Centro de Investigación del Cáncer
Instituto de Biología Molecular y Celular del Cáncer
(CSIC-USAL)

Roles of human VRK1 Ser-Thr kinase in the regulation of cell proliferation

PhD Thesis

David da Silva Moura

Salamanca, Spain

2016

D. Pedro Alfonso Lazo-Zbikowski Taracena, profesor de investigación del Consejo superior de Investigaciones Científicas (CSIC),

Certifica:

Que la memoria titulada **‘’Roles of human VRK1 Ser-Thr Kinase in the regulation of cell proliferation’’** presentada por el Máster en Biología **David da Silva Moura**, ha sido realizada bajo su dirección en el Instituto de Biología molecular y Celular del Cáncer y reúne, a su juicio, originalidad y contenidos suficientes para que sea presentada ante el tribunal correspondiente y optar al grado de doctor por la universidad de Salamanca.

Y para que así conste a efectos legales. Expide el presente certificado en Salamanca, a 29 de Enero de 2016.

Fdo. Pedro A. Lazo-Zbikowski Taracena

Esta memoria ha sido realizada siendo **David da Silva Moura** beneficiario de una beca predoctoral Formación de Personal Investigador (FPI; referencia BES-2011-046945) del Ministerio de Economía y Competitividad para la realización de la tesis doctoral (2011-2015). La memoria ha sido elaborada en el Programa de Doctorado Biociencias: Biología y Clínica del Cáncer y Medicina Traslacional.

La investigación en el laboratorio ha sido financiada por los siguientes proyectos:

Ministerio de Educación y Ciencia. CONSOLIDER-INGENIO2010 (CDS-007-0017)

Ministerio de Ciencia e Innovación (SAF2010-14935)

Junta de Castilla y León, Consejería de Educación (CSI006A11-2)

Ministerio de Economía y Competitividad (SAF2013-44810R)

Ministerio de Economía y Competitividad (SAF2014-57791-REDC)

Junta de Castilla y León, Consejería de Educación (CSI002U14)

Los resultados obtenidos a lo largo de esta Tesis Doctoral han sido publicados como artículos en las siguientes revistas:

DS Moura; IF Fernández; G Marín-Royo; I López-Sánchez; FM Vega; PA Lazo. Sox2 regulates and cooperates with VRK1 in cell cycle progression and differentiation – Submitted revised manuscript.

Marcella Salzano, Marta Sanz-García, Diana M Monsalve, **David S Moura** & Pedro A Lazo (2015) VRK1 chromatin kinase phosphorylates H2AX and is required for foci formation induced by DNA damage. Epigenetics, 2015, 10:5,373-383.

To my family,

specially to my wife and son

‘’All good work requires self-revelation’’

Sidney Lumet

Index

Glossary of abbreviations

A

ACA: Anti-centromere Antibody

AEG: Anophthalmia-Esophageal-Genital

AP-1: Activating Protein-1

APC: Anaphase-promoting Complex

APC/C: Anaphase-promoting Complex/ Cyclosome

APS: Ammonium Persulfate

ATF2: Activating Transcription Factor 2

ATM: Ataxia Telangiectasia Mutated

ATR: Ataxia Telangiectasia and Rad3-related Protein

AurKA: Aurora Kinase A

AurKB: Aurora Kinase B

AurKC: Aurora Kinase C

B

BAB: Basic-Acid-Basic

BAF: Barrier to Autointegration Factor

Bcl-xL: B cell Lymphoma-extra Large

BER: Base Excision Repair

BIRC5: Baculoviral IAP Repeat Containing 5

BMP4: Bone Morphogenetic Protein 4

BRCA1: Breast Cancer Associated 1

BSA: Bovine Serum Albumin

Bub1: Budding Uninhibited by Benzimidazoles 1

C

CAMK-IV: Calmodulin-dependent Kinase IV

CB: Cajal Body

CDK: Cyclin-dependent Kinase

cDNA: Complementary DNA

CDS: Coding DNA Sequence

ChIP: Chromatin Immunoprecipitation

Chk1: Checkpoint Kinase 1

Chk2: Checkpoint Kinase 2

CHX: Cycloheximide

CIP: Calf Intestinal

CK1: Casein Kinase 1

COX-2: Cyclooxygenase 2

CPC: Chromosomal Passenger Complex

CREB: cAMP Response Element-binding

CSC: Cancer Stem Cell

Ct: Cycle Threshold

D

DAPI: 4’,6’ Diamidino-2-Phenilindole

DDR: DNA Damage Response

DMEM: Dulbecco’s Modified-minimum Essential Medium

DMSO: Dimethyl Sulfoxide

DNA: Deoxyribonucleic Acid

DNA-PKcs: DNA-dependent Protein Kinase, Catalytic Subunit

DRAM: Damage-regulated Autophagy Modulator

DSB: Double-strand Break

DTT: Dithiothreitol

E

EDTA: Ethylenediaminetetraacetic Acid

EGF: Epidermal Growth Factor

EGTA: Ethylene Glycol Tetraacetic Acid

EMT: Epithelial-Mesenchymal Transition

ER: Endoplasmic Reticulum

ERK1/2: Extracellular Signal-regulated Kinase

ES: Ewing Sarcoma

ESC: Embryonic Stem Cell

EST: Expressed Sequences Tags

F

FACS: Fluorescence-activated Cell Sorting

FBS: Fetal Bovine Serum

FGF: Fibroblast Growth Factor

G

GAPDH: Glyceraldehyde 3-phosphate Dehydrogenase

GFAP: Glial Fibrillary Acidic Protein

GST: Glutathione S-Transferase

H

H: Hour

HeBS: HEPES-buffered Saline Solution

HMG: High-Mobility Group

HMSN: Hereditary Motor and Sensor Neuropathy

HP-1: Heterochromatin Protein-1

HR: Homologous Recombination

I

ICIS: Inner Centromere Kin-I Stimulator

IF: Immunofluorescence

IP: Immunoprecipitation

iPSC: Induced Pluripotent Stem Cell

IPTG: Isopropyl β-D-1-Thiogalactopyranoside

J

JNK: c-Jun N-terminal Kinase

K

Kb: Kilobase

kDa: Kilodalton

Klf4: Kruppel-like Factor 4

Knl1: Kinetochore-null protein 1

KSR1: Kinase Suppressor of Ras 1

L

LAP2: Lamina-associated Polypeptide 2

LB: Lysogeny Broth

LSCC: Lung Squamous Cell Carcinoma

M

M: Molar

MAN1: LEM Domain-containing Protein 3

MAP4K4: Mitogen-activated Protein Kinase Kinase Kinase 4

MAPK: Mitogen-activated Protein Kinase

MCAK: Mitotic Centromere-associated Kinesin

MDC1: Mediator of DNA Damage Checkpoint Protein 1

MDM2: Mouse Double Minute 2

MEK-1: Mitogen-activated Protein Kinase 1

mg: Milligram

min: Minute

Mklp1: Mitotic Kinesin-like Protein 1

mL: Milliliter

mm: Millimeter

mM: Millimolar

MMP2: Metalloproteinase-2

MMP3: Metalloproteinase-3

MMR: Mismatch Repair

MPS1: Monopolar Spindle 1

MRN: Mre11-Rad50-NBS1 Complex

MSC: Mesenchymal Stem Cell

N

NBS1: Nijmegen Breakage Syndrome Protein 1

NER: Nucleotide Excision Repair

NES: Nuclear Export Signal

NFAT: Nuclear Factor of Activated T Cells

NIS: Nuclear Import Signal

NHEJ: Non-homologous End-joining

NHK1: Nucleosomal Histone Kinase 1

NLS: Nuclear Localization Signal

Nm: Nanometer

nM: Nanomolar

NSCLC: Non-small Cell Lung Carcinoma

NT2/ D1: NTERA-2/ clone D1

O

Oct4: Octamer-binding Transcription Factor 4

ON: Overnight

P

PARP: Poly ADP Ribose Polymerase

PBS: Phosphate-buffered saline

PCR: Polymerase Chain Reaction

PI: Propidium Iodide

PIKK: Phosphoinositide 3-Kinase-related Protein Kinase

PKA: Protein Kinase A

PKC: Protein Kinase C

Plk1: Polo-like Kinase 1

Plk3: Polo-like Kinase 3

PMA: Phorbol 12-Myristate 13-Acetate

PMSF: Phenylmethylsulfonyl Fluoride

PPI: Polypropylenimine

PP1: Protein Phosphatase 1

PP2A: Protein Phosphatase 2A

PRKC1: Protein Kinase C iota type

R

RA: Retinoic Acid

Ran: Ras-related Nuclear Protein

RAR: Retinoic Acid Receptor

RARE: Retinoid Acid Response Element

RNA: Ribonucleic Acid

RNAi: RNA Interference

RNF8: Ring Finger Protein 8

RPMI: Roswell Park Memorial Institute Medium

RT: Room Temperature

RT-PCR: Reverse transcriptase PCR

RXR: Retinoid X Receptor

S

SAC: Spindle Assembly Checkpoint

SDS: Sodium Dodecyl Sulfate

SDS-PAGE: SDS-Polyacrylamide Gel Electrophoresis

Sgo1: Shugoshin-1

Sgo2: Shugoshin-2

shRNA: Small-hairpin RNA

siRNA: Small-interference RNA

SMC: Structural Maintenance of Chromosomes

Sox: Sry-related HMG Box

Sry: Sex-determining Region Y

SSB: Single-strand Break

T

TCA: Trichloroacetic Acid

TE: Tris-EDTA

TEMED: Tetramethylethylenediamine

TM: Melting Temperature

TNF-α: Tumor Necrosis Factor α

TSS: Transcription Start Site

U

UPP: Ubiquitin Proteasome Pathway

UV: Ultraviolet

V

VHL: Von Hippel-Lindau Tumor Supressor

VRK: Vaccinia-related Kinase

W

WB: Western Blot

WT: Wild type

#

53BP1: p53 Binding Protein 1

β-Me: β-Mercaptoethanol

µCi: Microcurie

µg: Microgram

µL: Microliter

µm: Micrometer

µM: Micromolar

ºC: Degree Celsius

Amino Acids		
Abbreviation		Amino Acid
A	Ala	Alanine
C	Cys	Cysteine
D	Asp	Aspartate
E	Glu	Glutamate
F	Phe	Phenylalanine
G	Gly	Glycine
H	His	Histidine
I	Ile	Isoleucine
K	Lys	Lysine
L	Leu	Leucine
M	Met	Methionine
N	Asn	Asparagine
P	Pro	Proline
Q	Gln	Glutamine
R	Arg	Arginine
S	Ser	Serine
T	Thr	Threonine
V	Val	Valine
W	Trp	Tryptophan
Y	Tyr	Tyrosine

Nitrogenous Bases	
A	Adenine
C	Cytosine
G	Guanine
T	Thymine
U	Uracil

List of Figures

List of Tables

Introduction

1. Cell division

Cell cycle or cell division includes a series of events that occur in a eukaryotic cell, involving its growth, division and replication and ending in the production of two identical daughter cells. Cell division is a tightly regulated process and is mainly characterized by DNA replication, chromosome condensation and segregation into two separate cells containing the same genetic information. This process was originally divided into two stages: i) mitosis or M phase and ii) interphase.

Mitosis, when the nuclear division occurs, is sub-divided in well-defined stages based on the reversible physical state of the chromosomes and spindle: i) prophase; ii) prometaphase; iii) metaphase; iv) anaphase, and v) telophase. The first stage is prophase, when the chromatin condensation and microtubules polymerization from the duplicated centrosomes begins. Prometaphase starts with the abrupt fragmentation of the nuclear envelope, exposing the chromosomes to the centrosome-radiating microtubules and ends with chromosomes correctly bi-orientated. In metaphase, chromosomes reach their most compacted state, lining-up in the equatorial plate of the mitotic spindle. A complex checkpoint mechanism – spindle assembly checkpoint (SAC) – determines whether the spindle is properly assembled and cells ready to divide. In anaphase, the sister chromatids separate, and finally in telophase, the chromosomes reach the poles, the nuclear membrane is formed around each set of chromosomes and the chromosomal chromatin begin to decondense into interphase-like conformation. Cytokinesis, or the division of the cytoplasm between the two daughter cells, is the final physical division of the cell that follows telophase and is therefore sometimes considered the last phase of mitosis. An important feature that characterizes mitosis is the high level of chromatin condensation, in comparison to interphase, in which the chromatin is less condensed, to facilitate easy access of the transcriptional machinery to the chromatin.

Chromatin condensation depends in part on the phosphorylation of the nucleosomal elements, histones, by protein kinases. A nucleosome is the fundamental subunit of chromatin and it is composed by around 147 DNA base pairs, wrapped around to an eight histone proteins core, including two copies of

histones H2A, H2B, H3, and H4. During mitosis, the highly condensed chromosomes become attached to the mitotic spindle through microtubules of tubulin radiating from the centrosomes. Microtubules attach to the chromosomes at their kinetochores and are able to pull the sister chromatids to opposite poles of the spindle. Here, SAC plays a key role determining whether the spindle is properly assembled and the cells ready to divide (Figure 1).

In turn, interphase occupies a much larger fraction of the cell cycle and includes three different phases: i) G1, ii) S phase and iii) G2. DNA replication occurs in the S phase. At the end of this phase there is an important checkpoint – DNA synthesis checkpoint - controlling whether the DNA has been successfully replicated and allowing the entrance into mitosis. The S phase is preceded by a gap called G1 during which cells prepare for DNA synthesis and is followed by a second gap called G2 during which the cell prepares for mitosis. At the end of G1 there is another important checkpoint – cell growth checkpoint – that regulates whether the cell is big enough and all the proteins necessary for replication were produced. At this point, cells can enter into the S phase or go to a resting state called G0 that accounts for the major part of the non-growing, non-proliferating ones (Figure 1) (Mitchison and Salmon, 2001; Paweletz, 2001).

The transition between the different phases of the cell cycle occurs in an orderly fashion and is regulated by numerous and different cellular proteins. Consequently, errors and malfunctions in this well-regulated process can lead to the accumulation of mutations, improper cell proliferation and culminates in the initiation and development of cancer. The most well-known key regulatory proteins are the serine (Ser/S) – threonine (Thr/T) cyclin-dependent kinases (CDKs) that are activated at specific stages of the cell cycle. These protein kinases remain stable during the cell cycle, but in turn the levels of their activating proteins, the cyclins, vary in order to specifically and sequentially activate a particular CDK. Briefly, to enter in G1 the three cyclin D types (D1, D2 and D3) complexes to CDK4 and CDK6, and to regulate the progression from G1 to S phase, cyclin E associates with CDK2. Besides, during S phase, cyclin A, binds to CDK2, and in late G2 and early mitosis the same cyclin complexes with CDK1 to promoter the entry into the M phase. Finally, the progression through mitosis is regulated by cyclin B in complex with CDK1 (Harashima et al., 2013; Vermeulen et al., 2003). However, not only CDK-cyclin complex are involved in

the control of cell cycle progression. In fact, several other proteins kinases (i.e. Auroras Kinases) and many transcriptional factors (i.e. p53) have been associated with the regulation of cell division by distinct mechanisms (Bolanos-Garcia, 2005; Eastman, 2004; Lazo and Santos, 2011; Malumbres and Barbacid, 2007). In this work, we explore the roles of Vaccinia-related kinase 1 (VRK1) in association with Aurora kinase B (AurKB) and with the reprogramming transcriptional factor SRY (Sex Determining Region Y)-Box 2 (Sox2) on the regulation of cell proliferation.

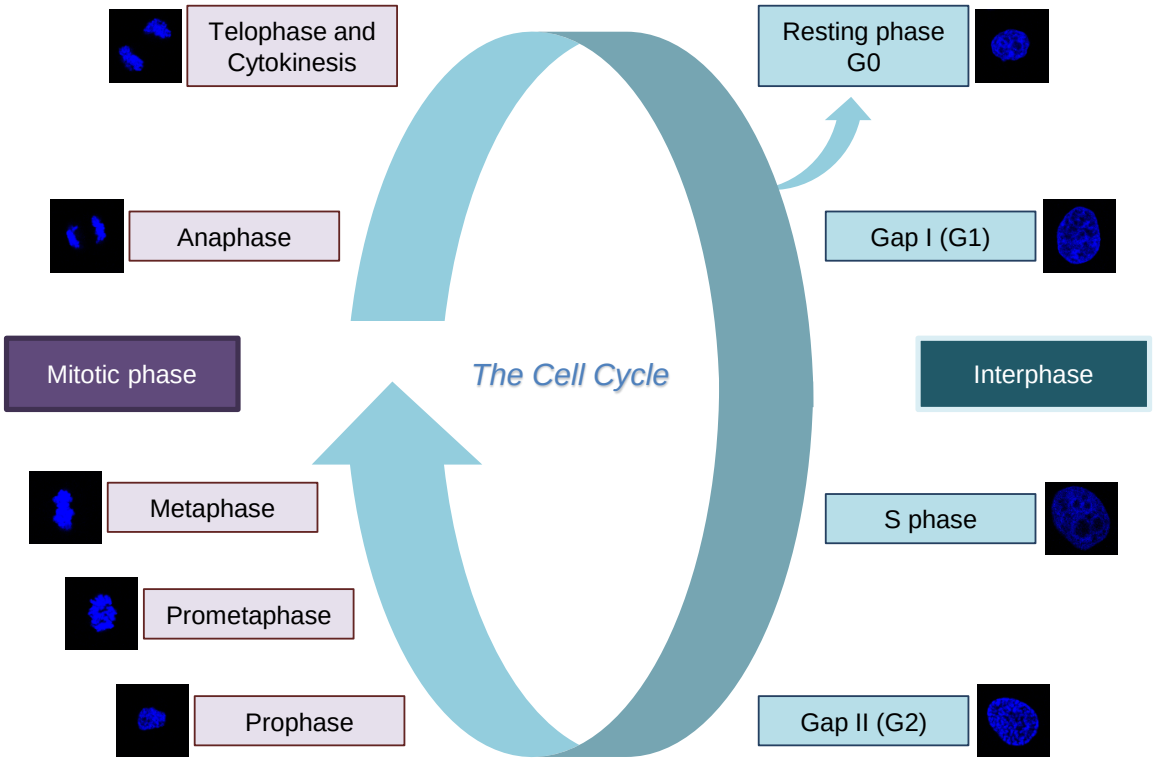

Figure 1 – **The cell cycle of animal cells** was originally divided into mitosis and interphase. In pioneering studies Flemming observed that the nuclear material, which he named chromatin, appeared distinctly in the cells. Nowadays it is known that he had successfully distinguished cells in interphase from cells in mitosis.

2. The protein kinases

The protein kinases are enzymes that catalyse the covalent ligation of a phosphate group to Ser, Thr or tyrosine (Tyr/Y) residues on specific cellular proteins. This process is called phosphorylation and it is a reversible posttranslational modification that mediates signal transduction in eukaryotic cells through changes on protein conformation, localization, molecular interactions,

stability and activity (Manning et al., 2002b; Pawson and Scott, 2005; Ubersax and Ferrell, 2007). Consequently, protein phosphorylation is a mechanism directly involved in the coordination of several biological processes such as angiogenesis, apoptosis, cell differentiation, DNA damage response (DDR), cellular growth, metabolism and migration (Shchemelinin et al., 2006). Any deregulation on these kinase proteins can lead to the development of a variety of diseases namely to cancer (Shchemelinin et al., 2006).

In general, protein kinases show a great homology in a specific sequence of 250-300 amino acids, which forms the kinase domain or catalytic domain (Hanks and Hunter, 1995; Higgins, 2001). This is an important feature that preserves the main function of these proteins in cellular pathways, which is the ability to transfer a phosphate group from ATP to neutral hydroxyl groups on the Ser, Thr and tyrosine (Tyr/Y) residues (Taylor and Kornev, 2011). The phosphorylation is a reversible process that can be accurately modulated by phosphatases, which eliminate the phosphate group from the hydroxyl groups on phosphorylated amino acids (Hunter, 1995). However, despite the overall kinase domain homology, differences in the activating sequences and in the amino and carboxyl terminal regions are critical to regulate protein kinases activity, negatively or positively, in response to cellular signals (Nolen et al., 2004).

The 518 genes, coding the respective proteins kinases, represent 2% of the human genome (Manning et al., 2002a; Manning et al., 2002b). Protein kinases are responsible for the phosphorylation of around 30% of the whole cellular proteins and, based in the specificity of the substrate, is sub-divided into three main sub-families:

a) Ser-Thr kinases
b) Tyr kinases
c) Dual kinases (Ser-Thr-Tyr kinases).

The phylogenetic of the human kinome was initially described in 2002 by Manning and colleagues, using public and proprietary genomic databases, complementary DNA (cDNA) and short sub-sequence of a cDNA sequence called Expressed Sequences Tags (EST) (Manning et al., 2002a; Manning et al., 2002b). This new classification follows another from 1995 by Hanks and Hunter, adding numerous new kinases to the kinase taxonomy (Hanks and Hunter, 1995). The kinases forming the human kinome can be grouped into eight different groups which are

in turn subdivided in families. In 2002, four new groups were added by Manning, among them the casein kinase I (CK1) group of kinases, which included the family of Ser-Thr kinases VRK (*Vaccinia-Related Kinase*) (Figure 2) (Manning et al., 2002b).

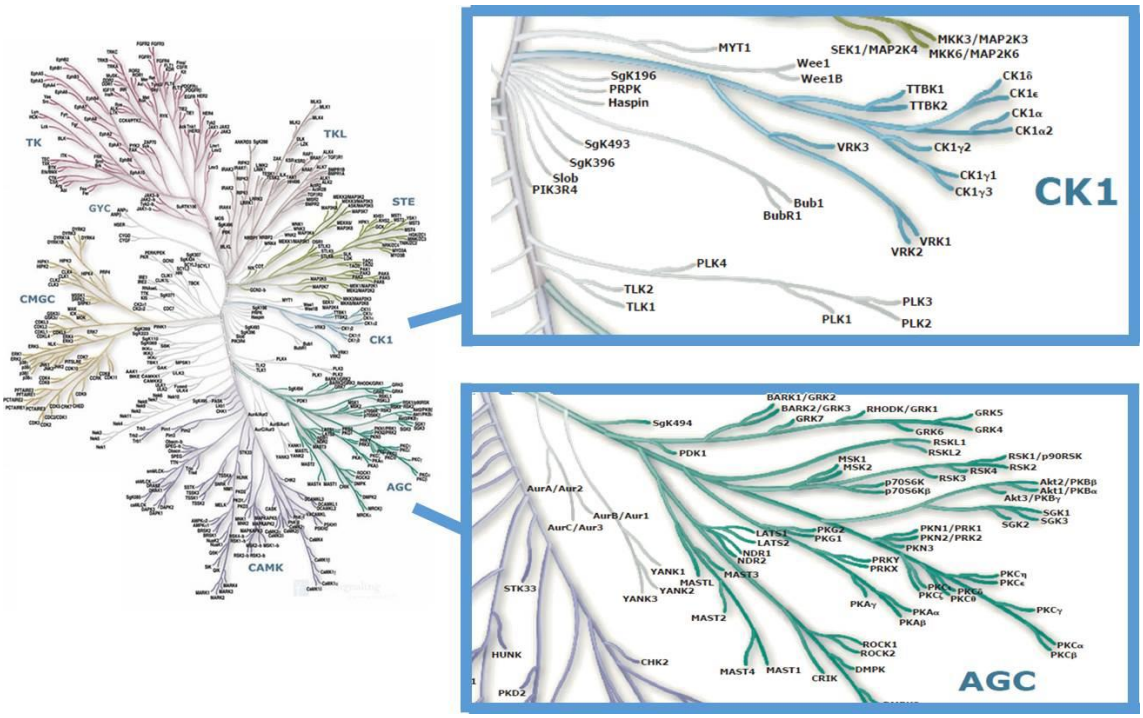

Figure 2 - **The human kinome** following the classification of 2002, from Manning and colleagues. In evidence the CK1 group, which contains the VRK family and the AGC group that includes Aurora family. Adapted from (Manning et al., 2002b).

3. The VRK family

The human VRK family belongs to the CK1 group of kinases and consists of three members: VRK1, VRK2 and VRK3. VRK1 and VRK2 have kinase activity, whereas VRK3 is a pseudo-kinase (without kinase activity), due to substitutions in key amino acids, present in its kinase domain, which disrupt invariant motifs essential to achieve a full catalytic activity (Nichols and Traktman, 2004). On the other hand, VRK2, due to alternative splicing of its mRNA, generates isoforms VRK2A and VRK2B, which mainly differ in their carboxyl-terminal (Blanco et al., 2006).

In 1997, Nezu and colleagues, using a cDNA library enriched in foetal genes from the liver, in a search for genes implicated in cell cycle regulation and

overexpressed in highly proliferating tissues, identified both VRK1 and VRK2 (Nezu et al., 1997). Due to the high homology between the B1R kinase and the *Vaccinia* virus, important to viral replication, this group of kinases received the name of *Vaccinia-related kinase* (Nichols and Traktman, 2004). Curiously, since B1R and VRK1 share 39% of homology between them, VRK1 expression was shown to partial rescue the DNA replication of a *Vaccinia* virus-B1R negative mutant sensible to temperature (Boyle and Traktman, 2004). Later in 2003, using cDNA library databases, the third kinase from the VRK family, the pseudo-kinase VRK3, was identified (Vega et al., 2003).

From an evolutionary point of view, it has been suggested that a unique ancestral gene was duplicated twice in vertebrates, creating the three genes of the VRK family, in contrast to invertebrates presenting a single original gene (Klerkx et al., 2009). In yeast, orthologous genes had not been identified, being the only ones described isoforms of CK1, such as the *Hrr25* gene of *Saccharomyces cerevisiae* or the *hhp1* gene of *Schizosaccharomyces pombe (Dhillon and Hoekstra, 1994)*. Interestingly, in *Caenorhabditis elegans* there is one orthologous gene to VRK1 codified by the *VRK-1* gene. This VRK1 orthologous gene is important to the proliferation of the germinal cells, through the direct regulation of CEP-1 (p53 orthologous gene) activity. The knockdown of *VRK-1*, using specific RNAi, is embryonic lethal due to defects in cell division (Kamath et al., 2003; Waters et al., 2010). Also, in nematodes, the importance of the VRK1 orthologous gene has been described regarding the phosphorylation of the barrier to autointegration factor (BAF), which regulates its localization and participation in the formation of the nuclear envelope (Gorjanacz et al., 2007). Moreover, in *Drosophila melanogaster* there is one orthologous gene of the VRK1 protein, the nucleosomal histone kinase-1 or NHK1. NHK1 is responsible for the phosphorylation of histone H2A, in the Thr119 residue, during mitosis and could partially regulate the localization of the AurKB in the inner centromere chromatin and therefore its activity during the early phases of cell division (Aihara et al., 2004; Brittle et al., 2007; van der Waal et al., 2012). NHK1 also phosphorylates BAF, regulating the affinity of this protein to the chromatin and to the nuclear membrane proteins, during the formation of the caryosome (Lancaster et al., 2007). In *Mus musculus*, as in humans, there are three orthologous genes, being the one of VRK1 originally nominated 51PK and described as a nuclear kinase

with high levels of auto-phosphorylation in Ser residues. All three kinases are expressed during embryonic development, reaching higher levels in highly proliferating organs such as liver, leucocytes, spleen and foetal thymus (Zelko et al., 1998). In adult rats, the levels of expression of each kinase depend on the cellular tissue (Vega et al., 2003). In general, we could assert that VRK proteins are present in all Holozoa.

3.1 The structure of VRK protein kinases

All VRK family members present high homology in the amino terminal region, in contrast to the carboxyl terminal region where there are several differences between them (Figure 3). The *VRK1* gene is located in the chromosomal region 14q32 and it codes a 396 amino acids protein. This protein presents in the N-terminus the catalytic domain (residues 35-275), containing not only the active Ser-Thr kinase domain (residues 175-185), but also the ATP binding domain (residues 43-71). In turn, the C-terminus of VRK1 contains a nuclear localization signal (NLS) (residues 356-360), a nuclear export signal (NES), and a basic-acid-basic domain (BAB) (residues 356-396), that is maintained between the orthologous genes (Aihara et al., 2004). Since the VRK1 carboxyl terminal region is only characteristic of this VRK member, it is assumed that this region is the responsible for the regulation of this kinase protein (Lopez-Borges and Lazo, 2000).

Regarding VRK2, this kinase protein has a 44% homology with VRK1, which can increase up to 53%, when comparing only the catalytic domain of both kinases. *VRK2* gene is located in the chromosomal region 2p16 and codes two isoforms due to mechanisms of alternative splicing: VRK2A and VRK2B. VRK2A consists of 508 amino acids and VRK2B consists of 397 amino acids. Overall, both VRK2A and VRK2B show a similar sequence until the amino acid 394, where the new exon, produced by alternative splicing, introduces a premature stop codon, which swaps the amino acids between 395 and 508, by three VEA (valine-glutamate-alanine) residues (Blanco et al., 2006). The N-terminus, which is similar between the two isoforms, comprises the ATP binding domain (residues 35-61) and the active kinase domain (residues 162-174). On the other hand, the C-terminus of VRK2A contains a hydrophobic transmembrane region (residues 492-508) and two overlapped BAB motifs, being the transmembrane region and

the BAB motifs absent in the truncated isoform VRK2B (Blanco et al., 2006; Nichols and Traktman, 2004). VRK1 and VRK2 are active kinases that have the ability to phosphorylate basic or acid proteins and present high autophosphorylation activity (Barcia et al., 2002; Lopez-Borges and Lazo, 2000).

At last, the 474 amino acid pseudo-kinase VRK3 is coded by the *VRK3* gene in the chromosomal region 19q13, and shows minor homology with VRK1 (33%) and VRK2 (23%). The amino terminal region of VRK3 contains the NLS whereas the carboxyl terminal region contains a degenerative kinase domain, due to alterations in key amino acids that lead to a null catalytic activity (Kang and Kim, 2006).

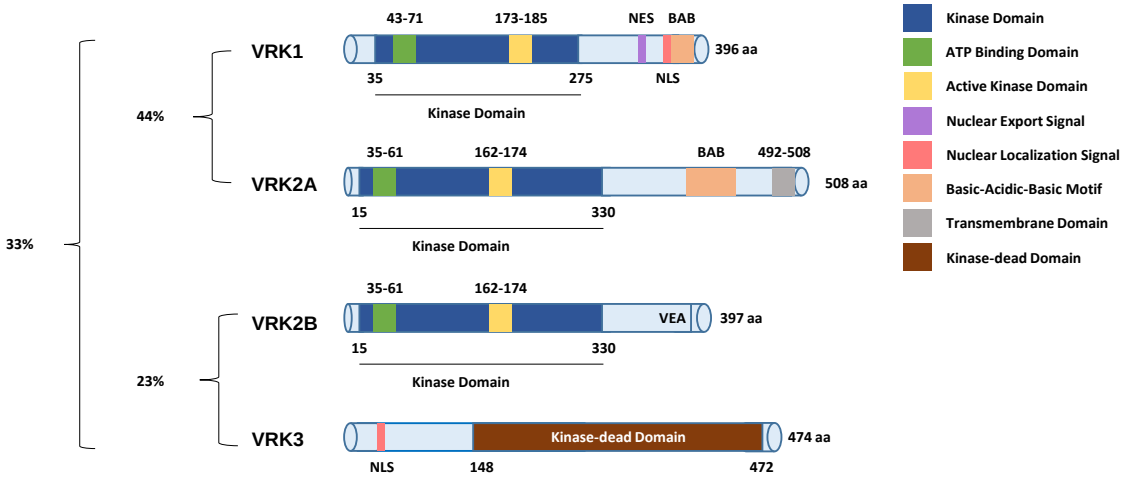

Figure 3 – Schematic representation of the structure of VRK family of protein kinases and the main domains and motifs of each kinase. The percentages relate to the level of homology between the three different members of the family.

Concerning the tri-dimensional structure of the VRK family members, they show an additional α-helix (αC4) in the activation domain that makes the kinases constitutively active (Scheeff et al., 2009). This is important since the members of the VRK family lack a conserved phosphorylation site in the activation loop in order to regulate the kinase activity, being equally active due to this extra helix. Nevertheless, in VRK3, several glycine residues in the G-loop (GxGxFG) are degraded and replaced by larger amino acids. These substitutions prevents the binding of ATP, as well as other modifications outside the G-loop and turn the VRK3 in a pseudo-kinase without kinase activity (Scheeff et al., 2009).

3.2 Subcellular localization of VRK protein kinases

VRK1 is typically a nuclear kinase, since it contains a NLS in the protein structure. In the nucleus, VRK1 was described to be in the nucleoplasm, nucleolus and was also associated with the chromatin (Andersen et al., 2005; Kang et al., 2007b; Valbuena et al., 2011b). However, it is important to notice that VRK1 subcellular localization depends on the cell type and cell growth conditions, as it can also be observed in the cytoplasm of a few cell lines.

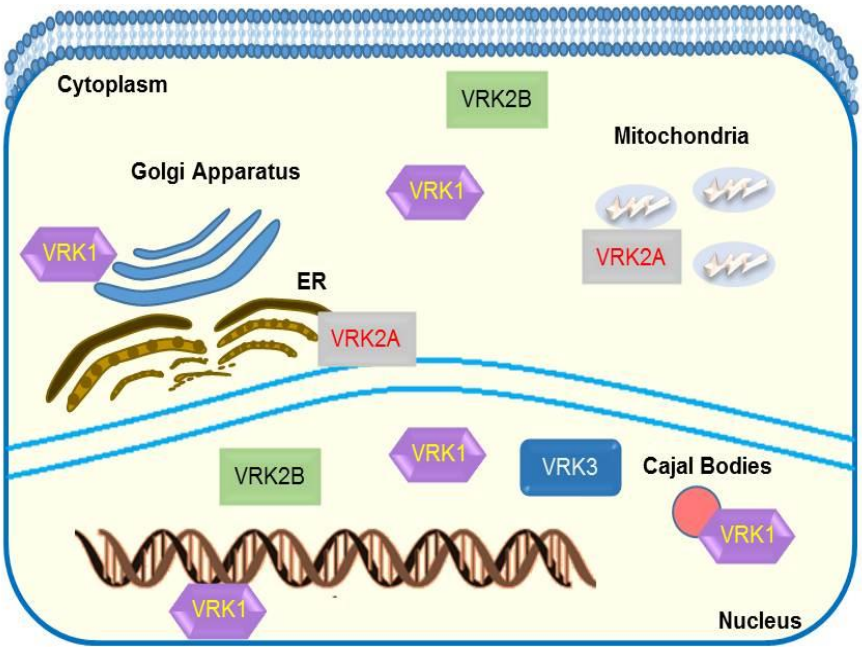

Figure 4 – Subcellular localization of VRK family of protein kinases. VRK1 is predominantly a nuclear kinase, being detected on the nucleoplasm, nucleolus and associated with the chromatin. In the cytosol, a smaller fraction is observed in the cytoplasm and associated with the Golgi apparatus.

Additionally, a subpopulation of VRK1 was also detected in the Golgi apparatus and VRK1 was described as being part of transcription complexes associated with the chromatin, alongside with histones and transcriptional factors (Figure 4) (Guermah et al., 2006; Valbuena et al., 2007a). VRK2 has two isoforms due to alternative splicing. The first isoform, VRK2A, is located anchored to the membranes of Golgi apparatus, endoplasmic reticulum (ER) and nuclear envelope, through the transmembrane domain. This domain is present in the carboxyl terminus region and has a hydrophobic nature. On the other hand, due to the absence of a transmembrane domain in its protein structure, VRK2B can be detected loose in the cytoplasm and in the nucleus (Figure 4). Finally, VRK3

has a nuclear localization, due to the NLS located in the amino terminal region of the protein kinase structure (Figure 3).

3.3 The human VRK1 kinase

The human VRK1 is the first member of the VRK family and it is the best characterized protein kinase of the group. VRK1 is ubiquitously expressed in all tissues, with particular high expression in highly proliferating tissues, such as liver and thymus or cancer cell lines (Nezu et al., 1997; Vega et al., 2003). Thus, based on VRK1 features and expression, this kinase has been related to cell cycle regulation and proliferation. Nowadays, new updates on this kinase have emerged, and several others functions have been associated with VRK1 (Valbuena et al., 2011b). In summary, VRK1 was described to participate in a broad group of processes such as: i) the correct progression of the cell cycle through transcriptional factors regulation; ii) DDR pathways; iii) modulation of p53 levels; iv) nuclear envelope breakdown; v) histone phosphorylation; vi) formation and maintenance of Cajal body (CB); vii) chromatin condensation and viii) fragmentation of the Golgi apparatus. VRK1 protein functions are described in detail in the following chapters and are summarized in the Table I.

3.3.1 Role of VRK1 in cell proliferation and cell cycle progression

VRK1 is an important regulator of proliferation and cell cycle progression. The majority of these observations were obtained from studies related with VRK1 expression. It was described that in normal squamous epithelium VRK1 is highly expressed near the highly proliferative basal layer, decreasing as the epithelial cells differentiate, and correlating positively with the proliferation marker Ki67. Moreover, in head and neck squamous cells tumours, VRK1 expression was described to correlate positively with proliferations markers, such as CDK2, CDK6, cyclin A, Ki67 and topoisomerase II and, negatively with cell cycle inhibitors such for example p16 and p27. Likewise, VRK1 was also described to positively correlate with the expression of proliferation marker p63 in pharynx squamous epithelium. Altogether, these results suggest that VRK1 behaves as a proliferation marker (Santos et al., 2006; Valbuena et al., 2008b; Valbuena et al., 2007a). Accordingly, it was also observed that the inhibition of VRK1 gene expression, using specific RNA interference (RNAi), reduces the levels of cyclin

A, cyclin D1, PCDNA, among other proliferation markers, leading to a cell cycle arrest in the G1 phase (Valbuena et al., 2008b; Valbuena et al., 2011b). Moreover, it was also observed the dependence of Ewing sarcoma (ES) cell lines on human VRK1. Here, knockdown of VRK1 with small hairpin RNA (shRNA) induced low proliferation and rapid onset of apoptosis on ES cell lines. A result supported by *in vivo* studies, demonstrated the clear reduction in tumour development after injection of VRK1-depleted SKNMC-ES cells. These results confirmed that VRK1 is critical for ES proliferation and survival, displaying the tumoral cells a marked higher sensitivity to the suppression of the kinase (Riggi et al., 2014).

Table I – List of VRK1 substrates

VRK1 Substrates		
Protein Substrate	**Residues Phosphorylated**	**Function**
53BP1	Ser25; Ser29	DNA damage repair
ATF2	Ser62; Thr73	Transcriptional activation
BAF	Thr2; Thr3; Ser4	Nuclear envelope break-down
c-Jun	Ser63; Ser73	Transcriptional activation
Coilin	Ser184	Cajal bodies assembly
CREB	Ser133	Cell cycle progression in G1/ S phase transition
Histone H2A.X	Ser139	DNA damage repair
Histone H2B	Unknown	Unknown
Histone H3	Thr3; Ser10	Chromatin condensation during mitosis
Histone H4	Unknown	Unknown
NBS1	Ser343	DNA damage repair
p53	Thr18	p53 activation and cell cycle arrest

In the table are represented the major VRK1 substrates described in the literature.

However, not all the tumours express the same levels of VRK1. As an example, lung carcinomas express variable levels of VRK1 depending on the subtype of the tumour. Squamous cell lung carcinomas have higher expression

of VRK1, when compared to adenocarcinomas. Curiously, squamous cell lung carcinomas present p53 mutations, which could indicate a tendency for tumours positive with p53 mutations to accumulate VRK1 (Valbuena et al., 2007b). Besides, in breast cancer, the levels of VRK1 expression diverge depending on tumour type. High levels of VRK1 could indicate poor prognosis in breast cancer, whereas low levels of VRK1 expression and other mitotic markers could indicate good prognosis in breast cancer (Fournier et al., 2006). The same conclusion was obtained in an independent study, in which it was shown that high expression of sixteen cell cycle-related kinases, including VRK1, correlated with poor prognosis in breast cancer (Finetti et al., 2008). Nevertheless, VRK1 is also involved in several other mechanisms associated with cell proliferation as explained in the next sections.

3.3.2 The implication of VRK1 on chromatin remodelling

The chromatin is the state in which the DNA is packed inside the cell, being the nucleosome the fundamental component of chromatin. The nucleosome contains approximately 147 base pairs of DNA, wrapped around of an octamer composed by two copies of the four core histones: H3, H4, H2A and H2B (Kouzarides, 2007; Smith and Shilatifard, 2010). The core histones are globular except for their amino-terminal ‘‘tails,’’ which are unstructured and vastly modified on their residues. These tails can be submitted to different posttranslational modifications, such as phosphorylation, acetylation, ADP ribosylation, deamination, (mono-; di-; tri-) methylation, proline isomerization, sumoylation or ubiquitination (Kouzarides, 2007). Histone modifications can change the active or repressive state of the chromatin, modulating the activity of histone chaperones, nucleosome remodelers, transcription factors and other histone modifiers (Baek, 2011) and, ultimately regulating chromatin condensation during mitosis, apoptosis, DDR, genome stability, replication and transcription (Berger, 2007; Costelloe et al., 2006; Hans and Dimitrov, 2001; Hurd et al., 2009; Kang et al., 2007b; Luijsterburg and van Attikum, 2011; Smith and Shilatifard, 2010; Valbuena et al., 2011b).

VRK1 directly participates on chromatin remodelling mostly through histone H3 phosphorylation on the residues Thr3 (H3T3ph) and Ser10 (H3S10ph). H3T3ph and H3S10ph are necessary for an accurate cell cycle

progression and are also phosphorylation targets of two other relevant mitotic kinases: Haspin, that phosphorylates H3T3, and AurKB, which phosphorylates H3S10 (Kang et al., 2007b; Valbuena et al., 2011b; Vazquez-Cedeira et al., 2011). Curiously, H3S10ph was also reported to be important for chromatin relaxation and transcription (Prigent and Dimitrov, 2003). Besides histone H3, VRK1 is also able to phosphorylate, in a smaller scale, H2A, H2B and H4. Altogether, it seems that VRK1, besides its involvement in the cell cycle progression during interphase, also contributes to chromatin condensation, and consequently to the G2/M transition, through histone phosphorylation (Kang et al., 2007b; Valbuena et al., 2011b). Lately, the potential role of VRK1 on histone acetylation and methylation has been also studied, and it appears that the kinase has an active role on the regulation of other histone modifications besides phosphorylation (Salzano et al., 2015).

3.3.3 Regulation of transcription factors by VRK1

VRK1 is a kinase with high autophosphorylation capacity, capable of phosphorylating both acidic and basic proteins. Interestingly, this particular characteristic is not shared with other kinases from the casein kinase 1 group. (Lopez-Borges and Lazo, 2000).

Among the numerous substrates of VRK1, several transcription factors are regulated by VRK1-phosphorylation, namely p53. The tumour suppressor p53 is important to maintain cell homeostasis, as it mediates cell cycle arrest in order to correct the detected ‘’errors’’ on the DNA. Otherwise, the cell undergoes apoptosis. The accumulation, stabilization and activation of p53, in response to cellular ‘’stress’’ is perfectly regulated, and this regulation occurs mostly due p53 phosphorylation and acetylation. VRK1 phosphorylates p53 on the Thr18 residue, blocking the binding of p53 to the negative modulator Mouse double minute 2 (Mdm2) and promoting the binding to p300 (Barcia et al., 2002; Dumaz and Meek, 1999). Thus, VRK1 avoids p53 degradation through the Mdm2-dependent ubiquitin proteasome pathway (UPP) and it increases the acetylation of lysine (Lys/K) 373 and Lys382 by the co-factor p300. This leads to the stabilization of the transcription factor (Vega et al., 2004a). On the other hand, VRK1 and p53 form an autoregulation loop, since VRK1 is tightly regulated by p53. The activation of p53 induces DRAM (damage-regulated autophagy modulator)

expression, which in turn promotes the degradation of VRK1 through lysosomal degradation in the autophagic pathway (Valbuena et al., 2011a; Valbuena et al., 2006b). In addition, p300 affects the specificity of p53 towards particular transcription targets while protecting VRK1 from degradation (Valbuena et al., 2008a).

Moreover, VRK1 phosphorylates c-Jun and the activating transcription factor 2 (ATF2). Both c-Jun and ATF2 are activating protein-1 (AP-1) transcription factors. The c-Jun protein regulates genetic expression, in response to stress, of cytokines and grow factors, controlling in turn several cellular mechanisms such as apoptosis, differentiation or proliferation. The activation of c-Jun occurs through direct phosphorylation by kinases belonging to the mitogen-activated protein (MAPK) kinase family, like the ERK1/2 (extracellular signal-regulated kinases) and JNK (c-Jun N-Terminal kinase) kinases (Chang and Karin, 2001). Additionally, VRK1 phosphorylates c-Jun in the Ser63 and Ser73 residues, which stabilizes and activates the transcriptional activity of c-Jun (Sevilla et al., 2004a). Regarding ATF2, the transcription factor belongs to the ATF/ CREB (cAMP response element-binding) family and, through the activation of genes involved in cell growth, differentiation and immune response, promotes proliferation and oncogenesis (van Dam and Castellazzi, 2001). ATF2 is phosphorylated by MAPKs as ERK, JNK and p38 (Bhoumik and Ronai, 2008), and as described recently, it is also phosphorylated by VRK1 on the Ser62 and Thr73 residues, which are phosphorylation targets of protein kinase A (PKA) and calmodulin-dependent kinase IV (CAMK-IV). Both Ser62 and Thr73 phosphorylation lead to the accumulation and transcriptional activation of ATF2 (Sevilla et al., 2004b). Furthermore, VRK1 is capable of phosphorylating the Ser133 residue of transcription factor CREB. This parallel VRK1-dependent activation of CREB and ATF2 increases the binding of both transcriptional factors to the promoter *CCND1*, enhancing the expression of cyclin D1 protein and promoting G1/ S phase transition (Sevilla et al., 2004b).

3.3.4 Role of VRK1 on the Golgi apparatus fragmentation

The fragmentation of the Golgi apparatus is a common feature that occurs during mitosis. More precisely, at the end of the cell cycle the redistribution of the organelles between the two daughter cells, requires fragmentation, dispersion

and assembly of the Golgi apparatus, in a process dependent on phosphorylation. Normally, this phosphorylation process leads to the fragmentation of the Golgi apparatus and it is attributed to MEK1 (mitogen-activated protein kinase 1) and Plk3 (polo-like kinase 3) (Ruan et al., 2004; Xie et al., 2004). Recently, also VRK1 has been described to actively participate in this fragmentation mechanisms. In short, VRK1 interacts with Plk3, forming a stable complex, co-localizing in the Golgi apparatus. Plk3 phosphorylates the Ser342 residue localized in the ‘’regulatory-carboxyl-terminal-region’’ of VRK1. Besides, it was observed that the down-regulation of VRK1, using small interfering RNA (siRNA), partially blocks MEK1 and Plk3 induced fragmentation of the Golgi apparatus. This was also observed when a VRK1 mutant without kinase activity was expressed. In summary, VRK1 is essential for the correct fragmentation of the Golgi apparatus at the G2/ M transition, playing a role downstream of the MEK1/ Plk3 pathway (Lopez-Sanchez et al., 2009).

3.3.5 VRK1 importance on the assembly of nuclear envelope

The nuclear envelope breakdown and assembly is a well-regulated mechanism that begins at early stages of mitosis and ends during telophase. Among the proteins involved in this breakdown-assembly process one of the most important is BAF. BAF is a small protein involved in the maintenance of the nuclear architecture. BAF binds the DNA and proteins with LEM motifs, namely emerin, lamina-associated polypeptide 2 (Lap2) and LEM domain-containing protein 3 (MAN1) that are localized in the internal nuclear membrane. Furthermore, BAF changes its sub-cellular location depending on the phase of the cell cycle. So, during interphase BAF is located in the internal nuclear membrane, playing a role on the anchorage of chromatin to the nuclear envelope while during the early stages of mitosis it is released from the chromatin and nuclear membrane proteins, playing a role in the chromatin condensation and nuclear envelope breakdown. On anaphase, BAF is located near the telomeres, enhancing the recruitment of proteins necessary for the nuclear envelope assembly (Haraguchi et al., 2001).

VRK1 phosphorylates BAF in three residues in the amino-terminal region: i) Thr2, ii) Thr3 and iii) Ser4. These phosphorylations, while slightly affected the binding of BAF to LEM-motif proteins, seriously affected the binding of BAF to the

chromatin and the subcellular localization of the protein. Thus, VRK1 phosphorylates BAF, releasing the protein from the DNA, facilitating chromatin condensation and nuclear envelope breakdown. In conclusion, VRK1 plays an important role in the nuclear envelope breakdown-assembly dynamics. (Molitor and Traktman, 2014; Nichols et al., 2006b; Zhuang et al., 2014).

3.3.6 Implication of VRK1 on DNA-damage response (DDR)

Cell homeostasis is regulated by several mechanisms like: proliferation, cell senescence and cell death, representing a fundamental balance for cell survival and maintenance of the DNA integrity the DDR. The DDR system has as fundamental functions the detection, signalling and repair of DNA breaks and mutations, induced by either endogenous cellular processes or by exogenous agents. When a break/mutation is detected, the cell cycle arrests in order to prevent the replication and propagation of damaged DNA to the daughter cells. DDR then activates the correct DNA damage repair pathway as a way to repair the DNA and maintain the DNA integrity. When the damage is efficiently repaired, cell re-enters the proliferative state, but if the damage is too severe, the cell undergoes apoptosis. Errors in the repair of DNA damage or non-repaired lesions can lead to tumorogenesis. Concerning the different types of DDR, these can be related to single-strand breaks (SSBs) such as BER (base excision repair), *in situ* repair, MMR (mismatch repair) and NER (nucleotide excision repair), or related to double-strand breaks (DSBs) like HR (homologous recombination) and NHEJR (non-homologous end-joining repair). Focusing only on DBSs, the most lethal form of DNA damage, numerous proteins are involved DNA repair. For instance the sensor proteins H2A.X, MRN (Mre11-Rad50-NBS1) complex and PIKKs (phosphoinositide 3-kinase-related protein kinase: ATM (ataxia telangiectasia mutated), ATR (ataxia telangiectasia and Rad3-related protein) and DNA-PKcs) that detect the lesions, the scaffold proteins breast cancer associated 1 (BRAC1) and mediator of DNA damage checkpoint protein 1 (MDC1), which recruit other proteins important for the repair, the transducing proteins checkpoint kinase 1 and 2 (Chk1 and Chk2) and PIKKS responsible for amplify the detection signal and the effector proteins cdc25 and p53 in control of the cell cycle arrest, reparation, senescence or apoptosis. Recently, also VRK1 has been described to be relevant regarding DDR mechanisms. (Fleck and Nielsen, 2004; Jackson

and Bartek, 2009; Lopez-Sanchez et al., 2014b; Salzano et al., 2015; Salzano et al., 2014; Sanz-Garcia et al., 2012).

Initially, evidence demonstrated that VRK1 is an early response protein, required for the formation of 53BP1 foci. In resting cells, the induction of DSBs with ionizing radiation activates VRK1, inducing the formation of p53-binding protein 1 (53BP1) foci in a VRK1-dependent manner. In addition, VRK1 specifically phosphorylates 53BP1 in starvation conditions. Knock-down of VRK1 using siRNA, results in defective 53BP1 foci formation, not only in number, but also in size. The use of a siRNA-mutant-resistance rescues the formation of 53BP1 foci, being the effect of VRK1 upon the foci formation independent of ATM and p53. In fact, VRK1 seems to act upstream of ATM since VRK1 knockdown avoids the activation of ATM and other kinases such as Chk2 and DNA-dependent protein kinase (DNA-PK) (Sanz-Garcia et al., 2012). Similar results were obtained using doxorubicin as damaging agent in breast cancer cell lines, which indicates that VRK1 is activated early independently of the type of DNA damage (Salzano et al., 2014). New evidence, supports the importance of VRK1 in DNA damage early response. VRK1 exists in a basal stable complex with p53, before UV-induced DNA damage activates VRK1, leading to the phosphorylation of p53 on the Thr18 residue as well as its accumulation. The VRK1-p53 basal complex seems to be important as an early-warning system to respond instantly after DNA damage (Lopez-Sanchez et al., 2014b). Moreover, VRK1 seems to affect Nijmegen Breakage syndrome protein 1 (NBS1) foci formation. Knock-down of VRK1 affects negatively the formation of NBS1 foci, being this phenotype rescued when using a mutant resistant to the siRNA, similarly to the results observed with 53BP1 foci formation. VRK1 interact and phosphorylates NBS1, leading to the correct formation of NBS1 foci. Moreover, VRK1 and ATM are necessary for NBS1 formation, avoiding the degradation of NBS1 by the ubiquitin proteasome pathway dependent of the ubiquitin-ligase E3 RNF8 (ring finger protein 8).

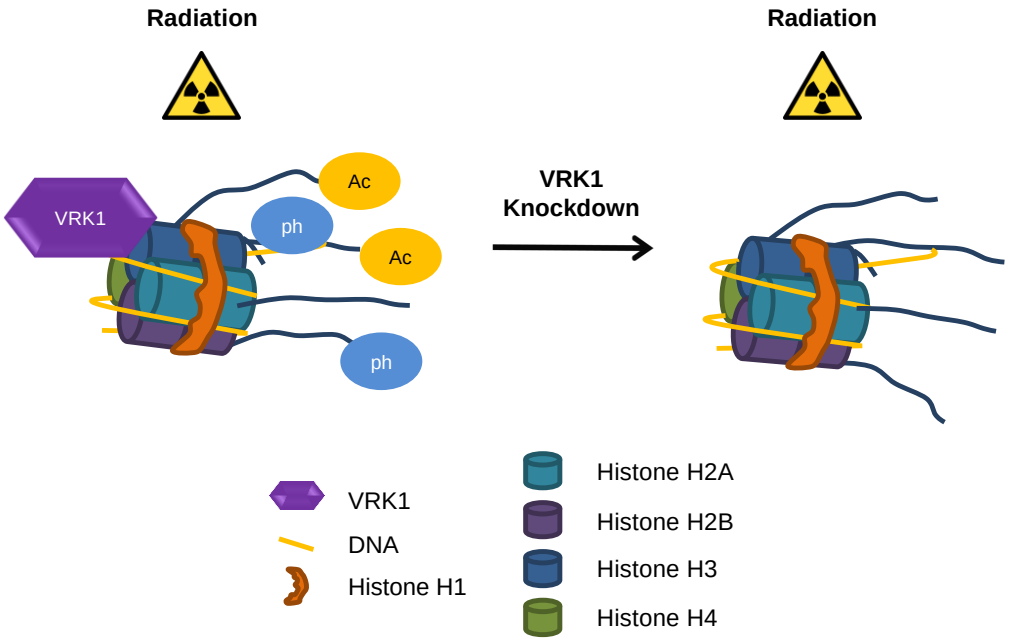

Figure 5 – Role of VRK1 on histone modifications under ionizing radiation. VRK1 knockdown, under ionizing radiation, induces loss of histone H2A.XSer139 phosphorylation and histones H3 and H4 acetylation.

Lately, VRK1 was also implicated in chromatin relaxation, under ionizing radiation conditions and independently of ATM. The acetylation of histone H3 and histone H4 are critical events for the relaxation of chromatin, which is important for DDR. Depletion of VRK1 causes the loss of histone acetylation, not only under DNA damage condition, but also in basal conditions. Moreover, VRK1 interacts and phosphorylates the histone H2A.X on the Ser139 residue, whereas VRK1 knockdown decreases the phosphorylation of histone H2A.X and γH2A.X foci formation upon ionizing radiation (Figure 5) (Salzano et al., 2015).

3.3.7 Neurodegeneration and VRK1

The importance of VRK1 covers a spectrum much wider than the regulation of cell cycle progression and proliferation or its implication in cancer. Indeed, it has been shown that VRK1 also plays an important role in the development and maintenance of the nervous system (Renbaum et al., 2009b; Wee et al., 2010). So, it is expected that the deregulation of VRK1 or mutations on this kinase could lead to the development of neurodegenerative diseases. VRK1 mutation R358X, with a stop within the NLS and forming a truncated VRK1, lacking its C-terminal region, has been associated with spinal muscular atrophy,

pontocerebellar hypoplasia and consequently child death. This mutation occurs in the VRK1-NLS domain and affects the normal nuclear localization of the kinase but not its activity. This syndrome only affects recessive homozygote children, having the heterozygosis a normal phenotype (Renbaum et al., 2009b). More recently, other VRK1 mutations (R89Q; R133C; V236M) were reported in hereditary motor and sensory neuropathies (HMSN)-related studies. VRK1 mutations, located in the kinase domain, may affect cell cycle progression and induce apoptosis of neuronal cells, but the effect of such mutations in the neurodegeneration process is not yet fully cleared (Gonzaga-Jauregui et al., 2013a; Najmabadi et al., 2011). Moreover, VRK1 seems to be important for the CBs correct assembly, more precisely to the recruitment of the scaffold protein coilin, essential to CBs assembly. VRK1 interacts with and phosphorylates, at least the Ser184 residue, on coilin regulating the formation of CBs. The VRK1-dependent phosphorylation of coilin on Ser184 occurs in mitosis, before the formation of the CBs, and is important for the stability of the scaffold protein. The loss of coilin phosphorylation results in disintegration of CBs and degradation of coilin in the proteasome (Cantarero et al., 2015; Gonzaga-Jauregui et al., 2013a; Sanz-Garcia et al., 2011)

3.3.8 VRK1 gene-trap hypomorphic transgenic mice

Hypomorphic mice expressing no more than 15% of VRK1 protein, comparing with wild-type mice, are viable but sterile. This sterility results from defects in spermatogenic cells proliferation, due to deficient mitosis and meiosis of the male reproductive cells. Also, VRK1 silencing does not affect other tissues, which may indicate a redundancy with the others members of the VRK family (Choi et al., 2010; Wiebe et al., 2010). Likewise, it was also reported that VRK1 knock-out dramatically affects the gametogenesis. Mice males were initially fertile, but gradually become sterile due to alterations in spermatogenesis, whereas female mice were totally sterile due to oocyte developmental defects (Schober et al., 2011). Recent report in VRK1-deficient ovaries supports the important role of VRK1 on gametogenesis and folliculogenesis (Kim et al., 2012a).

3.3.9 The regulation of human VRK1

The regulation of VRK1 activity, sub-cellular localization and expression is important for an accurate response to extra or intracellular stimulus. VRK1 expression is regulated by mitogens and growth factors, normally present in the serum, given that serum-free conditions decrease the levels of VRK1 and the re-introduction of serum in the cellular medium restores the levels of this kinase (Valbuena et al., 2008b). Additionally, transcription factors, such as E2F1 and Myc, activate the expression of *VRK1* gene promoter (Kang and Kim, 2008; Santos et al., 2006).

Recently, also the aberrant transcription factor EWS-FLI1 was described to activate the *VRK1* promoter. EWS-FLI1 multimers recruit acetyltransferases (p300) and methyltransferases, which open the chromatin and create *de novo* enhancers. Consequently, this new enhancer physically interacts and activates the promoter of *VRK1* (Figure 6). The interaction between the long distance enhancer, bounded to EWS-FLI1, and the *VRK1* promoter was confirmed in ES cell lines SKNMC and A673, where the knockdown of EWS-FLI1 also induced a decrease in VRK1 expression (Riggi et al., 2014).

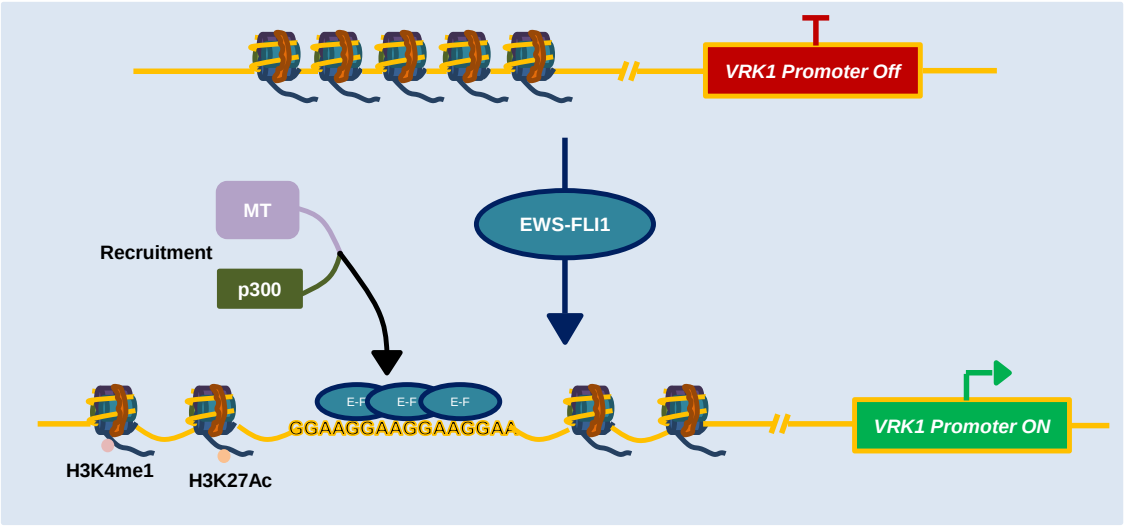

Figure 6 – Regulation of *VRK1* gene promoter by EWS-FLI1. The transcription factor binds to GGAA repeats, recruiting methyltransferases and acetyltransferases, relaxing the chromatin, creating *de novo* enhancers and activating the VRK1 gene promoter.

However, the most well-known regulation of VRK1 subcellular localization and activity is related with post-translational modifications on the protein. VRK1, like VRK2, has high autophosphorylation activity important to maintain the stability of the kinase, since the inactive kinase is less stable and has reduced lifetime (Lopez-Borges and Lazo, 2000). Besides, the *in vitro* phosphorylation of Thr355, located in the carboxyl-terminus region of VRK1, seems to be involved in the regulation of this kinase, although it remains unknown how it affects the localization or its activity (Barcia et al., 2002). This residue was also described to be phosphorylated by protein kinase C δ (PKCδ), which negatively regulates VRK1. More precisely, in DNA damage conditions, VRK1 is phosphorylated by PKCδ, arresting the cell cycle and consequently inducing p53-dependent cell death (Park et al., 2011). Another important residue is VRK1 Thr378, which is suggested to be phosphorylated by ATM and ATR in response to UV light (Stokes et al., 2007). Moreover, it was described that VRK1 levels increase after ionizing radiation or UV light exposure or treatment with DNA damage-inducing drugs, such as doxorubicin (Sanz-Garcia et al., 2012; Valbuena et al., 2011a). In addition, VRK1 can also be activated through stable interactions with other proteins. An example is Ras-related nuclear GTPase (Ran GTPase), identified by proteomics, which interacts and regulates VRK1 kinase activity. When VRK1 binds to RanGTP, the kinase is active, but when it binds to RanGDP the kinase is inactive. Besides VRK1, also VRK2A and VRK2B are similarly regulated by Ran GTPase (Sanz-Garcia et al., 2008). On the other hand, VRK1 interacts and it is regulated by macroH2A1.2. The interaction between VRK1 and macroH2A.1.2 seems to occur during interphase, avoiding the phosphorylation of histone H3 and BAF, without affecting the autophosphorylation activity of VRK1 (Kim et al., 2012c). MacroH2A has three isoforms (macroH2A1.1, macroH2A1.2 and macroH2A2) and differs from the conventional histone H2A in the C-terminus region, since it has a macro domain attached via a linker region. MacroH2A isoforms incorporate into the chromatin via their histone H2A-like region, changing the chromatin conformation and repressing transcription. Lately, macroH2A had also been associated with the transcriptional activation of differentiation genes in embryonic and adult stem cells, rendering them important in the establishment and maintenance of differentiated states (Chakravarthy et al., 2005; Creppe et al., 2012a; Creppe et al., 2012c; Pasque et al., 2012).

Finally, VRK1 can be regulated by kinase inhibitors and metals (Barcia-Sanjurjo et al., 2013; Vazquez-Cedeira et al., 2011). The sensibility of VRK proteins to other kinase inhibitors is relatively low, but the fact that VRK1 and VRK2 show different response to different kinase inhibitors implies that the development of specific inhibitors for each member of the VRK family is possible (Vazquez-Cedeira et al., 2011). In fact, luteolin was described as a specific inhibitor of VRK1, inhibiting VRK1 ability to phosphorylate both BAF and histone H3, due to a direct interaction with the kinase domain of VRK1. Furthermore, luteolin regulates the progression of cell cycle by VRK1 modulation, leading to the suppression of cell proliferation and induction of apoptosis (Kim et al., 2014).

3.4 The VRK2 kinase

VRK2 gene is located in the chromosomal region 2p16 and it produces two isoforms due to alternative mRNA splicing (Blanco et al., 2006). The isoform VRK2A contains 508 amino acids and is anchored to the membranes of endoplasmic reticulum, mitochondria and nuclear envelope by the carboxyl-terminal hydrophobic transmembrane domain. VRK2B consists of 397 amino acids and is observed freely in the nucleoplasm and cytoplasm, since the transmembrane domain, characteristic of the first isoform, is absent (Blanco et al., 2006; Nichols and Traktman, 2004). VRK2 expression is ubiquitous in the tissues, having the skeletal muscle, heart, pancreas and testis higher levels of protein expression (Nezu et al., 1997). On the other hand, VRK2A expression is observed in all the studied cell lines, whereas VRK2B expression was only observed in a few number of cell lines (Blanco et al., 2006; Fernandez et al., 2010). In breast cancer, it was observed that VRK2 expression correlated positively with estrogen and progesterone receptors and negatively with ErbB2. ErbB2 is overexpressed in 25%-30% breast cancer and it is a poor prognosis marker. Tumours positive to ErbB2 tend to lose part or completely VRK2 expression, which can indicate that VRK2 is a marker of good prognosis for breast cancer (Fernandez et al., 2010).

Regarding the substrates of VRK2, both isoforms share several of them due to the high homology on the catalytic domain. VRK2 isoforms have high autophosphorylation capacity and phosphorylate several substrates like casein, H2B and H3 histones, and myelin (Blanco et al., 2006; Nichols and Traktman,

2004; Sanz-Garcia et al., 2008). Moreover, it also phosphorylates VRK1 substrates like Thr18 on p53 or Ser2, Ser3 and Thr4 on BAF. However, it is important to notice that these phosphorylations by VRK2A are not associated with *in vivo* studies, since the nature of the carboxyl-terminal domain responsible for VRK2A cytoplasmic subcellular localization and regulation prevents the access of this kinase to the substrates. In fact, it was observed that only VRK2B phosphorylates p53 *in vivo*, leading to the stabilization and accumulation of the transcriptional factor, similar to what is observed with VRK1 phosphorylation (Blanco et al., 2006).

Regarding the function of human VRK2, the kinase has been described to participate in numerous cellular mechanisms. VRK2 modulates gene transcription in response to hypoxia, and cellular stress induced by interleukin 1β, mediated by JNK (Blanco et al., 2007; Blanco et al., 2008). Additionally, VRK2A in response to epidermal growth factor (EGF) acts as a negative modulator of ERK1/2 in the MAPK signal pathway (Fernandez et al., 2010). This function is dependent of VRK2A, MEK1 and KSR1 (kinase suppressor of Ras 1) direct interaction, and independent of VRK2A kinase activity (Fernandez et al., 2012). Moreover, it was observed that VRK2 isoforms phosphorylate the nuclear factor of activated T cells (NFAT) on the Ser32, after phorbol 12-myristate 13-acetate (PMA) stimulation. This phosphorylation activates NFAT and increases the transcription of *COX-2* (cyclooxygenase-2) promoter. Besides, it was also observed that the COX-2 protein and mRNA levels decrease after VRK2A-siRNA treatment without any alteration on the expression levels of NFAT. Also, VRK2 down-regulation reduced tumour cell invasion (Vazquez-Cedeira and Lazo, 2012). Finally, it was reported that VRK2 interacts with the anti-apoptotic protein B cell lymphoma-extra-large (Bcl-xL) and regulates negatively the expression of Bax, modulating the intrinsic pathway for apoptosis. Down-regulation of VRK2A leads to increased mitochondrial Bax protein level, and consecutively increased the release of cytochrome C as well as caspases activation, detected by Poly-ADP-ribose polymerase (PARP) processing. Low levels of VRK2A increase cell sensitivity to apoptosis via chemotherapeutic drugs such as camptothecin (Monsalve et al., 2013).

3.5 VRK3: the inactive member of the family

VRK3 is a pseudo-kinase protein without kinase activity, located on chromosome 19q13. This protein contains 474 amino acids and it is predominantly nuclear due to the NLS in the amino-terminal region (Nichols and Traktman, 2004; Vega et al., 2003). Since VRK3 lacks kinase activity and conserves the catalytic domain folding it was hypothesised that the protein kinase might have been retained as a scaffold or a regulatory binding partner (Scheeff et al., 2009). In fact, VRK3 forms a complex with Von Hippel-Lindau tumour suppressor (VHL) and ERK1/2, stimulating the phosphatase activity of VHL and leading to a decrease on ERK1/2 phosphorylated levels. Here, VRK3 negatively regulates the EKR1/2 signalling pathway. Moreover, it seems that PMA stimulation activates ERK1/2, increasing the levels of VRK3, creating a negative feedback in which ERK1/2 positively regulates the expression of VRK3 negative regulator. Finally, VRK3 does not correlates with proliferation since its expression is equal in high- or low-proliferative tissues (Kang and Kim, 2006, 2008).

4. The Aurora kinase family

The human Aurora kinases are a highly conserved protein kinase family that contain three catalytically active kinases: the Aurora kinase A (AurKA), the Aurora kinase B (AurKB) and the Aurora kinase C (AurKC) (Kamaraj et al., 2013). Unlike the other kinase families, this family has a eukaryotic protein kinase domain that doesn’t fit in any major group of protein kinases. As a result, Aurora family branches near to the AGC group of kinases, which was named after the protein kinase A (PKA), G (PKG) and C (PKC) families, but was not included in the family (Goldberg et al., 2006; Manning et al., 2002b).

The first member of Aurora family (AurKA) was initially described in 1995 by Glover and colleagues in *Drosophila* (Glover et al., 1995). They discovered that mutations in AurKA resulted in irregular centrosome separation and in the consequent formation of ‘’monopolar spindles’’. Because of that and reminiscent of the North Pole, it was given the name ‘’Aurora’’ to the discovered kinase, (Fu et al., 2007; Glover et al., 1995). Nowadays, it is well known that Auroras have homologues genes in numerous species, from *Saccharomyces cerevisiae* that has a single Aurora kinase named Ipl1, to *Caenorhabditis elegans*, *Drosophila*

melanogaster and *Xenopus laevis*, which has two types of Aurora kinases: AurKA and AurKB (Brittle et al., 2007; Crosio et al., 2002; Eyers et al., 2005). Mammals, besides AurKA and AurKB, encode a third member, ‘’unexpectedly’’ named, AurKC (Bolanos-Garcia, 2005; Kollareddy et al., 2008). Moreover, phylogenetic trees suggest that the Auroras kinase functions, in metazoans, have diverged during evolution from a single urochordate ancestor. AurKA is an orthologous gene line in cold-blooded vertebrates and mammals, while structurally similar AurKB and AurKC evolved later in evolution, in mammals due to a duplication of a cold-blooded vertebrate ancestral Aurora B/C gene (Brown et al., 2004).

The activity of Aurora kinases is mostly functional during mitosis, and therefore, these are vital mitotic kinases, essential for the regulation of cell cycle. In fact, several mitotic abnormalities and different types of cancer are associated with deregulation of Aurora kinases-dependent mechanisms such as, chromatin condensation, centromere function, spindle assembly, chromosome alignment, chromosome segregation and, cytokinesis (Bolanos-Garcia, 2005; Chu et al., 2011; Fu et al., 2007; Kamaraj et al., 2013; Wang et al., 2010). Aurora kinases are overexpressed in several types of tumors, such as breast or lung cancer, indicating that these kinases might be important in the tumorogenesis process (Kollareddy et al., 2008; Takeshita et al., 2013; Zhang et al., 2015). Indeed, it is important to notice that the maximal expression of Aurora kinases occurs in G2/M phases and that high activity of these kinases due to overexpression in cultured cells leads to a cancer-like phenotype associated with mitotic abnormities that generate genomic instability (Smith et al., 2005).

4.1 The structure of Aurora kinases

The Aurora family members are kinases that have an amino acid sequence length ranging between 309 and 403 and show a relatively small sequence convergence among species. For instance, AurKB shows an overall sequence identity of 84% between human and rodents. Auroras present a quite similar domain organization, having an amino-terminal domain of 39 to 129 residues in length, a central protein kinase domain, and a 15 to 20 residues carboxy-terminal domain. The catalytic kinase domain of the three members of Aurora family is highly conserved (around 71% between AurKA and AurKB), whereas the N-terminal of the Auroras shares low sequence conservation. This fact justifies the

selectivity of each Aurora kinase during protein-protein interactions (Carmena and Earnshaw, 2003; Kollareddy et al., 2008).

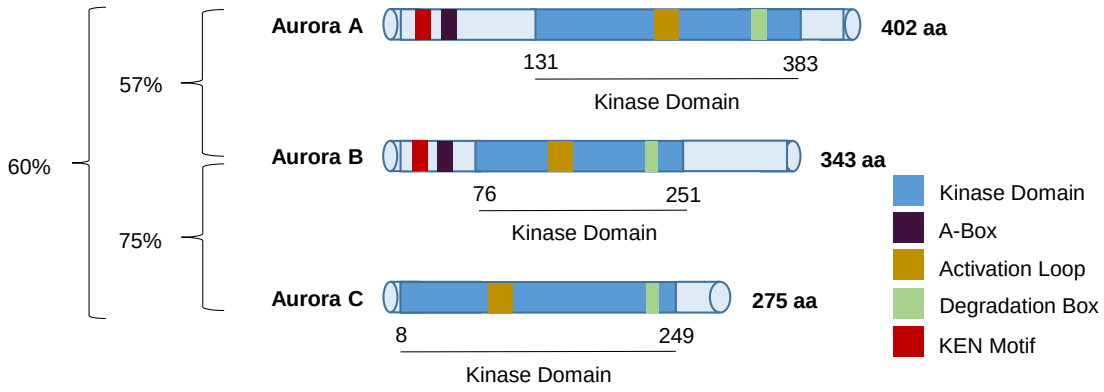

Figure 7 – Aurora protein kinases structure. The percentages are relative to the level of homology between the several Aurora family members.

Analysing the alignment of both AurKA and AurKB is possible to identify a conserved ‘’KEN’’ motif, covering from 11 to 18 residues, especially important to recognize Cdh1-dependent anaphase-promoting complex (APC) signals. Moreover, in the N-terminal region of AurKA and AurKB, lies an A-Box-activating motif or A-Box that confers functionality to a second motif, the Degradation box or D-Box that exists in the C-terminal region of kinases and is the target of Fizzy-related proteins, in the case of AurKA. These motifs are important to regulate the levels of AurKA on G1 phase entrance, leading to its degradation via APC/ cyclosome (APC/C)-UPP dependent on hCdh1 (Castro et al., 2002). In the case of AurKB, the kinase is equally degraded through APC/C-UPP dependent on hCdh1, and it possesses the same D-Box as AurKA. However, this degradation occurs through a different ubiquitin ligase, undergoing degradation by binding to the α-subunit C8 (HC8) of the human proteasome (Bolanos-Garcia, 2005; Stewart and Fang, 2005). Concerning AurKC degradation, mechanisms are still unclear. The three human Auroras present higher homology, when compared to homology among the VRK family members (Figure 7). Indeed, AurKB shows a 57% homology with AurKA and a higher score of 75% with the third member of the family the AurKC. AurKA shows 60% homology with AurKC (Brown et al., 2004; Carmena and Earnshaw, 2003; Cheetham et al., 2002).

4.2 Aurora kinases subcellular localization

Despite the high number of similarities in terms of sequences and structures, Aurora kinases are completely different regarding their subcellular localization. Therefore, AurKA is located in the pericentriolar structures, from the end of S phase until the beginning of the next G1 phase. During mitosis, AurKA spreads to the pole, more precisely to the proximal ends of spindle microtubules. In anaphase, most of AurKA is located on the polar microtubules, and in a fewer scale at the spindle midzone. In turn, AurKB is located alongside with INCENP at pericentromeric regions, during the late S phase until the late G2 phase, when AurKB becomes more diffusely located on the chromatin (Hayashi-Takanaka et al., 2009). In early prophase, AurKB and the other CPC proteins are partially located on the chromosomal arms, moving to the inner centromeres on the transition from prometaphase to metaphase (Nishiyama et al., 2013; van der Horst and Lens, 2014). This association seems to be dynamic, since centromeric AurKB continuously exchanges with a cytoplasmic pool. In the beginning of anaphase, AurKB gradually relocates to the midzone and to the cell cortex at the site of cleavage furrow ingression, persisting in this zone until the end of cytokinesis. The association with the central spindle microtubules during anaphase reduces considerably the mobility of AurKB. In cytokinesis, both AurKA and AurKB are concentrated in the midbody (Figure 8) (Carmena and Earnshaw, 2003; Carmena et al., 2014; Fu et al., 2007; Gohard et al., 2014; Vader and Lens, 2008; Wang et al., 2010; Wang et al., 2011).

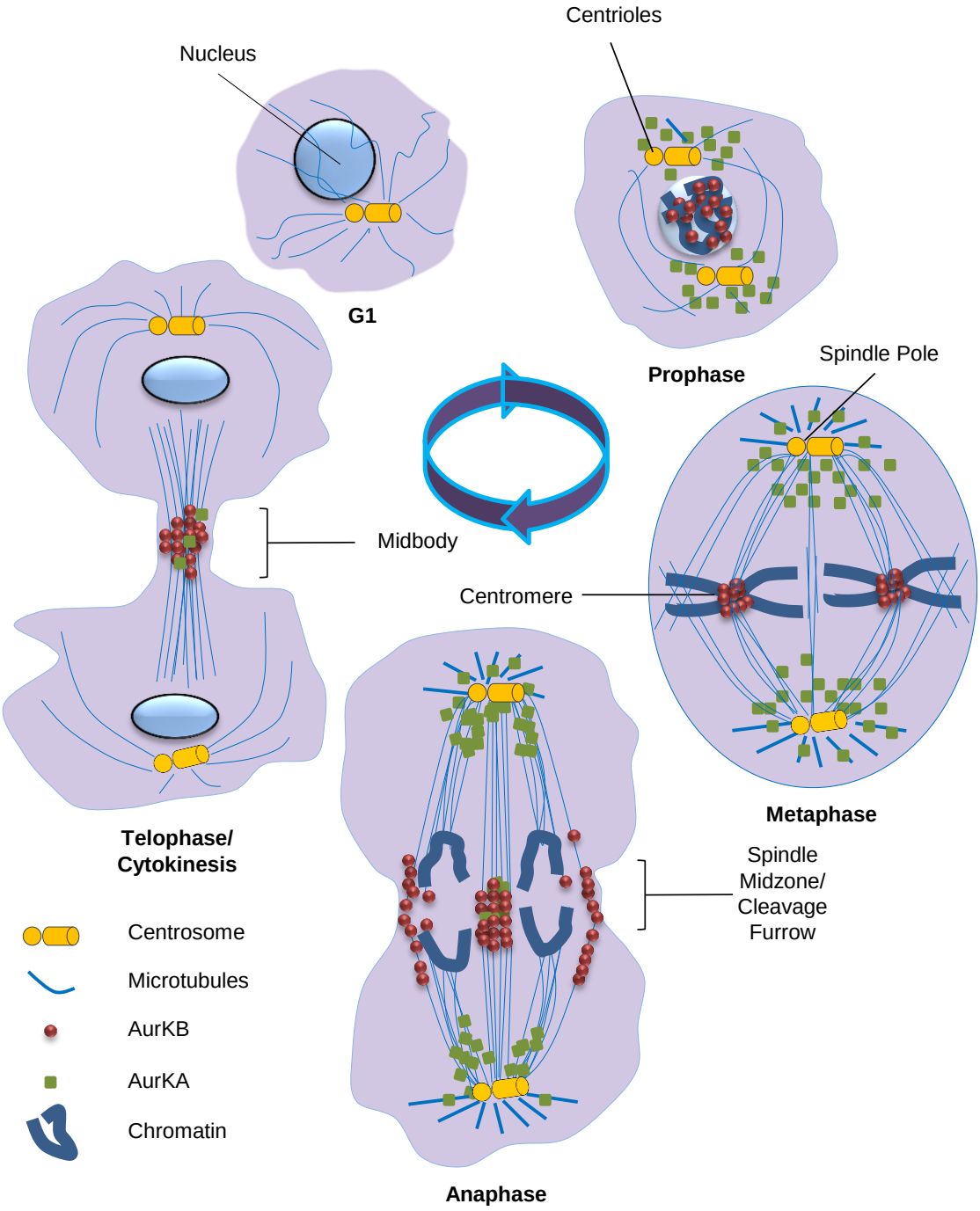

Figure 8 – Subcellular localization of AurKA and AurKB during cell cycle (Adapted from (Carmena and Earnshaw, 2003)).

The changes on AurKB localization occur alongside with at least three other proteins: INCENP, Survivin and Borealin. All four proteins are named ‘’chromosomal passengers’’, as they move precisely from different locations at specific times, and form the tightly regulated chromosomal passenger complex

(CPC) during mitosis (Figure 9) (Fu et al., 2007). In terms of localization, AurKC behaves similarly to AurKB.

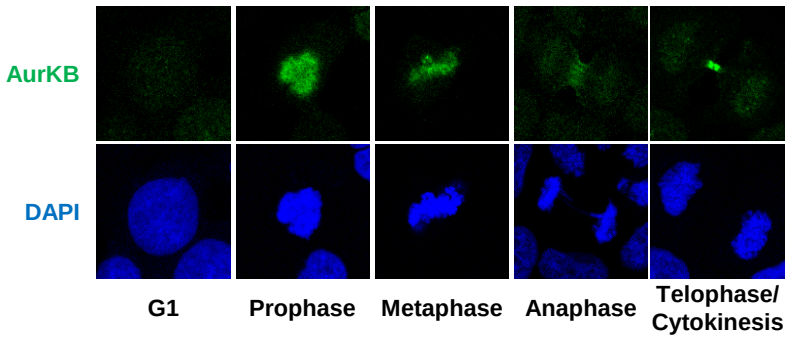

Figure 9 – Microscopy analysis of AurKB subcellular localization during cell cycle in HeLa cells. AurKB (green staining) and DNA (blue staining) (unpublished results).

4.3 The human AurKB

AurKB was first identified in 1998 by polymerase chain reaction (PCR) in a search for kinases overexpressed in colorectal tumours (Bischoff et al., 1998). AurKB is part of the CPC and is involved in the regulation of many mitotic processes. Therefore, AurKB expression peaks at the G2-M transition and its kinase activity is higher during mitosis. Chronologically, AurKB activity is important for chromosome condensation, sister chromatid cohesion, mitotic spindle assembly, correct chromosome bi-orientation, SAC, chromosome segregation and cytokinesis (Carmena and Earnshaw, 2003).

4.3.1 The role of AurKB on chromatin condensation

The condensation of chromosomes compacts the chromatin in order to avoid errors during sister chromatid segregation and is driven by the activity of the Condensin I and II complexes (Vagnarelli, 2012). In turn, AurKB plays an important role in this process by promoting the chromosomal association of the Condensin I complex during prometaphase and, maintaining this association in the late phases of mitosis. Furthermore, this regulation is probably due to direct phosphorylation of the three non-SMC (structural maintenance of chromosomes) subunits and, is specific of the Condensin I complex, since AurKB does not regulates the association of the Condensin II complex (Lipp et al., 2007).

Another important mechanism for chromosome condensation is the phosphorylation of the Ser10 residue, in the amino-terminal region of histone H3

by AurKB, at early G2 phase (Crosio et al., 2002). In *Tetrahymena* it has been shown that the mutation of this residue on histone H3, results in abnormal chromosome segregation and extensive chromosome loss during mitosis (Vader and Lens, 2008; Wei et al., 1998). Nevertheless, the similar mutation in budding yeast *Saccharomyces cerevisiae* didn't originate the same mitotic defects, perhaps due to differences in the chromosomal structure between the two species (Hsu et al., 2000; Vader and Lens, 2008).

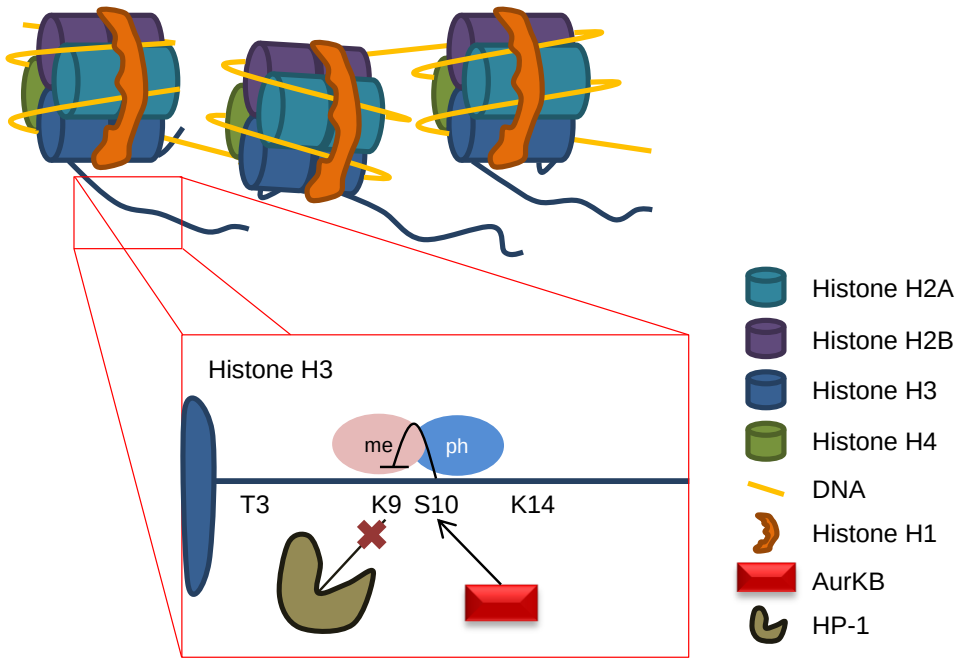

Figure 10 – Histone cross-talk between the phosphorylation of H3S10 and the methylation of H3Lys9. The phosphorylation of Histone H3 by AurKB, affects negatively the binding of the HP-1 to the chromatin.

In human cells, phosphorylation of H3S10, by AurKB, causes the displacement of the Heterochromatin Protein 1 (HP-1) family of proteins from the heterochromatin during mitosis. HP-1 recognizes and binds to the H3Lys9 when this residue is tri-methylated and it seems that the phosphorylation of the H3S10 is sufficient to eject the HP-1 from the chromatin, even when tri-methylation levels of H3Lys9 remain unaffected. In the same way, the inhibition or depletion of AurKB causes the retention of HP1 on mitotic chromosomes, suggesting that histone H3Ser10 phosphorylation is necessary for the dissociation of HP1 from chromatin in mitosis (Fischle et al., 2005; Hirota et al., 2005). However, it is unknown if the displacement of HP-1 from the chromatin is important for correct

chromosome condensation at the beginning of mitosis. These results suggest a possible histone modification cross-talk, in which the mitotic phosphorylation of H3Ser10, by AurKB, negatively affects the recognition of tri-methylation of the H3Lys9 by specific readers, as HP-1 (Figure 10) (Baek, 2011; Bannister and Kouzarides, 2011; Hirota et al., 2005; Kouzarides, 2007).

4.3.2 The role of AurKB on the cohesion of the sister chromatids

Chromosome cohesion depends on a ring-like Cohesin complex closely related with the Condensin complexes. The Cohesin proteins are responsible for maintaining the two sister chromatids trapped inside the ring structure until the metaphase to anaphase transition. So, at the metaphase-anaphase transition Cohesin removal is important for the correct progression of the cell cycle. Cohesin is removed through two different pathways, being the first one the ‘’prophase pathway’’ that depends on the activity of the mitotic kinases polo-like kinase 1 (Plk-1) and AurKB. Regarding the role of AurKB in this pathway, this kinase is an important player in the regulation of the Shugoshin-1 (Sgo-1) localization on the centromeres in mitosis. Thereby, Sgo-1 protects the centromeric Cohesin recruiting the PP2A (protein phosphatase 2A) complex to the centromeres. Downregulation of AurKB affects the centromeric localization of Sgo-1, leading to a more diffused localization along the chromosome arms. This alteration on Sgo-1 localization blocks the removal of the Cohesin-complexes placed on the chromosome. Cohesin of sister chromatids is removed in a separase-dependent manner, but no role has yet been assigned to AurKB in this mechanism (Dai et al., 2006; Gimenez-Abian et al., 2004; Watanabe, 2010).

4.3.3 The role of AurKB on the mitotic spindle assembly and chromosomal bi-orientation

The mitotic spindle assembly relies also on the activity of AurKB, has the inhibition or depletion of AurKB in *Xenopus* extracts disturbs the mitotic spindle formation (Kelly et al., 2007). Moreover, it seems that AurKB operates in parallel to the Ran-dependent pathway, phosphorylating two different substrates, important in the mitotic spindle assembly: i) the mitotic centromere-associated kinesin (MCAK) that is phosphorylated in several residues by AurKB and ii) the microtubule-destabilizing protein Stahtmin/ OP18, which is inhibited by AurKB

phosphorylation neighbouring the chromosomes (Kelly et al., 2007; Zhang et al., 2007). Concerning MCAK, the interplay between multiple phosphorylation sites of this protein, is critical for the temporal and spatial control of MCAK function. In fact, AurKB seems to phosphorylate MCAK in three different residues (Thr95, Ser110, Ser196), which creates a two-site phosphoregulatory mechanisms targeting MCAK to chromosome arms or to centromeres. MCAK binding to the chromatin precedes the centromeric location of the protein, and creates a pool of MCAK ready to load onto the centromeres. Phosphorylation of Thr95 associates MCAK with the chromosome arms, whereas the phosphorylation of Ser196 promotes de disassociation of the chromosome arms. The phosphorylation of Ser196 inhibits also the microtubule depolymerizing activity of MCAK. In turn, MCAK centromere targeting is accomplished by a balance between phosphorylation at Ser110 and dephosphorylation at Thr95. Centromeric MCAK is important for mal-attachment corrections of kinetochores to microtubules, critical for proper chromosome alignment and segregation. Because of that, centromeric MCAK at mal-attached kinetochores is hyper-phosphorylated on Ser110, but hypo-phosphorylated on Ser196 (Andrews et al., 2004; Zhang et al., 2007).

The kinetochores are structures assembled on the centromere, where the spindle apparatus attaches to a chromatid, during cell division (Vader and Lens, 2008). These structures are fundamental in order for the paired of chromatids to achieve bi-orientation on the mitotic spindle, since they participate on the microtubule capture, chromosome movement and checkpoint signalling. Bi-orientation is important for chromosomal segregation, where each of the two sister chromatids is attached to a different pole of the bipolar spindle. The tension caused by the pulling forces generated by the mitotic spindle on the two sister chromatids are counterbalanced by cohesion forces. When each kinetochore is attached to an opposite pole of the bipolar spindle it is called amphitelic attachment. Uncorrected attachments can occur when microtubules from the same pole bind both kinetochores (syntelic attachment), or when kinetochores attach microtubules from both poles (merotelic attachment). In both cases, AurKB activity destabilises the formed attachment, releasing the kinetochore for a new cycle of microtubule attachment, until it culminates in the production of

chromosome bi-orientation and faithful segregation of sister chromatids (Kalantzaki et al., 2015; Maiato et al., 2004; Meppelink et al., 2015).

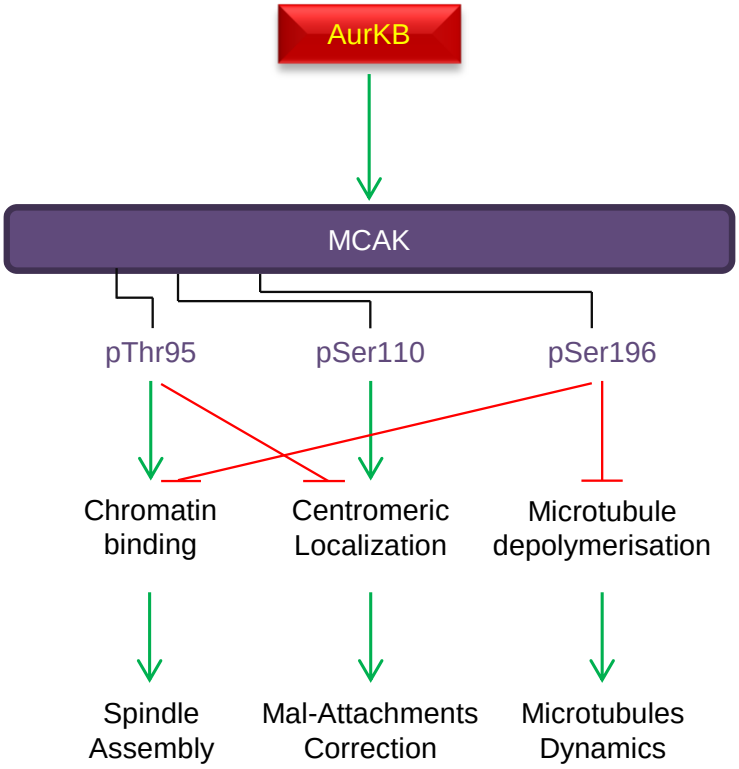

Figure 11 – Mitotic spindle assembly through AurKB-dependent regulation of MCAK localization and function.

In syntelic attachments, AurKB phosphorylates and regulates MCAK and two other important kinetochore microtubule-capture factors: Ncd80/Hec1 and Dam1 complex (Figure 11). AurKB-dependent phosphorylation of NCD80/ Hec-1 decreases the affinity of the complex to microtubules *in vitro* and mutations of the AurKB phosphorylation sites in NCD80/Hec-1 stabilise the interaction between microtubules and the kinetochore (DeLuca et al., 2011; Kalantzaki et al., 2015). Moreover, AurKB (Ipl1) phosphorylates some subunits of the Dam-1 complex in budding yeast, but none Dam-1 complex was found in mammals (Cheeseman et al., 2002). Contrariwise, AurKB corrects merotelic chromosomal attachments mostly through the regulation of MCAK complex during prometaphase. The regulation of MCAK by AurKB occurs, as previously described, at different levels (Figure 8) or indirectly, via inner centromere kin-I stimulator (ICIS), which interacts with AurKB and stimulates MCAK activity, or via Shugoshin-2 (Sgo2) AurKB-dependent phosphorylation that targets MCAK to centromeres (Ohi et al.,

2003; Tanno et al., 2010). Disruption of AurKB or MCAK increases chromosomal misalignment and missegregation due to improper kinetochore–microtubule attachments (Zhang et al., 2007).

4.3.4 The role of AurKB on the spindle assembly checkpoint

The SAC or mitotic checkpoint vigils the transition from metaphase to anaphase, preventing cell cycle progression in the presence of unattached or non bi-oriented chromosomes (Musacchio, 2011). As long as the amphitelic attachment state is not reached by all the chromosomes, SAC is active and avoids cell cycle progression to anaphase, through the regulation of APC/C activity. SAC includes core proteins such as: monopolar spindle 1 (Mps1), Mad1, Mad2, Mad3/ BubR1, budding uninhibited by benzimidazoles 1 (Bub1) and Bub3 (Lens and Medema, 2003). The activation of APC/C promotes anaphase and consequently mitotic exit, by targeting for degradation, via the 26S proteasome, essential mitotic regulators like Securin and Cyclin B, among other proteins (Musacchio, 2011; Sudakin et al., 1995). As previously mentioned, the APC/C functions in combination with two different specificity factors Cdc20 or Cdh1. Activation of APC/C^{Cdc20} is avoided by SAC through the formation of an inhibitory complex of Mad2, Mad3/ BubR1, Bub3 and Cdc20 proteins (Sudakin et al., 2001). All core proteins localise at kinetochores, being some of them (i.e. Mad1 and Mad2) completely displaced from microtubule-attached kinetochores, while others are retained (i.e. BubR1) in response to the amount of tension between sister kinetochores. Absence of tension, like unattached kinetochores, triggers SAC activation and AurKB seems to be required for SAC-dependent mitotic arrest induced by lack of tension (Lens and Medema, 2003; Maresca and Salmon, 2010; Shannon et al., 2002). This activation may be induced directly through the complete absence of attachments, or, indirectly due to the creation of unattached kinetochores (Pinsky and Biggins, 2005). AurKB activity is important to destabilise unreliable attachments between the spindle apparatus and the kinetochore. So, lack of tension activates AurKB, leading to the detachment of kinetochore-microtubule interaction lacking tension. This process recruits checkpoint proteins to the kinetochores and consequently leads to the inhibition of APC/C^{Cdc20} (Maresca and Salmon, 2010). Even though, the role of AurKB in the indirect pathway is clear, the potential role of AurKB in the direct pathway is

not quite yet understood (Vader et al., 2007). In fact, only few data in *Xenopus* and *Schizosaccharomyces pombe* show that AurKB activity is necessary for SAC response to unattached kinetochores (Kallio et al., 2002; Petersen and Hagan, 2003), but is still unclear whether there is a direct tension pathway triggering SAC in human cells, since tension and attachment are tightly linked (Vader and Lens, 2008). SAC failure can lead to premature anaphase entering with unattached or aberrantly attached kinetochores, resulting in improper chromosomal segregation, loss/gain of chromosomes and increased predisposition to cancer.

4.3.5 The role of AurKB on anaphase and cytokinesis

AurKB activity is necessary for the correct progression of cell cycle through anaphase and cytokinesis. After SAC inactivation, anaphase begins when Cyclin B1 and Securin are degraded by APC/C^{Cdc20}, which causes the reduction of Cdk1 activity and the segregation of sister chromatids (Lu et al., 2014; Meadows and Millar, 2015). From anaphase and beyond, AurKB is restricted to the central spindle/ midbody or it is transported by the microtubules to the cell cortex. On the central spindle, AurKB promotes the rapid switch in microtubules dynamic (anaphase) and the well-organized disassembly of the mitotic spindle (telophase) (Terada, 2001; Vader et al., 2007). Regarding cytokinesis, in which the cytoplasm is divided between the two newly-formed cells, each one containing a single nucleus, AurKB activity is also required. The equatorially division of the cytoplasm after chromosomal segregation, depends on the formation of a cleavage furrow, generated by the contraction of an actinomyosin ring (Werner and Glotzer, 2008). GTPase RhoA is important for the contractibility of the actinomyosin ring, since its activation (GTP-bound), regulates various cytokinesis effectors. The activity of RhoA during the last phase of cell division is controlled partially by a complex located on the central spindle, the centralspindlin, which in turn is regulated by AurKB. AurKB phosphorylates the centralspindlin-associated mitotic kinesin-like protein 1 (Mklp-1), controlling the normal function and localization of the complex and consequently the end of cytokinesis. AurKB inhibition, in late anaphase, leads to abnormal cytokinesis without disruption of the central spindle (Guse et al., 2005). Moreover, AurKB phosphorylates Desmin, glial fibrillary acidic protein (GFAP), Myosin II regulatory light chain and Vimentin, controlling the filament

assembly ability of these proteins and thus cytokinesis (Goto et al., 2003; Kawajiri et al., 2003; Kondo et al., 2013).

4.3.6 The regulation of AurKB

AurKB is regulated by activation, localization and degradation. Still, several AurKB-regulatory mechanisms are feedback loops in which AurKB plays an important role. Full AurKB activation and function depends on the autophosphorylation within the kinase activation segment, on Thr232, and binding to INCENP. AurKB binds to the IN-box motif within the carboxy-terminus region of the scaffold protein INCENP, and this interaction partially activates the kinase due to AurKB-activation loop changes. Yet, fully active AurKB is obtained only through the AurKB-dependent phosphorylation of an INCENP-transcription start site (TSS) motif, which possibly induces another conformational change within AurKB catalytic region (Sessa et al., 2005).

The CPC complex, besides AurKB and INCENP, includes the non-enzymatic subunits Borealin and Survivin, These two proteins are essential for proper AurKB localization during mitosis and they bind to INCENP amino-terminal (van der Horst and Lens, 2014). Indeed, mitotic-centromeric localization and function of CPC, and therefore of AurKB, depends on several phosphorylation feedback loops that generate docking points for Survivin and Borealin (van der Horst and Lens, 2014). So, the predominant theory is that Survivin and Borealin activates AurKB and guide the kinase to its different locations to facilitate the AurKB-mitotic substrates phosphorylation, and thus the AurKB-dependent functions (Carmena et al., 2012b).

AurKB localization and function on the inner centromere depends on the interaction between Survivin and Borealin with INCENP during (pro)metaphase (Klein et al., 2006; van der Horst and Lens, 2014; van der Waal et al., 2012; Wang et al., 2010). Survivin interacts with H3T3 phosphorylated, by Haspin and maybe by VRK1, and Borealin binds via Sgo1 and Sgo2 to H2AT120 phosphorylated, by Bub1 (Kang et al., 2007b; Valbuena et al., 2011b; van der Waal et al., 2012; Wang et al., 2010; Wang et al., 2011). Altogether, VRK1, Haspin and Bub1 control AurKB localization and activity though direct histone phosphorylation. These phosphorylation mechanisms are in turn regulated by AurKB, generating different feedback loops.

The phosphorylation of H3T3, by Haspin and possibly by VRK1, occurs in early mitosis and targets AurKB to locate in inner centromeres (Figure 12) (Kang et al., 2007b; Valbuena et al., 2011b; Wang et al., 2010). Nonetheless, the ability of Haspin to phosphorylate H3T3 is regulated by AurKB due to direct phosphorylation on various Ser and Thr residues (Wang et al., 2011). In fact, site directed mutation of these residues or AurKB inhibition strongly decreases H3T3ph, suggesting that AurKB regulates its own centromeric accumulation though Haspin regulation (Wang et al., 2011).

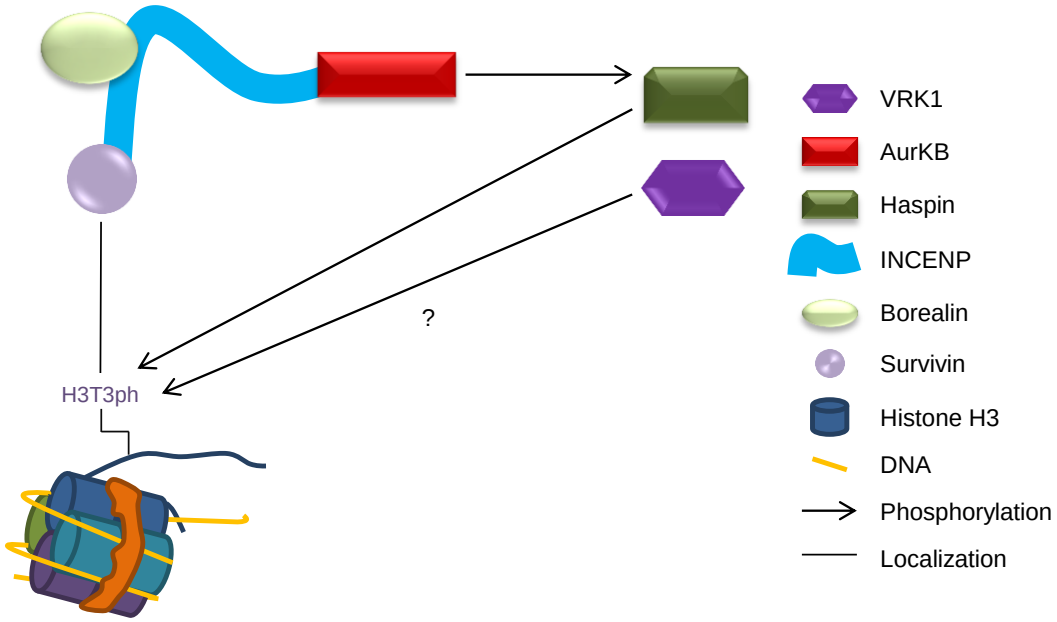

Figure 12 – Feedback loop targeting AurKB to inner centromere. The regulation loop involves the kinases AurKB, Haspin and potentially VRK1.

Moreover, AurKB regulates H3T3ph through Repo-Man Ser893 phosphorylation. PP1 (Protein Phosphatase 1) γ-Repo-Man phosphatase complex dephosphorylates H3T3ph and this activity is important to sustain H3T3ph restricted to the centromeres in (pro) metaphase (Qian et al., 2011). Therefore, AurKB activity regulates Repo-Man, by phosphorylation, avoiding its chromosomal targeting and allowing H3T3ph in the first place (Qian et al., 2011). To notice, that Repo-Man also interacts with PP2A, and this phosphatase dephosphorylates Repo-Man Ser893 phosphorylation (Qian et al., 2013). Instead, there is scant information about a possible feedback loop regulating AurKB/ CPC localization and activity involving VRK1 and AurKB. Yet, the fact that VRK1 phosphorylates directly H3T3 evokes a potential role for this kinase on the

centromeric accumulation of AurKB/ CPC (Figure 9) (Kang et al., 2007b; Valbuena et al., 2011b).

On the other hand, Bub1 kinase phosphorylates histone H2AT120, through an unknown regulatory mechanism. Yet, some data point to a possible feedback loop between Bub1 and AurKB via ATM. ATM phosphorylates Bub1 and supports Bub1-dependent H2AT120 phosphorylation during mitosis. This phosphorylation recruits Sgo1, which interacts with Borealin and consequently targets AurKB/ CPC to accumulate on the centromeres. Moreover, ATM is phosphorylated in mitosis by AurKB on the Ser1403 residue and this phosphorylation is important to activate ATM. Mitotic activity of ATM is independent of ATM-DNA damage activity. Altogether, these results suggest a potential loop involving the three kinases (Bihani and Hinds, 2011; van der Waal et al., 2012; Yang et al., 2011). Additionally, kinetochore localization of Bub1 is also essential for the H2AT120ph and relies on Mps1 activity not only in yeast but also in human cells. Mps1 is regulated by AurKB direct phosphorylation (van der Horst and Lens, 2014; Yamagishi et al., 2010). Thus, Mps1 is phosphorylated by AurKB and phosphorylates the kinetochore-null protein 1 (Knl1), enhancing the binding between Bub1 and Knl1. Then, Bub1 on the kinetochores phosphorylates H2AT120 and leads to CPC accumulation on the inner centromeres via Sgo1-Borealin interaction (van der Waal et al., 2012). Besides, also Plk1 seems to regulate AurKB localization and activity. Plk1 phosphorylates the Ser20 in Survivin and this phosphorylation seems to be relevant for proper activation of AurKB. Plk1 inhibition prevents AurKB activation and correct kinetochore-microtubule attachment (Chu et al., 2011). Instead, AurKB phosphorylates the Thr210 in Plk1 at centromere in early mitosis, activating the late kinase, and generating another feedback loop that enhances inner centromere localization and activity of CPC (Carmena et al., 2014; Carmena et al., 2012a).

5. Pluripotency reprogramming factors

The study of embryonic stem cells (ESCs) led to the discovery of induced pluripotent stem cells (iPSCs). ESCs can grow indefinitely, maintaining pluripotency, high proliferation potential, and the capability to differentiate in all three germ layers cell types (Martin, 1981). Therefore, ESCs might be used to

treat numerous disorders such as Alzheimer's and Parkinson's diseases or diabetes (Isobe et al., 2015). However, mostly due to ethical complications regarding the use of human embryos, the induction of pluripotent cells directly form the patient cells, became necessary.

Somatic cells can be reprogrammed, not only transferring their nuclear content into oocytes, but also by fusion with ESCs (Kim et al., 2009; Takahashi and Yamanaka, 2006). This indicates that both unfertilized eggs and ESCs hold factors that can convert a somatic cell into a pluripotent cell. Based on this fact, Takahashi and Yamanaka discovered that the introduction of four defined transcriptional factors, critical in the maintenance of ESC identity, could reprogram somatic cells into iPSCs. These factors are known as OSKM and include: Oct4 (octamer-binding transcription factor 4), Sox2, Klf4 (Kruppel-like factor 4) and c-Myc (Takahashi and Yamanaka, 2006). Previous evidence showed that other set of transcriptional factors (Sox2, Oct4, Nanog and Lin28) convert somatic cells into iPSCs (Yu et al., 2007) and nowadays it is known that the OSKM factors can be replaced by others functionally divergent factors and delivered by different systems (Kim et al., 2009; Soufi, 2014). OSKM factors are expressed in the early phases of development and are especially intriguing since Oct4, Sox2 and Klf4 can bind to DNA, engaging silent chromatin at distal enhancers and triggering gene activation, early in reprogramming (Gao et al., 2013). c-Myc, however, is not able to access closed chromatin (Zaret and Carroll, 2011). Reprogramming is accompanied by dynamic epigenetic modifications, essential for chromatin remodelling. This capacity of reprogramming factors is quite important, allowing the cell to adapt different chromatin states in alternative cell types. Likewise, it is also important to notice that OSKM factor can also interact between them. An example is the Oct4-Sox2 interaction, which seems important in terms of self-renewal, pluripotency and somatic cell reprogramming in mouse ESCs (Ding et al., 2012; van den Berg et al., 2010).

Nonetheless, reprogramming factors, such as c-Myc, Klf4, Nanog, Oct4 and Sox2 have also been associated with cancer development, mostly when these are overexpressed. These factors are vital players on transformation, tumorigenesis, tumour metastasis and tumour proliferation, but the precise underlying mechanisms are yet poorly understood. Moreover, reprogramming factors are also critical for cancer stem cells (CSCs) self-renewal. These cells

sustain tumour growth and resistance to conventional cancer therapy while exhibiting the ability to self-renew as well as give rise to differentiated tissue cells. CSCs may be related to the origin of cancer (Amini et al., 2014; Huang et al., 2014; Iv Santaliz-Ruiz et al., 2014; Li et al., 2012a; Liu et al., 2013a; Tan et al., 2006; Wang et al., 2014a; Yu et al., 2015).

5.1 The transcriptional factor Sox2

The *SOX2* gene was first discovered and characterized in humans in 1994. Sox2 belongs to the Sox (Sry-related HMG box) family of transcriptional factors, which are important in embryonic development and stem cell biology. *Sry* gene is located in the sex-determining region on the chromosome Y and is the mammalian testis-determining factor. This gene contains a peculiar high-mobility group (HMG) domain, essential for DNA recognition and binding. All the proteins containing a HMG domain with an amino acid motif 50% similar to the HMG domain of Sry are included in the Sox family (Gubbay et al., 1990; Sarkar and Hochedlinger, 2013; Sinclair et al., 1990). The Sox2 HMG domain recognizes DNA through the consensus sequence $^{A}/_{T}{}^{A}/_{T}$CAAAG (Bowles et al., 2000; Chambers and Tomlinson, 2009). Nonetheless, even if it is known that Sox2 binds to and activates numerous promoters like *CCND1* or *Baculoviral IAP Repeat Containing 5* (*BIRC5*) (Lin et al., 2012; Wu et al., 2012), it seems to be a relatively weak/ moderate activator of cellular transcription by itself. Accordingly, Sox2 associates with several others transcriptional factors in the activation of specific targets, like in the transcriptional activation of *NANOG* gene, in human ESCs, alongside with Oct4 (Kuroda et al., 2005). In cellular differentiation, Sox2 marks the immature cells of the early neuroepithelium and although the transcriptional factor is lost as cells differentiate, it is retained in adult neural stem cells (Fauquier et al., 2008). Similar observations were obtained in mouse cortex (Hagey and Muhr, 2014).

The *SOX2* gene is located on the chromosome 3q26.3-q27 and encodes a 317 amino acids protein belonging to the SoxB1 group of proteins. Sox2 proteins contain three main domains. The N-terminal (residues 1-40), containing a poly-glycine domain and the HMG domain (resides 41-109), which is fairly conserved between species and serves as potential binding site for protein partners (i.e. Oct4 and H2AFY) or to nuclear import signals (NIS) and NES. This

fact elucidates an important mechanism for Sox2 regulation. Moreover, Sox2 contains a transactivation domain (residues 110-317) that binds to promoters, activating or repressing target genes (Figure 13) (Collignon et al., 1996; Fang et al., 2011a).

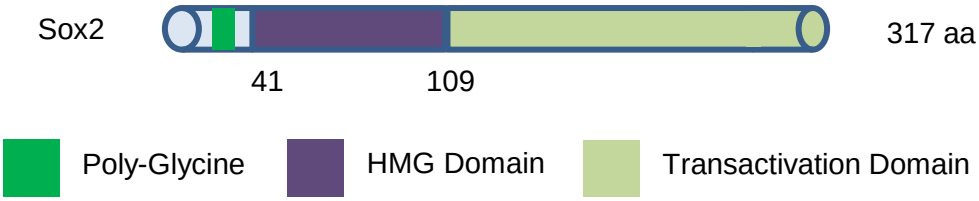

Figure 13 – The structure of Sox2 protein. The HMG domain is quite conserved between *Homo sapiens, Mus musculus and Danio reri.*

Besides its role in stem cell maintenance and cellular reprogramming, Sox2 has been also associated with anophthalmia-esophageal genital (AEG) syndrome that occurs in the presence of heterozygous mutations of *SOX2*. These mutations lead to abnormal development of ectodermal and endodermal tissues (Williamson et al., 2006). Additionally, Sox2 has been also shown to be strongly associated with numerous cancer types, acting in some cases as an oncogene, controlling the oncogenic signalling and promoting and maintaining CSCs (Liu et al., 2013c; Sarkar and Hochedlinger, 2013). CSCs overexpressing stem cell markers such as Sox2 are a critical attribute of tumours, providing resistance to therapy (Piva et al., 2014; Rothenberg et al., 2015).

5.2 Sox2 amplification in cancer

A particular feature observed in several cancer types, such as glioblastoma, lung cancer, and others is the amplification of *SOX2* 3q26.3 gene locus, which leads to an increased number of copies of the *Sox2* gene (Hussenet et al., 2010; Weina and Utikal, 2014). Such genetic aberrations can alter the progression of normal cell cycle, which could culminate in tumour development. Indeed, comparative genomic hybridization arrays showed that Sox2 was amplified in lung squamous cell carcinomas (LSCCs) and regulated genes involved in tumour formation, proliferation, cell migration, and cell growth (Hussenet et al., 2010). In addition, several others genes have been described to be co-amplified with *SOX2.* One example is the co-amplification, on chromosome

3q26, of the oncogene *PRKC1* (protein kinase C iota type) alongside with *SOX2* that determine the stem cell phenotype observed in lung squamous cell carcinoma (Justilien et al., 2014). In some cases, Sox2 amplification could be due to aberrant Sox2 transcription (Sox2 regulation at transcriptional level) generated by chromosome instability (Liu et al., 2013c).

Sox2 has been also reported to be overexpressed in many other cancer types like breast and colorectal cancer or even in ES or osteosarcoma. However, in these cases the overexpression of Sox2 is not related with gene amplification, indicating that the aberrant Sox2 expression is due to unidentified mechanisms (Basu-Roy et al., 2012; Leis et al., 2012; Lengerke et al., 2011; Lundberg et al., 2014; Riggi et al., 2010). The overexpression of Sox2 in various cancer types may indicate that reactivation of this transcriptional factor is an early step in tumour initiation since normal differentiated tissue present residual levels of Sox2.

5.3 Regulation of Sox2

The regulation of Sox2 could occur not only transcriptionally, but also due to translational and post-translational modifications. At the transcriptional level, even if Sox2 is overexpressed, mostly due to gene amplification, only one transcript occurs after Sox2 expression. In turn, in somatic cells, macroH2A regulates the expression of Sox2. MacroH2A isoforms are structural components of the repressed chromatin of pluripotency genes, such as Sox2, acting as an epigenetic barrier to pluripotency induction. Indeed, chromatin immunoprecipitation (ChIP) studies revealed that the macroH2A.1 isoform was greatly enriched in the chromatin of *SOX2* regulatory regions in mouse embryonic fibroblasts but not in adult neural stem cells, where this gene is highly expressed. The removal of macroH2A.1, macroH2A.2 or both increased the efficiency of pluripotency induction up to 25-fold, with reactivation of pluripotent genes (Pasque et al., 2012). Likewise, loss of macroH2A1 in ESCs resulted in the incomplete inactivation of pluripotent genes encoding key regulatory transcription factors such as Sox2, alongside with reduced or delayed activation of differentiation genes (Creppe et al., 2012a). Besides, the incorporation of macroH2A isoforms in the chromatin directly regulates the transcriptional activity of Sox2, due to re-arrangements in the chromatin structure.

Besides, Sox2 expression can be regulated by different signalling pathways, as occur in osteoblasts, where the expression of Sox2 is induced by fibroblast growth factor (FGF), inhibiting the Wnt signalling (Mansukhani et al., 2005). Also, the EWS-FLI1 protein, associated with the majority of ES cases and believed to be the initiation factor, induces the expression of stem cell markers, including Sox2, in mesenchymal stem cells (MSCs). As for VRK1, EWS-FLI1 opens the chromatin and creates *de novo* enhancers, which physically interact and activate the promoter of Sox2. Besides the direct effect on Sox2 promoter activation, EWS-FlI1 represses the promoter of miRNA-145, which is a repressor of Sox2, further enhancing the levels of the transcription factor (Riggi et al., 2014; Riggi et al., 2010; Xu et al., 2009).

Sox2 can also be inhibited by microRNAs, such as microRNA-126 (miR-126) and again by miRNA-145 at translational level (Riggi et al., 2010; Xu et al., 2009; Zhao et al., 2015). This last miRNA presents low levels in self-renewing human ESCs, and increases considerably during differentiation. Besides, pluripotency factors *OCT4*, *SOX2*, and *KLF4* are direct targets of miR-145, which represses the 3' untranslated regions of *OCT4*, *SOX2*, and *KLF4*. Thus, this suggests that this specific miRNA can inhibit the self-renewal process of human ESCs, and direct repress pluripotency genes such as *SOX2* and *OCT4* and, therefore promote lineage-restricted differentiation (Xu et al., 2009). Moreover, Sox2 is also regulated by post-translational modifications, for instance phosphorylation, methylation, SUMOylation, acetylation and ubiquitination. In summary, these post-translational modifications interfere with Sox2 stability and localization and consequently enhance or block it transcriptional activity (Jeong et al., 2010; Mao et al., 2015; Ouyang et al., 2015).

5.4 The contribution of Sox2 to cancer

Sox2 has been implicated, through numerous cellular pathways, in several hallmarks of cancer such as in cell proliferation and self-renewal of CSCs (Basu-Roy et al., 2012; Chen et al., 2008a; Chou et al., 2013; Fang et al., 2014; Fang et al., 2011b; Hutz et al., 2014; Lin et al., 2012), cell invasion, migration and metastasis (Fang et al., 2014; Han et al., 2012; Li et al., 2013; Singh et al., 2012; Xiang et al., 2011; Yang et al., 2014), or even cell survival and chemoresistance (Figure 14) (Chen et al., 2014; Chou et al., 2013; Eini et al., 2014; Jia et al., 2011;

Lin et al., 2012; Rothenberg et al., 2015). Some of the mechanisms underlying the role of Sox2 in such events will be explained in the following paragraphs.

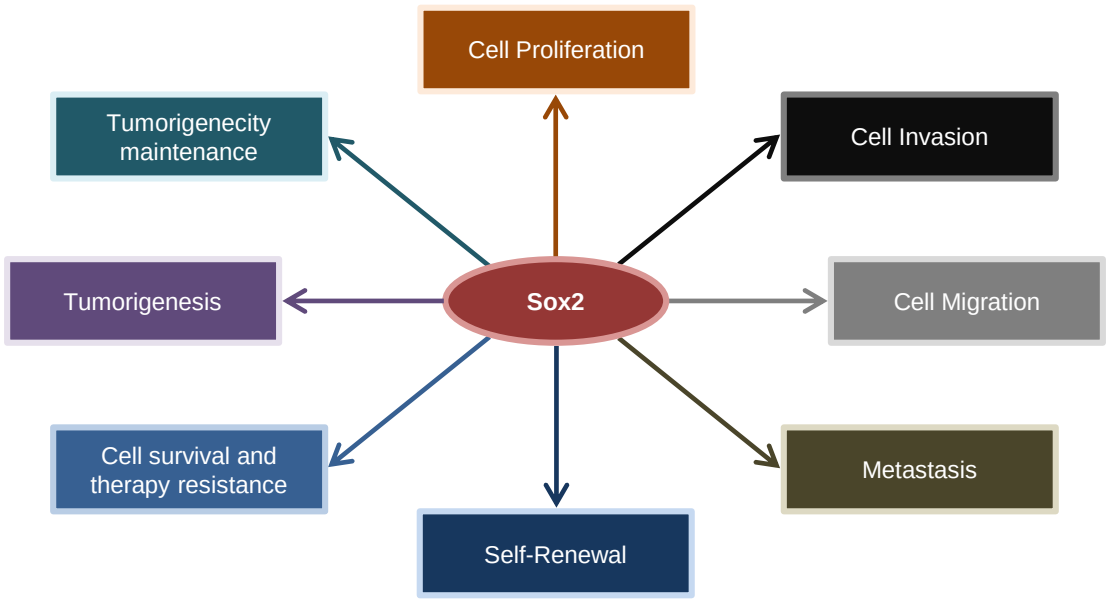

Figure 14 – Implication of Sox2 in cancer. Sox2 overexpression regulates many processes of cancerous cells (adapted from (Liu et al., 2013c)).

Cellular proliferation is strongly regulated by Sox2 in many cancer types and numerous publications ascertain the role of Sox2 in this process. For example, in pancreatic and gastric cancer, Sox2 knockdown caused cell growth inhibition, inducing cell cycle arrest, due to the transcriptional activation of p21 and p27, whereas Sox2 overexpression induced S-phase entry and cell proliferation through *CCND3* gene transcriptional activation (Herreros-Villanueva et al., 2013; Hutz et al., 2014). In fact, negative regulators of CDKs, such as the Kip/ Cip proteins that inhibit most cyclin-CDK complexes, seem to have a tight relationship with Sox2 and Sox2-dependent regulatory mechanisms. For instance, p27 levels seem to be relevant for *SOX2* gene repression in mice models. Cells and tissues from *p27* null mice, showed elevated levels of Sox2 and failed to repress Sox2 under differentiation stimuli. The negative regulator p27 binds, along with a complex of p130-E2F4-SIN3A, to the *SRR2* enhancer of the *SOX2* gene under differentiation and represses gene transcription (Li et al., 2012b). Similarly, treatment of the embryonal carcinoma cell line NTERA-2/ clone D1 (NT2/D1) with all-trans retinoic acid (RA) induces cell growth arrest and neural differentiation dependent of p27 expression. RA treatment reduces p27

degradation by the ubiquitin/ proteasome-dependent pathway, resulting in increased association of this protein with cyclin E/ Cdk2 complexes and suppression of their activity (Baldassarre et al., 2000). NT2-RA-dependent increase in p27 expression occurs inversely to Sox2, Oct4, Nanog, cyclin D1, Vimentin and Nestin downregulation and in parallel with upregulated levels of Pax6, Tau, βIII-Tubulin and Synapsin (Figure 15) (Kakhki et al., 2013; Megiorni et al., 2005; Pleasure and Lee, 1993; Podrygajlo et al., 2009; Spinella et al., 1999). Besides, it was also reported that NT2-RA-treatment activates p53, independently of the protein levels, contributing to NT2 RA-mediated G1 arrest (Curtin et al., 2001).

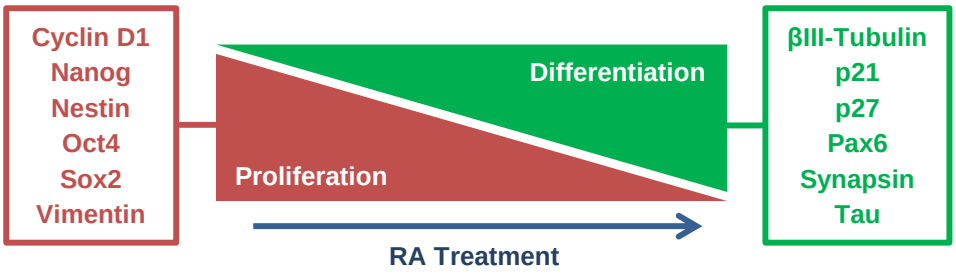

Figure 15 – NT2 cell line downregulated and upregulated proteins, upon retinoic acid (RA) differentiation. RA enhances cell cycle arrest and expression of protein associated with cell differentiation, over proliferation-related proteins.

Moreover, in LSCC, Sox2 downregulation induced the expression of the downstream target bone morphogenetic protein 4 (BMP4), causing cell proliferation inhibition. BMP4 is repressed by Sox2, as proved by ChIP analysis and luciferase assay, and reactivation of BMP4 signaling, upon Sox2 silencing, could partially induce cell cycle arrest as observed in cell-based experiments (Fang et al., 2014). Knockdown of Sox2 had been reported to reduce cell proliferation in many other cancer types such as glioblastoma (Fang et al., 2011b) and breast cancer (Stolzenburg et al., 2012).

Furthermore, Sox2 also contributes to maintain a less cellular differentiated state and the stemness characteristics of CSCs. For instance, Sox2 is required to maintain self-renewal proprieties of CSCs in osteosarcoma and antagonizes the pro-differentiation Wnt pathway. Sox2 depletion results in increased expression of cell cycle inhibitor p16 and p27 and in the activation of the Wnt pathway, which is critical for proper bone formation and, osteoblast

lineage commitment and maturation. Consistently, Sox2 depleted cells fail to form osteo-spheres and tumors in murine xenografts (Basu-Roy et al., 2012). Recently, it was reported that Sox2 antagonizes also the Hippo pathway to maintain CSCs in osteosarcoma (Basu-Roy et al., 2015). These results indicate that Sox2 play a critical role in maintain a self-renewing state in tumors of mesenchymal origin, just as observed in ES (Riggi et al., 2010). Besides osteosarcoma and Ewing sarcoma, the antagonizing effect of the Wnt pathway on Sox2 levels and in CSCs self-renewal was also described in nasopharyngeal carcinoma (Chan et al., 2015).

Contrariwise, it was reported that Sox2 can activate and act synergistically with the Wnt signalling-related protein β-catenin, promoting cell proliferation. In breast cancer, both proteins act together in the transcriptional activation of *CCND1* gene, facilitating G1/ S-phase transition and cell proliferation (Chen et al., 2008a). This same observation was reported in detail in colorectal cancer. Sox2 could reduce the expression of E-cadherin at plasma membranes, and therefore decrease the binding of β-catenin with of the adhesion complexes. Consequently, β-catenin is recruited to the nucleus by Wnt signalling components and activates downstream targets of the Wnt pathway such as c-Myc and cyclin D1. The activation of the Wnt pathway by Sox2 facilitated the epithelial-mesenchymal transition (EMT) process (Han et al., 2012).

Curiously, in colorectal cancer some reports showed that Sox2 is implicated in cell proliferation, while others reject the involvement of Sox2 in the proliferative process. While Sox2 knockdown, in SW620 colorectal cancer cell line, decreased their growth rates *in vitro*, and *in vivo* xenograft models, the overexpression of Sox2 significantly inhibited the proliferation of colorectal adenocarcinoma cells HT-29, SW480 and LoVo (Fang et al., 2010; Liu et al., 2013b). These contradictory results may be due to the fact that were used distinct colorectal cancer cell lines or due to different experimental conditions.

On the other hand, Sox2 was also implicated as a new regulator of cell invasion, migration and metastasis. In colorectal cancer, Sox2 mediates invasion and migration, *in vitro*, through matrix metalloproteinase-2 (MMP-2) activity (Han et al., 2012). Similarly, in melanoma, the downregulation of Sox2 resulted in decreased invasion *in vitro*, but in this case via metalloprotenase-3 (MMP-3) downregulation (Girouard et al., 2012). Furthermore, the invasive phenotype was

also confirmed in glioma, where Sox2 downregulation decrease migration and the overexpression of the transcriptional factor increases the number of migratory and invasive cells (Girouard et al., 2012), in laryngeal cancer, where Sox2 promotes invasion via PIK3/ Akt/ mTOR and MMP-2 activation (Yang et al., 2014), in ovarian cancer, through Src kinase activity (Wang et al., 2014b) and, in breast and prostate cancer, where it promotes metastasis through *CTNNB1* promoter activation and consequently by triggering EMT via Wnt/ β-catenin pathway (Li et al., 2013).

Sox2 is also an important player in cell survival pathways. For instance, in prostate cancer, Sox2 overexpression increases apoptotic resistance, in *in vitro* and *in vivo* experiments, due to the repression of ORAI1 (Jia et al., 2011). Moreover, in non-small cell lung carcinoma (NSCLC), Sox2 is also implicated in cell surviving, since its knockdown induces apoptosis via mitogen-activated protein kinase kinase kinase kinase 4 (MAP4K4) activation with increased expression of tumor necrosis factor-α (TNF-α) and p53, and loss of Survivin. Upon activation, MAPK4K translocates from the cytoplasm to the nucleus and activates some transcriptional factors such as, c-Myc, c-Jun and c-Fos to regulate the expression of key apoptosis-related proteins, such as TNF-α, p53 and Survivin (Chen et al., 2014). Inquiringly, Sox2 was also implicated in the activation of Survivin and the mitochondria-dependent apoptotic pathway inhibition in neural stem cells. This could indicate the existence of conserved regulatory mechanisms between cancer and neurological diseases (Feng et al., 2013) In addition, Sox2 downregulation has been reported to induce apoptosis in several other cancer types such as gastric cancer (Hutz et al., 2014) and lung tumors (Chou et al., 2013).

Hypothesis and Aims

Hypothesis

In this work we hypothesize that VRK1 participates in the regulation of cell proliferation, via two new and independent mechanisms. One by actively regulating AurKB and the other by regulating the balance between cell proliferation and cell differentiation.

Aims

Therefore this work was sub-divided into two main aims:

1) To characterize the role of the human kinase VRK1 in the control of the AurKB mitotic localization and activity;

2) To analyze the implication of the reprogramming transcriptional factor Sox2 in the regulation of human kinase VRK1 in the context of cellular proliferation and differentiation.

Material and Methods

1. Cell Lines

The cell lines used in this work and the respective culture medium used for the correct growth are represented in the Table II. Briefly, human embryonic kidney HEK293T, human cervix adenocarcinoma HeLa, human breast adenocarcinoma MCF7 and MDA-MB-231, human bone osteosarcoma U2OS and, human pluripotent embryonal carcinoma NT2/D1 (shortly abbreviated to NT2) cell lines were cultured in Dulbecco's modified Eagle's-low glucose (DMEM) medium (Sigma-Aldrich; St-Louis, MO, USA), with 10% fetal bovine serum (FBS) (Gibco® - Life Technologies-Invitrogen; Paisley, UK), 2mM L-glutamine, both the antibiotics penicillin (50units/mL) and streptomycin (50µg/mL) (Gibco®) and ciprofloxacin Kabi (10µg/mL) (Fresenius SE; Hesse, Germany). Human lung carcinoma A549 and human non-small cell lung carcinoma H1299 cell lines were cultured in Roswell Park Memorial Institute (RPMI) medium (Gibco®) supplemented with 10% FBS (Gibco®), 2mM L-glutamine (Gibco®), both the antibiotics penicillin (50units/mL) and streptomycin (50µg/mL) (Gibco®) and ciprofloxacin Kabi (10µg/mL) (Fresenius SE; Hesse, Germany). All the cell lines were cultured in culture treated flasks (BD Falcon™ - BD Biosciences; San Jose, CA, USA) in an incubator at 37ºC, 5% CO_2 and 98% of relative humidity.

The process of collecting the cells from the culture flasks was performed with trypsin-ethylenediaminetetraacetic acid (EDTA) (Gibco®), or with TrypLE™ express stable trypsin replacement reagent (Gibco®). This reagent is free of animal/ human derived components allowing a fast and effective cell harvesting without harm the cells or affecting intracellular pathways. Normally, the cell lines, after being harvested, were plated, accordingly with the experiment, in 10mm, 15mm or 20mm *Style* cell culture dishes. All the cell culture dishes were purchased from BD Falcon™ - BD Biosciences.

All the different cell lines were examined in an inverted microscope *Zeiss Axiovert 25* (Carl Zeiss AG; Jena, Germany).

Table II – Cell lines

Cell Lines				
Cell Line	**Organism**	**Tissue**	**Characteristics**	**Medium**
A549	Human	Lung carcinoma		RPMI 10% FBS
H1299	Human	Non-small cell lung carcinoma	p53-deficient	RPMI 10% FBS
HEK-293T	Human	Embryonic kidney	Express SV40 large antigen	DMEM 10% FBS
HeLa	Human	Cervix carcinoma	HPV-18 transformed	DMEM 10% FBS
MCF7	Human	Breast carcinoma	Luminal-type cell line	DMEM 10% FBS
MDA-MB-231	Human	Breast carcinoma	Basal-type cell line	DMEM 10% FBS
NTera-2 cd.D1	Human	Pluripotent embryonal carcinoma		DMEM 10% FBS
U2OS	Human	Bone osteosarcoma		DMEM 10% FBS

All the cell lines were cultured in the respective culture medium in normal conditions at 37ºC, 5% CO_2 and 98% relative humidity.

2. DNA-related assays

2.1 Extraction and purification of DNA plasmid from *Escherichia coli*

The alkaline lysis technique described in 1979, by Birnboim and Doly (Birnboim and Doly, 1979), was used to obtain deoxyribonucleic acid (DNA) plasmid from *Escherichia coli* (*E. coli*). In this method, the plasmids are attained after the *E. coli* lysis, together with the chromosomal DNA and protein denaturation. A process that depends on the alkalization of the bacteria with NaOH (sodium hydroxide) in the presence of the anionic detergent SDS (sodium dodecyl sulfate).

The extraction of high-purity DNA plasmid was performed using with the classic method of phenol-chloroform extraction, in which the proteins were

eliminated by a series of washings with phenol-chloroform and the DNA plasmid was precipitated with ethanol. Normally, the extraction of small-scale DNA plasmid (mini-prep) was performed using the commercial kit *NucleoSpin® plasmid* (MACHEREY-NAGEL; Dueren, Germany) following the company protocol. Briefly, saturated *E. coli* were pelleted in a microcentrifuge (Eppendorf; Hamburg, Germany) at 11000x*g* during 30s, discarding the supernatant. Next, the cells were lysed at room temperature (RT) and the cell lysate clarified by centrifugation at 11000x*g* during 5min. Next, the supernatant was decanted on a column with a silica membrane to bind the DNA (1min at 11000x*g*), washed twice (2min at 11000x*g*) and eluted in Tris-EDTA (TE) buffer solution (1min at 11000x*g*). On the other hand, the extraction of large-scale DNA plasmid (maxi-prep) was performed using the commercial kit *JETStar Plasmid Purification System* (Genomed; Löhne, Germany), adapted from the manufacturer's protocol. Initially, the *E. coli* were pelleted in an Avanti™ J-25 centrifuge (Beckman Coulter, Inc.; Pasadena, CA, USA), at 2500x*g* during 8min. Next, the cells were lysed at RT, neutralized and centrifuged at 12000x*g* for 10min. After loading the supernatant in a column, the column was washed once, and the DNA plasmid eluted. Then, the plasmid was precipitated with isopropanol (12000x*g* for 30min) and washed with ethanol 70% (12000x*g* for 15min). After that, the pellet was air dried around 10min and eluted in TE buffer solution.

2.2 Quantification of DNA plasmid

The final concentration of extracted and purified DNA plasmid was quantified by measuring the absorbance of each sample at 260nm, in one Hitachi U-2001 spectrophotometer (Hitachi High-Tech; Tokyo, Japan). In order to calculate the purity of DNA both the $A_{260/280}$ and $A_{260/230}$ absorbance ratios were taken into account. These two ratios should rank between 1.8 and 2.0, and if not, lower $A_{260/280}$ ratio indicates probably contamination by chemical compounds such as phenol, which is commonly used to purify the DNA or in a low-scale by proteins. In turn, lower $A_{260/230}$ ratio indicates probably contamination by phenolate ion, thiocyanates and other organic compounds found in some of the solutions used to extract and purify the DNA. Ratios below 1.7 were not accepted and the extraction and purification protocols were repeated. Later, the DNA concentration was confirmed by electrophoresis in 1% agarose gel.

2.3 Agarose gel electrophoresis

The DNA fragments were separated by electrophoresis, accordingly with their size and charge (due to the phosphate groups present in the DNA), in an agarose gel/ 1% TAE buffer (40mM Tris-acetate, pH 8.0 and 1mM EDTA). This buffer maintains the pH close to 8.0 during the electrophoresis, which is important since the DNA migration on the agarose gel depends on the DNA phosphate-negative charge and on the charged-ions present in the medium. Since DNA is negative-charged it migrates to the positive pole when submitted to an electrical field.

The visualization of the DNA fragments, in the agarose gel, was attained using ethidium bromide (0.5µg/ml), diluted in the electrophoresis buffer. Ethidium bromide is an agent that intercalates into the nitrogenous bases of the DNA and emits fluorescence when exposed to UV light. Then, the fluorescence emitted by the DNA fragments can be visualized and captured through a digital camera attached to the *Gel Doc* ^{TM} analyzer (Bio-Rad; Hercules, CA, USA). The results were impressed in thermal paper. Furthermore, it was used a molecular-weight size marker, the DNA ladder 1Kb (Promega; Madison, WI, USA), which facilitates the determination of the size of the different fragments captured with the analyzer from Bio-Rad.

2.4 Recombinant DNA and cloning

Recombinant DNA was obtained through the insertion of a specific coding DNA sequence (CDS) into a cloning vector. Usually, these CDSs were attained by PCR followed by the digestion of DNA fragments with restriction endonuclease enzyme(s) (Fermentas – Thermo Scientific; Ontario, Canada) or by digesting directly the CDS from another cloning vector. Meanwhile, the cloning vector was also digested with the same restriction endonuclease enzyme(s) used on the CDS digestion and dephosphorylated with the Calf intestinal (CIP) alkaline phosphatase (New England Biolabs, Inc.; Ipswich, MA, USA), to avoid re-ligation of the vector. All the restriction digestions were performed accordingly with the web tool *DoubleDigest* (Thermo Scientific; Waltham, MA, USA) and the primers used on the cloning process are represented on Table II. Thereafter, the digested CDS and the digested and dephosphorylated vector were ligated with the enzyme

T4 DNA-ligase (Promega), overnight (ON) at 14ºC on a thermocycler (Bio-Rad). Next, the constructions were transformed in competent *E. coli* bacteria (DH5α or BL21DE3), plated on LB (Lysogeny Broth) medium with ampicillin (10µg/mL) or kanamycin (25µg/mL), in conformity with the cloning vector resistance, and incubated ON at 37ºC. Since the vector had a specific resistance against one antibiotic, only the *E. coli* incorporating the cloning vector grew on the LB petri dish. Afterward, the DNA was extracted and purified by mini-prep, and the vector-CDS constructions analyzed by enzymatic digestion and DNA sequencing. The alignment of the DNA sequencings was performed with both *Chromas* (Technelysium Pty, Lda; South Brisbane, Australia) and *DS-Gene* (Accelrys, Inc.; San Diego, CA, USA) software.

2.5 *Escherichia coli* transformation

The recombinant DNA, as described in the chapter 2.4, was transformed in competent *E. coli* bacteria, such as DH5α or BL21DE3. The first strain (DH5α) is usually used to express DNA plasmid, and the second one (BL21DE3) used to express recombinant proteins. The transformation was performed through the heat shock method.

Briefly, a small amount of DNA (50-100ng) was added to the thawed bacteria strain, mixing homogenously and left incubating on ice around 30min. Subsequently, the heat shock transformation was done at 42ºC during 1min in a bath, moving quickly the cell/ DNA mixture to ice again (2min incubation). Next, 1mL of LB medium was added and the final cell/ DNA/ LB mixture grew at 37ºC on a shaking incubator between 45min to 60min. Later, the bacteria were plated in LB Petri dish with the specific antibiotic (ampicillin (10µg/mL) or kanamycin (25µg/mL)), in order to grow the bacteria expressing the resistance gene present in the cloning vector. The bacteria were incubated ON at 37ºC. Next day, the isolated colonies were picked to further analysis by enzymatic digestion and/or DNA sequencing. The positive colonies, expressing the recombinant DNA, were cryopreserved with sterile glycerol at 30% (v/v) (at -80ºC).

2.6 Site-directed mutagenesis

Site-directed mutagenesis was executed following the protocol from the commercial system *''QuickChange Site-Directed Mutagenesis''* (Stratagene; La Jolla, CA, USA).

Briefly, the PCR reaction was prepared using 20ng of DNA template, 125ng of each primer with the mutagenesis site included (Table III), 0.2mM dNTPs (Hoffman- La Roche; Basel, Switzerland), buffer 1x (100mM KCl, 100mM $(NH_4)_2SO_4$, 200mM Tris-HCl pH8.8, 20mM $MgSO_4$, 1% Triton X-100, BSA 1mg/mL) and 1 unit of Pfu turbo DNA polymerase (Stratagene) into a final volume of 50µl. Before adding the polymerase, the PCR reaction was incubated at 95ºC during 10min to denature the DNA strands. Subsequently to the addiction of the Pfu turbo DNA polymerase, the PCR was carried out during 16 cycles of:

- 0.5min at 95ºC (Denaturation)
- 1min at 55ºC (Annealing)
- 22min at 68ºC (Elongation).

Table III – List of primers

Primers		
Name	**Sequence 5'- 3'**	**Used to**
Flag-VRK1-F	CCGGATCCATGGACTACAAGGACGAC GATGAC	Amplify Flag-VRK1
NotI-VRK1-R	CCGCGGCCGCTTACTTCTGGACTCTC TTTCTGGTTCTTG	Amplify VRK1
SalI-VRK1-R	CCCGTCGACTTACTTCTGGACTCTCT TTCTGGTTCTTG	Amplify VRK1
HA-VRK1-F	CCATGGGATCCATGTACGACGTTCCT GATTACGCTAGCC	Amplify HA-VRK1
SOX2F	CCCGGATCCGCCATGTACAACATGAT GGAGACGGAGCTG	Amplify SOX2
SOX2R	CCCGAATTCGCCTCACATGTGTGAGA GGGGCAGTGTGCC	Amplify SOX2
GAPDH5'	GGTCTTACTCCTTGGAGGCCATGTG	Amplify GAPDH for RT-PCR
GAPDH3'	ACCTAACTACATGGTTTACATGTT	Amplify GAPDH for RT-PCR

macroH2A2-F	TGCTGGCAGTTGCCAATGACGA	Amplify macroH2A2 for RT-PCR
macroH2A2-R	CGTTTCCGACTTGCCTTTGGTC	Amplify macroH2A2 for RT-PCR
OCT4-F	AAGCGATCAAGCAGCGACTAT	Amplify OCT4 for RT-PCR
OCT4-R	GGAAAGGGACCGAGGAGTACA	Amplify OCT4 for RT-PCR
Pex2hVRK1F	CCAACGAGCTGCAAAACC	Amplify VRK1 for RT-PCR
Pex2hVRK1R	TGTCATGTAGACCAGACCCCC	Amplify VRK1 for RT-PCR
SOX2-F	ACCTCTTCCTCCCACTCC	Amplify SOX2 for RT-PCR
SOX2-R	TCCCATTTCCCTCGTTTT	Amplify SOX2 for RT-PCR
AurBK106R-F	CCATTTCATCGTGGCGCTCAGGGCCT CTTCAAGTCCCAGA	Mutagenesis of Aurora B on Lysine 106 to Arginine
AurBK106R-R	TCTGGGACTTGAAGAGGACCCTGAGC GCCACGATGAAATGG	Mutagenesis of Aurora B on Lysine 106 to Arginine
VRK1-F-T51I	CCAAGGAGGCTTTGGCTGTATATATC TTGCTGATATGA	Mutagenesis of VRK1 on Threonine 51 to Isoleucine
VRK1-R-T51I	TCATATCAGCAAGATATATACAGCCAA AGCCTCCTTGGCC	Mutagenesis of VRK1 on Threonine 51 to Isoleucine

*Used in phenotypic rescue

Subsequently to PCR, the DNA template was eliminated by the enzyme DpnI (Fermentas – Thermo Scientific), which cuts the methylated and hemimethylated DNA, but not the mutated copies, allowing the selection of the latter ones. As usual, the PCR product was transformed in *E. coli* DH5α, selecting the positive colonies through the specific antibiotic resistance, and the DNA extracted and purified with the kit *NucleoSpin® plasmid* (MACHEREY-NAGEL) as described in the chapter 2.1. To confirm the correct substitution of the nucleotide, the DNA was sequentiated and the results analyzed with *Chromas* (Technelysium Pty, Lda) and *DS-Gene* (Accelrys, Inc.) software.

2.7 Cell cycle analysis

The propidium iodide (PI) staining was used for cell cycle analysis. PI molecule has the ability to intercalate the double helix of the DNA emitting self-fluorescence that can be detected by fluorescence-activated cell sorting (FACS). These allows the rate-analysis of cell cycle stages (G0/G1; S-phase; G2/M).

Initially, cells were seeded in 10mm *Style* cell culture dishes and incubated with the appropriated treatment. Then, cells were fixed in 70% ethanol (Sigma-Aldrich) in 1x phosphate buffered saline (PBS) for 30min. After the removal of the fixation agent, through centrifugation, the cells were stained with a solution of 0.5% PI (1mg/mL) (Sigma-Aldrich) and 0.5% RNAase (Sigma-Aldrich) in 1x PBS, in the absence of light for 1h. Finally, the cells were acquired (20000 events) in a FACSort Cytometer (Becton Dickinson; Franklin Lakes, NJ, USA) and the analysis of the results was performed using both *Paint-a-Gate* (Becton Dickinson; Franklin Lakes, NJ, USA) and *ModFit* softwares (Verity Software House; Topsham, ME, USA).

3. RNA-related assays

3.1 RNA extraction

The cells were seeded in 10mm *Style* cell culture dishes and 24h later they were submitted to the respective treatment or transfection. Then, the cells were scraped and the pellet was recovered to a 2ml eppendorf and centrifuged. The medium was carefully removed and the cell pellet was resuspended in 1ml of TRIzol® (Invitrogen™ – Life Technologies; Carlsbad, CA, USA), for 5min incubation. Next, the mixture was careful homogenized with chloroform (Merck; Whitehouse Station, NJ, United States of America) and after 2min of incubation at RT, the tubes were centrifuged at 4ºC at 13500x*g* during 15min. At this point three phases were distinguishable according to the particles that constitute it:

- Upper aqueous phase of ribonucleic acid (RNA)
- Middle white phase of DNA
- Lower red phase of proteins.

The upper-RNA phase was transferred to a new eppendorf and 2-propanol (Merck) was added to the mixture. Afterwards, the tubes were incubated for

10min on ice and centrifuged at 4ºC, at 13500x*g,* during 10min. Finally, the supernatant was eliminated, 75% ethanol (Sigma-Aldrich) was added and after a 5min centrifugation at 4ºC at 13500x*g*, the pellet was resuspended in RNase-free water (Qiagen; Venlo, Netherlands).

3.2 RNA purification

Purification of RNA was performed with the *RNeasy® Mini Kit* (Qiagen), following manufacturer's instructions. Briefly, the extracted RNA was homogenized in lysis buffer complemented with β-mercaptoethanol (β-ME) (Sigma-Aldrich) and 100% ethanol (Sigma-Aldrich). Then, the complete volume was transferred to a RNA-purification column and centrifuged at 9350x*g* for 15s at RT. Next, the RNA was washed with distinct *washing membrane-bound RNA* buffers (9350x*g* for 15s at RT), through the RNA-purification column and finally, the RNA was eluted in RNase-free water (Qiagen).

3.3 Evaluation of RNA quality

The RNA was quantified with the spectrophotometer NANOdrop (NanoDrop Technologies; Wilmington, DE, USA) and the 260nM/280nM and 260/230nM ratios were analyzed in order to evaluate the quality of the RNA. Ideally, both ratios (A2660/A2880 and 260/230) should be near to 2.0. In those cases where ratio was lower than 1.7, the RNA was re-purified since it indicates that the sample may be contaminated with proteins and/ or organics compounds.

3.4 Quantitative RT-PCR

Quantitative reverse transcriptase-PCR (qRT-PCR) is a reliable and effective technique that allows the amplification and quantification of a particular RNA molecule. This system uses the activity of reverse transcriptase enzyme to transform RNA in DNA, which is amplified by PCR. The number of copies of the target oligonucleotide can be precisely quantified, at the beginning of the reaction, through the cycle threshold (Ct), that it is defined as the number of cycles required for the fluorescent signal to pass the threshold (i.e. exceeds the background level). Ct levels are inversely proportional to the amount of nucleic acid in the samples. Moreover, for qRT-PCR is necessary to have specific primers to amplify the precise fragment that we want to analyze the expression. The primers were

designed according to the sequences obtained in the PubMed database for each gene and taking into account that the amplicon should be around 90 to 110bps and the melting temperature (TM) must be of 60-61ºC.

The qRT-PCR was prepared using 100ng of the purified RNA (diluted at 50µg/µL), the primers designed for each target gene (Table II) and the commercial kit *iScript™ One-Step RT-PCR Kit With SYBR® Green* (Bio-Rad) in a total volume of 25µL. The reaction was performed in one thermocycler *iCycler* (Bio-Rad) and the data analyzed using the *BioRad iQ5* software (Bio-Rad), exporting the CT values, the mean CT values and the standard deviations to an excel file. The melting curve was examined to determine if only one clean peak per primer was observed.

In each experiment, the RNA levels of each target gene were normalized to the RNA levels of the housekeeping gene glyceraldehyde 3-phosphate dehydrogenase (GAPDH), which was determined for each sample. The normalization of the values is essential to avoid high variability of results.

4. Protein-related assays

4.1 Purification of glutathione S-transferase fusion proteins

The expression and purification of glutathione S-Transferase (GST)-tagged proteins, is a technique extremely useful to produce large amounts of protein, to use in a wide range of studies, including antigen and vaccine production, molecular immunology and structural, biochemical and cell biology studies. The expression and purification was obtained from *E. coli* Bl21DE3 strain, which was previously transformed with a pGEX-4T-GST plasmid containing the protein to express. This plasmid has an inducible *lac* promoter that can be chemically activated by lactose or any lactose-analogue, such the isopropyl β-D-1-thiogalactopyranoside (IPTG).

Briefly, the bacteria expressing the GST-tagged proteins of interest were pre-incubated ON, at 37ºC, in LB medium with ampicillin (50µg/mL). Then, the pre-inoculum was diluted in fresh LB with ampicillin (1:10 dilution) and this dilution incubated at 37ºC under agitation, until achieve an optical density between 0.6-0.8 (600nm). At this point the bacteria are in exponential growth and, it possible to induce the expression of the protein. The expression of the protein was

accomplished with 0.2mM IPTG (Roche Applied Science), under agitation, at 37ºC for 2 to 4h. Next, the bacteria culture was centrifuged at 4000x*g*, during 10min, and the pellet resuspended in lysis buffer (1% triton x-100, 0.2µg/mL lyzosyme, 1mM phenylmethylsulfonyl fluoride (PMSF), 5mM dithiothreitol (DTT), 10µg/mL aprotinin and 10µg/mL leupeptin in 1x PBS). The suspension was submitted to sonication using the sonicator *Misonic XL2010* (Misonix Inc.; Farmingdale, NY, USA), performing 3 to 5 short ‘’10s’’ bursts, alternated with ‘’10s’’ on ice. Subsequently, the suspension was incubated at 4ºC, for 30min and centrifuged, at 10000x*g*, for 30min.

At this point, all the soluble proteins and GST-tagged protein are in the supernatant. However, to confirm that in fact the protein of interest is present in the soluble fraction, it was collected an aliquot from the pellet and another from the supernatant, which were analyzed in one gel. Afterward, the soluble fraction was incubated ON, at low agitation, with the resin *Glutathione Sepharose 4B beads* (GE Healthcare; Buckinghamshire, UK), which has a high-affinity to the GST-tagged proteins. When the time of incubation was over, the resin was washed several times with 1x PBS with proteases inhibitors, at 400x*g*, during 3min (4ºC), and the GST-tagged protein eluted from the resin with a solution of 10mM glutathione reduced in 50mM Tris-HCl (pH 8.0), at 4ºC, during 4h to 12h in rotation. The eluted protein was separated from the resin by centrifugation, at 400x*g* for 3min. In the end, the purification of GST-tagged protein was confirmed by sodium dodecyl sulfate polyacrylamide gel electrophoresis (SDS-PAGE) followed by Coomassie blue staining or Western blot (WB). The protein levels were quantified by colorimetry, through the *Bio-Rad protein assay* (Bio-Rad), using bovine serum albumin (BSA) in order to build the standard curve.

4.2 Protein extraction

The cells were scraped in cold 1x PBS and transferred to an eppendorf. After centrifugation, the PBS was removed, the pellet resuspended in lysis buffer, and the cell lysate incubated on ice, during 20min. Finally, the tubes were centrifuged for 20min at 16100x*g* (4ºC) and the pellet was removed.

The protein extracts were obtained using two different lysis buffers: the Suave and the RIPA buffers. The lysis buffer Suave was prepared using 50mM Tris-HCl (pH 8.0), 1mM EDTA, 150mM NaCl and 1% triton X-100 in milliQ H_2O

and the lysis buffer RIPA was prepared using 150mM NaCl (sodium chloride), 1.5mM $MgCl_2$ (magnesium chloride), 10mM NaF (sodium fluoride), 4mM EDTA, 50mM Hepes, 1% triton X-100, 0.1% SDS and 10% glycerol in milliQ H_2O. At the time of the lysis, the buffers were complemented with phosphatases inhibitors (1mM NaF and 1mM NaOv (sodium orthovanadate)) and proteases inhibitors (1mM PMSF, 10µg/mL aprotinin and 10µg/mL leupeptin). The cell lysates were always kept on ice.

4.3 Acid extraction of histones

Histones were acid extracted, according to Shechter and colleagues protocol (Shechter et al., 2007). Briefly, culture cells (3 x 10^6 cells/ ml) were collected, pelleted and once washed with 1x PBS. Next, the cells were centrifuged (10min, 300x*g*) and the pellet lysed in a hypotonic lysis buffer (10mM Tris-HCl pH 8.0; 1mM KCl (potassium chloride); 1.5mM $MgCl_2$; 1mM DTT, supplemented with proteases and phosphatases inhibitors) for 30min, at 4ºC, on rotation. Them, the intact nuclei were recovered by centrifugation, at 4ºC, (10min, 10000x*g*), and after discard the supernatant with a pipette, they were re-suspended very well in 0.4N H_2SO_4 (sulfuric acid) (Merck). If required, the samples were submitted to vortex until all the clumps were dissolved, and only at this time they were incubated ON with rotation, at 4ºC. Next day, the samples were centrifuged (10min, 16000x*g*), at 4ºC, to remove nuclear debris, and the supernatant, containing the histone fraction, was transferred to a new eppendorf.

Subsequently, the histones were precipitated with trichloroacetic acid (TCA) (Merck), adding the acid drop by drop and mixing the solution gently by inversion, until a 33% final TCA concentration in solution. At this point, the solution seemed lightly milky and it was incubated on ice around 90min. Later, the histones were recovered by centrifugation, at 4ºC (10min, 16000x*g*), and the pellet-containing histones was carefully washed with ice-cold acetone (Merck), at 4ºC (5min, 16000x*g*). Next, the supernatant was discarded with a pipette and the histone pellet air-dried, during 20 to 30min at RT. Finally, the histones were very well resuspended in milliQ H_2O, quantified by Bradford protein assay and 5µg to 7.5µg protein was boiled 5min at 100ºC, in sample buffer. The histones posttranslational modifications were analyzed by electrophoresis in 12.5% SDS-PAGE for WB.

4.4 High-salt extraction of histones

The high-salt extraction was performed following the protocol from Shechter and colleagues (Shechter et al., 2007). Initially, the culture cells were collected, pelleted and once washed with 1x PBS. Then, the cells were centrifuged (5 min, 6500x*g*), and lysed in an extraction buffer (10mM HEPES (pH 7.9), 10mM KCl, 1.5mM $MgCl_2$, 0.34M sucrose, 10% glycerol, 0.2% NP40, 1mM NaF and 1mM NaOv, 1mM PMSF, 10µg/mL aprotinin and 10µg/mL leupeptin in milliQ H_2O), during 10min on ice. Then, the cell lysate was centrifuged, at 4ºC, during 5min (6500x*g*) and the pellet (nuclei) washed with extraction buffer (without NP40) and centrifuged, at 4ºC, for 5min (6500x*g*). Afterward, the nuclei were lysed with a no-salt buffer (3mM EDTA, 0.2mM ethylene glycol tetraacetic acid (EGTA), 1mM NaF and 1mM NaOv, 1mM PMSF, 10µg/mL aprotinin and 10µg/mL leupeptin in milliQ H_2O), during 30min at 4ºC with rotation. Subsequently, the chromatin was pelleted by micro-centrifugation, at 4ºC, for 5min (6500x*g*) and lysed in a high-salt solubilization buffer (10mM Tris-HCl (pH 8.0), 2.5M NaCl and 0.05% NP40 in milliQ H_2O) for 30min with rotation, at 4ºC. Successively, the solution was centrifuged, at 4ºC, for 10min (16000x*g*) and the supernatant, containing the histones, was submitted to dialysis using a 16mm dialysis tubing (Serva; Heidelberg, Germany) during 2h and changing the dialysis medium (10mM Tris-HCl (pH 8.0) in 2L milliQ H_2O) once. Finally, the histones extracts were quantified, by Bradford protein assay, and boiled 5min, at 100ºC, in sample buffer.

4.5 Chromatin isolation by cell fractionation

The isolation of chromatin was executed following the method described by Wysocka and colleagues in 2001 (Wysocka et al., 2001) and using the commercial kit *NE-PER nuclear and cytoplasmic extraction reagents* (Thermo Scientific). The protocol was the following: the cells were harvested with 1xPBS, lysed with the cytoplasmic extraction buffer, provided by the kit, during 10min on ice, and the cytoplasm was separated from the nuclei by centrifugation (10min; 16000x*g*). Next, the nuclei were lysed, during 40min on ice, with the nuclear extraction buffer, provided with the kit, and the nucleoplasm separated from the chromatin by centrifugation (10min; 16000x*g*). Then, the chromatin was

resuspended in chromatin buffer (10mM HEPES (pH 7.9), 10mM KCl, 1mM $MgCl_2$, 10% glycerol, 1mM $CaCl_2$ (calcium chloride), 1mM EDTA, 1mM NaF and 1mM NaOv, 1mM PMSF, 10µg/mL aprotinin and 10µg/mL leupeptin in milliQ H_2O), complemented with 5units of *Micrococcal nuclease* (Sigma-Aldrich), and the mix incubated, at 37ºC, for 45min. The *Micrococcal nuclease* reaction was stopped with 10mM EGTA and the cytoplasm, nucleoplasm and chromatin fractions handled for SDS-PAGE and WB.

4.6 Protein quantification

The protein extracts were quantified using the Bradford method. The Bradford method for protein quantification is a colorimetric assay able to determine the amount of protein in each sample, by measuring the absorbance from the established Bradford reagent-protein complexes. The Bradford reagent (use the dye G-250 Coomassie blue) alone is red and turns to blue, when specific and relatively stable complexes are established with proteins. This changes the maximum absorbance from 465nm to 595nm. Higher protein concentrations lead to stronger shades of blue. The extracts were quantified with the reagent *Bio-Rad protein assay* (Bio-Rad), using BSA to build the standard curve. Usually, six standards were prepared, diluting the BSA in milliQ H_2O, and the samples were prepared by adding 2 and 3 µl of the protein extract to the appropriate amount of milliQ H_2O and Bradford reagent, up to a total volume of 1ml. After homogenization, absorbance was read in a spectrophotometer (Bio-Rad), at 595nm, and the protein concentration determined according to the Beer-Lambert Law.

4.7 SDS-PAGE electrophoresis

The separation of proteins was performed, accordingly with their size, in denaturating conditions, through SDS-PAGE vertical electrophoresis. SDS is an anionic detergent with the ability to linearize and to bond to proteins, giving them a uniform negative charge, due to the sulfate groups present in the molecule, which masks the protein charge. Thus, the proteins have a ratio charge/ mass uniform that allows their separation by size.

For immunoblotting, three different resolving gels were used according to the size of the target protein(s). To small proteins (<30kDa) were used 12.5%

acrylamide gels, to proteins between 30-100kDa, 10% acrylamide gels and to larger proteins (>100kDa), 7.5% acrylamide gels. The resolving gels were prepared with 7.5%-12.5% acrylamide, 0.13%-0.4% bis-acrylamide, in 0.375M Tris-HCl (pH 8.8) and 3.5mM SDS. On the other hand, the stacking gel was prepared with 4.8% acrylamide, 0.128% bis-acrylamide in 0.125M Tris-HCl (pH 6.8) and 3.5mM SDS on top of the resolving gel. To solidify both the resolving and the stacking gels, it was added the catalysts agent ammonium persulfate (APS) and tetramethylethylenediamine (TEMED). Before being loaded on the acrylamide gel, the samples were re-suspended in sample buffer (62.5mM Tris-HCl (pH6.8), 10% glycerol, 2.3% SDS, 0.1% bromophenol blue, and 5% β-ME) and boiled at 100ºC, during 5min. The electrophoresis was performed in denaturating conditions in the appropriated buffer (25mM Tris-HCl, 200mM glycine and 1.7mM SDS) and using the protein ladder *Precision plus Protein™ Standards Dual Color* (Bio-Rad).

4.8 Staining protein gels with Coomassie blue

The visualization of proteins in polyacrylamide gels was achieved by Coomassie Blue staining. Coomassie Blue was prepared with 0.5% *Coomassie brilliant blue R250* (Merck), 50% methanol (Sigma-Aldrich) and 10% acetic acid, glacial (Merck). This solution was added directly on the polyacrylamide gels (5min incubation on agitation), and it was washed out with a washing solution of 50% methanol (Sigma-Aldrich) and 10% acetic acid, glacial (Merck). When the protein bands where visible the gels were transferred to *Whatman 3M* paper and dried during 2h, at 80ºC, in a gel dryer (Bio-Rad).

4.9 Transference and Western Blot

Following SDS-PAGE electrophoresis, the proteins were transferred to PVDF *Immobilon-P* or *Immobilon-FL* membranes (Millipore), following the protocol described by Towbin (Towbin et al., 1979). Firstly, the membranes were activated for 2min in methanol (Sigma-Aldrich) and equilibrated 2min in milliQ H2O. Then, the transference (90min; 90V; 4ºC) was performed with a transference buffer (25mM Tris HCl, 19.2mM glycine and 10%-20% methanol in milliQ H2O), which varies on methanol concentration due to the size of the proteins that we want to analyze. Smaller proteins used higher methanol

concentrations and larger proteins used lower methanol concentrations. If necessary, PVDF membranes were incubated for 5-10 minutes with red Ponceau (chapter 4.8) to determine whether the transference was perfectly achieved. Next, the membranes were washed several times in TBS-T (25mM Tris-HCl (pH 8.0), 50mM NaCl, 2.5mM KCl and 0.1% Tween-20 (Sigma-Aldrich) in milliQ H2O) and the membranes blocked in 5% non-fat dried milk or BSA, in TBS-T (1h at RT).

Afterward, the membranes were incubated with the specific primary antibody, following the datasheet instructions (Table IV). Normally the primary antibodies were prepared in 1%BSA-TBS-T or in TBS-T and the incubations times were 1h to 2h, at RT, or ON, at 4ºC. Subsequently, the membrane was washed (3x, 10min washes with TBS-T) and incubated with the secondary antibody. Both the secondary antibodies *Goat Anti-Mouse IgG, DyLight™ 680* (red colored) and *Goat Anti-Rabbit IgG, DyLight™ 800* (green colored) (Thermo Scientific) were incubated at 1:10000 dilutions in TBS-T, during 1h (in the dark). Successively, the membranes were washed with TBS-T (3x, 10min washes) and scanned in the *LI-COR Odyssey Infrared Imaging System* (LI-COR Biosciences; Lincoln, NE, USA) that detects the fluorescence associated with the secondary antibody.

Sporadically, the secondary antibody used was conjugated with peroxidase (*ECL Anti-Mouse IgG, Horseradish peroxidase-Linked Species-Specific Whole Antibody* (Amersham Biosciences; Amersham, UK) or *Anti-Rabbit IgG (Whole Molecule) Peroxidase Conjugate* (Sigma-Aldrich)). In these cases, after a 1h incubation with the secondary antibody (1:10000), the luminescence was detected with the *ECL Western Blotting Detection Reagent* (5min incubation) (Amersham Biosciences) through X-ray film (Fujifilm; Tokyo, Japan).

Table IV. List of antibodies

Antibodies				
Antibody	**Type**	**Dilution (WB/IF)**	**MW(kDa)**	**Origin**
Acetyl-Histone 4	Rabbit polyclonal	1:1000	14	Millipore

Acetyl-Histone H2A (Lys5)	Rabbit polyclonal	1:1000	14	Cell Signaling
Acetyl-Histone H3 (Lys14)	Rabbit polyclonal	1:1000	17	Millipore
Acetyl-Histone H3 (Lys9)	Rabbit polyclonal	1:1000	17	Millipore
AU5-Tag	Mouse monoclonal	1:1000		Covance
AU5-Tag	Rabbit polyclonal	1:1000		Covance
AurKB	Rabbit monoclonal	1:1000/ 1:100	39	Abcam
AurKB	Rabbit polyclonal	1:100	39	Santa Cruz
CREB	Mouse monoclonal	1:1000	43	Cell Signaling
Cyclin A	Rabbit polyclonal	1:1000	54	Santa Cruz
Cyclin B1	Rabbit Polyclonal	1:2000	55	Santa Cruz
Cyclin D1 (M20)	Rabbit polyclonal	1:1000	37	Santa Cruz
E-cadherin	Mouse monoclonal	1:1000	135	BD
Flag-Tag	Rabbit polyclonal	1:1000		Sigma-Aldrich
Flag-Tag (M2)	Mouse monoclonal	1:1000		Sigma-Aldrich
Flag-Tag (M5)	Mouse monoclonal	1:1000		Sigma-Aldrich
GFP-Tag	Mouse monoclonal	1:1000		Santa Cruz
GST-Tag (B-14)	Mouse monoclonal	1:1000		Santa Cruz
H2A.X	Rabbit polyclonal	1:1000	15	Cell Signaling
HA-Tag	Rabbit polyclonal	1:1000		Sigma-Aldrich
HA-Tag (F-7)	Mouse monoclonal	1:1000		Santa Cruz
Histone H3	Rabbit polyclonal	1:5000	17	Cell Signaling
Lamin A/C (H110)	Rabbit polyclonal	1:500	50-41	Santa Cruz
Lamin B (M-20)	Goat polyclonal	1:500	66	Santa Cruz
Myc-Tag	Mouse monoclonal	1:1000		Millipore
Myc-Tag	Rabbit polyclonal	1:1000		Millipore
N-cadherin	Rabbit polyclonal	1:200	130	Santa Cruz
Nanog (D73G4) XP™	Rabbit monoclonal	1:1000	40	Cell Signaling
Oct4	Rabbit monoclonal	1:1000	45	Cell Signaling

p27	Mouse monoclonal	1:1000	27	BD
p53 (DO-1)	Mouse monoclonal	1:1000	53	Santa Cruz
p53 (Pab 1801)	Mouse monoclonal	1:1000	53	Santa Cruz
p53 (phospho 18)	Rabbit polyclonal	1:1000	53	Abcam
PAX6	Rabbit polyclonal	1:1000	46	Abcam
PCNA	Mouse monoclonal	1:1000	36	Santa Cruz
Phospho-CREB (Ser133)	Rabbit polyclonal	1:1000	43	Cell Signaling
Phospho-Histone H2A.X (Ser139)	Rabbit polyclonal	1:1000	15	Cell Signaling
Phospho-Histone H3 (Ser10)	Rabbit polyclonal	1:500/ 1:100	17	Millipore
Phospho-Histone H3 (Thr3)	Rabbit polyclonal	1:5000/ 1:100	17	Millipore
Phospho-Rb (Ser807/811)	Rabbit polyclonal	1:1000	110	Cell Signaling
Rb (C-15)	Rabbit polyclonal	1:1000	110	Santa Cruz
Sox2 (D6D9) XP™	Rabbit monoclonal	1:1000/ 1:100	40	Cell Signaling
Sox2 (E-4)	Mouse monoclonal	1:500	40	Santa Cruz
Sox2 (Y-17)	Goat polyclonal	1:500	40	Santa Cruz
Trimethyl Histone H3 (Lys 4)	Rabbit polyclonal	1:1000	17	Cell Signaling
Trimethyl-Histone H3 (Lys 9)	Rabbit polyclonal	1:500	17	Millipore
Trimethyl-Histone H3 (Lys 9) 6F12-H4	Mouse monoclonal	1:1000	17	Millipore
V5-Tag (SV5-Pk1)	Mouse monoclonal	1:1000		Abcam
V5-Tag (G-14)	Rabbit polyclonal	1:1000		Santa Cruz
Vimentin	Mouse monoclonal	1:1000	54	Abcam
Vimentin	Rabbit polyclonal	1:1000	54	Cell Signaling
VRK1 (1B5)	Mouse monoclonal	1:1000/ 1:200	45	Own Production
VRK1 (1F6)	Mouse monoclonal	1:1000/ 1:200	45	Own Production

VRK1 (N-Term)	Rabbit polyclonal	1:1000/ 1:200	45	Sigma-Aldrich
VRK1 (VC)	Rabbit polyclonal	1:1000	45	Own Production
VRK1 (VE)	Rabbit polyclonal	1:1000	45	Own Production
α-Tubulin	Rabbit polyclonal	1:500	50	Santa Cruz
α-Tubulin	Mouse monoclonal	1:500	50	Santa Cruz
β-actin	Mouse monoclonal	1:5000	42	Sigma-Aldrich
βIII-Tubulin	Rabbit polyclonal	1:1000	55	Biolegend

The antibodies were used for WB following the manufacturer's instructions.

4.10 Ponceau S staining

In particular experiments, the PVDF membranes were submitted to Ponceau S staining, in order to verify whether the transference was correctly performed. In these cases, the membranes were incubated around 5min with a solution of 0.2% Ponceau S (*3*-Hydroxy-4-[2-sulfo-4-(*4*-sulfophenylazo)-phenylazo]-2, 7-naphthalenedisulfonic acid), 3% 5-sulfosalicylic acid, 3% trifluoroacetic acid and 1% acetic acid. Following the incubation, the membranes were washed until the bands were visualized.

5. Transfection assays

5.1 Transfection with *JetPEI™*

The overexpression of proteins was mediated by cell transfection with DNA plasmids (Table V). Initially, the cells were platted in *Style* cell culture dishes, 24h before to transfection, in order to obtain a 50% to 70% of confluence at the time of the transfection. Then, the transfections were performed with *JetPEI™* (Polyplus Transfection SA; New York, NY, USA), following the manufacturer's instructions. This polymer based reagent (polypropylenimine (PPI)) compacts the DNA inside positive charged particles that adhere to the negative charged proteoglycan proteins in the cell surface, allowing their entrance in the cell by endocytosis. Usually, the DNA was re-suspended in 150mM NaCl and the *JetPEI™* (also re-suspended in 150mM NaCl) was added

in a 2:1 proportion to the DNA. The quantity of DNA used was specific for each DNA plasmid, however the DNA final concentration, in solution, was maintained identical intra-experiments. Later, the mix was incubated between 20min to 30min and added dropwise to the cells.

Table V. List of DNA plasmids

DNA Plasmids			
DNA Plasmid	**Vector**	**Insert**	**Used to**
HA-VRK1	pCEFL-HA	VRK1	Eukaryotic expression; Tag on N-terminus
HA-VRK1 (K179E)	pCEFL-HA	VRK1 (K179E) (Kinase inactive)	Eukaryotic expression; Tag on N-terminus
HA-VRK1 RX	pCEFL-HA	VRK1 (R358X)	Eukaryotic expression; Tag on N-terminus
HA-VRK1 (Y202A)	pCEFL-HA	VRK1 (Y202A)	Eukaryotic expression; Tag on N-terminus
HA-VRK1 (Y202D)	pCEFL-HA	VRK1 (Y204A)	Eukaryotic expression; Tag on N-terminus
HA-VRK1 (Y204A)	pCEFL-HA	VRK1 (Y204A)	Eukaryotic expression; Tag on N-terminus
HA-VRK1 (Y204D)	pCEFL-HA	VRK1 (Y204D)	Eukaryotic expression; Tag on N-terminus
HA-VRK1 (T224A)	pCEFL-HA	VRK1 (T224A)	Eukaryotic expression; Tag on N-terminus
HA-VRK1 (T224D)	pCEFL-HA	VRK1 (T224D)	Eukaryotic expression; Tag on N-terminus
HA-VRK1 (T228A)	pCEFL-HA	VRK1 (T228A)	Eukaryotic expression; Tag on N-terminus
HA-VRK1 (T228E)	pCEFL-HA	VRK1 (T228E)	Eukaryotic expression; Tag on N-terminus
GST-VRK1	pCEFL-GST	VRK1	Eukaryotic expression; Tag on N-terminus
GST-VRK1 C	pCEFL-GST	VRK1 C-Terminus (aa 267-396)	Eukaryotic expression; Tag on N-terminus
VRK1-Myc	pcDNA3.1	VRK1	Eukaryotic expression; Tag on C-terminus

VRK1-NL-Myc	pcDNA3.1	VRK1 N-Terminus (aa 1-332)	Eukaryotic expression; Tag on C-terminus
VRK1-NC-Myc	pcDNA3.1	VRK1 N-Terminus (aa 1-267)	Eukaryotic expression; Tag on C-terminus
pGEX-GST-VRK1	pGEX4T1-GST	VRK1	Expression of GST fusion protein in *E. Coli*
pGEX-GST-VRK1 (K179E)	pGEX4T1-GST	VRK1 (K179E) (Kinase inactive)	Expression of GST fusion protein in *E. Coli*
pGEX-p53 (1-85)	pGEX-2T	Murine p53 (aa 1-85)	Expression of GST fusion protein in *E. Coli*
pGEX-GST-VRK1 (Y202A)	pGEX4T1-GST	VRK1 (Y202A)	Expression of GST fusion protein in *E. Coli*
pGEX-GST-VRK1 (Y202D)	pGEX4T1-GST	VRK1 (Y202D)	Expression of GST fusion protein in *E. Coli*
pGEX-GST-VRK1 (Y204A)	pGEX4T1-GST	VRK1 (Y204A)	Expression of GST fusion protein in *E. Coli*
pGEX-GST-VRK1 (Y204D)	pGEX4T1-GST	VRK1 (Y204D)	Expression of GST fusion protein in *E. Coli*
pGEX-GST-VRK1 (T224A)	pGEX4T1-GST	VRK1 (T224A)	Expression of GST fusion protein in *E. Coli*
pGEX-GST-VRK1 (T224D)	pGEX4T1-GST	VRK1 (T224D)	Expression of GST fusion protein in *E. Coli*
pGEX-GST-VRK1 (T228A)	pGEX4T1-GST	VRK1 (T228A)	Expression of GST fusion protein in *E. Coli*
pGEX-GST-VRK1 (T228E)	pGEX4T1-GST	VRK1 (T228E)	Expression of GST fusion protein in *E. Coli*
pDEST3.1_nV5-AurkA	pDEST3.1_nV5	Aurora A	Eukaryotic expression
pDEST3.1_nV5-AurkB	pDEST3.1_nV5	Aurora B	Eukaryotic expression
pDEST3.1_nV5-AurkB (K106R)	pDEST3.1_nV5	Aurora B (K106R) (Kinase inactive)	Eukaryotic expression
pGEX-GST-AurkB	pGEX4T1-GST	Aurora B	Expression of GST fusion protein in *E. Coli*
pGEX-GST-AurkB (K106R)	pGEX4T1-GST	Aurora B (K106R) (Kinase inactive)	Expression of GST fusion protein in *E. Coli*
pCMV6-SOX2-Myc	pCMV6-Entry (Myc/DDK tagged)	SOX2	Eukaryotic expression

pGEX-GST-SOX2	pGEX4T1-GST	SOX2	Expression of GST fusion protein in *E. Coli*
pCMV6-OCT4-Myc	pCMV6-Entry (Myc/DDK tagged)	OCT4	Eukaryotic expression
pCMV6-KLF4-Myc	pCMV6-Entry (Myc/DDK tagged)	KLF4	Eukaryotic expression
VRK1-Luc (-1028+52)	pGL2-Luc	VRK1 promoter (-1028+52)	Eukaryotic expression
VRK1-Luc (-791+52)	pGL2-Luc	VRK1 promoter (-791+52)	Eukaryotic expression
VRK1-Luc (-264+52)	pGL2-Luc	VRK1 promoter (-264+52)	Eukaryotic expression
VRK1-Luc (-131+52)	pGL2-Luc	VRK1 promoter (-131+52)	Eukaryotic expression
CycD1-Luc (-1745 +134)	pA3	Cyclin D1 promoter (-1745+52)	Eukaryotic expression
Survivin-Luc	pGL2-Luc	Survivin promoter	Eukaryotic expression

5.2 Transfection with *Lipofectamine™*

The suppression of VRK1 and Sox2 expression were attained using specific siRNA (Table VI), from *Dharmacon RNA Technologies* (Dharmacon, Inc.; Lafayette, CO, USA) or *OriGene Technologies* (Rockville, MD, USA), respectively. Simultaneously, it was used the *ON-TARGET plus siControl Nontargeting siRNA* (Dharmacon, Inc.), without any target on human cells, as negative control.

The genetic suppression, with siRNA, was accomplished using *Lipofectamine™* (Invitrogen) reagent, which contains lipid subunits that can produce liposomes in aqueous environments. The liposomes have a cationic nature that can form a complex with DNA (negative charged), avoiding the electrostatic repulsion of the cellular membrane (also negative charged). This allows the fusion of the complex with the cellular membrane and it penetration into the cell. The protocol used for siRNA-gene silencing was the following: cells were platted without antibiotic and when the correct confluence was achieved they were transfected with *Lipofectamine™*. This reagent was diluted in *Opti-MEM* (Gibco®) and it was added to the siRNA (100nM-200nM concentration) re-

suspended in *Opti-MEM* for a 20min incubation. Finally the mix containing the siRNA and the *Lipofectamine*^{TM} was added dropwise to the cells. The antibiotic was re-introduced to the medium 24h later.

Table VI. List of siRNA

RNAi		
Name	**Sequence 5'- 3'**	**Used to**
SOX2 Trilencer-27 Human siRNA		RNA Interference against SOX2
DOLRA siVRK1-01 (Thermo) Forward	GAAAGAGAGUCCAGAAGUAUUUU	RNA Interference against VRK1*
DOLRA siVRK1-01 (Thermo) Reverse	AAUACUUCUGGACUCUCUUUCUU	RNA Interference against VRK1*
siVRK1-02	CAAGGAACCUGGUGUUGAAUU	RNA Interference against VRK1
siVRK1-03	GGAAUGGAAAGUAGGAUUA	RNA Interference against VRK1
siVRK1-09	AGGUGUACUUGGUAGAUUA	RNA Interference against VRK1

*Used to phenotypic rescue

6. Viral transduction

Cell transduction uses a viral vector as a packaging device to introduce into the cell foreign DNA. Herein, it was used two different types of viral vectors to deliver the overexpressing protein or the shRNA of interest (Table VII) into the cell: lentiviruses and retroviruses. The main difference between these two types, from an experimental standpoint, is that lentiviruses are capable of transduce non-dividing and actively dividing cells, whereas retroviruses can only transduce mitotically active cells. This means that lentiviruses are more efficient transducing several cell types than retroviruses. Both the two viral vector systems use the gag, pol, and env genes for packaging. Nonetheless, the isoforms of these proteins used are different and lentiviral vectors may not be efficiently packaged by retroviral packaging systems and vice versa. Here, the lentiviral system used the *pCMV-dRp8.91* (gag-pol genes) and the *pMD26-VSV-G* (env gene) packing

vectors and the retroviral system used the *pCMVdr.9.91* (gag-pol-env genes) packing vector.

The protocol used for cell transduction was the following: on the first day, the HEK293T were platted in order to obtain the necessary confluence at the time of transfection. Then, the HEK293T cells were transfected with 10µg DNA and the respective packing vectors, diluted in 0.25M $CaCl_2$ and 2x HEPES-buffered saline solution (HeBS). Less than 20h after the transfection, the HEK293T cells were washed with 1x PBS and the medium of the cells was refreshed. On the next mourning the medium was refreshed once again and the target cells were platted. On the following day, the target cells were transduced adding directly the HEK293T cells medium over them. The medium was filtered with 0.45µm polysulfone filters (Pall Corporation; Ann Harbor, MI, USA) and it was supplemented with 4µg/mL polybrene (Sigma-Aldrich). Polybrene is a small and positively charged molecule that has the capacity to bind to cell surfaces and neutralizes it charge. This is important because it allows the viral glycoproteins to bind more efficiently to their receptors, because it reduces the repulsion between sialic acid-containing molecules leading to an increased efficiency of transduction. Lastly, the target cells were selected with 1µg/mL puromycin (Sigma-Aldrich) or in the cases in which the viral vectors weren't puromycin-resistant, the transduction was evaluated through the emission of fluorescence.

Table VII. Lentiviral and retroviral vectors

Viral Vectors			
Viral Vector	**Vector**	**Insert**	**Used to**
pLKO.1-shVRK1-H1	pLKO.1 [1]	shVRK1	shRNA against VRK1
pLKO.1-shVRK1-H3	pLKO.1 [1]	shVRK1	shRNA against VRK1
pLKO.1-shVRK1-H5	pLKO.1 [1]	shVRK1	shRNA against VRK1
pSUPERIOR-siVRK1-01	pSuperior [2]	siVRK1	RNA Interference against VRK1
pSUPERIOR-siVRK1-03	pSuperior [2]	siVRK1	RNA Interference against VRK1

pBabe-HA-VRK1	pBabe [2]	VRK1	VRK1 expression; Tag on N-terminus
pQCXIP-VRK1	pQCXIP [2]	VRK1	VRK1 expression
pLVX-IRES-zsGreen-HA-VRK1	pLVX-IRES-zsGreen [1]	VRK1	VRK1 expression; Tag on N-terminus
pLVX-IRES-tdTomato-HA-VRK1	pLVX-IRES-tdTomato [1]	VRK1	VRK1 expression; Tag on N-terminus
pBabe-Sox2	pBabe[2]	Sox2	Sox2 expression

[1] Lentiviral vector; [2] retroviral vector

7. Protein-protein interaction assays

7.1 Immunoprecipitation

Immunoprecipitation (IP) was executed using between 0.5mg to 2.0mg of total protein extracts, in a 1mL total volume. Initially, the protein extracts were incubated with the equilibrated resin *Gammabind plus Sepharose* (GE Healthcare), during 1h, at 4ºC, on a rotator. This initial incubation serves to eliminate everything that can bind nonspecifically to the resin. Subsequently, the resin was eliminated by low-rotation centrifugation and the pre-cleaned extracts were incubated with the specific antibody, ON, with rotation, at 4ºC. Typically, the antibodies were used at concentrations between 1:50 to 1:500, depending on the datasheet instructions and as control negative it was used an unspecific antibody. Then, the extracts were incubated once again with equilibrated *Gammabind Sepharose* during 2h, at 4ºC, on rotation. This second incubation serves to bind the antibody and consequently precipitate the protein bonded to it. Next, the *Gammabind Sepharose* was washed with lysis buffer at 4ºC, resuspended on sample buffer and boiled at 100ªC for further analysis by SDS-PAGE and WB. Also important to mention is the fact that the *Gammabind Sepharose* was equilibrated through a sequence of several washes with lysis buffer at 4ºC.

7.2 Pull-down assay

Pull-down assay was used to verify whether a specific protein (endogenous or transfected) interacted with the precipitated GST-tagged protein,

which was transfected in the eukaryotic cell. Briefly, the cells were transfected with the GST-fusion protein and they were lysed with the lysis buffer Suave, since a lysis buffer more aggressive could disrupt the interactions between the proteins. Afterward, between 0.5mg to 2.0mg of total protein extracts was incubated ON, at 4ºC, with the resin *Glutathione Sepharose 4B beads* (GE Healthcare), which was washed in the following day with lysis buffer at 4ºC, by low-rotation centrifugation. Finally, the beads were resuspended on sample buffer, boiled at 100ºC and analyzed by SDS-PAGE and WB. Like the *Gammabind Sepharose,* the *Glutathione Sepharose* was equilibrated washing it with lysis buffer at 4ºC, by low-rotation centrifugation. In the pull-down assay, it was used as negative control the GST protein, by itself.

8. Immunofluorescence and confocal microscopy

Immunofluorescence (IF) assays were used to analyze the levels and subcellular localization of endogenous or exogenous proteins in culture cells.

Briefly, the cells were cultured with or without 0.01% poly-L-lysine (Sigma-Aldrich), which increases the cellular adhesion to the glass, in coverslips (Thermo Scientific) placed in 10mm *Style* culture dishes. Then and after 48h to 96h, depending on the experiment, the cells were washed with 1xPBS and fixed with 3% paraformaldehyde (Sigma-Aldrich), during 30min, at RT. Next, the cells were treated with 20nM glycine during 15min to reduce the excess of aldehyde groups after the fixation, and permeabilized with 0.2% triton X-100 in 1xPBS, during 30min. Successively, the cells were blocked with 1% BSA in 1xPBS with azide, during 1h, at RT, or ON, at 4ºC. Afterward, the cells were incubated with the primary antibodies diluted in 1%BSA in 1xPBS with azide. The first primary antibody was incubated ON, at 4ºC, and the second one (always from a different host in relation to the first primary antibody) was incubated between 2 to 4h, at RT. Subsequently, the cells were washed with 1xPBS and incubated with the secondary antibodies. The secondary antibodies were linked to the cyanine fluorophore Cy2 (*Cy™2-conjugated AffiniPure Goat anti-Rabbit/ anti-Mouse (H+L))* or Cy3 (*Cy™3-conjugated AffiniPure Goat anti-Rabbit/ anti-Mouse (H+L))* (Jackson ImmunoResearch; West Grove, PA, USA) and were used always at 1:1000 dilution in 1%BSA in 1xPBS, for 1h, at RT, in the dark. Besides and from

this point until the end, the cells were always maintained in the dark to preserve the fluorophore. Later, the cells were washed with 1x PBS and the nuclear DNA was counterstained with 4', 6-diamidino-2-phenylindole, also called DAPI (Vector Labs; Burlingame, CA, USA). The excess of DAPI was removed with 1xPBS and the coverslips were mounted in microscope slides (LineaLab; Badalona, Spain) using *MOWIOL® 4-88* (Calbiochem; Billerica, MA, USA).

Finally, a *Leica TCS SP5* inverted fluorescence microscope (Leica Microsystems; Wetzlar, Germany) connected to a digital video camera *Leica DC100* (Leica Microsystems) was used to obtain the confocal microscopy images and the confocal image analysis was completed using the *LAS AF Lite* (Leica Microsystems).

9. Luciferase reporter assay

Reporter gene luciferase was used to study gene expression and cellular events coupled to gene expression. Usually, the promoter of interest was cloned into an expression vector with the luciferase reporter gene and then transfected into cells. Since the luciferase gene is downstream to the promoter, after the activation or repression, by a transcriptional factor complex, the expression of the luciferase gene respond equitably. Usually, this occurs because the transcriptional factor recognizes specific sequences in the transfected promoter, binding to them and leading to the transactivation of the luciferase reporter gene and to the synthesis of the protein luciferase. Afterward, the luciferase catalyzes the oxidation of luciferin, using ATP and Mg^{2+}, which produces oxyluciferin that emitted light at 556nm. The light was quantified with a *Lumat LB 9507* luminometer (Berthold Technologies; Oak Ridge, TN, USA).

The quantification of the luciferase reporter gene activity was performed with the commercial kit *Dual-Luciferase reporter assay system* (Promega), following the manufacturer's instructions. The assay was performed always in triplicate and repeated at least 3 times. *Student's t-test* was used to analyze data and the DNA plasmids used for gene reporter assay are represented in the Table IV.

10. Kinase assays

10.1 *In vitro* kinase assay with radiolabeled ATP

The Ser-Thr kinase activity was studied through *in vitro* kinase assays using radiolabeled ATP [γ-^{32}P]. This technique was performed using either GST-fusion kinase proteins, expressed in *E. coli,* or immunoprecipitated (endogenous or transfected) protein kinase from cell extracts. Moreover, it was also used a specific buffer to casein kinases (20mM Tris-HCl (pH 7.5), 5mM $MgCl_2$, 0.5mM DTT and 150mM KCl), 5μM cold ATP, 5μCi (0.1μM) [γ-^{32}P] ATP and specific substrates, such as recombinant proteins (e.g. GST-p53, GST-VRK1 K179E or GST-Aurora B K106R) or commercial human histone H3 (Upstate® - Millipore; Billerica, MA, USA).

The phosphorylation reaction was incubated during 30min, at 30ºC, with agitation (800rpm), in a *Thermomixer Compact* (Eppendorf). The phosphorylation conditions were the same for either recombinant protein kinase or immunoprecipitated kinase. Afterward, the phosphorylation reactions were resuspended on sample buffer, boiled at 100ºC and analyzed by SDS-PAGE and WB. The radioactive bands were detected exposing directly the ray-x film (Fujifilm) to the membranes between several minutes to several hours. The loading controls were stained with Ponceau S red or detected using specific antibodies against the protein or the tag.

10.2 *In vitro* kinase assay with cold ATP

On the other hand, if the phosphorylation site was known, the Ser-Thr kinase activity was also analyzed by *in vitro* kinase assays with cold ATP and phospho-specific antibodies. Like the *in vitro* kinase assay using radiolabeled ATP, it was used GST-fusion kinase proteins, expressed in *E. coli,* or otherwise immunoprecipitated (endogenous or transfected) protein kinase from cell extracts. The reactions were executed in the presence of the same casein kinase buffer, 10μM cold ATP and specific phosphorylation substrates, such as the GST-p53 or the commercial human histone H3 (Upstate®). Also, the phosphorylation reaction was incubated during 30min, at 30ºC, with agitation (800rpm) in a Thermomixer (Eppendorf). Then, the phosphorylation reactions were resuspended on sample buffer, boiled at 100ºC and analyzed by SDS-PAGE and

WB with phospho-specific antibodies. The loading controls were detected with antibodies against the protein or the tag.

11. Cell cycle synchronization

The study of the regulatory events that occurred in the cell, dependently of the cell cycle, required the synchronization (or cell arrest) of the general unsynchronized cell population into specific cell cycle phases. In our case, this synchronization was obtained due serum deprivation and drug-dependent methods. Succinctly, cells were synchronized in G0/G1 due to serum starvation during 72h, in S phase by double thymidine (2mM) block and in G2/ M by double thymidine (2mM) block followed by nocodazole (0.33μM) arrest. Moreover, the cells arrested with nocodazole were released from this drug and harvested 30min, 60min, 90min, 180min, 360min and 720min after the release, to obtain cell populations at different stages of the mitosis.

Thymidine causes the cell arrest in the S phase because it blocks the DNA synthesis by inhibiting the synthesis of specific nucleotides (i.e. generates negative feedback on the production of deoxycytidine triphosphate from cytidine-5'-phosphate). Nocodazole causes the cell arrest at G2/ M because it inhibits the microtubule function, which blocks the normal spindle assembly in early mitosis (Harper, 2005).

12. NTERA-2 cd.D1 cell differentiation

The differentiation of NT2 into a neuron-like phenotype was performed adding 10μM RA, during 14 days, and renewing the cell medium 2 in 2 days. At the same time that the medium was replaced, an experimental point was harvested to qRT-PCR and SDS-PAGE for WB, and the morphology analyzed by phase-contrast microscopy. RA is a metabolite of vitamin A that mediates the functions of this vitamin required for epithelial differentiation and embryo development (Marill et al., 2003). This action occurs mainly through the retinoic acid receptor (RAR) and retinoid X receptor (RXR) nuclear heterodimer or by the covalent binding of RA to cell macromolecules. On NT2 RA direct binds to RAR, which bounds to DNA as a heterodimer with RXR in the retinoic acid response

elements (RAREs). This heterodimer affects the transcription of different sets of genes controlling differentiation and proliferation.

13. Immunohistochemistry

Biopsies from normal human tonsil were obtained with informed consent, fixed in formalin and embedded in paraffin. Sections were sliced (3µm thick), transferred to positively (silanized) charged-surface glass slides and dried ON, at 62ºC. Next, the sections were dewaxed and rehydrated through an increased series of ethanol and washed with PBS. To desmask antigens, the slides were treated in a PT Link of DAKO for one cycle of 20min, at 95ºC, without boiling and with a buffer pH8.0. Subsequently, the sections were left tempering and washed with PBS. Immunodetection was performed with the DAKO EnVision Visualization Method (DAKO), with diaminobenzidine chromogen as substrate. Sections were counterstained with haematoxylin. VRK1 was detected with the VC polyclonal antibody (1:30) and Sox2 with monoclonal antibody Sox2 (E-4) (1:30) (Santa Cruz). For immunofluorescence, the tissue sections, after antigen retrieval, were blocked with 2% nonfat dry milk and 0.1% Triton in PBS, washed with PBS and incubated ON with both primary antibodies (1:30 each one). Afterward, after wash the slides with PBS, the sections were incubated with the secondary antibodies α-mouse Cy3 (1:100) (Jackson ImmunoResearch) and α-rabbit Alexa Fluor 488 (1:100) (Molecular Probes; Eugene, OR) during 2h, at RT. Following the staining, the slides were washed with PBS and incubated with DAPI for 5min. Cells were mounted with Vectashield (Vector Laboratories, Burlingame, CA) and analyzed with a LEICA SP5 DMI-6000B (Leica Microsystems) confocal microscope.

14. Ubiquitination and protein stability assays

In ubiquitination assays, cells were treated with 20 µM MG-132 proteasome inhibitor (Calbiochem). Moreover, cycloheximide (Sigma-Aldrich) was used, at 50 µg/ml, for protein stability studies.

Results

Part 1. Implication of VRK1 in the regulation of AurKB mitotic localization and activity

1.1 VRK1 and AurKB mutual regulation

VRK1 is a protein kinase essential for the correct cell cycle progression during interphase and was also recently reported to be involved in the regulation of mitosis, controlling chromatin condensation, nuclear envelope assembly and disassembly, and Golgi fragmentation. Likewise, AurKB was described as a key protein kinase implicated in the control of numerous mitotic processes, such as centromere function, chromatin condensation, spindle assembly, chromosome alignment and segregation and, cytokinesis. Inquiringly, AurKB share some phosphorylation substrates with VRK1, of which protrude the histone H3, and the transcriptional factor p53 (Bolanos-Garcia, 2005; Kang et al., 2007b; Valbuena et al., 2008b; Vega et al., 2004a).

In line with all this, we tested whether VRK1 could co-operate with AurKB on the same regulatory processes, using a known common substrate of both kinases: the histone H3. Accordingly, it was performed a kinase assay with radiolabeled [γ-^{32}P] ATP using as substrate the human histone H3 combined with recombinant proteins GST-AurKB-K106R inactive kinase and GST-VRK1, or with recombinant proteins GST-VRK1-K179E inactive kinase and GST-AurKB. GST-AurKB-K106R was mutated in the ATP binding site and therefore was inactive and VRK1 protein with the K179E substitution, in the active kinase domain, lacks both autophosphorylation and kinase activity. Proteins were incubated for 30 minutes at 30ºC. We demonstrated that VRK1-dependent phosphorylation of histone H3 and the autophosphorylation activity of this kinase were affected negatively by AurKB. Similarly, AurKB-dependent phosphorylation of histone H3 and the autophosphorylation activity of AurKB were affected negatively by VRK1 (Figure 16A). The quantification of histone H3 phosphorylation and autophosphorylation activities were performed using *ImageJ* and represented in a graphic (Figure 16B).

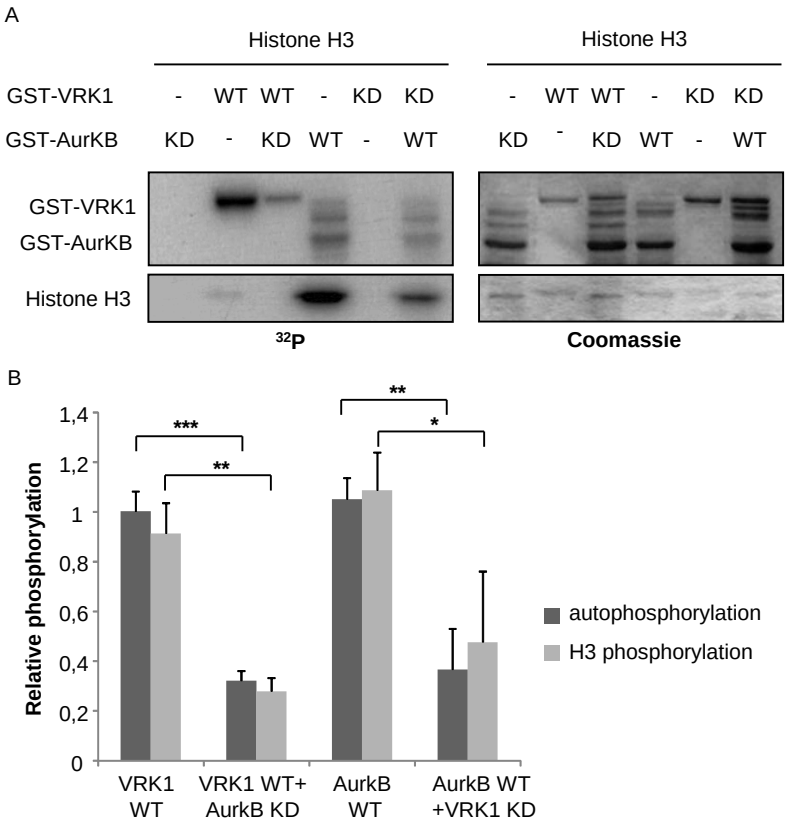

Figure 16. VRK1 and AurKB inhibits the kinase activity of one another. A) Kinase assay with recombinant proteins GST-VRK1 (pGEX-GST-VRK1 and pGEX-GST-VRK1-K179E) and GST-AurKB (pGEX-GST-AurKB and pGEX-GST-AurKB-K106R), and human histone H3 as phosphorylation substrate. Proteins were incubated for 30 minutes at 30ºC in presence of ATP and radiolabeled [γ-^{32}P] ATP. The gels were stained with Coomassie Blue to analyze the controls and the incorporated radioactivity was detected. B) The autophosphorylation and histone H3 phosphorylation activities were quantified using *ImageJ* and represented in a graphic. (Student's Test: *<0.05; **<0.005; ***<0.0005).

Additionally, we intended to confirm the results obtained in the Figure 16, through a kinase assay with cold ATP and specific histone H3-phosphorylation antibodies. VRK1 was demonstrated to phosphorylate two residues in the histone H3: the Thr3 (H3T3ph) and the Ser10 (H3S10ph) sites (Kang et al., 2007b). Curiously, both this two phosphorylations were also described to be directly (H3S10ph) and indirectly (H3T3ph) affected by AurKB (Hirota et al., 2005; Wang et al., 2011). Since VRK1 seemed to share at least one direct phosphorylation residue (H3S10ph) and thereby it may be a setback in the intended experiment, we performed several assays to confirm that in fact VRK1 phosphorylates H3T3

and H3S10 residues. First, we performed an IP assay to analyze whether VRK1 interacts with histone H3. VRK1 was immunoprecipitated with a mouse monoclonal anti-VRK1 (1F6) antibody and histone H3 was detected by immunoblot with a rabbit polyclonal anti-histone H3 antibody. It was shown that VRK1 interacts with histone H3 in unsynchronized cells (Figure 17A). Subsequently, it was performed a knockdown assay using siRNAs targeting VRK1 (siVRK1-02 and siVRK1-03), to analyze the effect of VRK1 depletion on the levels of H3T3ph and H3S10ph. A siRNA (siControl) lacking a specific target was used as control. 72 hours post-transfection, the histones were extracted using a high-salt extraction protocol and, H3T3ph was detected using a rabbit polyclonal anti-H3T3ph antibody and H3S10ph was detected using a rabbit monoclonal anti-H3S10ph antibody. It was demonstrated that VRK1 downregulation induces a decline in both H3T3ph and H3S10ph (Figure 17B). Similar result was obtained using shRNAs targeting VRK1 (pLKO-shVRK1-01 and pLKO-shVRK1-03). After 7 days of puromycin selection, the histones were extracted using an acid extraction protocol and, H3T3ph was detected using a rabbit polyclonal anti-H3T3ph antibody and H3S10ph was detected using a rabbit monoclonal anti-H3S10ph antibody. Once again, VRK1 knockdown decreases the levels of H3T3ph and H3S10ph (Figure 17C). However, in this later experiment it was observed that VRK1 downregulation led to a reduction on the levels of others mitotic markers such as AurKB and Rb phosphorylation. This observation indicates that the decline on the histone H3 phosphorylations may be due to the G0/ G1 cell cycle arrest, induced by the VRK1 depletion, instead of being a consequence of the lack of direct phosphorylation. Therefore, to verify which histone H3 residues were direct phosphorylation sites of VRK1, we performed a kinase assay using GST-VRK1 and human histone H3 as substrate. Besides, it was also studied the AurKB direct phosphorylation of histone H3 using GST-AurKB and human histone H3 as substrate. Recombinant proteins were incubated 30 minutes at 30ºC in the presence of the substrate. H3T3ph was detected using a rabbit polyclonal anti-H3T3ph antibody and H3S10ph was detected using a rabbit monoclonal anti-H3S10ph antibody. We observed that VRK1 only phosphorylated directly H3T3 and AurKB, as described in the literature, only phosphorylated H3S10 (Figure 17D).

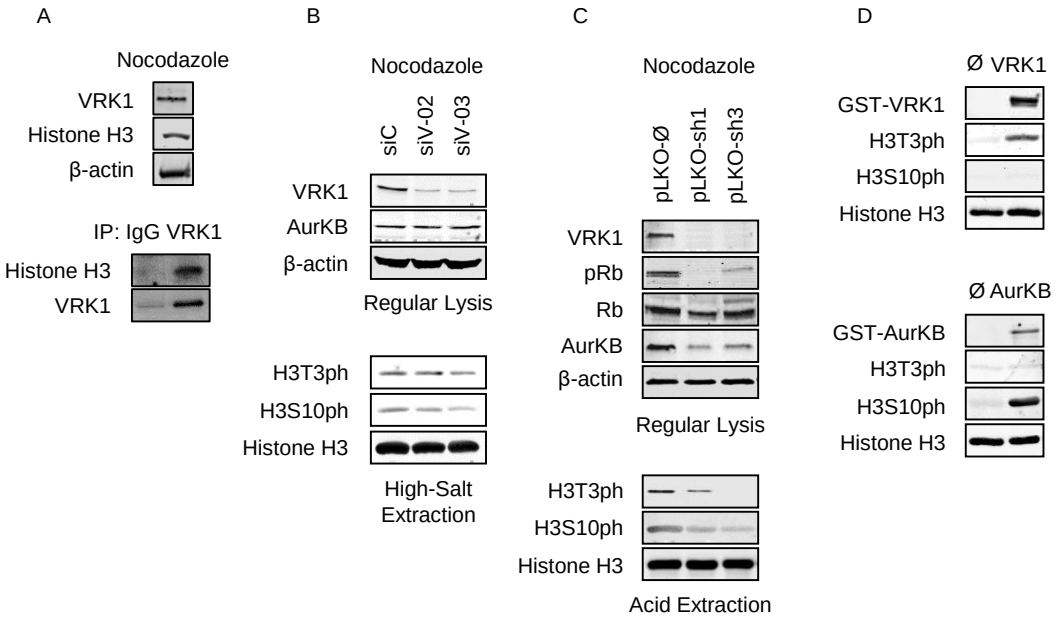

Figure 17. VRK1 interacts with and phosphorylates histone H3 in the Thr3 residue. A) VRK1 was immunoprecipitated with a mouse monoclonal anti-VRK1 (1F6) antibody and histone H3 was detected by immunoblot with a rabbit polyclonal anti-histone H3 antibody. B) The knockdown of VRK1 was performed, during 72 hours, and using specific VRK1-siRNAs (siVRK1-02 = siV-02; siVRK1-03 = siV-03). A siRNA lacking a specific target (siControl = siC) was used as control. C) VRK1 knockdown was obtained after cell transduction with shRNAs (pLKO-shVRK1-01 = pLKO-sh1) and pLKO-shVRK1-03 = pLKO-sh3) and puromycin selection. The pLKO empty vector was used as negative control. D) Kinase assay with GST (pGEX-GST) and recombinant proteins GST-VRK1 (pGEX-GST-VRK1) or GST-AurKB (pGEX-GST-AurKB), and histone H3 as a substrate. Proteins were incubated for 30 minutes at 30ºC in presence of ATP. H3T3ph was detected, by immunoblot, with a rabbit polyclonal anti-H3T3ph and H3S10ph was detected, by WB, with a rabbit monoclonal anti-H3S10ph antibody (B, C and D).

As demonstrated, Thr3 residue on histone H3 is a specific phosphorylation site of VRK1 and histone H3-Ser10 residue is a direct phosphorylation site of AurKB. Since both kinases target distinct phosphorylation sites on the histone H3, the results obtained in the Figure 16 can be confirmed by kinase assay with cold ATP using human histone H3 as substrate and specific antibodies against its phosphorylations. Initially, we focused on the inhibitory effect of AurKB on VRK1 activity. So, a stable concentration GST-VRK1 was incubated alongside with increased concentrations of GST-AurKB or GST-AurKB-K106R and human histone H3 as substrate. Proteins were incubated for 30 minutes at 30ºC in

presence of ATP and H3T3ph was detected using a rabbit polyclonal anti-H3T3ph antibody. It was observed that AurKB affected negatively the phosphorylation of histone H3 by VRK1. This effect was independent of AurKB activity and was AurKB-dose dependent. The H3T3ph levels were quantified using *ImageJ* and represented in a graphic (Figure 18A and Figure 18B). Similarly, GST-VRK1 was incubated with increasing concentrations of inactive GST-AurKB-K106R and GST-p53 as substrate. Proteins were incubated for 30 minutes at 30ºC in the presence of ATP and p53T18ph was detected using a rabbit polyclonal anti-p53T18ph antibody. It was showed that VRK1 activity, on p53T18, decreased in the presence of AurKB (Figure 18C).

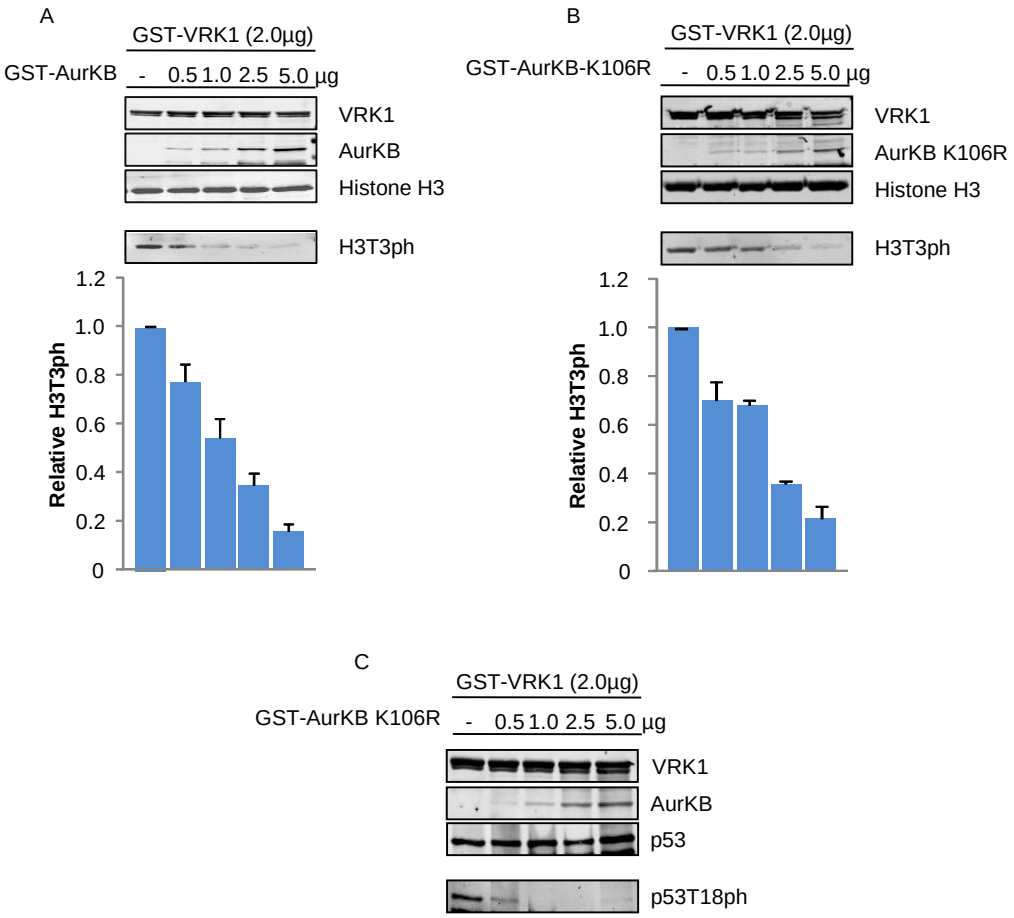

Figure 18. AurKB disturbs H3T3ph and p53T18ph by VRK1. The effect is independently of AurKB activity and is AurKB-dose dependent**.** A) Kinase assay with 2.0µg GST-VRK1 (pGEX-GST-VRK1), alongside with increasing doses (0.0, 0.5, 1.0, 2.5 and 5.0µg) of GST-AurKB (pGEX-GST-AurKB) and histone H3 as substrate. B) Kinase assay with 2.0µg GST-VRK1 (pGEX-GST-VRK1), alongside with increasing concentrations (0.0, 0.5, 1.0, 2.5 and 5.0µg) of inactive GST-AurKB-K106R (pGEX-GST-AurKB-K106R) and histone H3 as substrate. C) Kinase assay with 2.0µg GST-VRK1 (pGEX-GST-VRK1), alongside with increasing concentrations (0.0, 0.5, 1.0, 2.5 and 5.0µg) of inactive GST-AurKB-K106R (pGEX-GST-AurKB-K106R) and GST-p53 (pGEX-GST-p53) as substrate. Proteins were incubated for 30 minutes at 30ºC in presence of ATP. H3T3ph was detected using a rabbit polyclonal anti-H3T3ph antibody (A and B) and p53T18ph was detected using a rabbit polyclonal anti-p53T18ph antibody (C). The levels of H3T3ph were quantified with *ImageJ* and represent in a graphic (N=3).

Next, we focused on the inhibitory effect of VRK1 on AurKB activity. Thus, a fixed concentration of GST-AurKB was incubated with increased concentrations of GST-VRK1 or GST-VRK1-K179E, and human histone H3 as substrate. Proteins were incubated for 30 minutes at 30ºC in presence of ATP and H3S10ph

was detected using a rabbit monoclonal anti-H3S10ph antibody. It was perceived that VRK1 affected negatively the phosphorylation of histone H3 by AurKB. This effect was independent of VRK1 activity and was VRK1-dose dependent. The H3S10ph levels were quantified using *ImageJ* and represented in a graphic (Figure 19).

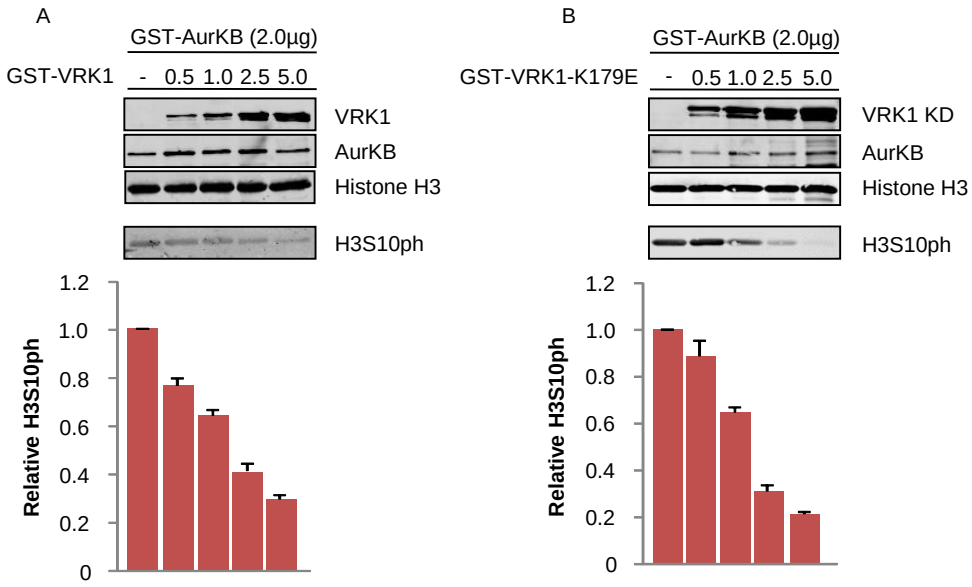

Figure 19. VRK1 disturbs H3S10ph by AurKB. The effect is independently of VRK1 activity and is VRK1-dose dependent. A) Kinase assay with 2.0µg GST-AurKB (pGEX-GST-AurKB), alongside with increasing doses (0.0, 0.5, 1.0, 2.5 and 5.0µg) of active GST-VRK1 (pGEX-GST-VRK1) and histone H3 as substrate. B) Kinase assay with 2.0µg GST-AurKB (pGEX-GST-AurKB), alongside with increasing doses (0.0, 0.5, 1.0, 2.5 and 5.0µg) of inactive GST-VRK1-K179E (pGEX-GST-VRK1-K179E) and histone H3 as substrate. Proteins were incubated for 30 minutes at 30ºC in presence of ATP. H3S10ph was detected using a rabbit monoclonal anti-H3S10ph antibody. The levels of H3S10ph were quantified with *ImageJ* and represent in a graphic (N=3).

Then, it was evaluated whether the knockdown of VRK1 affected the ability of AurKB to phosphorylate the Ser10 residue on histone H3 by kinase assay with cold ATP and specific antibody against H3S10ph. Since the presence of VRK1 inhibits AurKB, it was expected that the absence of VRK1 may increase the phosphorylation of H3S10 by AurKB. Therefore, endogenous AurKB was immunoprecipitated with a rabbit polyclonal anti-AurKB antibody, from HEK293T cells, in which VRK1 was downregulated during 72 hours with a siRNA (siVRK1-02). A siControl lacking a specific target was used as control and a non-specific

rabbit polyclonal anti-HA antibody was used as control of IP. Consequently, immunoprecipitated AurKB was incubated with human histone H3 as substrate for 30 minutes at 30ºC in the presence of ATP and H3S10ph was detected using a rabbit monoclonal anti-H3S10ph antibody. It was not observed any change on the phosphorylation levels of histone H3 by AurKB, after the knockdown of VRK1, comparing to the control (Figure 20).

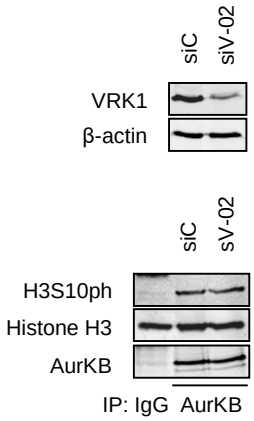

Figure 20. VRK1 knockdown does not affect the phosphorylation of histone H3 on the Ser10 residue by AurKB. VRK1 was depleted using a specific siRNA (siVRK1-02 = siV-02) and a siRNA lacking a specific target (siControl = siC) was used as control. Afterward, AurKB was immunoprecipitated with a rabbit polyclonal anti-AurKB and as control of IP it was used a rabbit polyclonal anti-HA antibody. Next, immunoprecipitated AurKB was used in a kinase assay with histone H3 as substrate. Proteins were incubated for 30 minutes at 30ºC in presence of ATP. H3S10ph was detected using a rabbit monoclonal anti-H3S10ph antibody and AurKB was detected using a rabbit monoclonal anti-AurKB antibody.

1.2 VRK1 interaction with AurKB

Next, we decided to analyze the potential interaction between both VRK1 and AurKB, since they are regulating, either by simply interaction or by interaction and direct phosphorylation, the kinase activity of one another. Thus, we studied the interaction between endogenous VRK1 and transfected AurKB protein in HEK293T cells. Likewise, we also evaluated whether transfected AurKA interacted with endogenous VRK1. Accordingly, the cells were transfected with both V5-AurKA and V5-AurKB plasmids and V5-tagged proteins were immunoprecipitated using a rabbit polyclonal anti-V5 antibody. VRK1 was

detected, by immunoblot, with a mouse monoclonal anti-VRK1 (1B5) antibody. We observed that endogenous VRK1 interacted with transfected AurKA and AurKB (Figure 21).

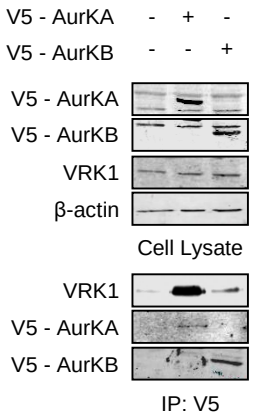

Figure 21. VRK1 endogenous protein interacts with transfected AurKA and AurKB. HEK293T cells were transfected with V5-AurKA (pDEST3.1_nV5-AurKA) and V5-AurKB (pcDNA3.1/nV5-DEST-AurKB) during 48 hours. Next, the extracts were immunoprecipitated with a rabbit polyclonal anti-V5 antibody. By immunoblot, VRK1 was detected using a mouse monoclonal anti-VRK1 (1B5) antibody and V5-tagged aurora kinases were detected using a mouse monoclonal anti-V5 antibody.

Even though VRK1 interacted also with AurKA we decided to pursuit the studies only with AurKB, since AurKB was described previously to phosphorylate or affect indirectly the same VRK1 phosphorylation residues on histone H3 (Thr3 and Ser10), and thereby it seemed more likely to share with VRK1 some mitotic regulatory mechanisms (Carmena and Earnshaw, 2003).

Subsequently, we confirm the interaction between transfected VRK1 and transfected AurKB through IP and pull-down assay. Firstly, HA-VRK1 and V5-AurKB were transfected in HeLa cell line. Then, HA-VRK1 was immunoprecipitated using a rabbit polyclonal anti-HA antibody. V5-AurKB was detected, by WB, using a mouse monoclonal anti-V5 antibody, confirming that both kinases interacted (Figure 22A). Moreover, GST-VRK1 active and GST-VRK1-K179E inactive were transfected with V5-AurKB in HEK293T cells. Pull-down experiments confirm that AurKB and VRK1 formed a stable complex and that this interaction was independent of VRK1 activity (Figure 22B). Similar result was obtained by IP assay. (Figure 22C).

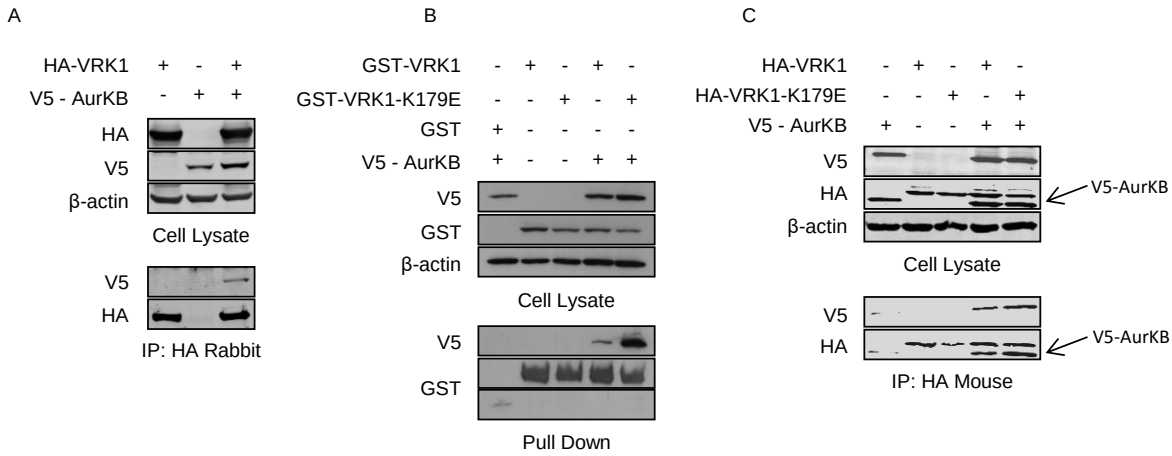

Figure 22. VRK1 interacts with AurKB. The interaction is independent of VRK1 activity. A) HeLa cells were transfected with V5-AurKB (pcDNA3.1/nV5-DEST-AurKB) and HA-VRK1 (pCEFL HA-VRK1). Cell extracts were immunoprecipitated with a rabbit polyclonal anti-HA antibody and AurKB was detected, by immunoblot, with a mouse monoclonal anti-V5 antibody. B) HEK293T cells were transfected with V5-AurKB (pcDNA3.1/nV5-DEST-AurKB) and with GST-VRK1 (pCEFL-GST-VRK1) or GST-VRK1-K179E (pCEFL-GST-VRK1 K179E). Cell extracts were incubated with glutathione sepharose overnight and AurKB was detected, by immunoblot, with a mouse monoclonal anti-V5 antibody. C) HEK293T cells were transfected with V5-AurKB (pcDNA3.1/nV5-DEST-AurkB) and with HA-VRK1 (pCEFL-HA-VRK1) or HA-VRK1 K179E (pCEFL-HA-VRK1 K179E). VRK1 proteins were immunoprecipitated with a mouse monoclonal anti-HA antibody and AurKB was detected using a rabbit polyclonal anti-V5 antibody.

Moreover, we intended to analyze the VRK1 region with which AurKB interacted. Thus, HEK293T cells were transfected with V5-AurKB and with myc-tagged VRK1 plasmids coding for different protein regions: VRK1 wild type (pCDNA3.1-VRK1-myc (1-396)), VRK1 large amino terminal (pCDNA3.1-VRK1-myc-LA (1-332)), VRK1 short amino terminal (pCDNA3.1-VRK1-myc-SA (1-267)) and VRK1 carboxy terminal (pCEFL-GST-VRK1-C (267-396)). After V5-AurKB IP, VRK1 proteins were detected using antibodies anti-myc or anti-GST. We observed that the interaction of AurKB occurred with all the four VRK1 constructions. This results suggests that AurKB interacts with both the amino and carboxy terminals of VRK1 (Figure 23).

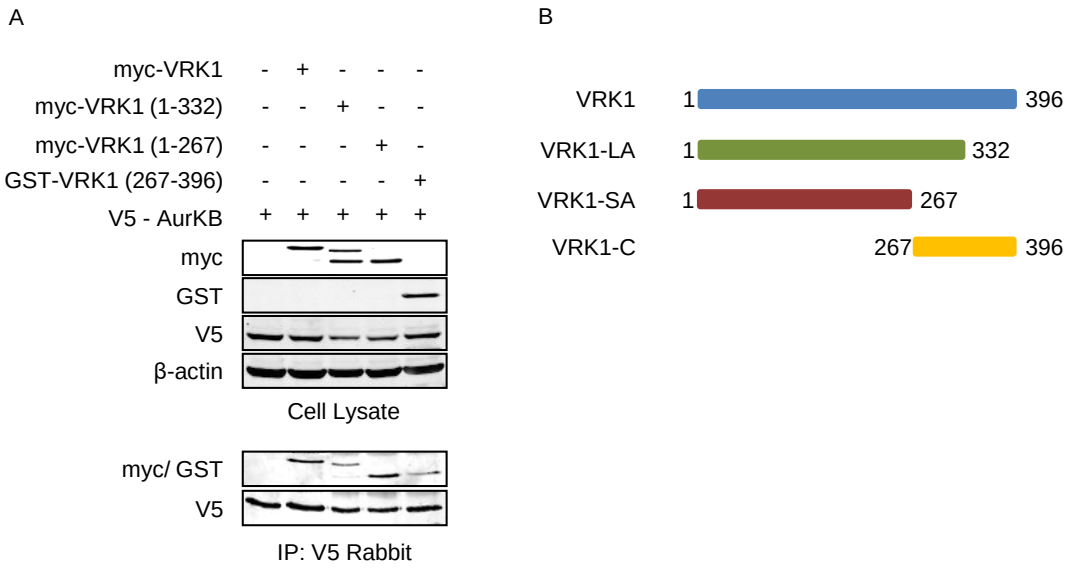

Figure 23. VRK1 interacts trough both amino and carboxy terminal regions with AurKB. A) HEK293T cells were transfected, with V5-AurKB (pcDNA3.1/nV5-DEST-AurKB) and with different VRK1 plasmids: VRK1 wild type (pCDNA3.1-VRK1-myc (1-396)), VRK1 large amino terminal (pCDNA3.1-VRK1-myc-LA (1-332)), VRK1 short amino terminal (pCDNA3.1-VRK1-myc-SA (1-267)) and VRK1 carboxy terminal (pCEFL-GST-VRK1-C (267-396)). V5-AurKB was immunoprecipitated with a rabbit polyclonal anti-V5 antibody and VRK1 proteins were detected, by WB, with a mouse monoclonal anti-myc antibody or with a mouse monoclonal anti-GST antibody. B) Schematic representation of VRK1 plasmids used in the immunoprecipitation assay.

Next, we aim to analyze the interaction between both endogenous VRK1 and AurKB protein kinases, since the interaction was quite consistent between the two transfected proteins. Accordingly, HeLa cells were lysed and endogenous VRK1 was immunoprecipitated using a mouse monoclonal anti-VRK1 (1B5) antibody, which recognizes mainly the nuclear VRK1 population. Nonetheless in these conditions and, oppositely to what was expected, AurKB protein kinase was not detected, by immunoblot, in the VRK1 immunoprecipitate (Figure 24).

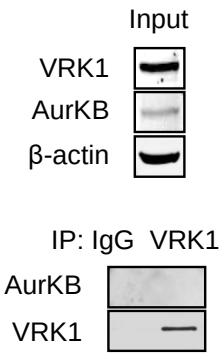

Figure 24. Endogenous VRK1 does not interact with endogenous AurKB in unsynchronized cells. HeLa cells were lysed and VRK1 was immunoprecipitated with a mouse monoclonal anti-VRK1 (1B5) antibody. A mouse monoclonal anti-HA antibody was used as control of IP (IgG). AurKB was analyzed, by WB, using a rabbit monoclonal anti-AurKB antibody.

It is known that AurKB localization and levels depend on the cell cycle stage in which the cell are (Ruchaud et al., 2007). Thus, we confirm this observation, by IF, in HeLa cell line. Indeed, we observed that AurKB levels increase significantly from interphase to mitosis, and that the kinase localization change during mitosis. Initially AurKB seems to localize in the chromatin arms and potentially in centromeres, changing its localization during the metaphase to anaphase transition, moving to the spindle midzone (Figure 25).

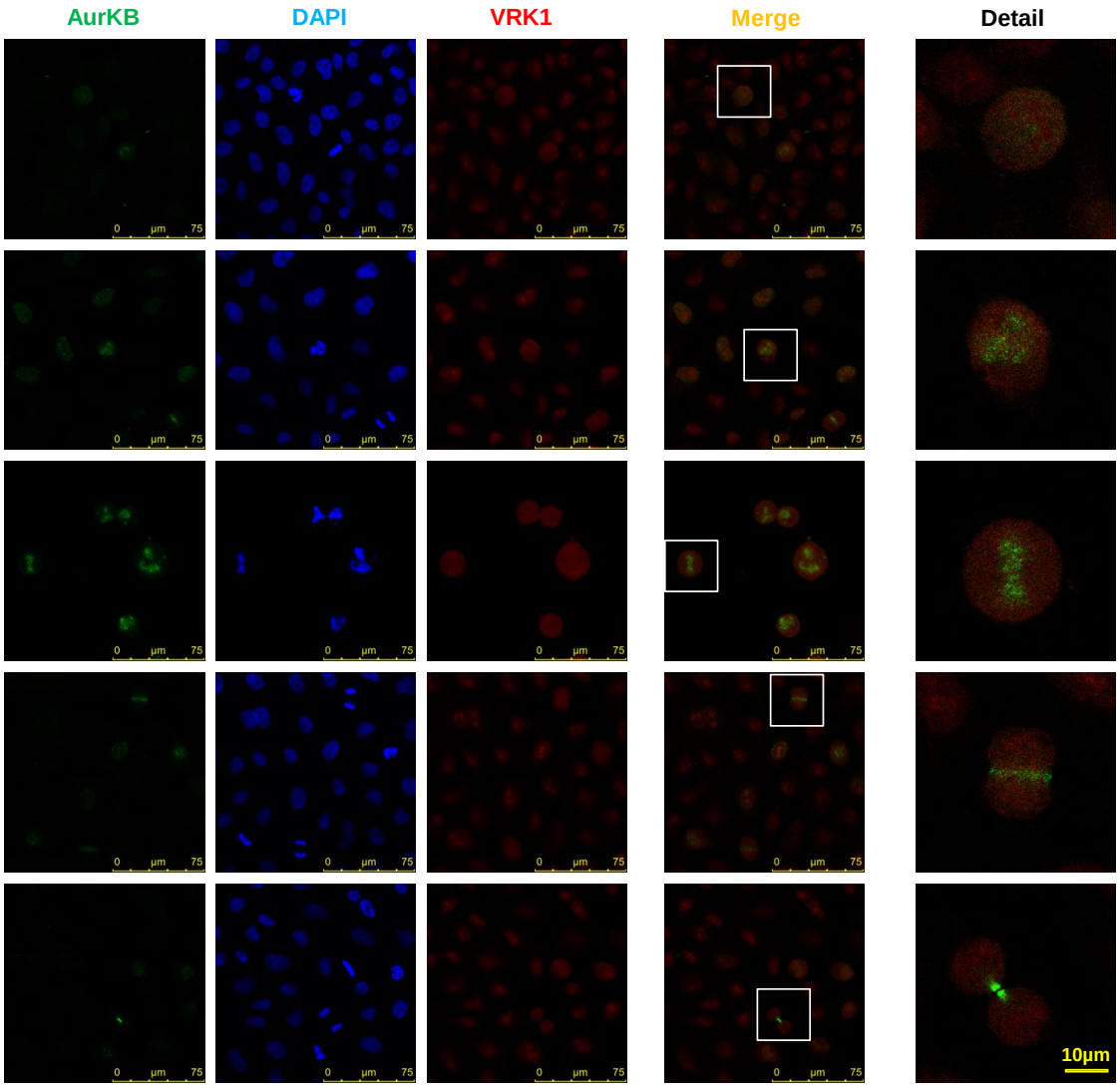

Figure 25. The levels and localization of AurKB are cell cycle-dependent. In HeLa cells, VRK1 was detected with a mouse monoclonal anti-VRK1 (1B5) antibody and AurKB was detected using a rabbit monoclonal anti-AurKB antibody. Chromatin was stained with DAPI.

Consequently and since AurKB levels and localization depends on cell cycle phase (Figure 25), we decided to analyze the interaction between VRK1 and AurKB in the context of cell cycle. Therefore, we arrested U2OS cells at different time points of cell division: at G0-early G1, by serum starvation during 72 hours, in S phase after double thymidine block and in early mitosis after double thymidine block, followed by 13 hours nocodazole treatment. Moreover and to obtain cells at different points of mitosis, the cells were released from nocodazole arrest and harvested 30, 60, 90, 180, 360 and 720 minutes post the release. The mechanism by which thymidine and nocodazole caused cell cycle arrest is

described in the chapter 11 of material and methods and the alteration made in the cell line used, was due to the fact that osteosarcoma U2OS cell line was more suitable to perform cell cycle arrest experiments, compared to HeLa cell line. VRK1 was immunoprecipitated with a mouse monoclonal anti-VRK1 (1B5) antibody and AurKB was detected, by immunoblot, with a rabbit monoclonal anti-AurKB antibody. Acid extracted histone H3 phosphorylations were detected, by immunoblot, with a rabbit polyclonal anti-H3T3ph antibody and a rabbit monoclonal anti-H3S10ph antibody. It was observed that VRK1-AurKB complex appeared in cells arrested with nocodazole, decreasing considerably 60 minutes after drug release (Figure 26A). At this point, as observed by FACS, the majority of the cells are in mitosis, suggesting that the interaction between VRK1 and AurKB occurs in mitosis (Figure 26B).

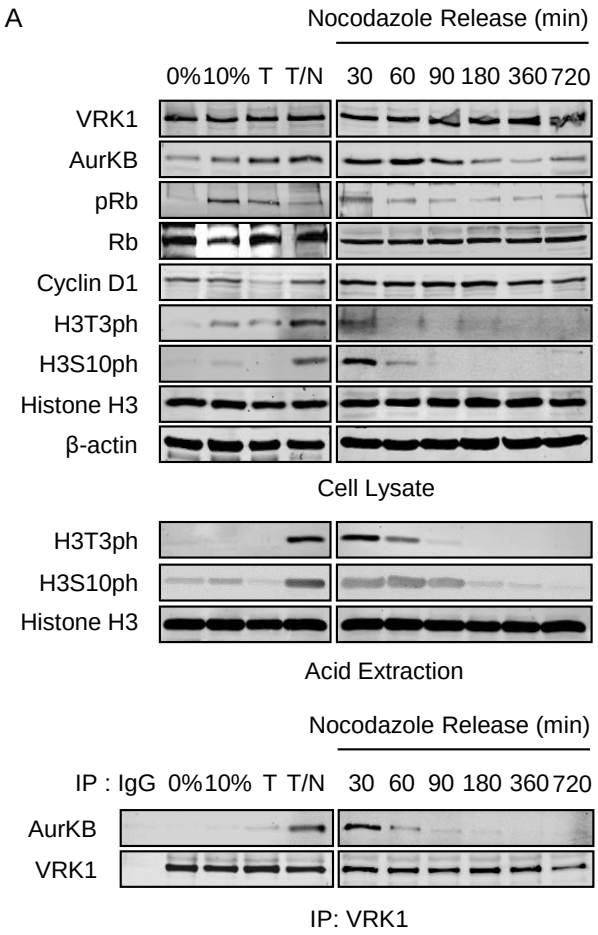

B

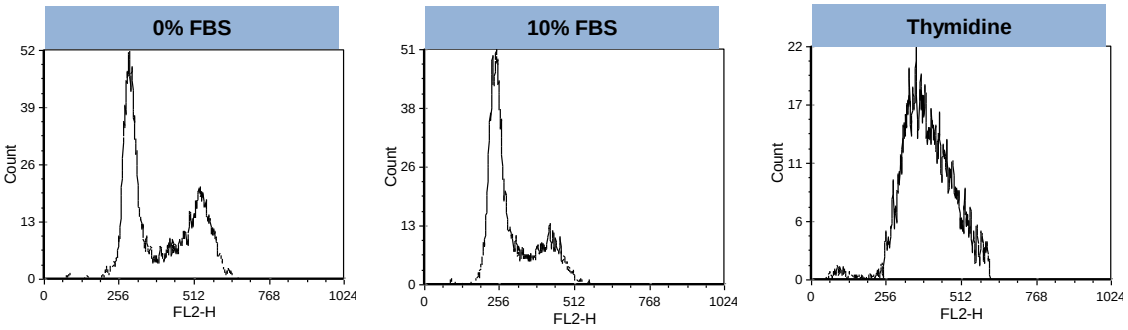

Cell Cycle Phase	%
G0/G1	51,07
G1/S	10,68
G2/M	33,68

Cell Cycle Phase	%
G0/G1	65,65
G1/S	9,46
G2/M	20,43

Cell Cycle Phase	%
G0/G1	45,73
G1/S	36,82
G2/M	11,55

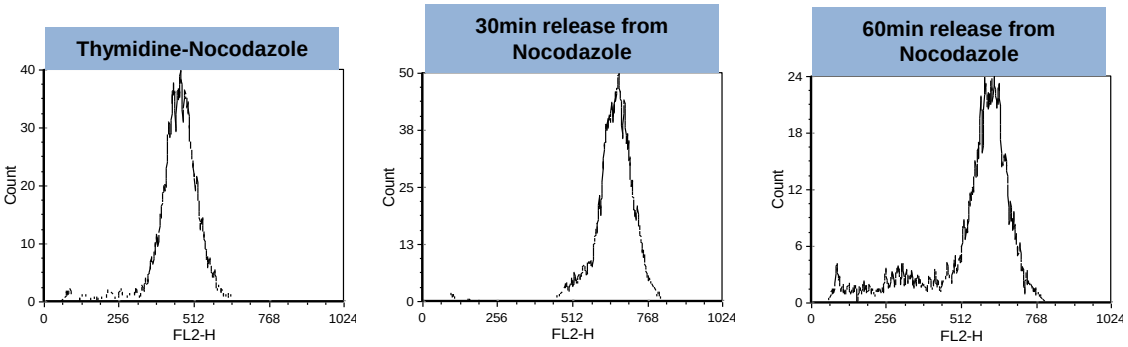

Cell Cycle Phase	%
G0/G1	2,80
G1/S	0,72
G2/M	93,48

Cell Cycle Phase	%
G0/G1	1,11
G1/S	0,30
G2/M	95,75

Cell Cycle Phase	%
G0/G1	10,70
G1/S	1,27
G2/M	80,50

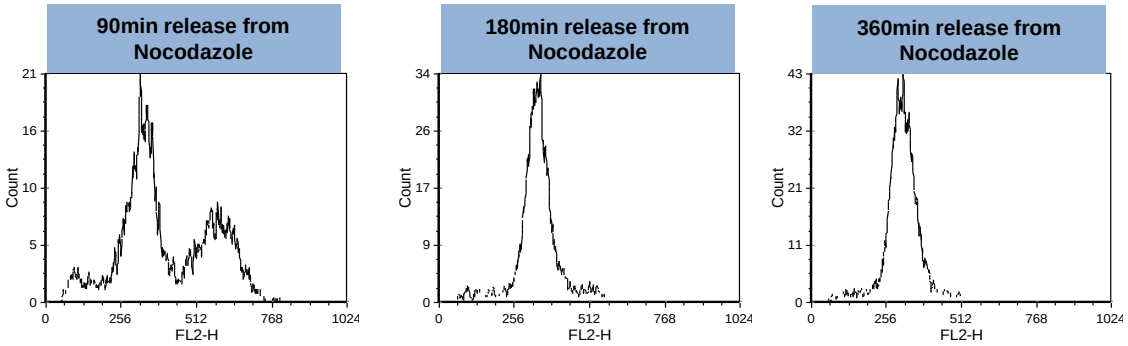

Cell Cycle Phase	%
G0/G1	50,86
G1/S	1,84
G2/M	36,18

Cell Cycle Phase	%
G0/G1	87,47
G1/S	1,61
G2/M	4,81

Cell Cycle Phase	%
G0/G1	92,54
G1/S	0,95
G2/M	1,42

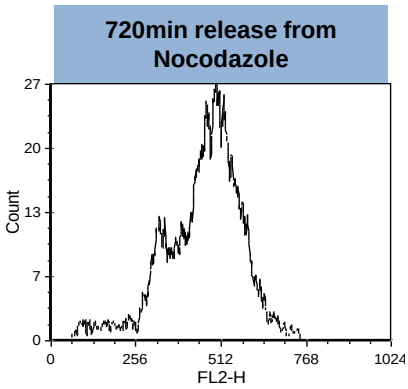

Cell Cycle Phase	%
G0/G1	14,89
G1/S	11,74
G2/M	64,65

Figure 26. VRK1 interacts with AurKB during mitosis. A) U2OS cells were arrested at G0/G1 (0%) with serum-free medium for 72 hours, arrested in S phase (T) after double thymidine block or in early mitosis (T/N) after double thymidine block followed by nocodazole arrest. Furthermore, the cells were released from nocodazole arrest during 720 minutes, being the cells harvested at different time periods (30, 60, 90, and 180, 360 and 720 minutes). Unsynchronized cells (10%) were maintained in normal conditions during the time of the experiment. Next, the extracts were immunoprecipitated with a mouse monoclonal anti-VRK1 (1B5) antibody or with a mouse monoclonal anti-HA antibody as IP control (IgG). By immunoblot, AurKB was detected using a rabbit monoclonal anti-AurKB antibody and VRK1 was detected using a rabbit polyclonal anti-VRK1 antibody. B) FACS analysis.

Next, we decided to study which population of VRK1 and AurKB was interacting. It is known that VRK1 is a chromatin-associated kinase involved in chromatin remodeling, affecting histone post-translational modifications, such as phosphorylation, acetylation and methylations. Still, VRK1 is also detected in the cytoplasm and in the nucleoplasm as we confirmed here (Figure 27A) (Salzano et al., 2015). In turn, AurKB was described to be associated with centromeric chromatin, in the early stages of mitosis, and was also identified in the cytoplasm (Murata-Hori and Wang, 2002; Wang et al., 2010). Therefore, we had executed a fractionation cytoplasm, nucleoplasm and chromatin with nocodazole arrested cells to analyze which kinases population participates in the complex formation. Nocodazole arrest cell cycle in early mitosis, more precisely at prometaphase. Since the nuclear membrane was disrupted in prophase and it is impossible to differentiate between cytoplasm and nucleoplasm, both fractions were taken into account together and named cytoplasm. After U2OS cell fractionation, each fraction was immunoprecipitated with a mouse monoclonal anti-VRK1 (1B5) antibody and AurKB was detected, by immunoblot, with a rabbit monoclonal anti-AurKB antibody. It was observed that VRK1 and AurKB interacted independently of their localization, in nocodazole arrested cells (Figure 27B). Unsynchronized

cells were used as control of synchronization and α-tubulin and histone H3 as cytoplasm and chromatin markers, respectively.

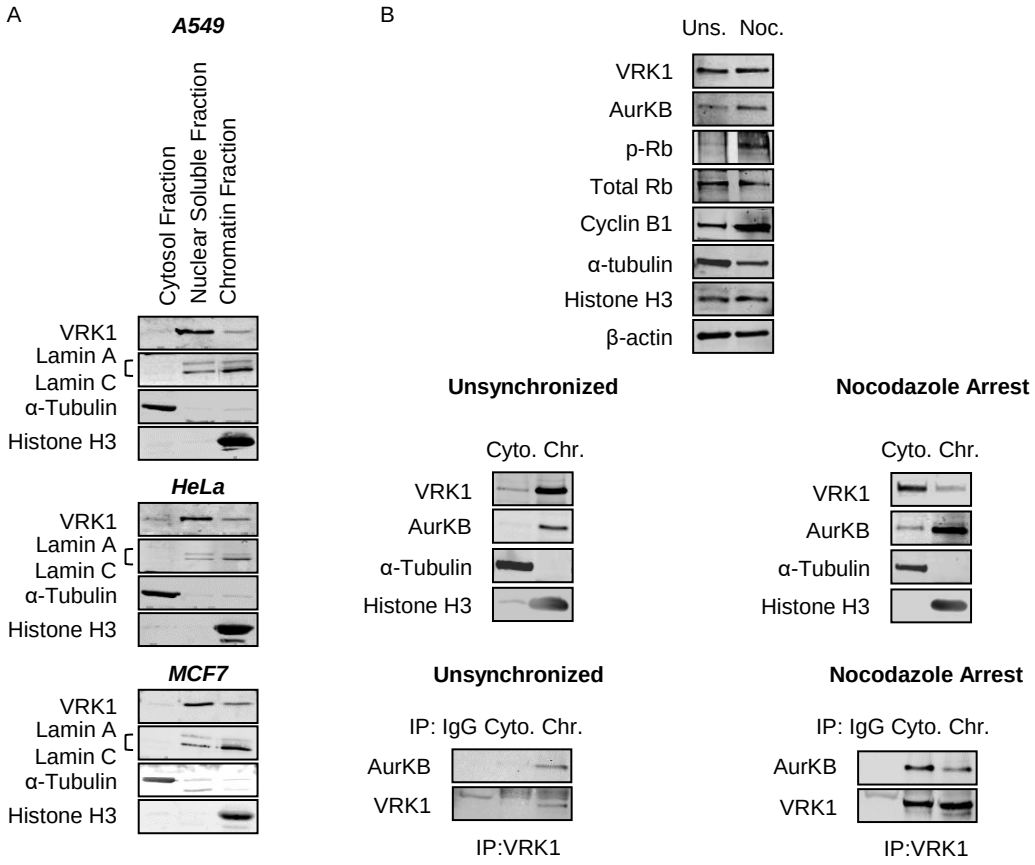

Figure 27. VRK1 and AurKB interaction is independent of their localization. A) VRK1 was detected in the cytoplasm, nucleoplasm and chromatin fractions in A549, HeLa and MCF7 cell line after cell fractionation. B) U2OS cells were fractionated and VRK1 was immunoprecipitated, from unsynchronized and nocodazole arrested cells, with a mouse monoclonal anti-VRK1 (1B5) antibody or with a mouse monoclonal anti-HA antibody (IgG) as control. AurKB was detected, by immunoblot, using a rabbit monoclonal anti-AurKB antibody. A-tubulin and histone H3 were used as cytoplasm and chromatin controls, respectively. Uns. = Unsynchronized. Noc. = Nocodazole arrest. Cyto. = Cytoplasm and nucleoplasm fractions. Chr. = Chromatin fraction.

Besides the phosphorylation of histone H3 on Thr3 and Ser10, we decided to analyze additional histone H3 modifications, such as H3K4me3, H3K9me3, H3K9ac and H3K14ac in the context of cell cycle. So, HeLa cells were arrested at G0/G1 through 72 hours of serum starvation, in S-phase through double thymidine block and in early mitosis after double thymidine block, followed by 13 hours of treatment with nocodazole. Besides and to obtain cells at different stages

of mitosis, the cells were nocodazole-released and harvested 30, 60, 90, 180, 360 and 720 minutes after the release. Histone H3 was detected using a rabbit polyclonal anti-histone H3 antibody, H3K4me3 was detected using a rabbit polyclonal anti-H3K4me3, H3K9me3 was detected using a rabbit polyclonal anti-H3K9me3 antibody, H3K9ac was detected using a rabbit polyclonal anti-H3K9ac antibody and H3K14ac was detected using a rabbit polyclonal anti-H3K14ac antibody. VRK1 and AurKB were detected with a mouse monoclonal anti-VRK1 (1F6) antibody and a rabbit monoclonal anti-AurKB antibody, respectively. Nevertheless, it was not perceived any extraordinary result, besides the fact that H3K9me3 seems to vary inversely to H3S10ph (histone crosstalk) as previous described (Figure 28) (Bannister and Kouzarides, 2011).

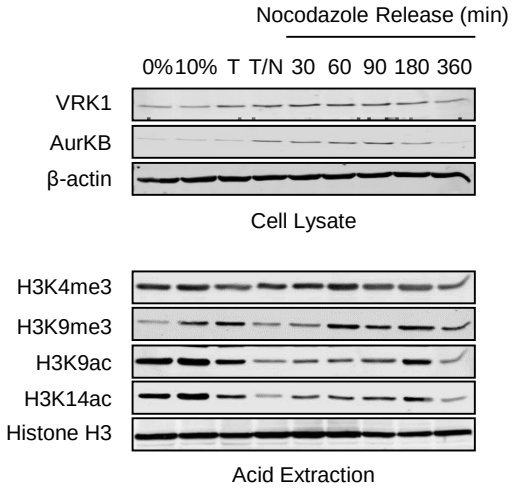

Figure 28. Histone H3 post-translational modifications during cell cycle. H3K9me3 seems to fluctuate inversely to H3S10ph. Histones were extracted using an acid extraction protocol, from HeLa cells synchronized at different stages of cell cycle, as explained in Figure 21.

1.3 VRK1 co-localization with AurKB during cell cycle

Afterward, VRK1 and AurKB co-localization was analyzed in U2OS and HeLa cell line, by IF. Since both the kinases interacted during mitosis (Figure 26), it was expected that VRK1 and AurKB co-localize during any mitotic stage. Concerning U2OS cell line, the cells were arrested at G0/G1 by serum starvation during 72 hours, in S-phase with double thymidine block and in early mitosis after double thymidine block, followed by 13 hours of nocodazole treatment. Moreover and to obtain cells at different points of mitosis, the cells were released from

nocodazole arrest and harvested 30, 60, 90, 180, 360 and 720 minutes post the release. VRK1 was detected using two different antibodies recognizing different kinase populations. It was used a mouse monoclonal anti-VRK1 (1B5), which recognizes specifically the nuclear VRK1 population (Figure 29A) and a mouse monoclonal anti-VRK1 (1F6) that recognizes specifically the cytoplasmic VRK1 population (Figure 29B). AurKB was detected using a rabbit monoclonal anti-AurKB antibody and the chromatin was stained with DAPI. The co-localization studies were performed in a *Leica TCS SP5* inverted fluorescence microscope connected to a digital video camera used to obtain the confocal microscopy images, which were analysed using the *LAS AF Lite*. In both cases, it was not observed any co-localization between VRK1 and AurKB at any stage of cell division cycle in U2OS (Figure 29).

Similar results were obtained in HeLa cell line. Once again, HeLa cells were arrested at G0-early G1 through serum starvation during 72 hours, in S-phase after double thymidine block and in early mitosis after double thymidine block, followed by 13 hours of nocodazole treatment. Then and to attain cells at different stages of mitosis, the cells were released from nocodazole arrest and harvested 30, 60, 90, 180, 360 and 720 minutes after being released. VRK1 was detected using the same two mouse monoclonal anti-VRK1 (1B5) and anti-VRK1 (1F6) antibodies, AurKB was detected with a rabbit monoclonal anti-AurKB antibody and chromatin was stained with DAPI (Figure 30). The representation of Figure 30 was elaborated distinctly from Figure 29, due to the fact that HeLa cell line showed a larger cell cycle comparing with U2OS cell line. So, in HeLa cells, each experimental point represented mostly a cell cycle stage, whereas in U2OS cells each experimental point included various mitotic stages, which made it impossible to attribute to each experimental point a stage of mitosis. Co-localization analysis was executed drawing a straight line on the more likely co-localization site, and evaluated directly with the specific tool provided by *LAS AF Lite* software (Figure 30C).

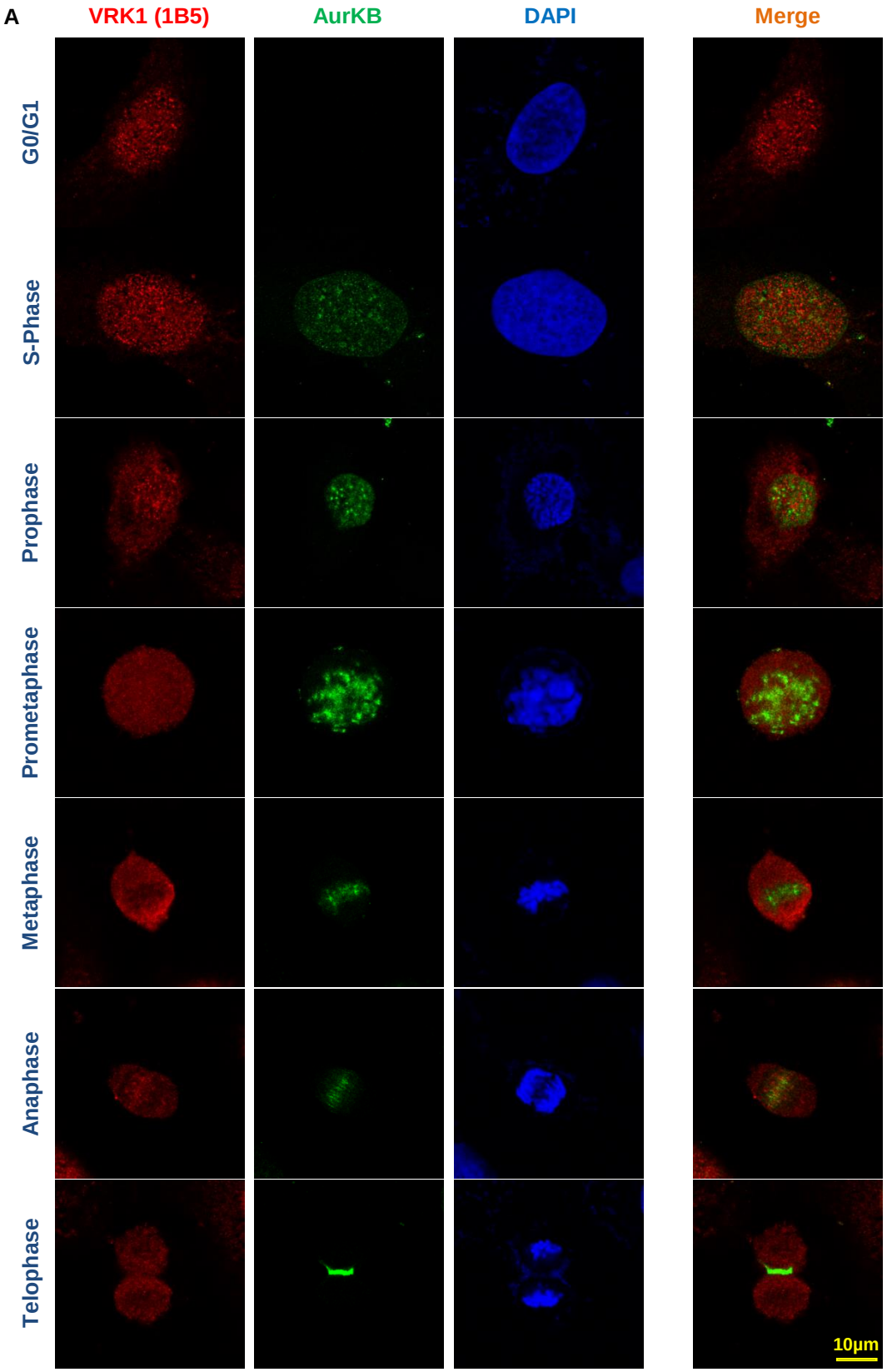
A
VRK1 (1B5)
AurKB
DAPI
Merge
G0/G1
S-Phase
Prophase
Prometaphase
Metaphase
Anaphase
Telophase
10µm

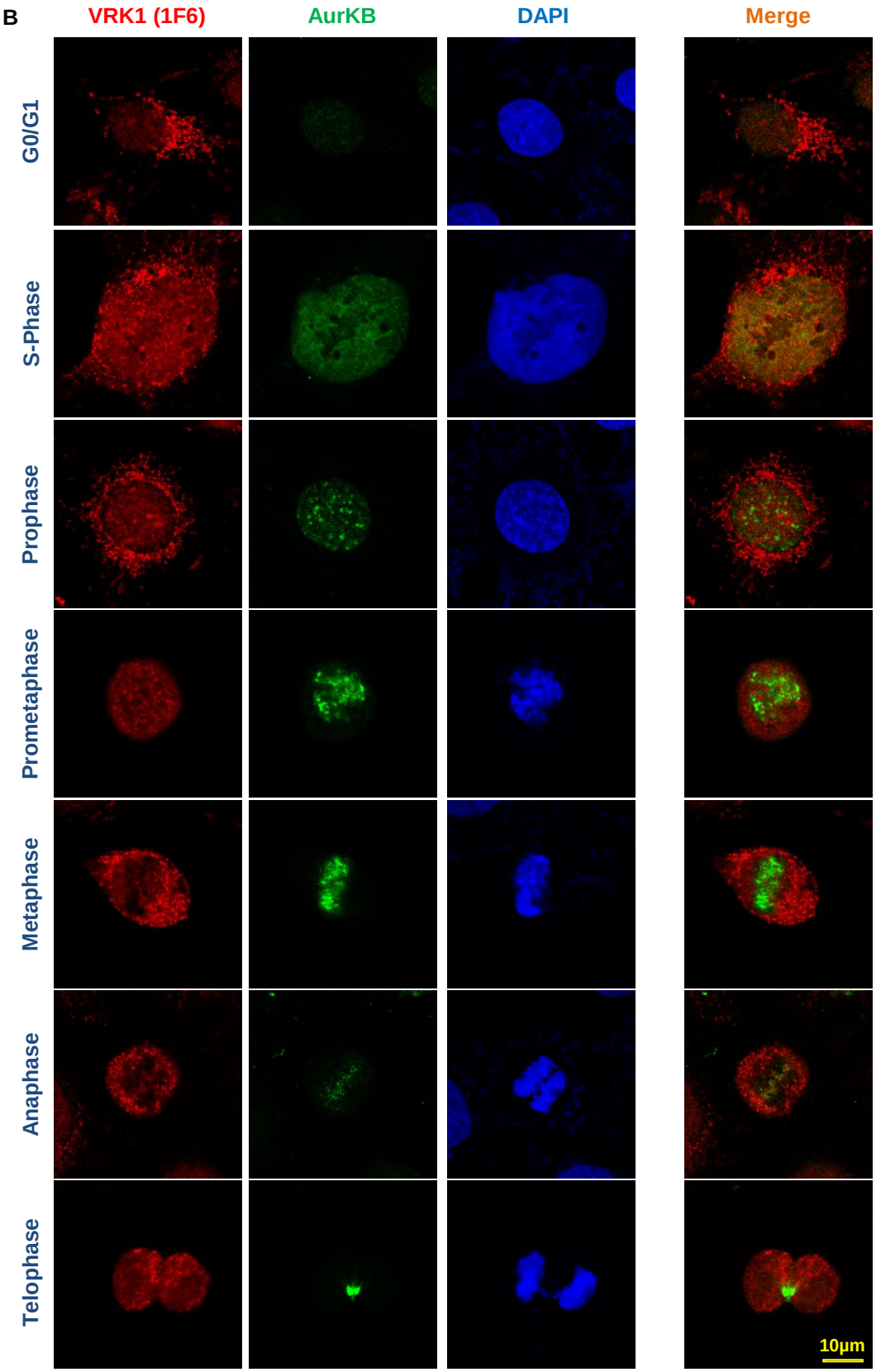
B
VRK1 (1F6)
AurKB
DAPI
Merge
G0/G1
S-Phase
Prophase
Prometaphase
Metaphase
Anaphase
Telophase
10μm

Figure 29. VRK1 and AurKB don’t co-localize in U2OS cell line. U2OS cells, arrested at each point of cell cycle, were analyzed by IF. The protocol used was the same of Figure 26. VRK1 was detected with a mouse monoclonal anti-VRK1 (1B5) antibody (A) or with a mouse monoclonal anti-VRK1 (1F6) antibody (B). AurKB was detected using a rabbit monoclonal anti-AurKB antibody. Chromatin was stained with DAPI.

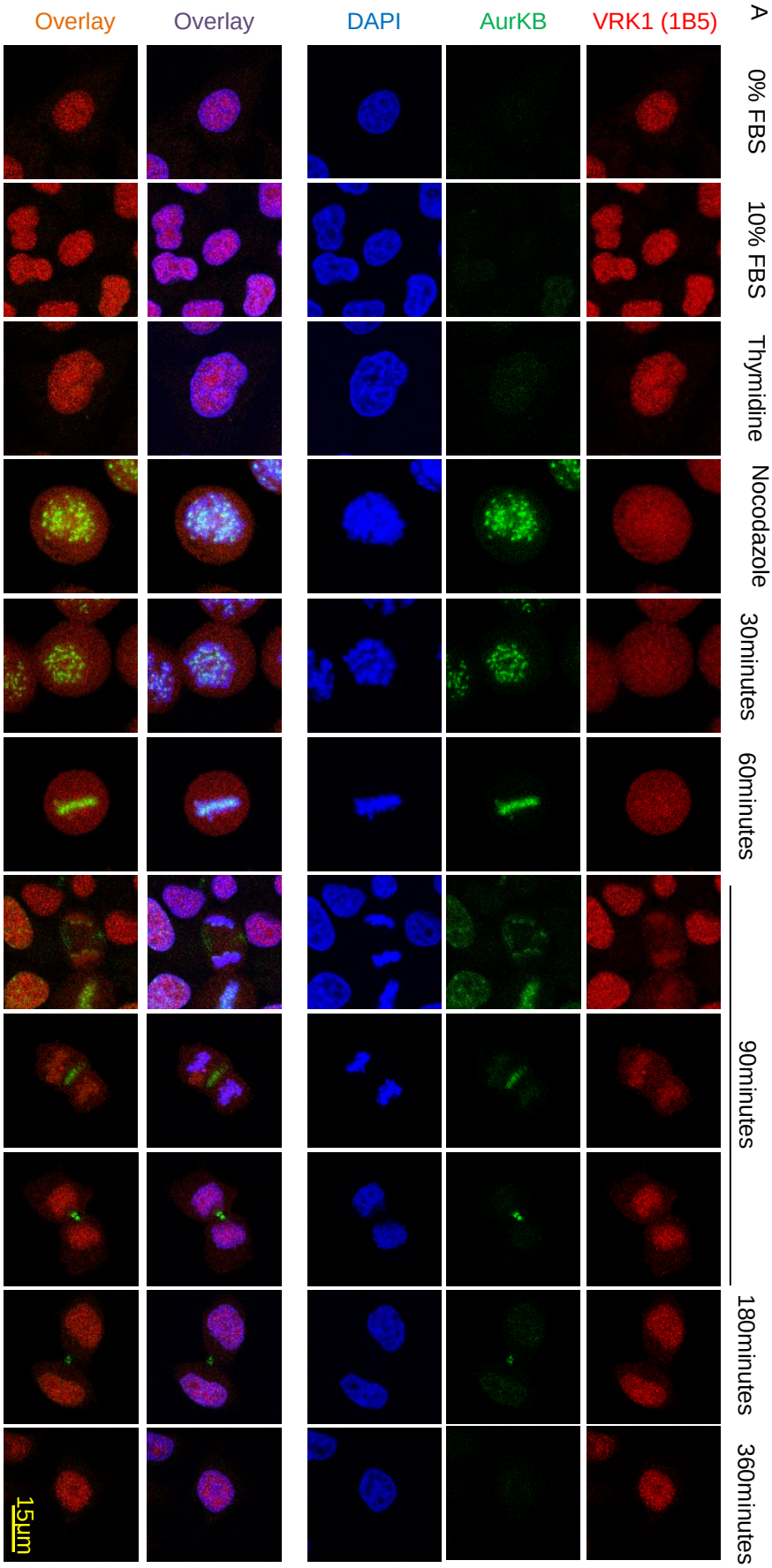
A
VRK1 (1B5)
AurKB
DAPI
Overlay
Overlay
0% FBS
10% FBS
Thymidine
Thymidine/ Nocodazole
30minutes
60minutes
90minutes
180minutes
360minutes
Nocodazole Release
15µm

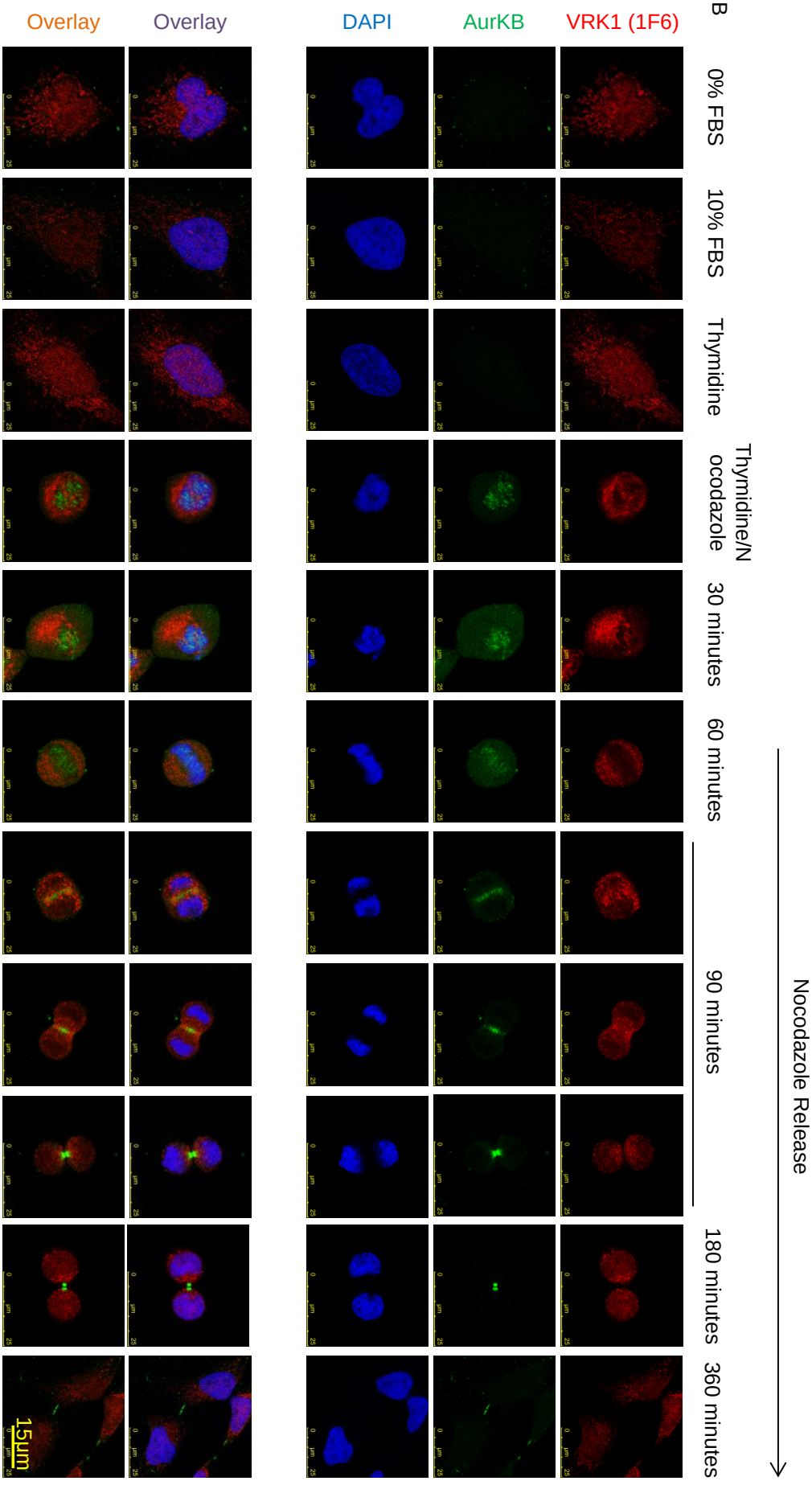
B
VRK1 (1F6)
AurKB
DAPI
Overlay
Overlay
0% FBS
10% FBS
Thymidine
Thymidine/Nocodazole
30 minutes
60 minutes
90 minutes
180 minutes
360 minutes
Nocodazole Release
15µm

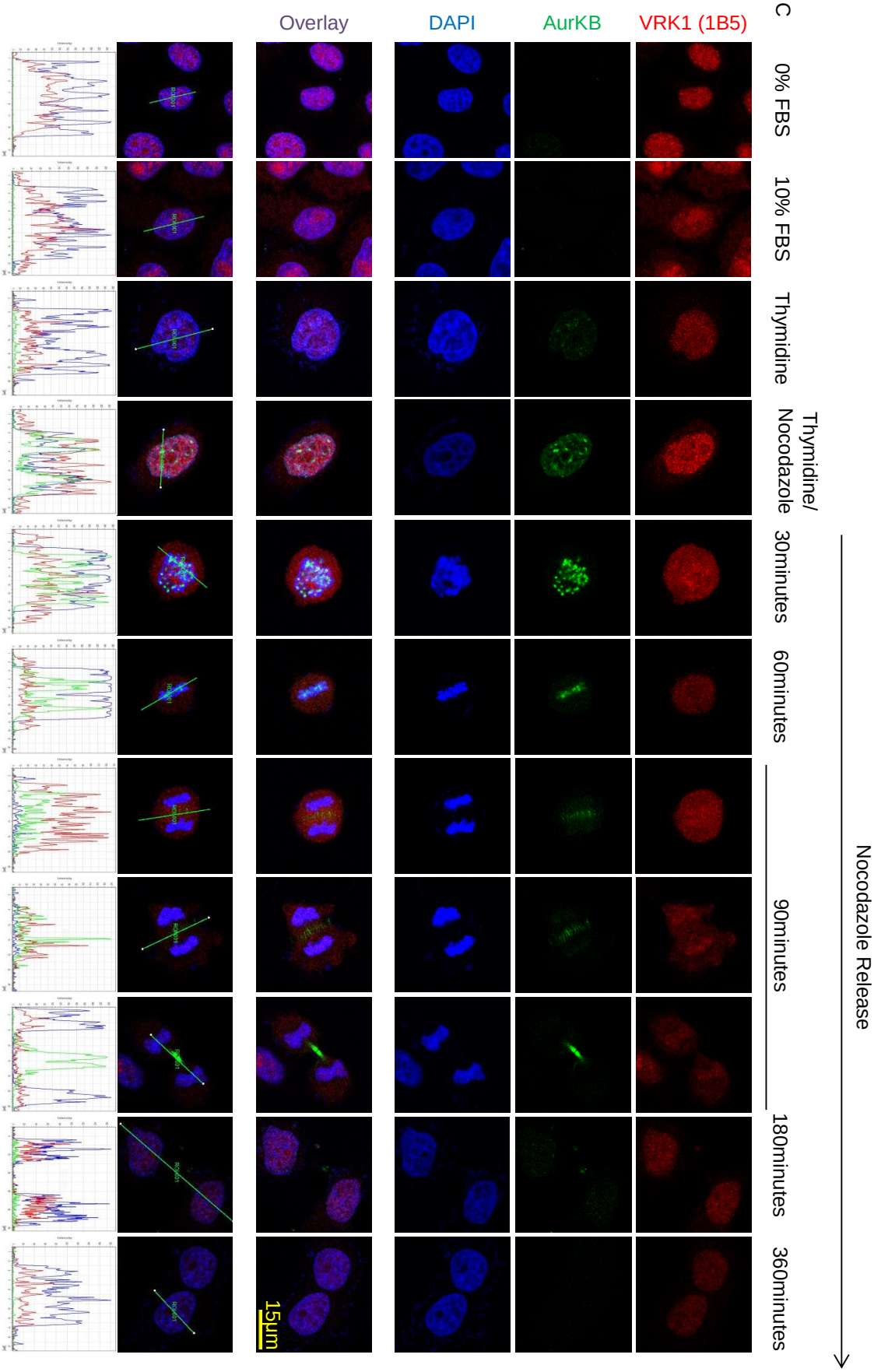
VRK1 (1B5)
AurKB
DAPI
Overlay
C
0% FBS
10% FBS
Thymidine
Thymidine/
Nocodazole
30minutes
60minutes
90minutes
180minutes
360minutes
Nocodazole Release
15µm

Figure 30. VRK1 and AurKB don't co-localize in HeLa cell line. HeLa cells were analyzed, by IF, after being arrested at different stages of cell cycle. The protocol used was the same of Figure 26. VRK1 was detected with a mouse monoclonal anti-VRK1 (1B5) antibody (A and C) or with a mouse monoclonal anti-VRK1 (1F6) antibody (B). AurKB was detected using a rabbit monoclonal anti-AurKB antibody. Chromatin was stained with DAPI. Co-localization studies were performed drawing a straight line on the potential co-localization site, and analyzed directly with the specific tool provided by *LAS AF Lite* software (C).

Moreover, it is known that phosphorylation of histone H3 on the Thr3 residue is critical for the localization of CPC/ AurKB in centromeres, in the early stages of mitosis, and that during metaphase to anaphase transition, AurKB re-locates to the midzone spindle, in line with a decrease in H3T3ph (Carmena and Earnshaw, 2003; Wang et al., 2010; Wang et al., 2011). Therefore we intended to verify, by IF, such behavior of H3T3ph in U2OS and HeLa cell lines and confirm that the in fact AurKB re-location and H3T3ph decrease may be related. Besides, immunoblot data showed a quick decline in H3T3ph, after nocodazole release, which is consistent with the loss of VRK1-AurKB interaction (Figure 26A). So, it could be important to analyze H3T3ph in the context of cell cycle, to limit the stages of mitosis in which both the kinases interact. H3S10ph, which is a phosphorylation AurKB-dependent and occurs mostly during mitosis, was used as control of antibody specificity. The protocol used to arrest cells at distinct points of mitosis was the same as previous described in this chapter and VRK1 was detected using a mouse monoclonal anti-VRK1 (1B5) antibody, H3T3ph was detected using a rabbit polyclonal anti-H3T3ph and H3S10ph was detected using a rabbit monoclonal anti-H3S10ph antibody. DAPI was used to stain chromatin. Indeed, it was observed that H3T3ph appeared early in mitosis and lasted until anaphase (Figure 31A and Figure 31C), and this correlates with the change observed in AurKB localization (Figure 29 and Figure 30). In turn, H3S10ph decreased continuously during cell cycle, but histone phosphorylation was still detectable in the late phases of mitosis, in U2OS cell line (Figure 31B). Yet, in HeLa cell line maybe due the slighter stain of H3S10ph, it seemed to disappear during the anaphase to telophase transition (Figure 31D). Unfortunately, H3T3ph, H3S10ph and AurKB antibodies were all from the same species and co-

localization studies were limited. Due to the same motive previously mentioned, U2OS and HeLa cell line figures were alternatively represented.

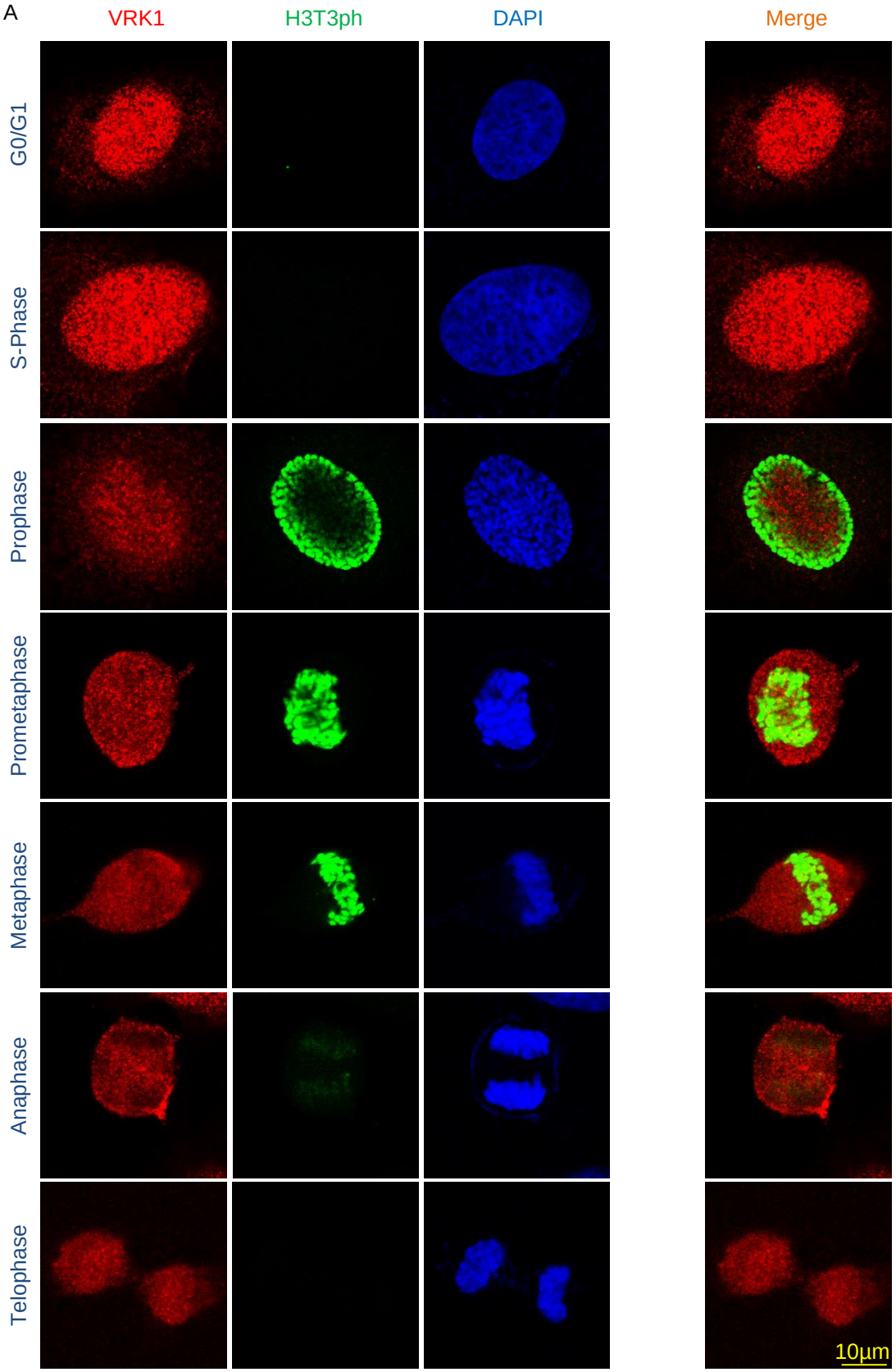

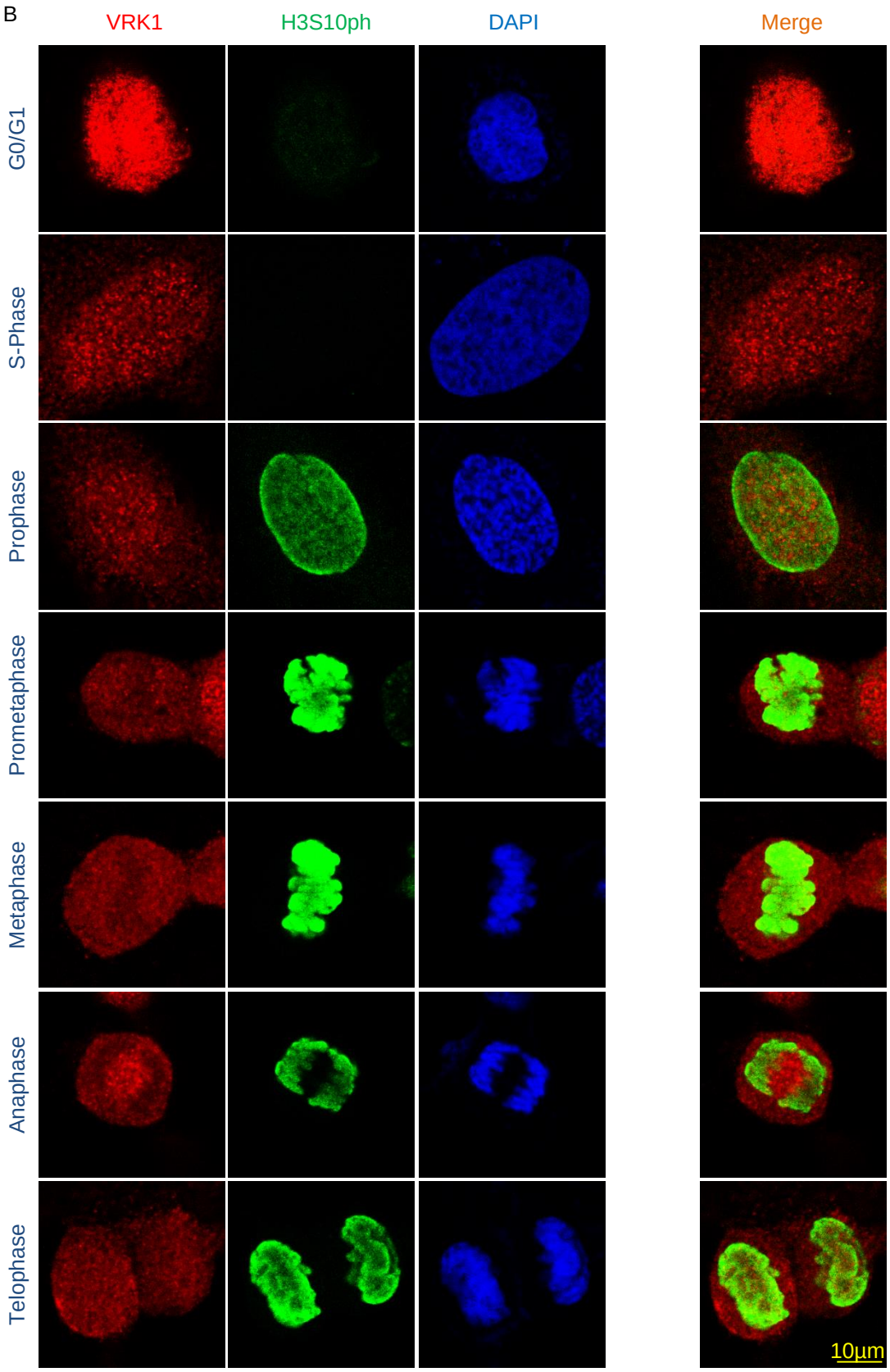
B
VRK1
H3S10ph
DAPI
Merge
G0/G1
S-Phase
Prophase
Prometaphase
Metaphase
Anaphase
Telophase
10µm

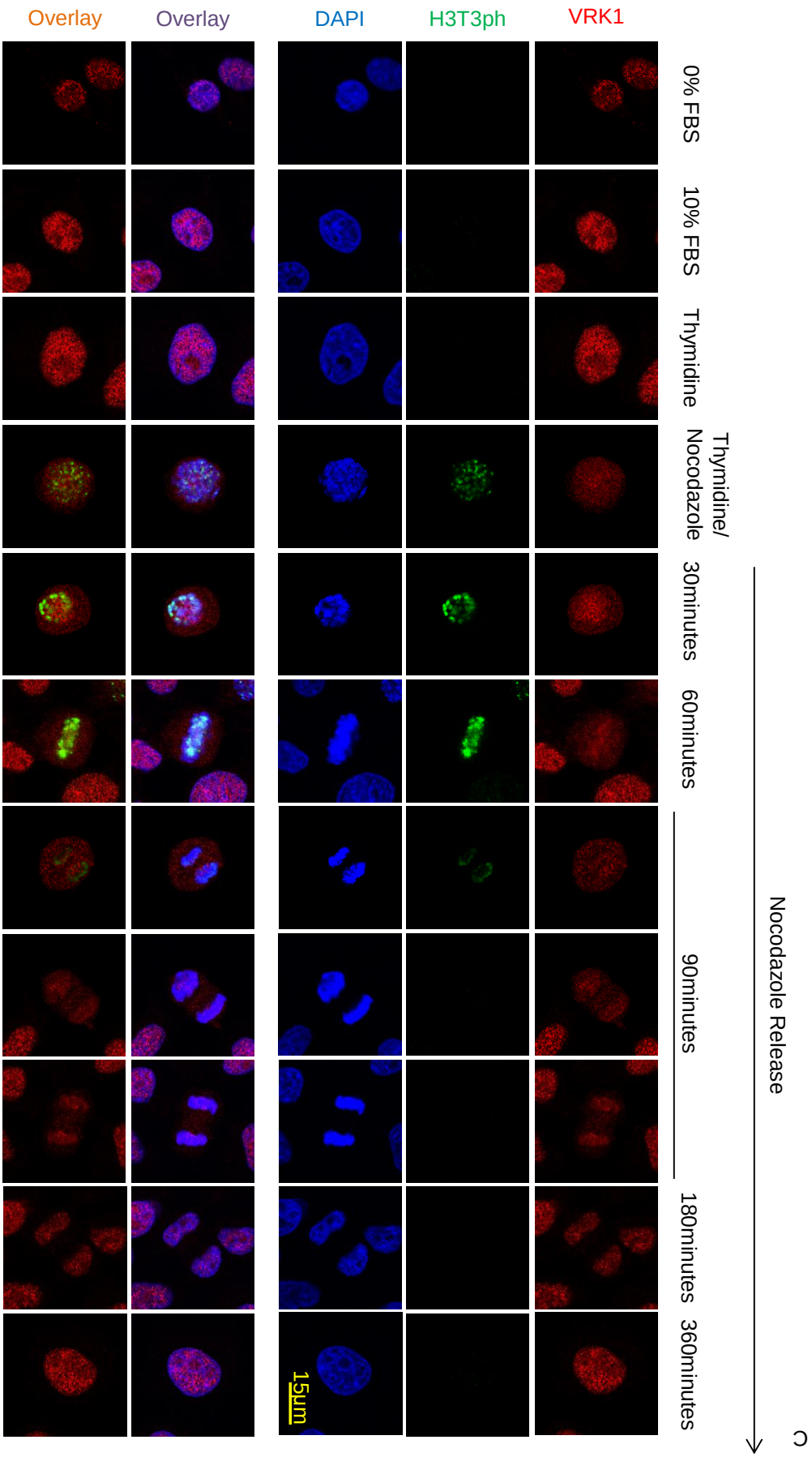
Overlay
Overlay
DAPI
H3T3ph
VRK1
0% FBS
10% FBS
Thymidine
Thymidine/ Nocodazole
30minutes
60minutes
90minutes
180minutes
360minutes
Nocodazole Release
C
15μm

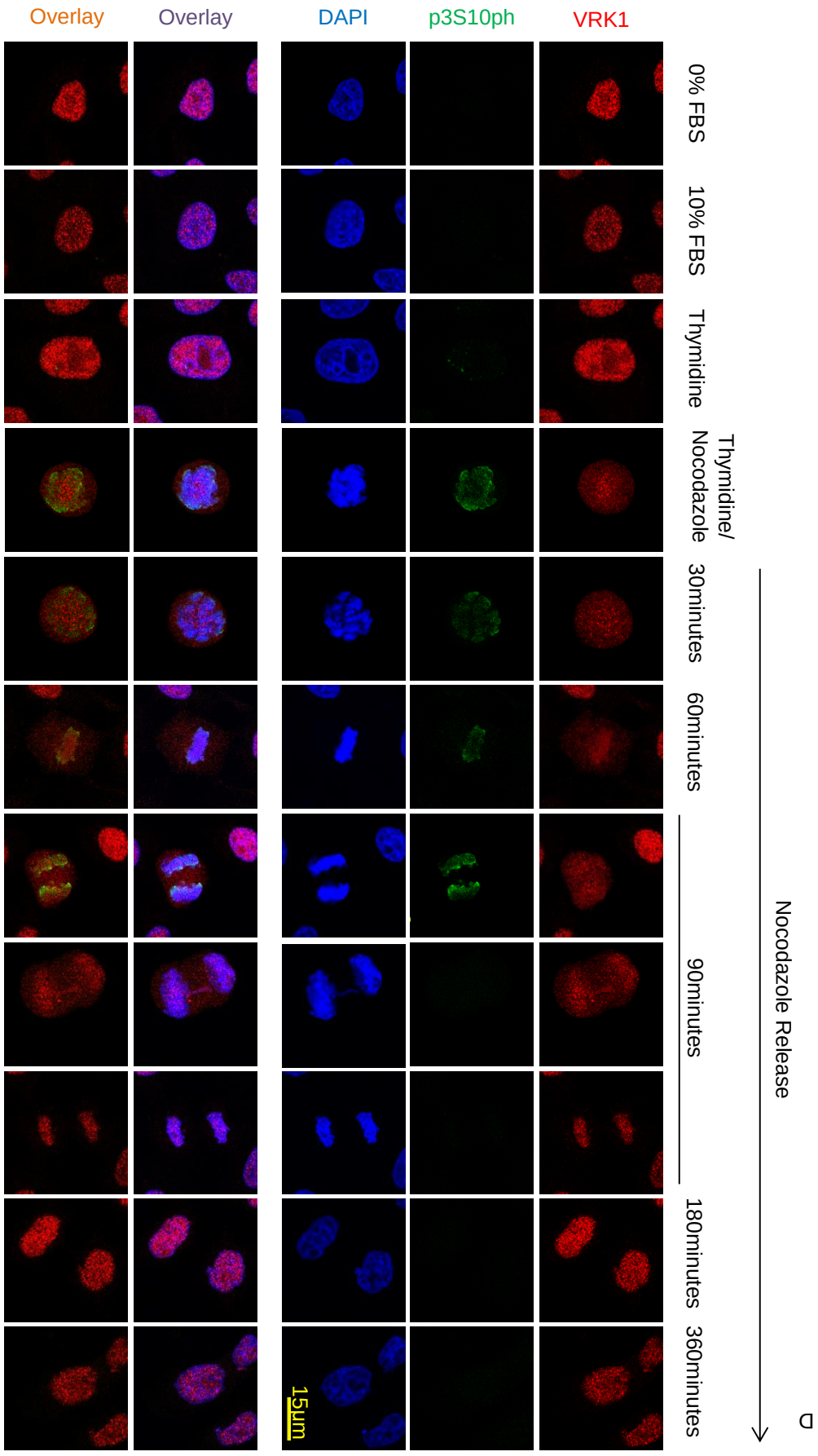
Overlay
Overlay
DAPI
p3S10ph
VRK1
0% FBS
10% FBS
Thymidine
Thymidine/ Nocodazole
30minutes
60minutes
90minutes
180minutes
360minutes
Nocodazole Release
15um

Figure 31. H3T3ph and H3S10ph levels during cell cycle. U2OS (A and B) and HeLa (C and D) cell lines were analyzed, by IF, after being arrested at different stages of cell cycle. The protocol used was the same of Figure 26. VRK1 was detected with a mouse monoclonal anti-VRK1 (1B5) antibody, H3T3ph was detected using a rabbit polyclonal anti-H3T3ph antibody (A and C) and H3S10ph was detected using a rabbit monoclonal anti-H3S10ph antibody (B and D). Chromatin was stained with DAPI.

1.4 Regulation of kinase activity by phosphorylation

At this point we knew that VRK1 and AurKB formed a stable complex during mitosis, which affected the kinase activity of one another. Furthermore, it is recognized that VRK1 is a highly active kinase that phosphorylates numerous substrates such as p53, histone H3, coilin, histone H2A.X or CREB (Cantarero et al., 2015; Kang et al., 2007b; Salzano et al., 2015; Vega et al., 2004a). Also, AurKB is very active during mitosis, and phosphorylates various protein substrates such as histone H3 and MCAK or even other protein kinases like Haspin and ATM (Hirota et al., 2005; Wang et al., 2011; Yang et al., 2011; Zhang et al., 2007). Thus, it is likely that these two kinase may be regulating one another by direct phosphorylation. Accordingly, there were performed two separated kinase assays with radiolabeled ATP to verify whether VRK1 phosphorylates AurKB or if AurKB phosphorylates VRK1. Similar experiment was performed initially, to the Figure 16, but we expected to discard that the presence of histone H3 on the mix, in combination with VRK1 and AurKB recombinant proteins, could weight on the result obtained.

First, GST-AurKB-K106R was incubated with GST-VRK1 and GST-p53 was used as positive control. We observed that AurKB was not a direct substrate of VRK1 (Figure 32A) in such conditions. Secondly, inactive GST-VRK1-K179E was incubated with GST-AurKB and purified human histone H3 was used as positive control. Again, the result was negative, meaning that VRK1 was not an AurKB-direct substrate in these conditions (Figure 32B). Both kinase assays were performed in the presence of cold ATP and radiolabeled ATP [γ-^{32}P] and were incubated in a thermomixer at 30ºC during 30 minutes.

Once again, we detected a slight decrease in the autophosphorylation of both active VRK1 (Figure 32A) and AurKB (Figure 32B), when incubated

combined. This observation confirmed that the interaction between the two kinases affected the kinase capability of one another.

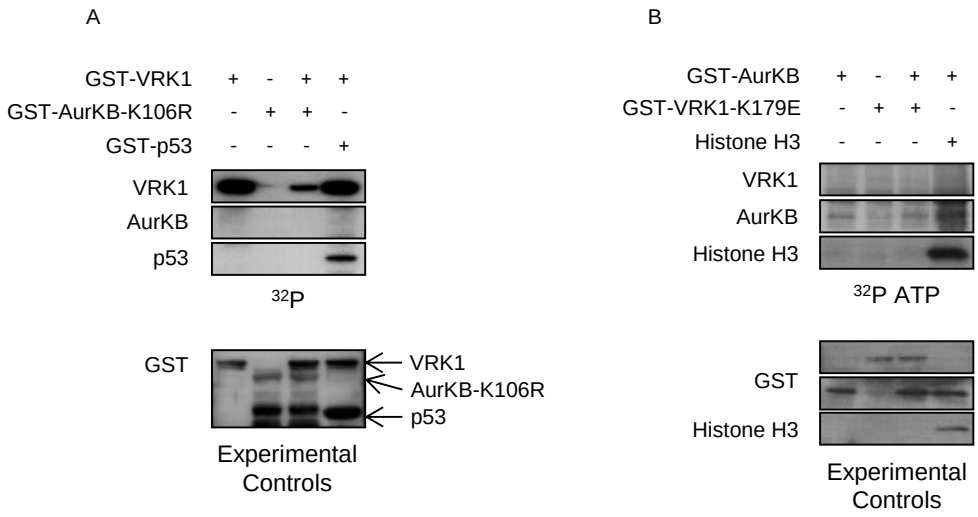

Figure 32. A) AurKB is not a direct substrate of VRK1. B) VRK1 is not a direct substrate of AurKB. A) A) Inactive GST-AurKB-K106R (pGEX-GST-AurKB-K106R) was incubated with GST-VRK1 (pGEX-GST-VRK1) and with GST-p53 (pGEX-GST-p53) as positive control. B) Inactive GST-VRK1-K179E (pGEX-GST-VRK1-K179E) was incubated with GST-AurKB (pGEX-GST-AurKB) and purified human histone H3 was used as positive control. Both kinase assays were performed in the presence of cold ATP and radiolabeled [γ-^{32}P] ATP, in a thermomixer at 30ºC during 30 minutes. The incorporated radioactivity was detected exposing the ray-x film to the membranes.

1.5 VRK1 effect on the ubiquitination and stability of AurKB

Furthermore, we had also analyzed the potential role of VRK1 on the ubiquitination and stability of AurKB, since both kinases are peculiarly connected through the mitotic process. It is known that ubiquitination of AurKB regulates the CPC/ AurKB localization in the central spindle during anaphase or the kinase degradation (Maerki et al., 2009; Teng et al., 2012). In turn, VRK1 had been demonstrated to protect coilin from ubiquitination and degradation in the proteasome (Cantarero et al., 2015). Accordingly, VRK1 may also be relevant in the stabilization of AurKB levels, regulating the ubiquitination of the kinase. Initially, the effect of VRK1 downregulation on the AurKB ubiquitination was performed in HEK293T cells, in the presence or absence of MG132, a specific, potent and reversible proteasome inhibitor. Briefly, cells were first transfected

with a siRNA targeting VRK1 (siVRK1-02), or with a siRNA (siControl) lacking a specific target. Next day, the same cells were transfected with V5-AurKB and HA-Ubiquitin, and 36 hours later they were treated ON with 20µM MG132. MG132 non-treated cells were maintained as part of experiment as control of drug efficiency. Then, from cells extracts treated or not-treated with MG132, V5-AurKB was immunoprecipitated with a mouse monoclonal anti-V5 antibody or HA-Ubiquitin was immunoprecipitated with a rabbit polyclonal anti-HA antibody. V5-AurKB was detected, by immunoblot, with a mouse monoclonal anti-V5 antibody or with a rabbit polyclonal anti-V5 antibody. HA-Ubiquitin was detected, by immunoblot, with a mouse monoclonal anti-HA antibody or with a rabbit polyclonal anti-HA antibody. The choice of antibody used in the immunoblot depended of the antibody used in the IP, to minimize cross-reactivity between antibodies from the same species. It was observed that VRK1 knockdown led to a decrease in AurKB polyubiquitination (over 70 kDa), independently of MG132 treatment, after HA-Ubiquitin IP. The same result is observed after IP of V5-AurKB, in MG132 treated cells, but is not perceptible in MG132 non-treated cells. Nevertheless, it was observed that VRK1 knockdown induced an overall protein ubiquitination decrease in cell lysate comparing to the control (Figure 33).

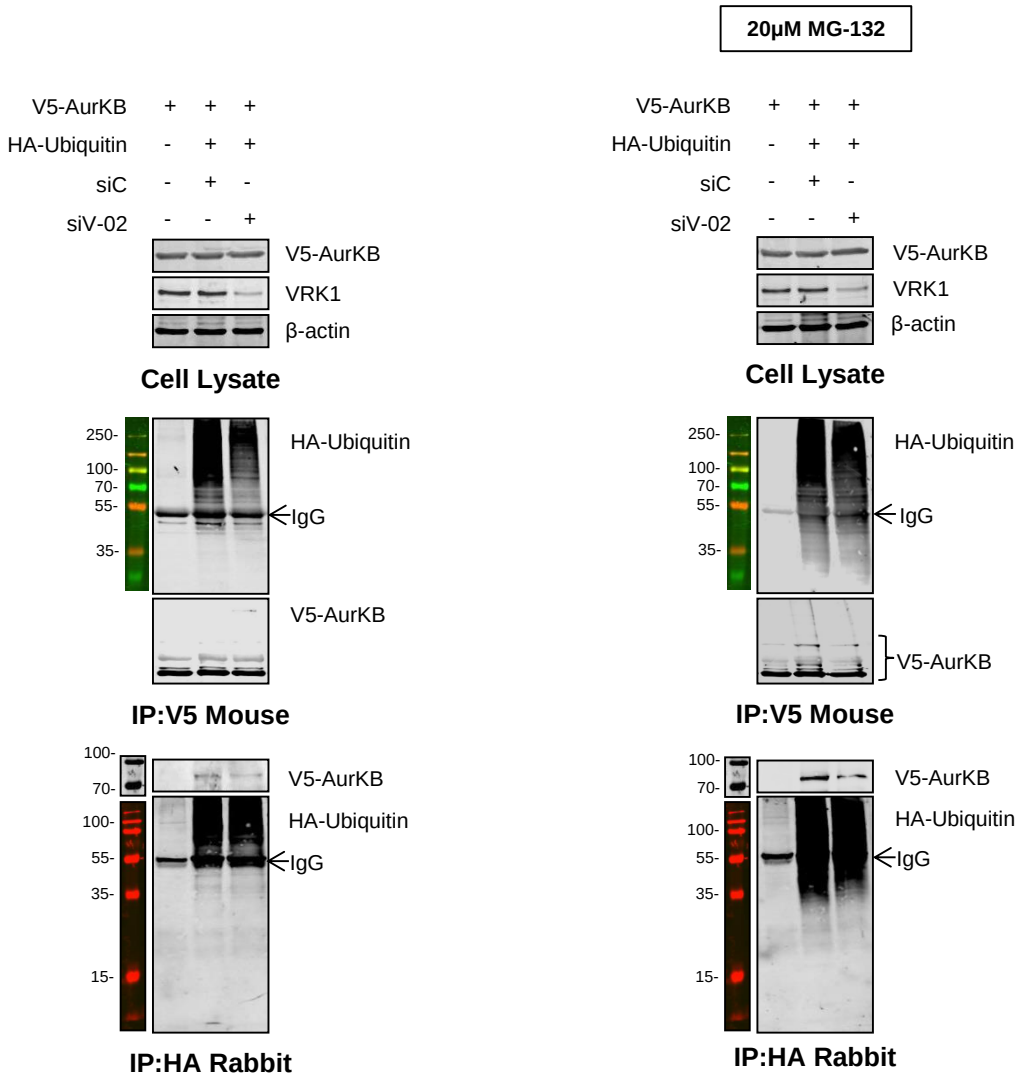

Figure 33. VRK1 knockdown interferes with AurKB ubiquitination. VRK1 was downregulated, in HEK293T cells, using a specific VRK1-siRNA (siVRK1-02 = siV-02) and a siRNA lacking a specific target (siControl = siC) was used as control. Then, V5-AurKB (pcDNA3.1/nV5-DEST-AurKB) and HA-Ubiquitin (pSSK-HA-Ubiquitin) were transfected and later the cells were overnight treated with MG132. MG132 non-treated cells were also used as part of experiment. Next, V5-AurKB was immunoprecipitated with a mouse monoclonal anti-V5 and HA-Ubiquitin was immunoprecipitated with a rabbit polyclonal anti-HA antibody. V5-AurKB was detected, by immunoblot, with a mouse monoclonal anti-V5 antibody or with a rabbit polyclonal anti-V5 antibody. HA-Ubiquitin was detected, by immunoblot, with a mouse monoclonal anti-HA antibody or with a rabbit polyclonal anti-HA antibody.

Afterwards, AurKB stability was evaluated in VRK1 overexpression and knockdown conditions, by CHX chase assay. VRK1 was downregulated, during 72 hours, using a particular VRK1-siRNA (siVRK1-02), and a non-specific siRNA

was used as control (siControl). On the other hand, HA-VRK1 was overexpressed alongside with V5-AurKB, during 48 hours. Empty vector was used as control and transfected together with V5-AurKB. Once CHX was added, the cells were harvest at different times (4, 8, 12 and 24 hours) and the extracts processed.

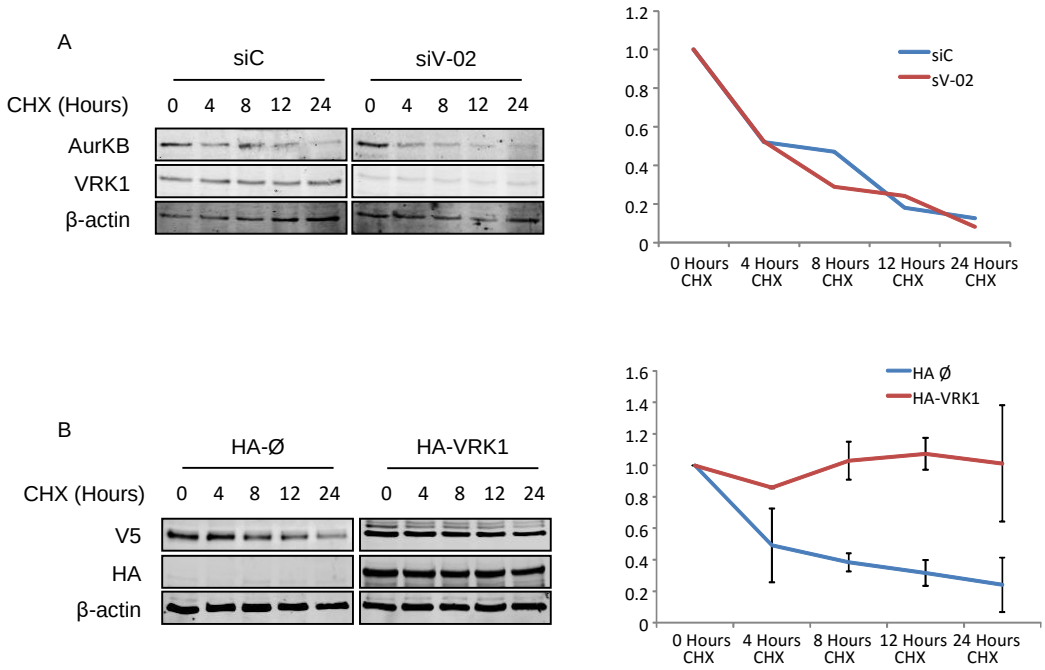

Figure 34. VRK1 overexpression stabilizes transfected AurKB, but VRK1 knockdown did not affect endogenous AurKB stability. A) In HEK293T cells, VRK1 was downregulated, during 72 hours, using a specific VRK1-siRNA (siVRK1-02 = siV-02) and a siRNA lacking a specific target (siControl = siC) was used as control. By immunoblot analysis, endogenous VRK1 was detected with a rabbit polyclonal anti-VRK1 (VC) antibody, endogenous AurKB was detected using a rabbit monoclonal anti-AurKB antibody. B) V5-AurKB (pcDNA3.1/nV5-DEST-AurKB) and HA-VRK1 (pCEFL-HA-VRK1) or HA-ø (pCEFL-HA-ø) were transfected in HEK293T cells. By immunoblot analysis, V5-AurKB was detected with a mouse monoclonal anti-V5 antibody and HA-VRK1 was detected with a rabbit polyclonal anti-HA antibody. In both experiments cells were harvest 4, 8, 12 and 24 hours after cycloheximide (CHX) treatment. Endogenous and transfected AurKB levels were quantified using *ImageJ* and represented in a graphic.

By immunoblot analysis, endogenous VRK1 was detected with a rabbit polyclonal anti-VRK1 (VC) antibody, endogenous AurKB was detected using a rabbit monoclonal anti-AurKB antibody, HA-VRK1 was detected using a rabbit polyclonal anti-HA antibody and V5-AurKB was detected using a mouse monoclonal anti-V5 antibody. The AurKB protein levels were quantified using

ImageJ and represented in a graphic. It was observed that VRK1 knockdown did not changed endogenous AurKB stability (Figure 34A), but VRK1 overexpression seemed to increase V5-AurKB stability, comparing to the control (Figure 34B).

1.6 Regulation of AurKB localization during mitosis by VRK1

CPC, and therefore AurKB, locates and accumulates during the early stages of mitosis on chromatin, more precisely, on centromeres. A localization that has been described to depend on the phosphorylation of histone H3 on Thr3 by Haspin, and on the phosphorylation of histone H2A on Thr120 by Bub1. H3T3ph serves as a docking site for Survivin and the H2AT120ph as a docking site for Borealin via Sgo1. Accordingly, loss of H3T3ph leads to CPC-AurKB missed localization on the centromeres and increased AurKB dispersion on the chromatin (Wang et al., 2010; Wang et al., 2011; Watanabe, 2010). Thus and since H3T3 is a direct phosphorylation target of VRK1, it seems likely that AurKB centromeric localization, may depend on VRK1 activity. Thereby, we began to analyze, by IF, the effect of VRK1 downregulation on AurKB localization in nocodazole arrested cells. In U2OS cell line, VRK1 was downregulated using a specific VRK1-siRNA (siVRK1-02), and a siRNA lacking a precise target was used as control (siControl). 60 hours later the cells were treated with nocodazole for 13 hours. Unsynchronized cells, transfected with siControl, were used as control of drug efficiency. By IF, AurKB was detected using a rabbit monoclonal anti-AurKB antibody and VRK1 was detected using a mouse monoclonal anti-VRK1 (1B5) antibody. Chromatin was stained with DAPI. As expected, was observed that AurKB localization seemed to change from a centromeric state to a chromatin diffuse state (Figure 35).

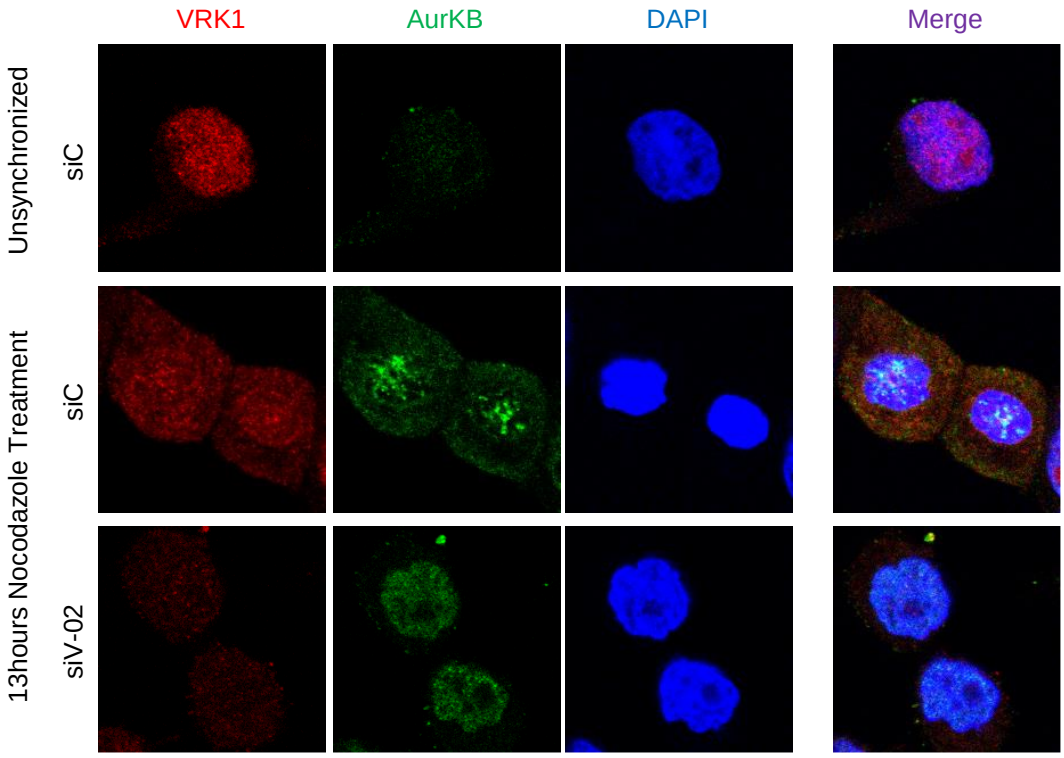

Figure 35. VRK1 downregulation re-locates AurKB from centromeres. In U2OS cells**,** VRK1 was downregulated using a specific VRK1-siRNA (siVRK1-02 = siV-02) and a non-specific siRNA (siControl = siC) was used as control. 60 hours later cells were treated with nocodazole, during 13 hours. Unsynchronized cells, transfected with siC, were used as control of drug efficiency. By IF, VRK1 was detected with a mouse monoclonal anti-VRK1 (1B5) antibody and AurKB was detected using a rabbit monoclonal anti-AurKB antibody. Chromatin was stained with DAPI.

At the same time, and using the same VRK1-knockdown protocol used in Figure 34, the effect of VRK1 downregulation on H3T3ph levels was confirmed, by IF, in nocodazole-arrested U2OS cells. Once again, unsynchronized cells transfected with siControl were used as control of drug efficiency. By IF, H3T3ph was detected using a rabbit polyclonal anti-H3T3ph antibody and VRK1 was detected using a mouse monoclonal anti-VRK1 (1B5) antibody. Chromatin was stained with DAPI. As previous determined, VRK1 downregulation led to a decrease in the levels of H3T3ph (Figure 36).

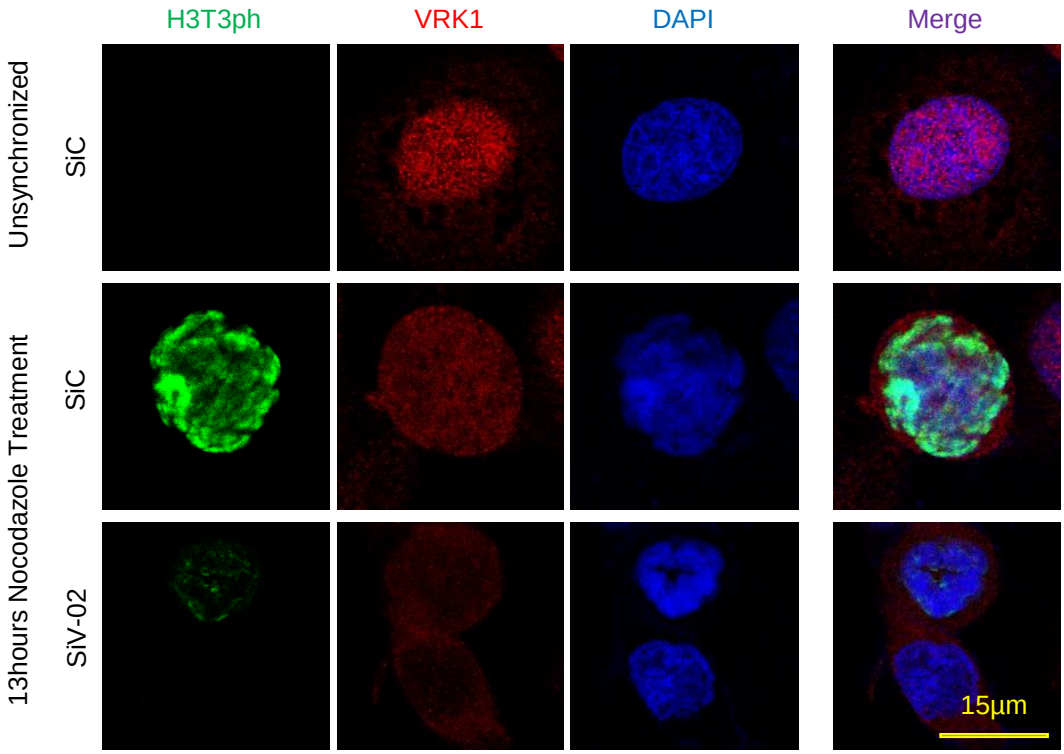

Figure 36. H3T3ph is negatively affect by VRK1 downregulation. In U2OS cells, VRK1 was downregulated using a specific VRK1-siRNA (siVRK1-02 = siV-02) and a non-specific siRNA (siControl = siC) was used as control. 60 hours later cells were treated with nocodazole, during 13 hours. Unsynchronized cells, transfected with siC, were used as control of drug efficiency. By IF, VRK1 was detected with a mouse monoclonal anti-VRK1 (1B5) antibody and H3T3ph was detected using a rabbit polyclonal anti-H3T3ph antibody. Chromatin was stained with DAPI.

Next, we aimed to analyze the co-localization of AurKB with centromeres, under VRK1 downregulation conditions. Again, U2OS cells were treated with a siRNA targeting VRK1 (siVRK1-02) or with a siRNA control (siControl), and 60 hours later the cells were incubated with nocodazole during 13 hours. Unsynchronized cells, transfected with siControl, were used as control of drug efficiency. By IF, AurKB was detected using a rabbit monoclonal anti-AurKB antibody and centromeres were detected using a human anti-centromere antibody (ACA) (Figure 37A). Chromatin was stained with DAPI.

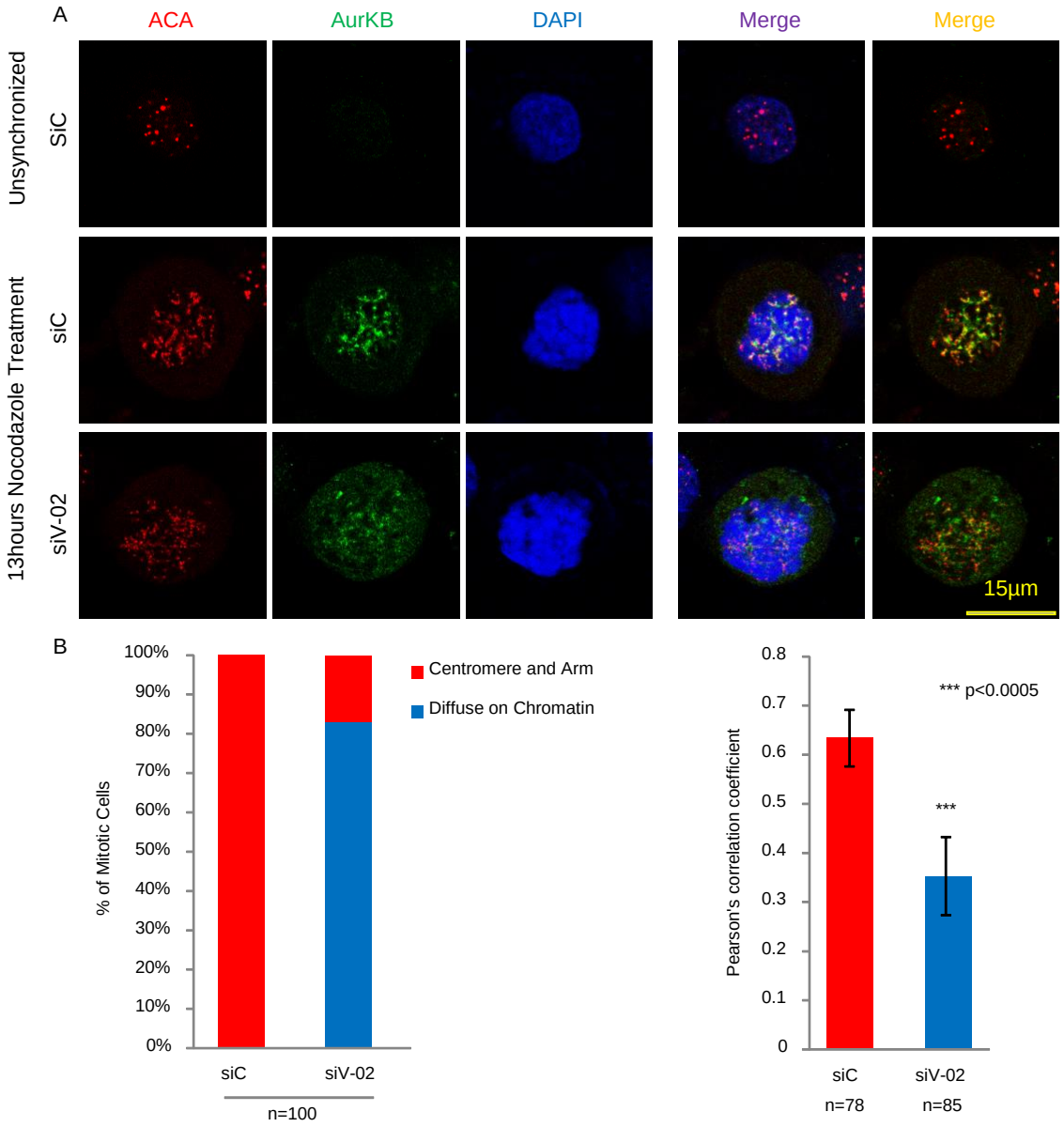

Figure 37. AurKB fails to locate in the centromeres in the absence of VRK1. A) In U2OS cells, VRK1 was downregulated using a specific VRK1-siRNA (siVRK1-02 = siV-02) and a non-specific siRNA (siControl = siC) was used as control. 60 hours later cells were treated with nocodazole, during 13 hours. Unsynchronized cells, transfected with siC, were used as control of drug efficiency. By IF, centromeres were detected with a human anti-centromere antibody (ACA) and AurKB was detected using a rabbit monoclonal anti-AurKB antibody. Chromatin was stained with DAPI. B) A total of 100 cells were counted concerning the distribution of AurKB on centromeres and chromosome arm or diffused on the chromatin (Chi-square statistic is significant at $p<0.01$). Pearson's correlation coefficient value was calculated separately for each cell, giving us the value of overlapping red and green pixels in each nucleus. (Student's Test: *<0.05; **<0.005; ***<0.0005).

Co-localization studies were performed by two distinct methods: the first by analyzing the images and the distribution of AurKB on centromeres and chromosome arms, or diffused on the chromatin, and the second calculating the Pearson's correlation coefficient value separately for each cell. This coefficient gave us the value of overlapped red and green pixels in each nucleus (Figure 37B). This experiment confirmed that VRK1 downregulation re-located AurKB from centromeres to a more diffused state on the chromatin. The result is sustained by the decreased number of cells with yellow dots, consequence of diminished ACA and AurKB co-localization, and by the reduced overlapping pixels calculated by Pearson's correlation coefficient (Figure 37).

Besides AurKB co-localization with ACA, also a potential co-localization between VRK1 and ACA was analyzed in unsynchronized and nocodazole arrested cells. By IF, VRK1 was detected using a rabbit polyclonal anti-VRK1 antibody and centromeres were detected using a human anti-centromere antibody (ACA). Chromatin was stained with DAPI. We did not observe any co-localization between VRK1 and centromeres. Neither during G1 (unsynchronized cells) nor during prometaphase (nocodazole arrested cells) (Figure 38).

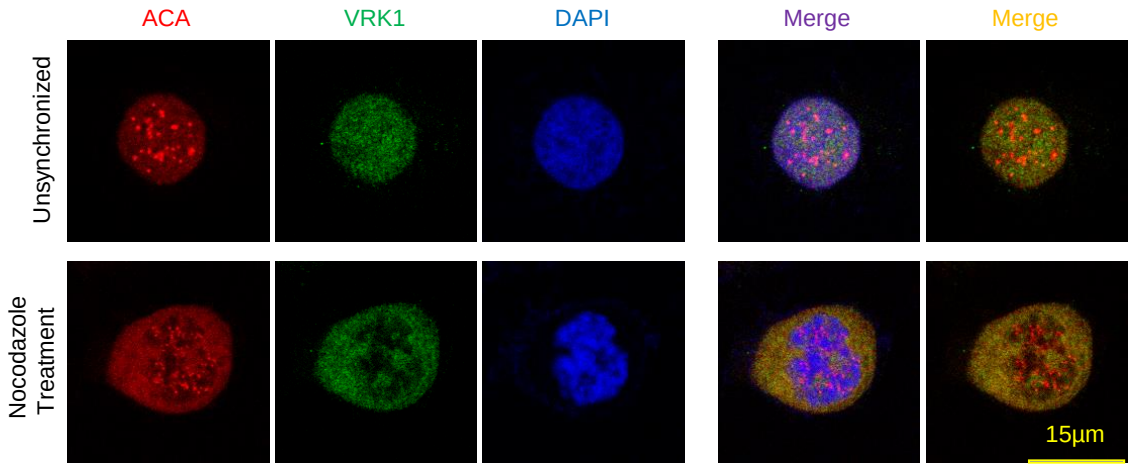

Figure 38. VRK1 is not located at centromeres in early stages of mitosis. U2OS cells were treated with nocodazole, during 13 hours and unsynchronized cells were used as control of drug efficiency. By IF, centromeres were detected with a human anti-centromere antibody (ACA) and VRK1 was detected using a rabbit polyclonal anti-VRK1 antibody. Chromatin was stained with DAPI.

VRK1 knockdown led to the re-location of AurKB from centromeres to a more diffuse state on the chromatin. An observation that may be related to the loss of H3T3ph and consequently to the disruption of CPC/ AurKB interaction with histone H3. Therefore, we aimed to verify whether the change on AurKB mitotic localization, observed after the knockdown of VRK1, is related to the loss of interaction between histone H3 and AurKB. For that reason, U2OS cells were transfected with a siRNA targeting VRK1 (siVRK1-02) or a siRNA control (siControl), lacking a specific target, and 60 hours later they were treated with nocodazole during 13 hours. Unsynchronized cells, transfected with siControl, were used as control of drug efficiency. Afterwards, AurKB was immunoprecipitated with a rabbit polyclonal anti-AurKB antibody and histone H3 was detected, by immunoblot, with a rabbit polyclonal anti-histone H3 antibody. Additionally, histones were extracted using an acid extraction protocol and H3T3ph was detected, by immunoblot, with a rabbit polyclonal anti-H3T3ph antibody. We confirmed that AurKB and histone H3 interacted in nocodazole arrested cells, and that the downregulation of VRK1 led to a decrease on this interaction. The loss of histone H3 and AurKB interaction occurs in line with the decline observed in H3T3ph levels in VRK1-knockdown conditions. The loss of interaction is independent of changes in the levels of AurKB (Figure 39).

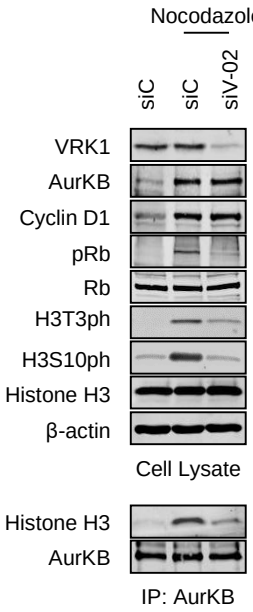

Figure 39. Histone H3 and AurKB interaction is loss when VRK1 is downregulated.

VRK1 was downregulated using a specific VRK1-siRNA (siVRK1-02 = siV-02) and a non-specific siRNA (siControl = siC) was used as control. 60 hours later cells were treated with nocodazole, during 13 hours. Unsynchronized cells, transfected with siC, were used as control of drug efficiency. Afterward, AurKB was immunoprecipitated with a rabbit polyclonal anti-AurKB antibody and histone H3 was detected, by immunoblot, with a rabbit polyclonal anti-histone H3 antibody. Furthermore, histones were extracted by acid extraction and H3T3ph was detected, by immunoblot, with a rabbit polyclonal anti-H3T3ph antibody.

Part 2. Regulation of VRK1 by Sox2 during cell proliferation and differentiation

1.1 VRK1 and Sox2 co-localization

The implication of both Sox2 and VRK1 in cell proliferation led us to determine whether there is a relationship between these two proteins (Basu-Roy et al., 2012; Santos et al., 2006; Tompkins et al., 2011; Valbuena et al., 2008b). Firstly, we intended to verify the pattern of VRK1 and Sox2 protein expression in a stratified squamous epithelium of a normal human tonsil. Sox2 was detected using a mouse monoclonal anti-Sox2 antibody and VRK1 was detected using a rabbit polyclonal anti-VRK1 antibody. We observed that VRK1 and Sox2 showed a similar localization, overlapping consistently within the proliferative amplification compartment and decreasing their protein expression as epithelial cells were terminally differentiated. Moreover, VRK1 was also detected in normal and tumoral lymphoid follicles, while Sox2 was only detected in tumoral lymphoid follicles (Figure 40).

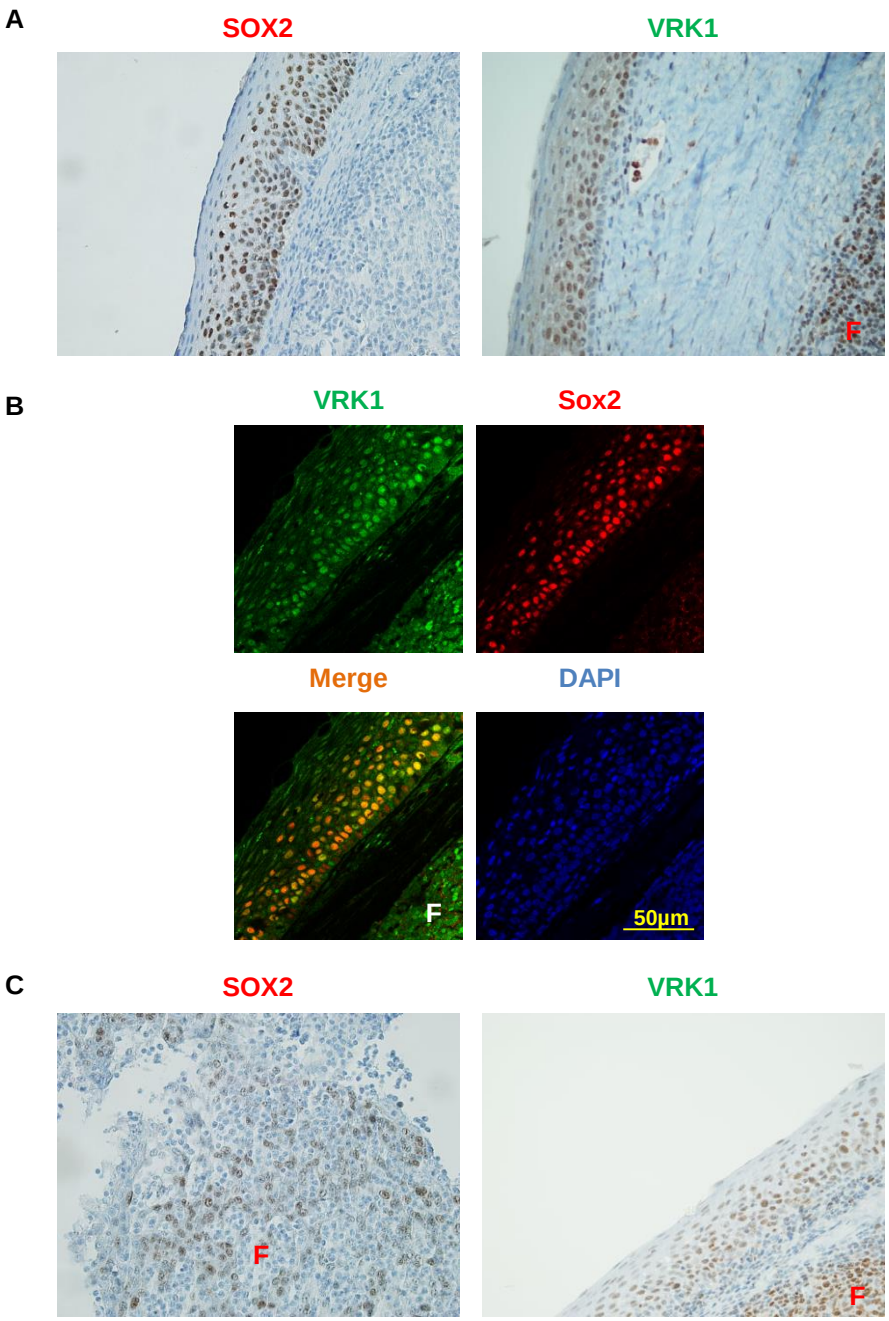

Figure 40. VRK1 and Sox2 co-localize in a stratified squamous epithelium of a normal human tonsil. A and B) Normal human tonsil. C) Tumoral human tonsil. By IHC and fluorescent IHC Sox2 was detected using a mouse monoclonal anti-Sox2 antibody and VRK1 was detected using a rabbit polyclonal anti-VRK1 antibody. Chromatin was stained with DAPI. F = Follicular tissue. The images were amplified 400x.

Next, we examined the VRK1 and Sox2 potential relationship in several cancer cell lines: MCF7 and MDA-MB-231 breast cancer cell lines, and NT2, a teratocarcinoma cell line that can differentiate into neurons. As both proteins co-

localize in a stratified squamous epithelium of a normal human tonsil, it was expected similar result among cell lines.

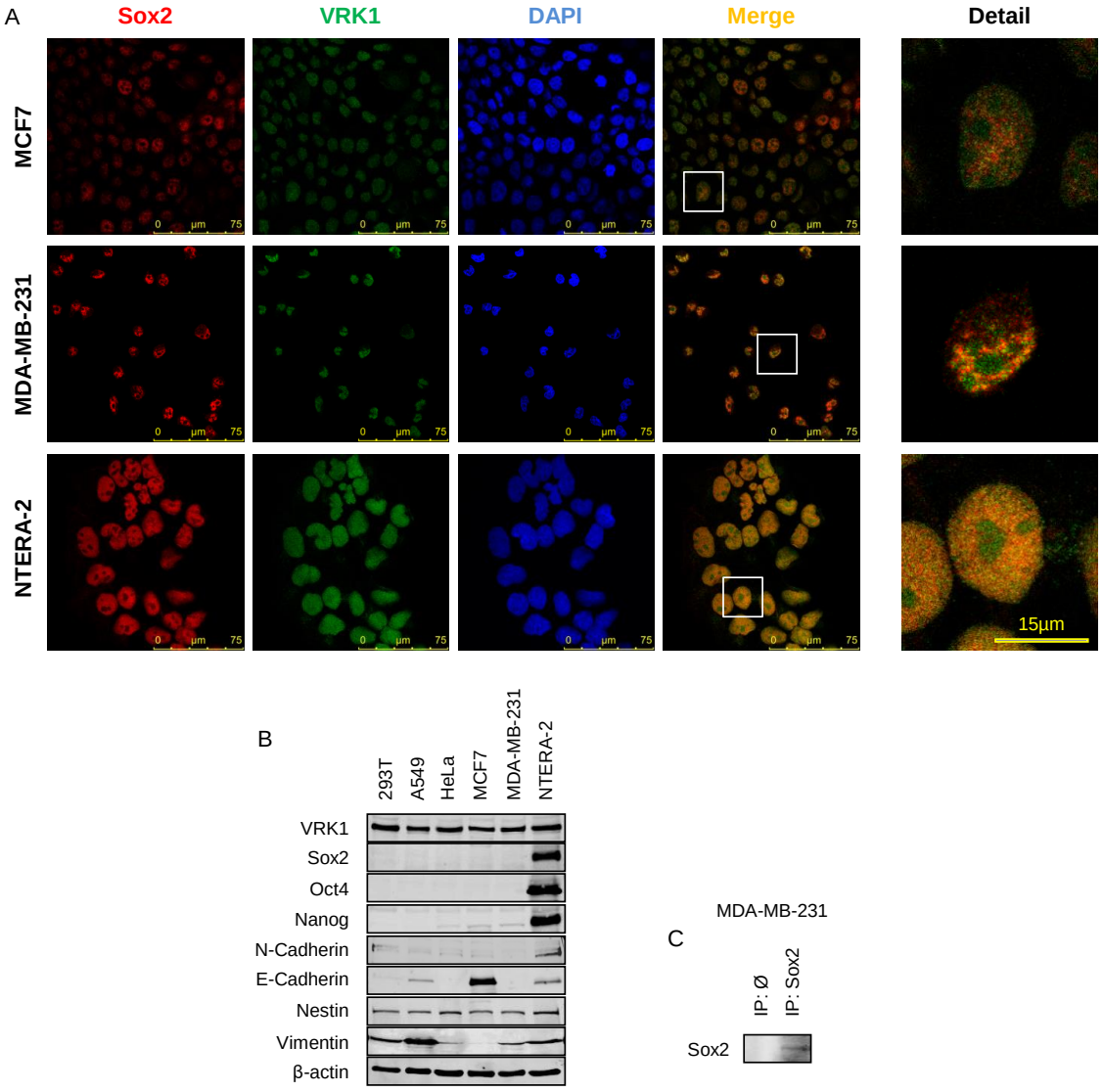

Figure 41. VRK1 and Sox2 co-localize in NTERA-2, MCF7 and MDA-MB-231 cell lines. A) Sox2 was detected using a mouse monoclonal anti-Sox2 antibody and VRK1 was detected using a rabbit polyclonal anti-VRK1 antibody. Chromatin was stained with DAPI. B) Endogenous levels of Sox2 were detected, by immunoblot, with a rabbit monoclonal anti-Sox2 antibody. C) Sox2 protein levels were immunoprecipitated with a mouse monoclonal anti-Sox2 antibody and detected, by immunoblot, using a goat monoclonal anti-Sox2 antibody.

Besides, the protein levels of reprogramming factor Sox2 were evaluated, by immunoblot, since they had been reported to be residual and imperceptible in somatic cancer cell lines. By IF, Sox2 was detected using a mouse monoclonal

anti-Sox2 antibody and VRK1 was detected using a rabbit polyclonal anti-VRK1 antibody. Chromatin was stained with DAPI. By immunoblot, Sox2 was detected using a rabbit monoclonal anti-Sox2 antibody. We observed that NT2 cells have high levels of both Sox2 and VRK1 proteins (Figure 41B) and that MDA-MB-231 low endogenous levels of Sox2 became detectable, by immunoblot, after IP (Figure 41C). Although Sox2 expression levels varied among cell lines, nuclear co-localization of Sox2 and VRK1 was confirmed by IF in NT2, MDA-MB-231 and MCF7 cell lines (Figure 41A).

1.2 VRK1 interaction with reprogramming factor Sox2

VRK1 is a chromatin kinase that establishes stable complexes with several transcription factors such as p53, ATF2 and c-Jun (Lopez-Sanchez et al., 2014a; Sevilla et al., 2004a; Sevilla et al., 2004b). Therefore and since VRK1 and Sox2 co-localize in human cancer cell lines and in a stratified squamous epithelium of a normal human tonsil, it is likely that both proteins interact, forming a stable protein complex. So, we performed reciprocal IPs of endogenous VRK1 and Sox2 proteins from extracts of MDA-MB-231, NT2 and HEK293T cells. The extracts were immunoprecipitated or with a mouse monoclonal anti-VRK1 (1B5) antibody or with a mouse monoclonal anti-Sox2 antibody. By immunoblot, Sox2 was detected using a goat polyclonal anti-Sox2 antibody and VRK1 was detected using a rabbit polyclonal anti-VRK1 antibody (VC). In the three cell lines, Sox2 was detected in the VRK1 immunoprecipitate, and reciprocally VRK1 was also detected in the Sox2 immunoprecipitate (Figure 42).

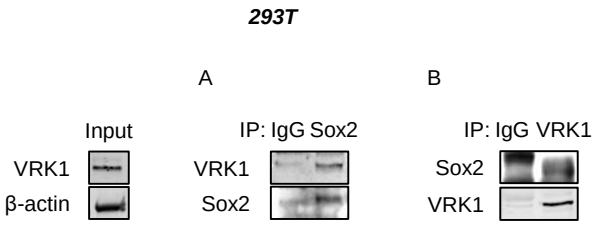

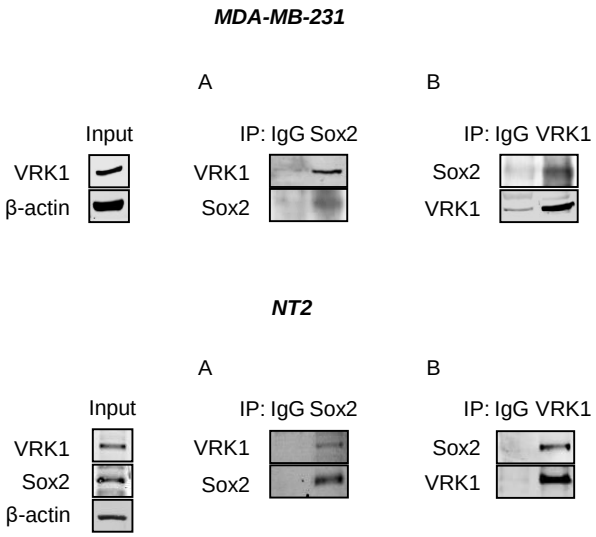

Figure 42. VRK1 and Sox2 interact in NTERA-2, MCF7 and MDA-MB-231 cell lines. A) Sox2 was immunoprecipitated with a mouse monoclonal anti-Sox2 antibody and VRK1 was detected with a rabbit polyclonal anti-VRK1 (VC) antibody. A mouse monoclonal anti-HA (IgG) antibody was used as control of IP. B) VRK1 was immunoprecipitated with a mouse monoclonal anti-VRK1 (1B5) antibody and Sox2 was detected a goat polyclonal anti-Sox2 antibody (HEK293T and MDA-MB-231) or with a rabbit polyclonal anti-Sox2 antibody (NT2). A mouse monoclonal anti-HA (IgG) antibody was used as control of IP.

Moreover, the stable VRK1-Sox2 protein interaction was confirmed by IP of transfected tagged-proteins. Therefore, myc-FLAG-Sox2 was transfected alone or alongside with HA-VRK1 in HEK293T cells. Then, protein extracts were immunoprecipitated with a rabbit polyclonal anti-FLAG antibody, or with a rabbit polyclonal anti-HA antibody or with a rabbit polyclonal anti-VRK1 (VC) antibody. VRK1 was detected in Sox2 immunoprecipitate with a mouse monoclonal anti-HA antibody or with a mouse monoclonal anti-VRK1 (1B5) antibody. Sox2 was detected in VRK1 immunoprecipitate with a mouse monoclonal anti-FLAG antibody. In all the experiments VRK1 interacted with Sox2, confirming the results obtained previously (Figure 43A-D). Additionally, a stable concentration of HA-VRK1 was transfected with increased doses of myc-FLAG-Sox2. Then, Sox2 was immunoprecipitated, from protein extracts, with a rabbit polyclonal anti-FLAG antibody and VRK1 was detected with a mouse monoclonal anti-HA antibody. Again, we observed that VRK1 and Sox2 interacted, being the interaction, in this case dependent on Sox2 concentration (Figure 43E).

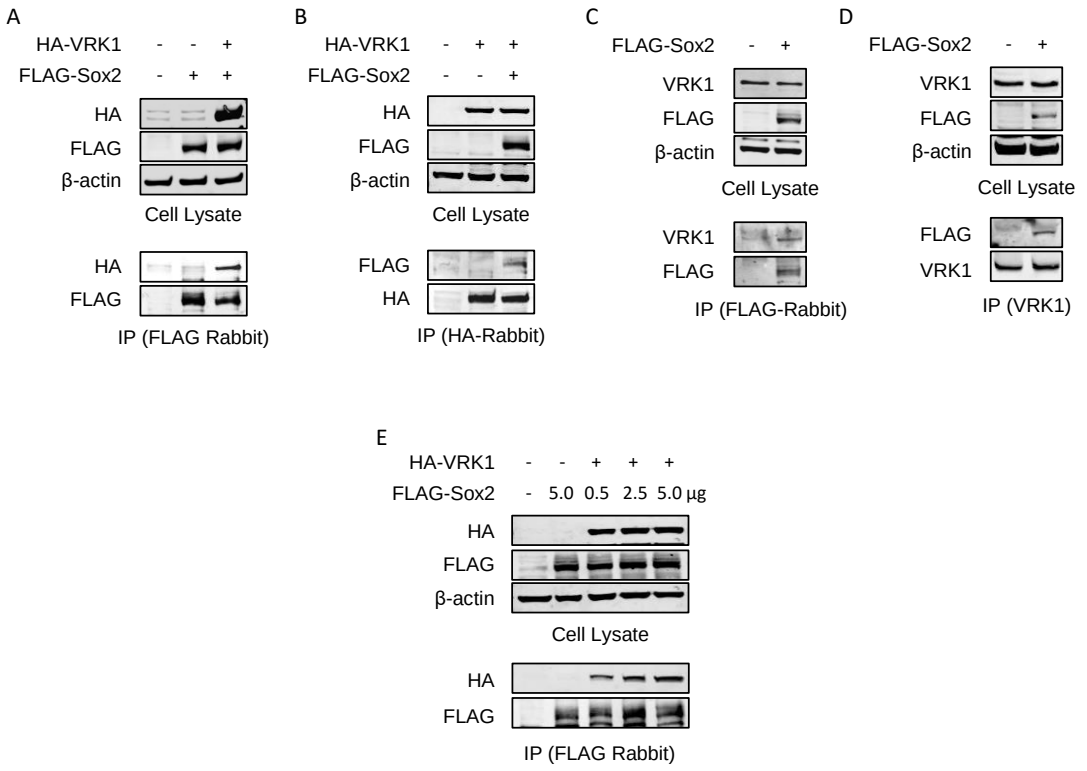

Figure 43. VRK1 and Sox2 transfected proteins interact. The interaction depends on Sox2 levels. A) HEK293T cells were transfected with pCMV6-myc-FLAG-Sox2 and pCEFL-HA-VRK1. Sox2 was immunoprecipitated with a rabbit polyclonal anti-FLAG antibody and VRK1 was detected, by immunoblot, with a mouse monoclonal anti-HA antibody. B) HEK293T cells were transfected with pCEFL-HA-VRK1 and pCMV6-myc-FLAG-Sox2. VRK1 was immunoprecipitated with a rabbit polyclonal anti-HA antibody and Sox2 was detected, by immunoblot, with a mouse monoclonal anti-FLAG antibody. C) FLAG-Tagged Sox2 (pCMV6-myc-FLAG-Sox2) was transfected in HEK293T cells and Sox2 was immunoprecipitated with a rabbit polyclonal anti-FLAG antibody. VRK1 was detected with a mouse monoclonal anti-VRK1 (1B5) antibody. D) FLAG-Tagged Sox2 (pCMV6-myc-FLAG-Sox2) was transfected in HEK293T cells and VRK1 was immunoprecipitated with a rabbit polyclonal anti-VRK1 (VC) antibody. A rabbit polyclonal anti-HA (IgG) antibody was used as control of IP. Sox2 was detected with a mouse monoclonal anti-FLAG antibody. E) HEK293T cells were transfected with a stable concentration of pCEFL-HA-VRK1 and increased doses of pCMV6-myc-FLAG-Sox2. Sox2 was immunoprecipitated with a rabbit polyclonal anti-FLAG antibody and VRK1 was detected, by immunoblot, with a mouse monoclonal anti-HA antibody.

Also, we intended to analyze the VRK1 region with which Sox2 interacted. Firstly, HEK293T cells were transfected with myc-FLAG-Sox2 (pCMV6-myc-FLAG-Sox2) together with GST-tagged VRK1 plasmids: VRK1 wild type (pCEFL-

GST-VRK1), VRK1 carboxy terminal (pCEFL-GST-VRK1-C (267-396)) or VRK1 truncated kinase (pCEFL-GST-VRK1-R358X). Sox2 was immunoprecipitated with a rabbit polyclonal anti-FLAG antibody and VRK1 plasmids were detected, by immunoblot, with a mouse monoclonal anti-GST-antibody. Secondly, HEK293T cells were transfected with VRK1 wild type (pCDNA3.1-VRK1-myc (1-396)) or with VRK1 large amino terminal (pCDNA3.1-VRK1-myc-LA (1-332)). Endogenous Sox2 was immunoprecipitated with a mouse monoclonal anti-Sox2 antibody and VRK1 plasmids were detected, by immunoblot with a rabbit polyclonal anti-myc antibody. We observed that VRK1 interacted with Sox2 through both amino and carboxy terminals (Figure 44).

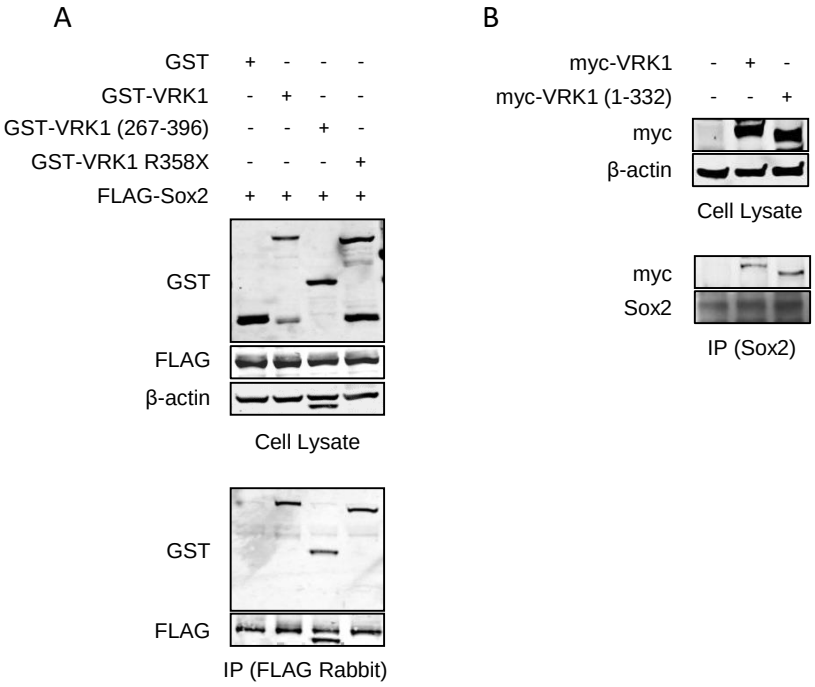

Figure 44. VRK1 interacts trough both amino and carboxy terminal with Sox2. A) myc-FLAG-Sox2 (pCMV6-myc-FLAG-Sox2) and GST-tagged VRK1 plasmids (VRK1 wild type (pCEFL-GST-VRK1), VRK1 carboxy terminal (pCEFL-GST-VRK1-C (267-396)) or VRK1 truncated kinase (pCEFL-GST-VRK1-R358X)) were transfected in HEK293T cells. Sox2 was immunoprecipitated with a rabbit polyclonal anti-FLAG antibody and VRK1 plasmids were detected, by immunoblot, with a mouse monoclonal anti-GST-antibody. B) HEK293T cells were transfected with myc-VRK1 wild type (pCDNA3.1-VRK1-myc (1-396)) or with myc-VRK1 large amino terminal (pCDNA3.1-VRK1-myc-LA (1-332)). Endogenous Sox2 was immunoprecipitated with a mouse monoclonal anti-Sox2 antibody and VRK1 plasmids were detected, by immunoblot, with a rabbit polyclonal anti-myc antibody.

1.3 Sox2 is a phosphorylation target of VRK1

The chromatin associated VRK1 phosphorylates several transcriptional factors, such as p53, ATF2 and c-Jun, with which the kinase interact (Lopez-Sanchez et al., 2014b; Sevilla et al., 2004a; Sevilla et al., 2004b). Therefore, it is possible that Sox2 may be phosphorylated by VRK1. In order to analyze the potential phosphorylation of Sox2 by VRK1, HEK2293T cells were transfected with myc-FLAG-Sox2 (pCMV6-myc-FLAG-Sox2) or with myc-FLAG empty vector (pCMV6-myc-FLAG-ø). Then, the protein extracts were immunoprecipitated with a mouse monoclonal anti-myc antibody and incubated, in a thermomixer at 30ºC during 30 minutes, with recombinant proteins GST-VRK1 (pGEX-GST-VRK1) and GST-VRK1-K179E (pCEFL-GST-VRK1-K179E), in the presence of cold ATP and radiolabeled ATP [γ-^{32}P]. It was observed that Sox2 was a phosphorylation target of VRK1 (Figure 45).

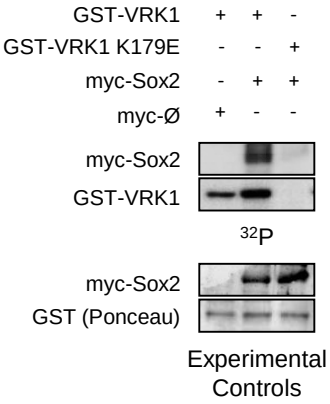

Figure 45. VRK1 phosphorylates Sox2. HEK293T cells were transfected with myc-FLAG-Sox2 (pCMV6-myc-FLAG-Sox2) or with myc-FLAG empty vector (pCMV6-myc-FLAG-ø) and Sox2 was immunoprecipitated with a mouse monoclonal anti-myc antibody. Immunoprecipitated myc-Sox2 was incubated with recombinant proteins GST-VRK1 (pGEX-GST-VRK1) and GST-VRK1-K179E (pCEFL-GST-VRK1-K179E) in the presence of cold ATP and radiolabeled [γ-^{32}P] ATP, in a thermomixer at 30ºC during 30 minutes. The incorporated radioactivity was detected exposing the ray-x film to the membranes.

1.4 Sox2 is implicated in the regulation of cell proliferation

The co-localization of Sox2 and VRK1 in the proliferation compartment, as well as their interaction, suggested that both proteins are likely to be involved in the regulation of cell proliferation. Indeed, it was reported that the loss of VRK1 reduced WS1 fibroblasts cell proliferation (Valbuena et al., 2008b) and likewise, some data indicated that Sox2 may also be involved in the control of cell proliferation (Basu-Roy et al., 2012; Chen et al., 2008a). Therefore, in MDA-MB-231 cells, we evaluated the effect of Sox2 or VRK1 depletion on cell proliferation (Figure 46).

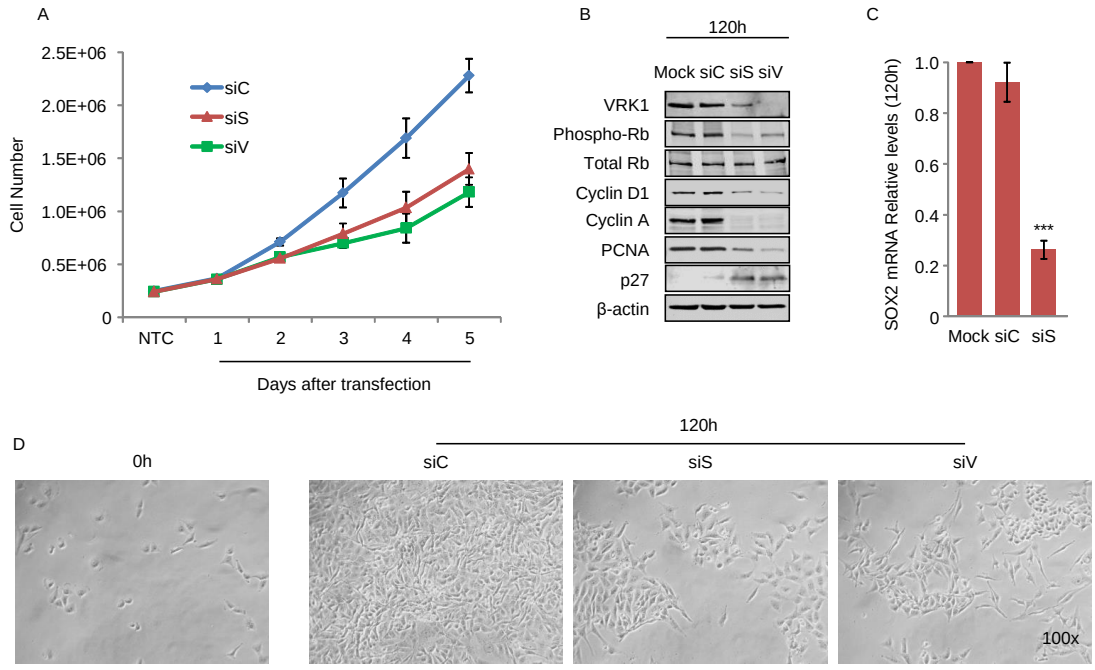

Figure 46. Depletion of Sox2 results in loss of proliferation. An equal number of MDA-MB-231 cells were transfected with siRNAs targeting specifically Sox2 (siSox2 = siS) and VRK1 (siVRK1-02 = siV) or with a siRNA lacking a precise target (siControl = siC). Lipofectamine-treated cells (mock) were used to exclude a possible effect of the reagent on cell proliferation. Then, the cells were harvested during 5 days and the cell number counted. The results show the mean of three experiments, in which each point was determined in triplicate (A). Proliferative markers were analyzed by immunoblot (B) and the mRNA levels of Sox2 determined by qRT-PCR (C). (Student's Test: *<0.05; **<0.005; ***<0.0005). Confluence images were acquired on a microscope, at 100x magnification, in the first and final day of the experiment (D).

The cells were transfected with siRNAs targeting specifically Sox2 (siSox2) and VRK1 (siVRK1-02) or with a siRNA lacking a precise target (siControl). Then, the cells were harvest at 24, 48, 72, 96 and 120 hours, and the living ones counted using a haemocytometer. The depletion of Sox2 was verified by qRT-PCR, since the protein levels were undetectable by immunoblot, and protein extracts were obtained to analyze cell cycle associated markers. We observed that Sox2 or VRK1 downregulation caused a similar reduction in the rate of cell duplication, and the loss of phospho-Rb, cyclins D1 and A, PCNA, all associated with active proliferation. Depletion of Sox2 or VRK1 also resulted in accumulation of p27, an inhibitor of cell cycle progression (Figure 46).

1.5 Sox2-dependent activation of *VRK1* gene expression

Sox2 is a transcriptional factor that executes its function mostly through the regulation of target gene promoters (Soufi, 2014). Besides, we demonstrated that Sox2 was implicated in the control of cell proliferation (Figure 46) and it is known that VRK1 is an important proliferation-associated kinase (Valbuena et al., 2008b). Accordingly, we speculated whether Sox2 was regulating *VRK1* gene expression. In order to verify such hypothesis, MDA-MB-231 were transduced with a retroviral construct overexpressing Sox2 (pBabe.puro-Sox2) and the effect on VRK1 protein levels was evaluated by immunoblot and IF. Additionally, the effect of Sox2 overexpression on VRK1 mRNA was also evaluated. We observed that Sox2 high levels induced an increase of endogenous VRK1 protein, which was detected by IF (Figure 47A) and by immunoblot analysis (Figure 47B). Moreover, the effect of Sox2 overexpression caused an increase in the expression of VRK1 mRNA levels, indicating that Sox2 is regulating the *VRK1* gene (Figure 47C). The same experiment was performed in MCF7 breast cancer line, obtaining similar results concerning the expression of VRK1 protein (Figure 48). The VRK1 protein levels detected by immunoblot analysis were quantified with *ImageJ* and normalize to β-actin protein levels. The VRK1 and Sox2 corrected total cell fluorescence was also quantified with *ImageJ*.

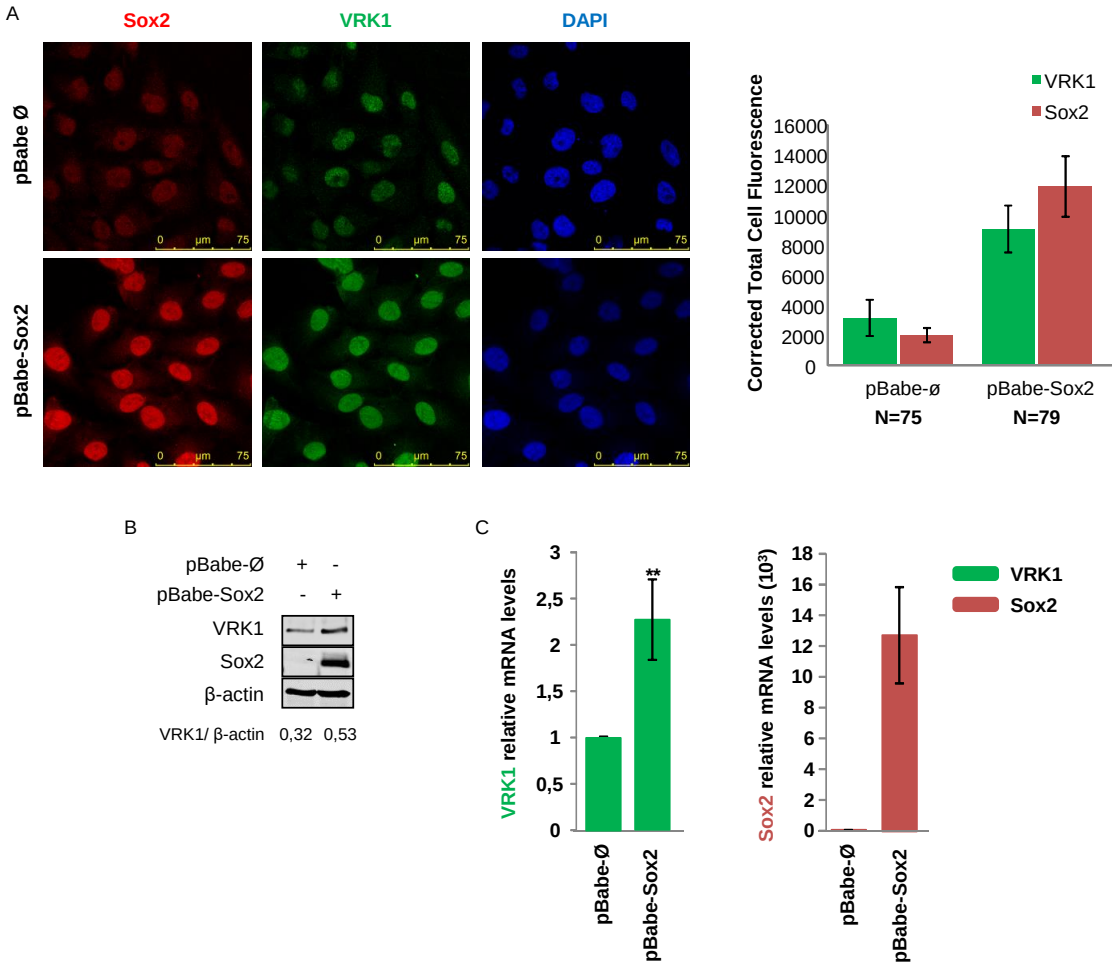

Figure 47. Sox2 overexpression upregulates VRK1 protein and mRNA levels in MDA-MB-231 cell line. MDA-MB-231 cells were transfected with pBabe.puro-Sox2 or with pBabe-ø empty vector. A) VRK1 protein levels were detected, by IF, with a rabbit polyclonal anti-VRK1 antibody and the corrected total cell fluorescence was quantified with *ImageJ* (Student's Test: *<0.05; **<0.005; ***<0.0005). B) VRK1 protein levels were detected, by immunoblot analysis, with a rabbit polyclonal anti-VRK1 antibody and quantified with *ImageJ.* Quantified VRK1 protein levels were normalize to quantified β-actin protein levels. C) VRK1 and Sox2 mRNA levels were determined by qRT-PCR and normalized to GAPDH mRNA levels. The experiment was performed in triplicate, three times (Student's Test: *<0.05; **<0.005; ***<0.0005).

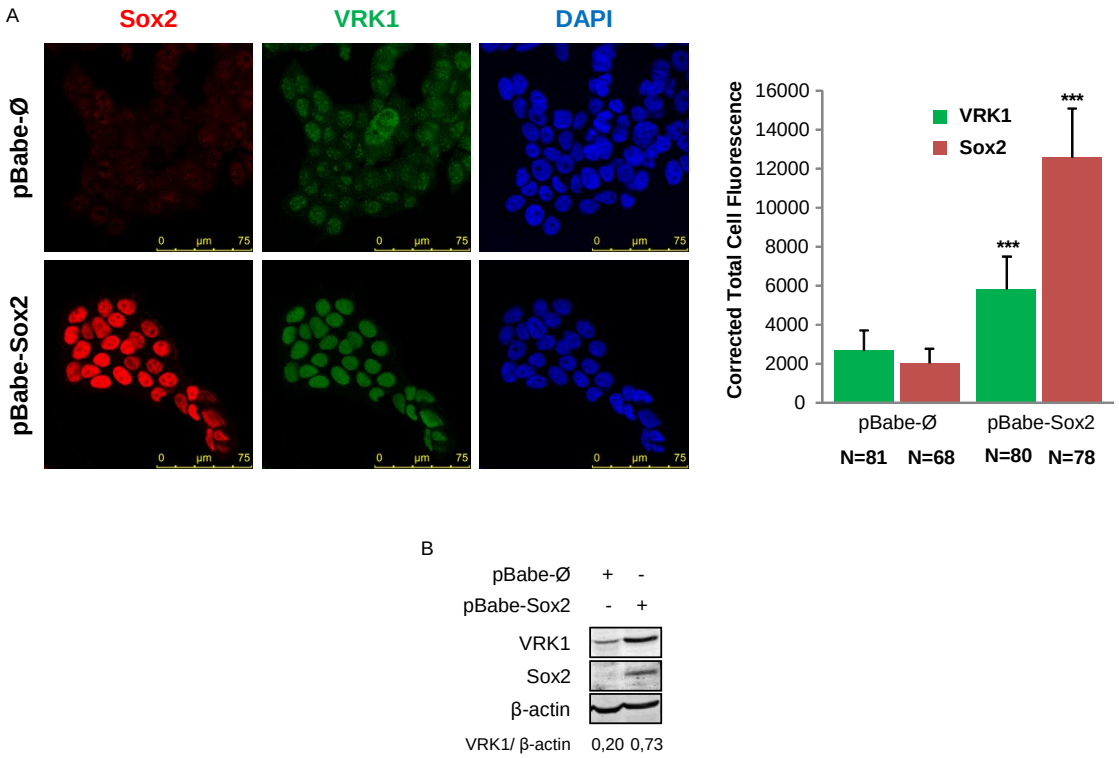

Figure 48. Sox2 overexpression upregulates VRK1 protein levels in MCF7 cell line. MCF7 cells were transfected with pBabe.puro-Sox2 or with pBabe-ø empty vector. A) VRK1 protein levels were detected, by IF, with a rabbit polyclonal anti-VRK1 antibody and the corrected total cell fluorescence was quantified with *ImageJ* (Student's Test: *<0.05; **<0.005; ***<0.0005). B) VRK1 protein levels were detected, by immunoblot analysis, with a rabbit polyclonal anti-VRK1 antibody and quantified with *ImageJ.* Quantified VRK1 protein levels were normalize to quantified β-actin protein levels.

Next and because Sox2 is a transcription factor, we tested whether the *VRK1* (-1028 to +52) proximal gene promoter, cloned in a luciferase reporter plasmid, was directly regulated by Sox2. Therefore, MDA-MB-231 cells were transfected with different amounts of pCMV6-myc-FLAG-Sox2 and with a plasmid expressing the long proximal VRK1 promoter (-1028 to + 52) region, cloned in pGL2-b-luciferase vector. Renilla-luciferase was used as internal control. We observed that *VRK1* proximal gene promoter was activated in a dose dependent manner by Sox2 overexpression (Figure 49). Similar result was obtained in HEK293T cell line (Figure 50).

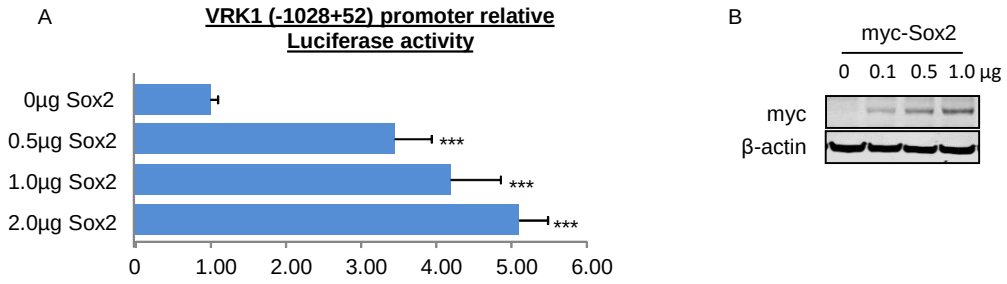

Figure 49. Sox2 overexpression activates *VRK1* proximal gene promoter in MDA-MB-231 cells. A) VRK1 (-1028+52) promoter relative luciferase activity. MDA-MB-231 cells were transfected with increased doses (0.5, 1.0 and 2.0µg) of pCMV6-myc-FLAG-Sox2, with pGL2-b-luciferase-VRK1 (-1028+52) vector and Renilla-luciferase as internal control. Besides, pGL2-Control plasmid expressing luciferase under the SV40 promoter was used as positive control and pGL2-basic, a promoter-less plasmid, was used as negative and background control. The experiment was performed in triplicate, three times (Student's Test: *<0.05; **<0.005; ***<0.0005). B) Immunoblot analysis.

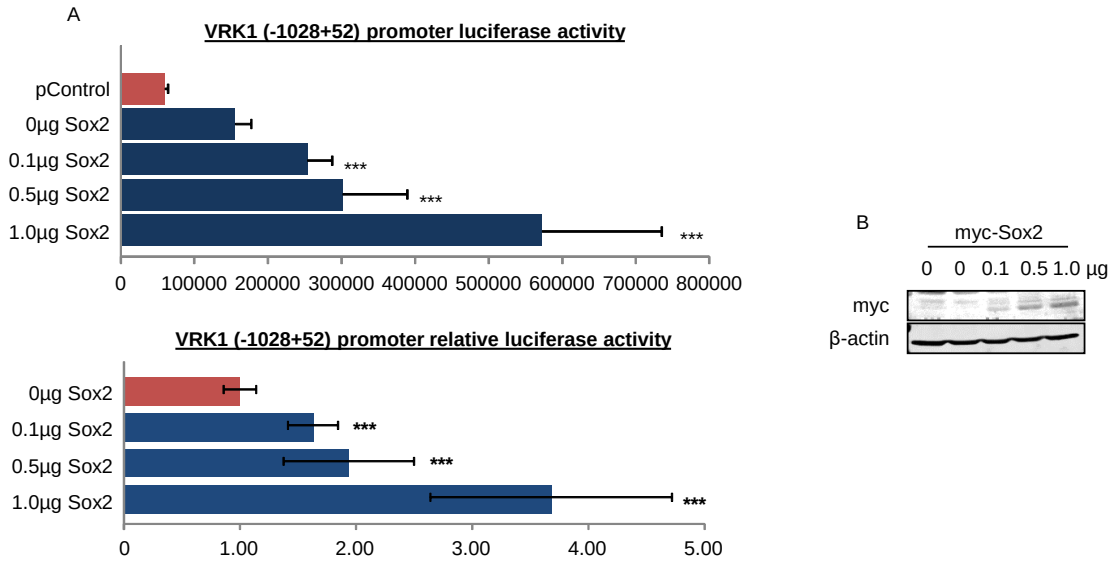

Figure 50. Sox2 overexpression activates *VRK1* proximal gene promoter in HEK293T cells. A) VRK1 (-1028+52 promoter) absolute (up) and relative (down) luciferase activity. HEK293T cells were transfected with increased doses (0.1, 0.5 and 1.0µg) of pCMV6-myc-FLAG-Sox2, with pGL2-b-luciferase-VRK1 (-1028+52) vector and Renilla-luciferase as internal control. Besides, pGL2-Control plasmid expressing luciferase under the SV40 promoter was used as positive control and pGL2-basic, a promoter-less plasmid, was used as negative and background control. The experiment was performed in triplicate, three times (Student's Test: *<0.05; **<0.005; ***<0.0005). B) Immunoblot analysis.

The proximal *VRK1* (-1028 to +52) gene promoter contains four consensus target sequences for Sox2 (Bowles et al., 2000; Chambers and Tomlinson, 2009; Fang et al., 2011b). Nevertheless, the DNA motifs are restricted between -1028 to -264 region (Figure 51).

Figure 51. Sox2 targets the proximal promoter (-1028+52) of the human *VRK1* gene. The DNA motifs that are Sox2 transcription factor targets are indicated in red.

Therefore, we intended to verify whether the activation of *VRK1* promoter, by Sox2 overexpression, was loss when the consensus target sequences for Sox2 were absent. HEK293T cells were transfected with different amounts of pCMV6-myc-FLAG-Sox2 and with a plasmid expressing a shorter proximal *VRK1*

promoter (-264 to + 52) region, cloned in pGL2-b-luciferase vector. Renilla-luciferase was used as internal control. It was demonstrated that Sox2 had no effect on the activation of *VRK1* promoter comprised between residues -264 to +52. This shorter promoter region shows a higher level of expression, reflecting the lack of some regulatory elements (Figure 52).

Altogether, these results indicated that the effect of Sox2 on *VRK1* promoter is mediated by the region comprised between residues -1028 to -264 that contains four consensus target sequences for Sox2.

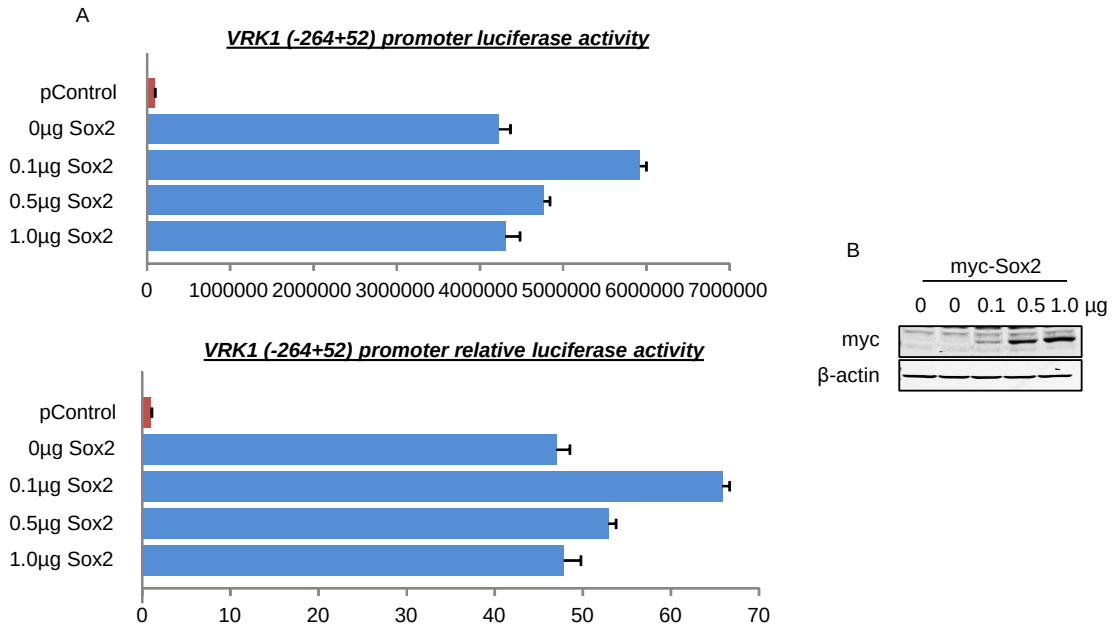

Figure 52. Sox2 overexpression has no effect on shorter *VRK1* proximal gene promoter. A) VRK1 (-264+52 promoter) absolute (up) and relative (down) luciferase activity. HEK293T cells were transfected with increased doses (0.1, 0.5 and 1.0µg) of pCMV6-myc-FLAG-Sox2, with pGL2-b-luciferase-VRK1 (-264+52) vector and Renilla-luciferase as internal control. Besides, pGL2-Control plasmid expressing luciferase under the SV40 promoter was used as positive control and pGL2-basic, a promoter-less plasmid, was used as negative and background control. The experiment was performed in triplicate, three times (Student's Test: *<0.05; **<0.005; ***<0.0005). B) Immunoblot analysis.

1.6 Sox2 and VRK1 co-operation in *CCND1* gene activation

Neither Sox2 nor VRK1 are direct regulators of cell cycle initiation and progression. Accordingly, both proteins have to regulate key genes or proteins implicated in cell cycle, among which *CCND1* is a major candidate. It is known that the transcriptional factor Sox2 initiates cell division in the stem cell compartment and regulates cell cycle G1/S transition, which is mediated by cyclin D1 (Boumahdi et al., 2014; Chen et al., 2008b). In turn, VRK1 also assists cell cycle progression and is able to activate the *CCND1* gene promoter, through the direct phosphorylation of CREB1. VRK1 depletion causes cell cycle arrest in G0/G1 (Kang et al., 2008a; Santos et al., 2006; Valbuena et al., 2008b). Accordingly, we verified the potential co-operation between VRK1 and Sox2 in the activation of the proximal *CCND1* gene promoter. Therefore, MDA-MB-231 cells were transfected with Sox2 tagged with flag-myc and/or HA-VRK1, alongside with a plasmid expressing the long proximal *CCND1* promotor (-1745 to +134), which was clones in a pGL2-b-luciferase vector. Renilla-luciferase was used as internal control. We showed that Sox2 and VRK1 individually activated the *CCND1* gene promoter, with a nearly fivefold stronger activation for Sox2 (Figure 53A and Figure 53B). However, the combination of both Sox2 and VRK1 resulted in a higher activation of *CCND1* gene expression, indicating that Sox2 and VRK1 proteins co-operate in the activation of *CCND1* gene expression and thus, they can contribute together to cell cycle progression and proliferation (Figure 53C).

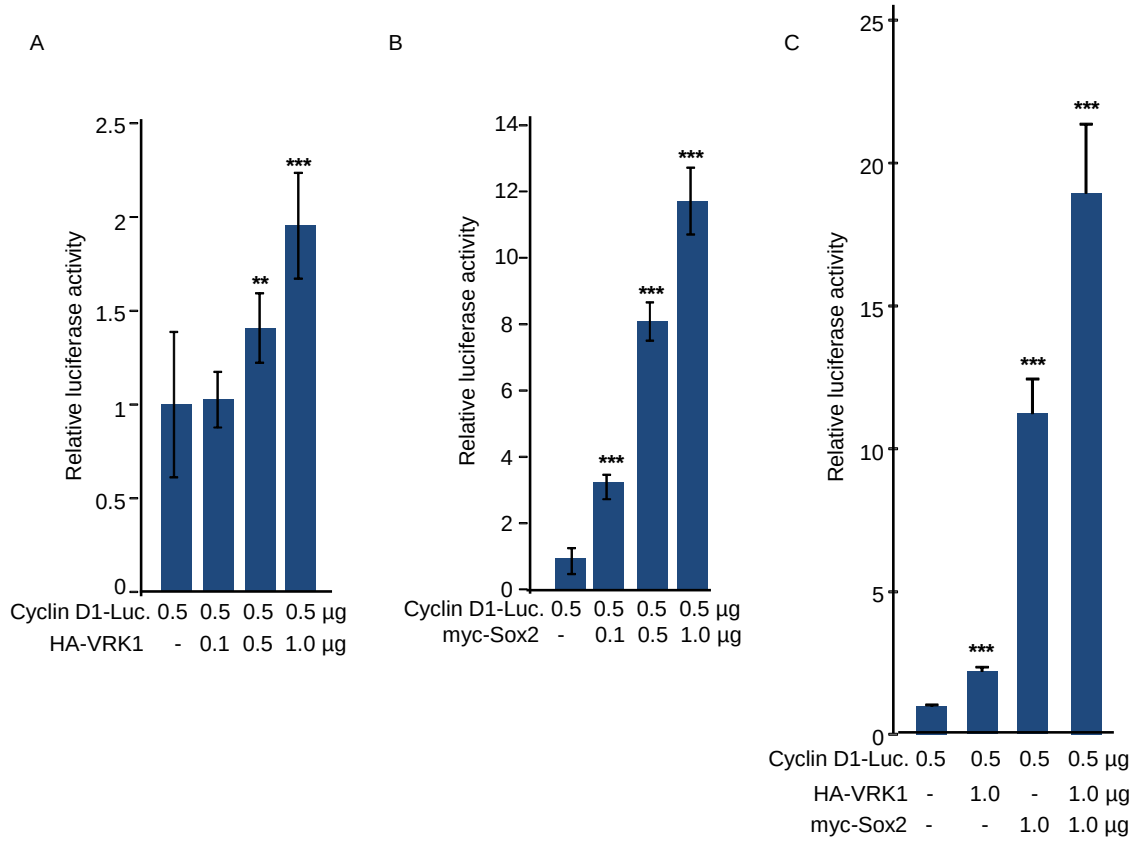

Figure 53. Sox2 co-operates with VRK1 on the activation of *CCND1* gene promoter. A) MDA-MB-231 cells were transfected with pA3-CycD1-Prom-Luc (-1745 +134) and increasing amounts of HA-VRK1 (pCEFL-HA-VRK1). B) MDA-MB-231 cells were transfected with pA3-CycD1-Prom-Luc (-1745 +134) and increasing concentrations of myc-FLAG-Sox2 (pCMV6-myc-FLAG-SOX2). C) MDA-MB-231 cells were transfected with pA3-CycD1-Prom-Luc (-1745 +134), with HA-VRK1 (pCEFL-HA-VRK1) and with myc-FLAG-Sox2 (pCMV6-myc-FLAG-SOX2). All the experiments were also transfected with Renilla-luciferase as internal control, with pGL2-Control plasmid expressing luciferase under the SV40 promoter as positive control and with pGL2-basic, a promoter-less plasmid, as negative and background control. The experiment was performed in triplicate, three times (Student's Test: *<0.05; **<0.005; ***<0.0005).

1.7 VRK1 modulates *SOX2* gene expression

The VRK1 activity is controlled by auto-regulatory loops with some of its targets, as has been described in the context of p53 (Valbuena et al., 2007b; Valbuena et al., 2006a). Therefore, we studied whether there is a cross regulation between VRK1 and Sox2 expression. First, the effect of VRK1 downregulation on the level of Sox2 protein and mRNA was determined, by IF and qRT-PCR, in

MDA-MB-231 cell line. VRK1 was depleted using two different siRNAs (siVRK1-02 or siVRK1-09) and a non-targeting siRNA (siControl) was used as control. Moreover, serum-free cells were maintained to determine whether the potential effect of VRK1 depletion on Sox2 levels may be due cell cycle arrest. We observed that VRK1 downregulation resulted in an increased intracellular level of Sox2 protein and mRNA, in MDA-MB-231 cells. An effect not related with the consequent cell cycle arrest induced by VRK1 depletion (Figure 54). Similar result was attained in MCF7 (Figure 55) and NT2 (Figure 56).

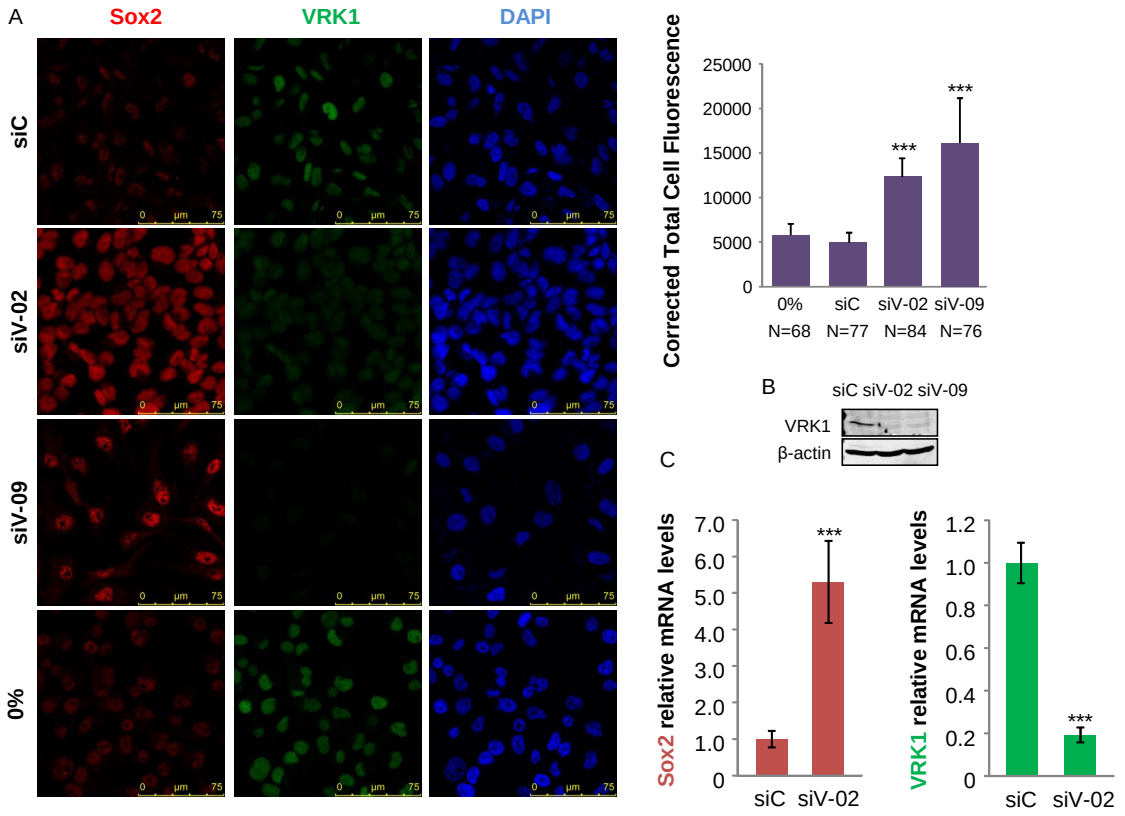

Figure 54. VRK1 depletion upregulates Sox2 in MDA-MB-231 cell line. MDA-MB-231 cells were transfected with siRNAs targeting VRK1 (siVRK1-02 = siV-02; siVRK1-09 = siV-09) and a non-targeting siRNA (siControl = siC) was used as control. Serum-free cells (0%) were used as control of cell cycle arrest. By IF, Sox2 was detected using a mouse monoclonal anti-Sox2 antibody and VRK1 was detected using a rabbit polyclonal anti-VRK1 antibody. Chromatin was stained with DAPI. Corrected total cell fluorescence was calculated using *ImageJ* (A). VRK1 knockdown was confirmed by immunoblot analysis (B). *SOX2* mRNA levels were quantified by real-time qRT-PCR and normalize with *GAPDH* mRNA levels. The experiment was performed in triplicate, three times (C). (Student's Test: *<0.05; **<0.005; ***<0.0005).

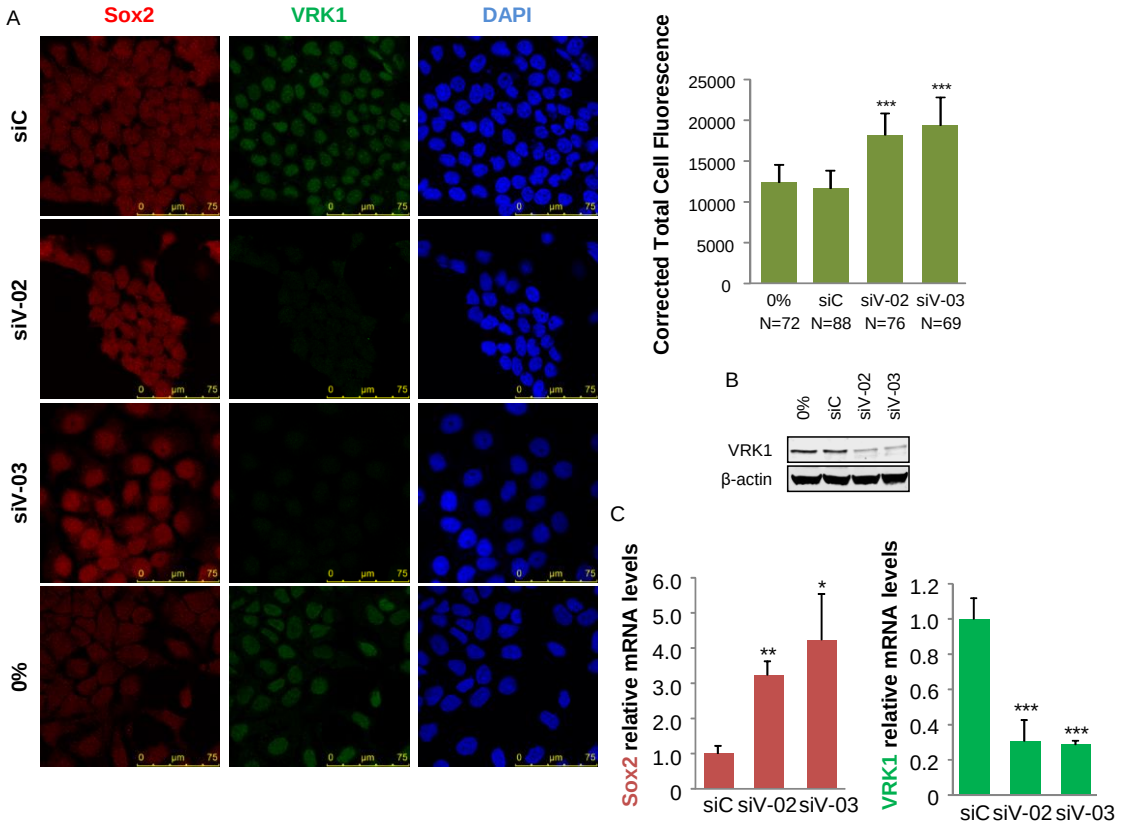

Figure 55. VRK1 depletion upregulates Sox2 in MCF7 cell line. MCF7 cells were transfected with siRNAs targeting VRK1 (siVRK1-02 = siV-02; siVRK1-03 = siV-03) and a non-targeting siRNA (siControl = siC) was used as control. Serum-free cells (0%) were used as control of cell cycle arrest. By immunofluorescence, Sox2 was detected using a mouse monoclonal anti-Sox2 antibody and VRK1 was detected using a rabbit polyclonal anti-VRK1 antibody. Chromatin was stained with DAPI. Corrected total cell fluorescence was calculated using *ImageJ* (A). VRK1 knockdown was confirmed by immunoblot analysis (B). *Sox2* mRNA levels were quantified by real-time qRT-PCR and normalize with *GAPDH* mRNA levels. The experiment was performed in triplicate, three times (C). (Student's Test: *<0.05; **<0.005; ***<0.0005).

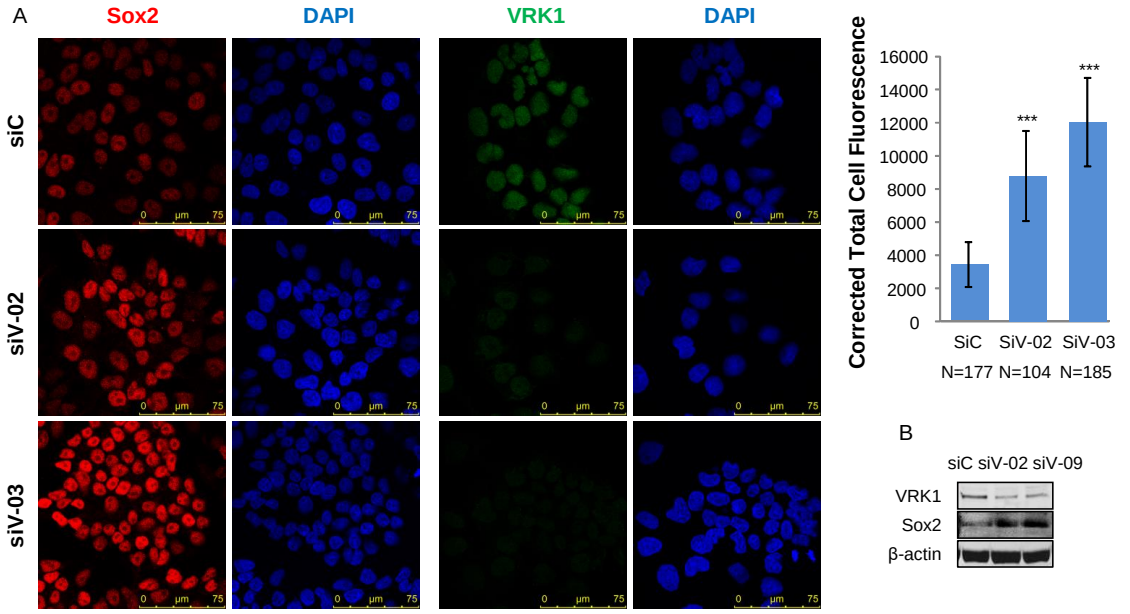

Figure 56. VRK1 depletion upregulates Sox2 in NT2 cell line. NT2 cells were transfected with siRNAs targeting VRK1 (siVRK1-02 = siV-02; siVRK1-03 = siV-03) and a non-targeting siRNA (siControl = siC) was used as control. By immunofluorescence, Sox2 was detected using a mouse monoclonal anti-Sox2 antibody and VRK1 was detected using a rabbit polyclonal anti-VRK1 antibody. Chromatin was stained with DAPI. Corrected total cell fluorescence was calculated using *ImageJ* (A). The effect of VRK1 knockdown on Sox2 protein levels was confirmed by immunoblot analysis. Sox2 was detected using a rabbit monoclonal anti-Sox2 antibody (B). (Student's Test: *<0.05; **<0.005; ***<0.0005).

Moreover and to further confirm the regulation of *SOX2* gene expression by VRK1, it was performed an opposed experiment. Therefore, VRK1 was overexpressed in MDA-MB-231 cell line with a retroviral plasmid vector overexpressing VRK1 (pQCXIP-VRK1) and the effect on Sox2 protein levels was evaluated by immunoblot and IF. Additionally, the effect of VRK1 overexpression on *SOX2* mRNA levels was evaluated by qRT-PCR. We observed that VRK1 overexpression led to the loss of Sox2 nuclear fluorescence, in comparison to the control. The effect was a consequence of a decrease in the level of *SOX2* mRNA (Figure 57). The result observed upon Sox2 protein levels was verified in stable a HeLa cell line overexpressing VRK1, but no effect was observed on the level of *SOX2* mRNA (Figure 58). Due to difficulties to transfect or transduce undifferentiated NT2 cell line, the overexpression of VRK1 was not achieved.

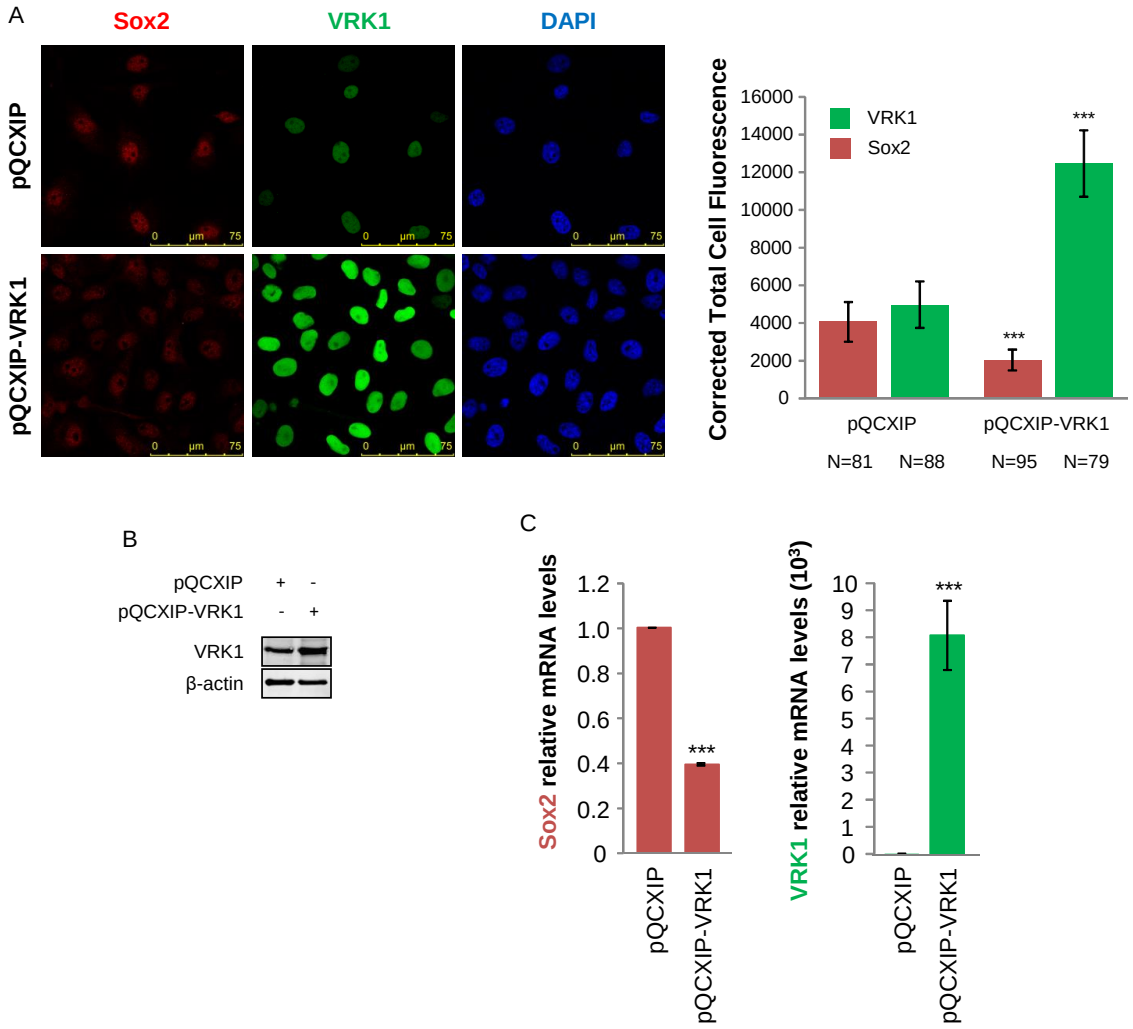

Figure 57. VRK1 overexpression downregulates Sox2 in MDA-MB-231 cell line. MDA-MB-231 cells were transduced with pQCXIP-VRK1 and pQCXIP empty vector was used as control. By immunofluorescence Sox2 was detected using a mouse monoclonal anti-Sox2 antibody and VRK1 was detected using a rabbit polyclonal anti-VRK1 antibody. Chromatin was stained with DAPI. Corrected total cell fluorescence was calculated using *ImageJ* (A). VRK1 overexpression was confirmed by immunoblot analysis (B). *SOX2* mRNA levels were quantified by real-time qRT-PCR and normalize with *GAPDH* mRNA levels. The experiment was performed in triplicate, three times (C). (Student's Test: *<0.05; **<0.005; ***<0.0005).

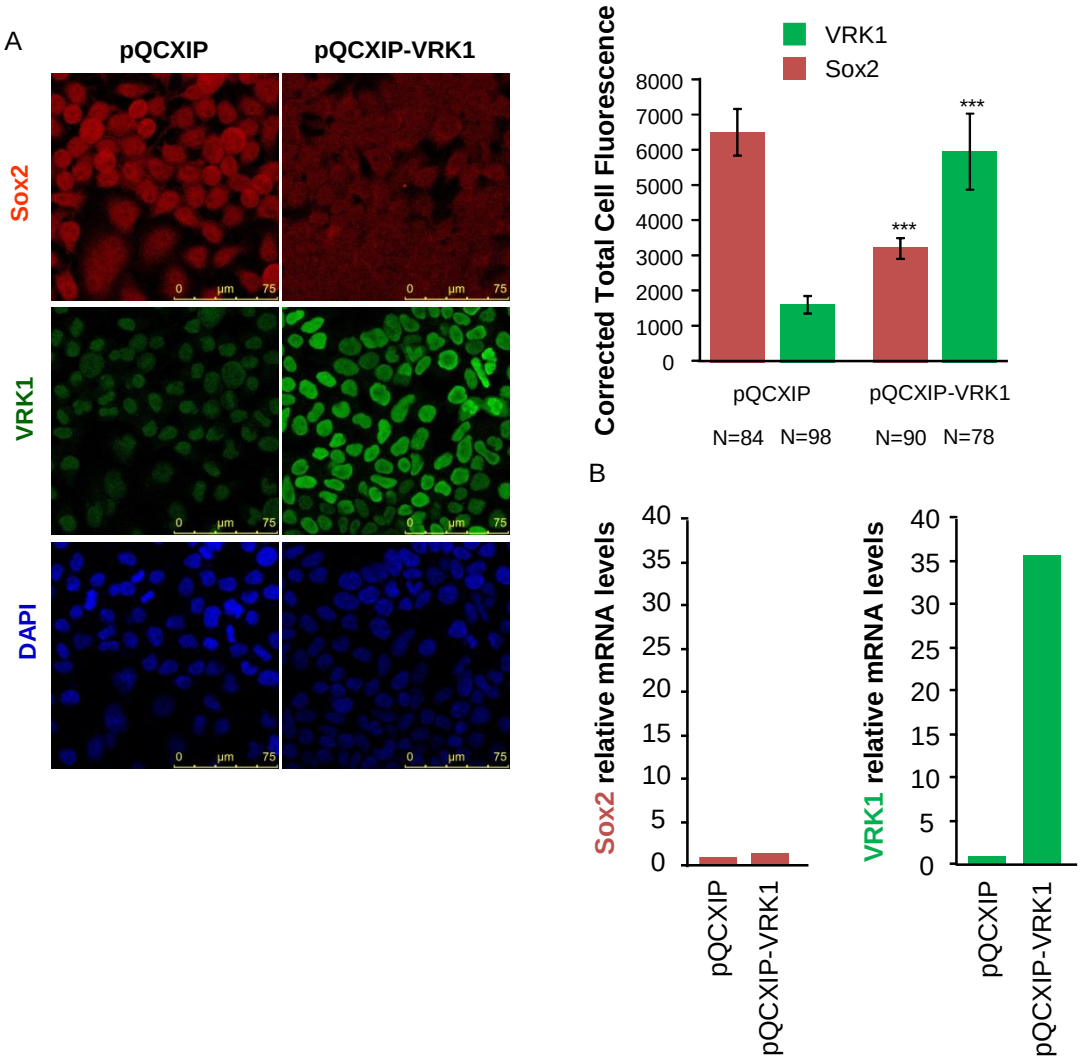

Figure 58. Stable VRK1-overexpressing HeLa cell line does not show alterations on Sox2 levels. HeLa cells were transduced with pQCXIP-VRK1 and pQCXIP empty vector was used as control. Then, the cells were selected with puromycin and a HeLa-VRK1-overexpressing pool was created. By immunofluorescence, Sox2 was detected using a mouse monoclonal anti-Sox2 antibody and VRK1 was detected using a rabbit polyclonal anti-VRK1 antibody. Chromatin was stained with DAPI. Corrected total cell fluorescence was calculated using *ImageJ* (A). *SOX2* mRNA levels were quantified by real-time qRT-PCR and normalize with *GAPDH* mRNA levels. The experiment was performed in triplicate, twice (B). (Student's Test: *<0.05; **<0.005; ***<0.0005).

1.8 Effect of cell differentiation on VRK1 and Sox2 levels

Sox2 plays an important role in the early decision of stem cells and VRK1 was reported to have a significant role in the initiation of cell proliferation (Boumahdi et al., 2014; Molitor and Traktman, 2013; Valbuena et al., 2008b;

Valbuena et al., 2011c). Therefore and since the initiation of cell lineage differentiation requires an asymmetric cell division, we decided to study the fate of Sox2 and VRK1 along the NT2 cell differentiation process induced with RA. The retinoid induces the rapid differentiation of NT2 cells into neurons (Pleasure and Lee, 1993). NT2 differentiation was performed during 14 days, changing the medium three times a week. Simultaneously, the cells were harvested every 48 hours, extracting mRNA for qRT-PCR and protein for immunoblot analysis. IF was done in the day 14.

We observed that the induction of cell differentiation resulted in a significant loss of reprogramming factor Sox2, Oct4, Nanog, alongside with a decrease in the proliferation markers VRK1, cyclins D1 and B1 proteins (Figure 59A and Figure 60B). The reduction of Sox2, VRK1, cyclin D1 Oct4 and Nanog protein levels, induced by RA, was also confirmed by the loss of their nuclear fluorescence (Figure 59B, Figure 60A and Figure 61). The differentiation state of the cells was also confirmed by the RA-induced morphological reorganization of α-tubulin observed by IF (Figure 60A), and through the detection of the corresponding increase in N-cadherin, βII-tubulin, PAX6 and CREB phosphorylated in Ser133, by immunoblot (Figure 59A) or by IF (Figure 61). Moreover, to determine whether these changes in protein levels were due to changes in gene expression we also determined, by qRT-PCR, the expression of *SOX2*, *OCT4*, *VRK1* and *H2AFY2* genes. *H2AFY2* codes for the macroH2A2 histone, an inhibitor of cell proliferation associated with terminal differentiation (Gaspar-Maia et al., 2013; Schnoder et al., 2015). RA induced a decrease of *SOX2*, *OCT4* and *VRK1* expression, while the *macroH2A2* expression increases to very high levels in the last days of the differentiation process (Figure 59C).

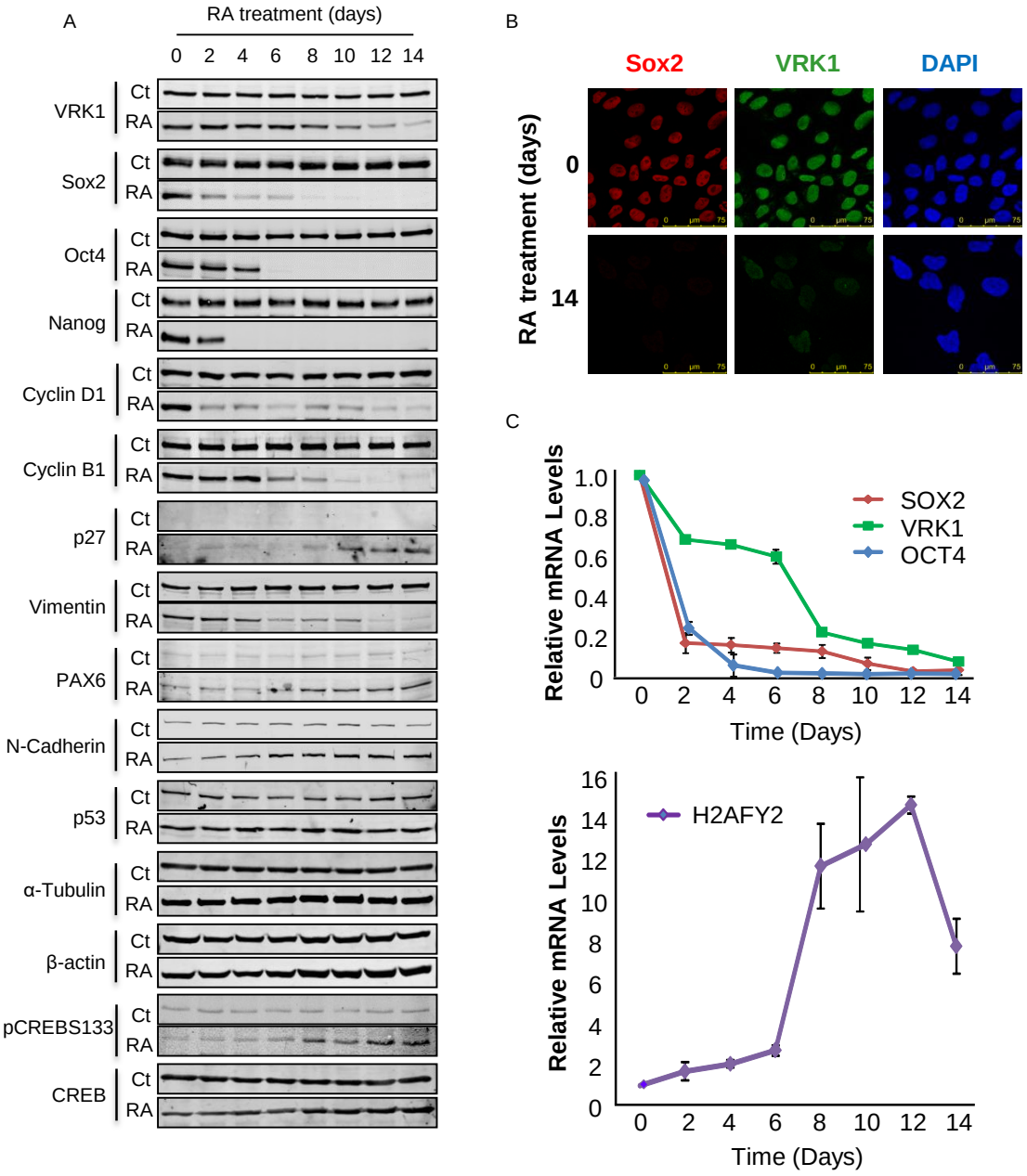

Figure 59. NT2 differentiation results in the loss of Sox2 and VRK1. A) Time course of the expression of different proteins in NT2 cells induced to differentiate with retinoic acid (RA). Sox2 was detected with a rabbit monoclonal anti-Sox2 antibody and VRK1, was detected with a rabbit polyclonal anti-VRK1 (VC) antibody. B) The expression of Sox2 and VRK1 proteins in NT2 cells was detected by immunofluorescence before and after induction of differentiation with retinoic acid (RA). Sox2 was detected using a mouse monoclonal anti-SOX2 antibody and VRK1 was detected using a rabbit polyclonal anti-VRK1antibody. Chromatin was stained with DAPI. C) Effect of RA-induced differentiation of NT2 cells on the gene expression levels *SOX2*, *OCT4*, *VRK1* and *H2AFY2*. Total RNA was extracted at the indicated times and the qRT-PCR was performed three times, in triplicate.

A

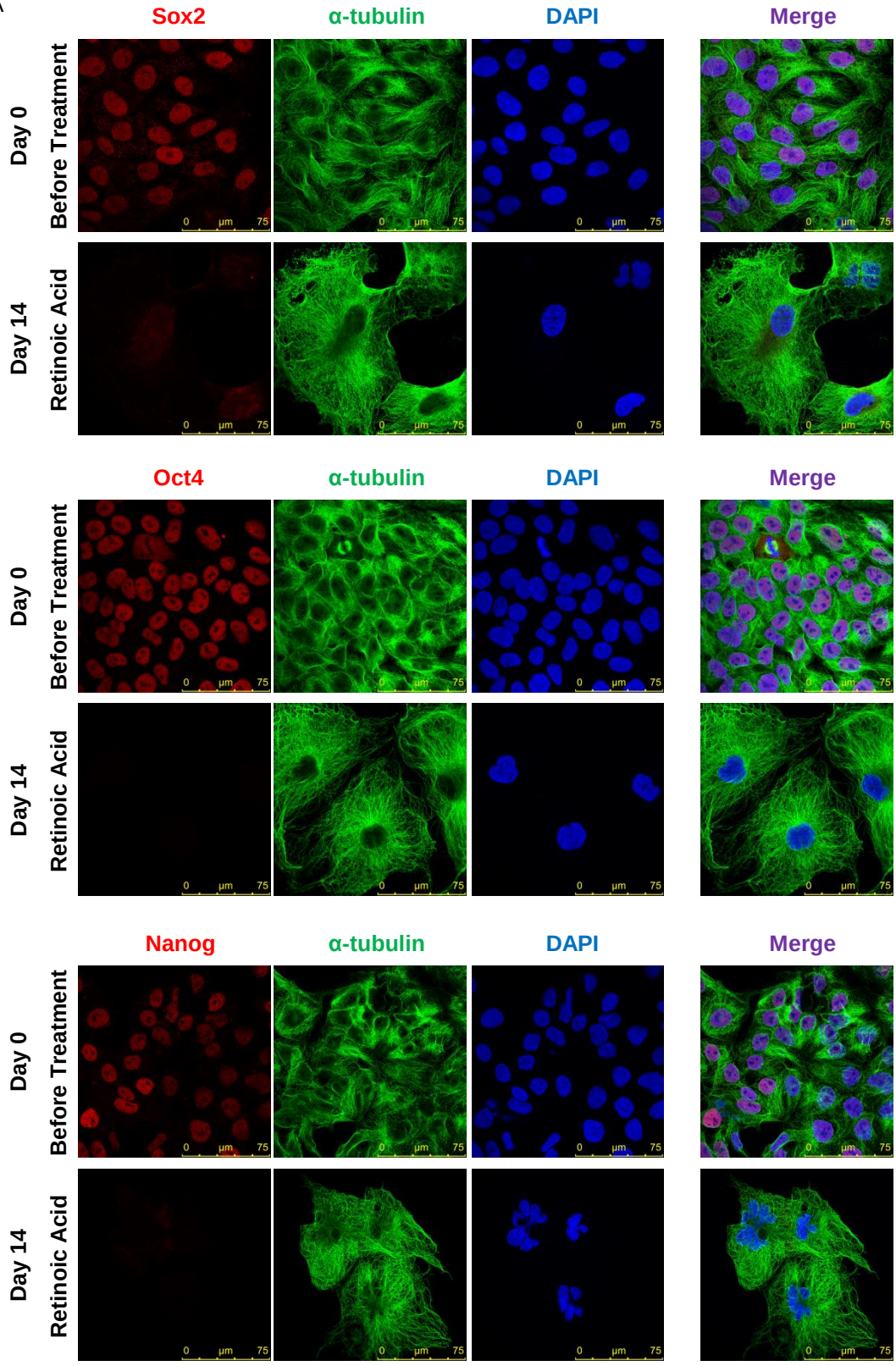
Sox2
α-tubulin
DAPI
Merge
Day 0
Before Treatment
Day 14
Retinoic Acid
Oct4
α-tubulin
DAPI
Merge
Day 0
Before Treatment
Day 14
Retinoic Acid
Nanog
α-tubulin
DAPI
Merge
Day 0
Before Treatment
Day 14
Retinoic Acid

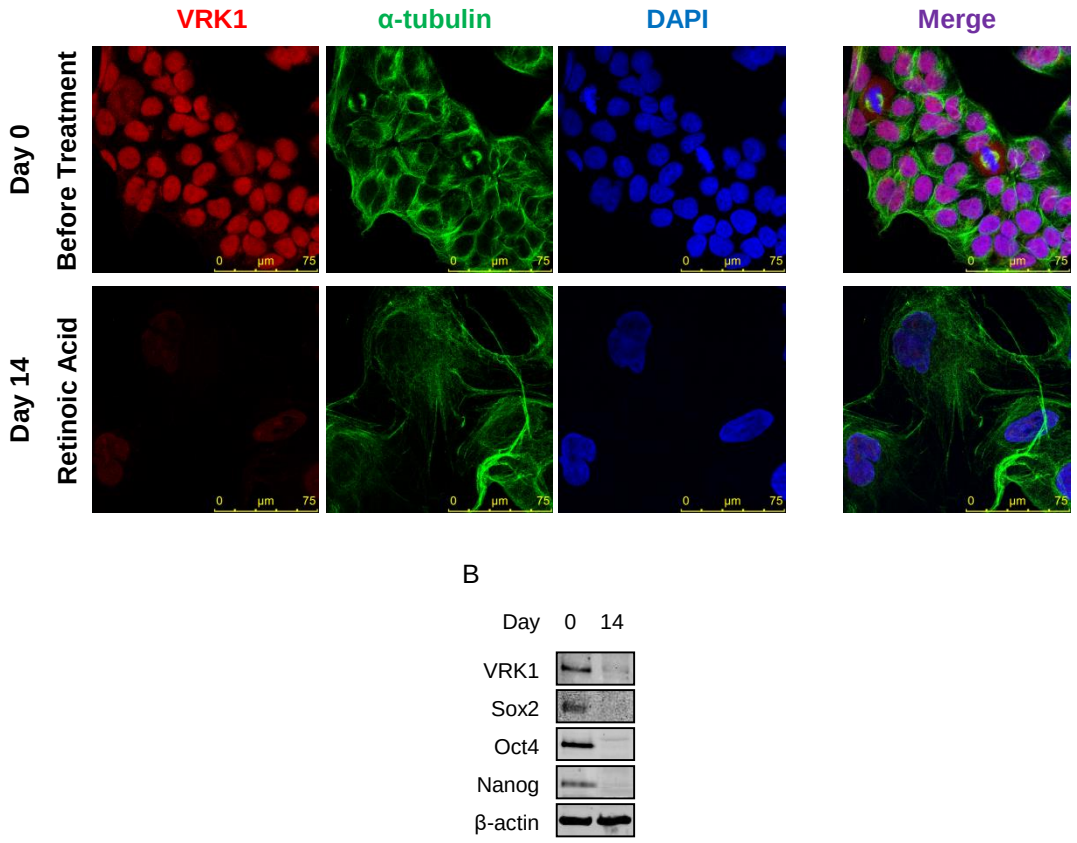

Figure 60. NT2 differentiation results in the loss of Sox2, Oct4, Nanog and VRK1, alongside with morphological reorganization of α-tubulin. A) The expression of VRK1 and reprogramming factors Sox2, Oct4 and Nanog, was detected by immunofluorescence before and after induction of NT2 differentiation with retinoic acid (RA). The morphological organization of α-Tubulin was also evaluated. Sox2 was detected using a mouse monoclonal anti-SOX2 antibody, Oct4 was detected using a rabbit monoclonal anti-Oct4 antibody, Nanog was detected with a rabbit monoclonal anti-Nanog antibody and VRK1 was detected using a mouse monoclonal anti-VRK1 (1B5) antibody. A-tubulin was detected with a rabbit polyclonal anti-α-tubulin antibody. Chromatin was stained with DAPI. B) The effect of RA-induced differentiation of NT2 cells on the expression of VRK1, Sox2, Oct4 and Nanog was confirmed by immunoblot.

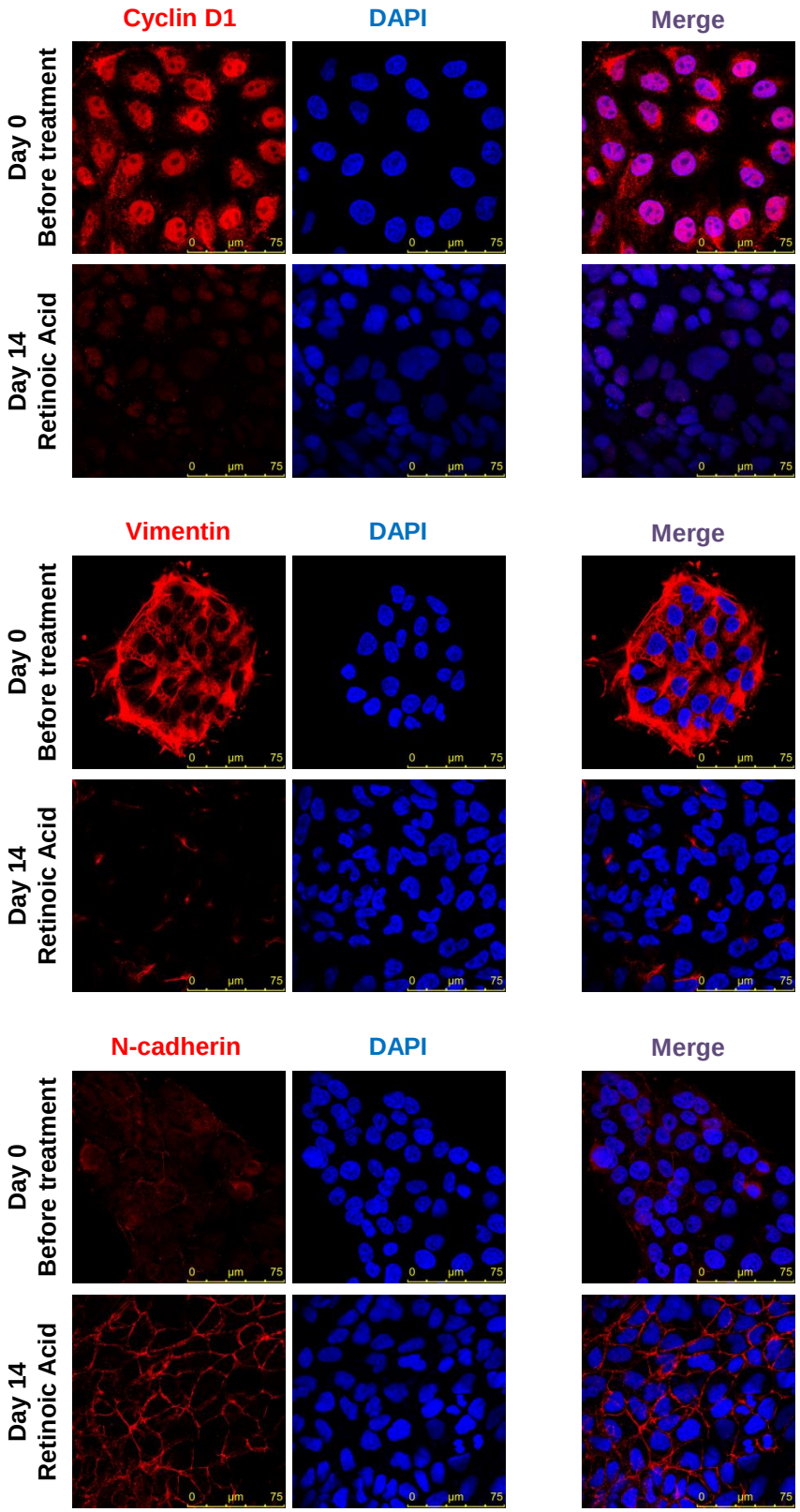
Cyclin D1
DAPI
Merge
Day 0
Before treatment
Day 14
Retinoic Acid
Vimentin
DAPI
Merge
Day 0
Before treatment
Day 14
Retinoic Acid
N-cadherin
DAPI
Merge
Day 0
Before treatment
Day 14
Retinoic Acid

Figure 61. Cyclin D1 and vimentin protein levels decrease during cell differentiation, while N-cadherin protein levels increase. NT2 were differentiated with retinoic acid (RA) during 14 days and cyclin D1, Vimentin and N-cadherin levels were analyzed by IF. Cyclin D1 was detected with a rabbit polyclonal anti-cyclin D1 antibody, Vimentin was detected with a mouse monoclonal anti-Vimentin antibody and N-cadherin was detected with a rabbit polyclonal anti-N-cadherin antibody. Chromatin was stained with DAPI.

Furthermore, NT2 cells were maintained under RA-differentiation conditions during 4 weeks, to verify whether proliferative proteins, such as VRK1 or cyclins, increase subsequently to the initial decrease observed during the initial 14 days. We observed that the protein levels of VRK1 and cyclins B1 and D1 remained low during the differentiation process (Figure 62).

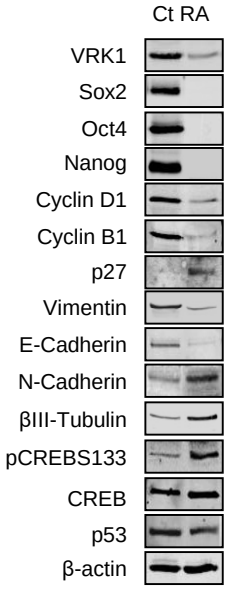

Figure 62. VRK1 levels remain low after 4 weeks of NT2 RA-differentiation. NT2 were differentiated with retinoic acid (RA) during 4 weeks and the protein expression of VRK1 was analyzed, by immunoblot, with a rabbit polyclonal anti-VRK1 (VC) antibody.

VRK1 is regulated directly by Sox2. Thus, we aimed to confirm that VRK1 is regulated by Sox2 in partially differentiated NT2 cells, where the levels of VRK1 already started to decline. Important to mention that differentiated NT2 are easily transfected, contrarily to undifferentiated NT2. Therefore, differentiated NT2 were transduced with a retroviral vector overexpressing Sox2 (pBabe.puro-Sox2) and the effect on VRK1 protein levels was evaluated by immunoblot. We observed

that the re-introduction of Sox2 into the cells, led to an increase in VRK1 protein levels (Figure 63).

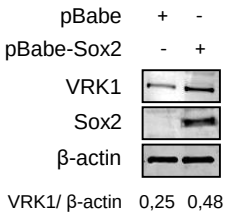

Figure 63. VRK1 levels are restored in RA-differentiated NT2 cells after Sox2 expression. NT2 cells were transfected with pBabe.puro-Sox2 and pBabe.puro empty vector, after 7 days of retinoic acid (RA) treatment. The protein expression of VRK1 was analyzed, by immunoblot, with a rabbit polyclonal anti-VRK1 (VC) antibody. The quantification of VRK1 protein levels was executed with *ImageJ* and its protein levels were normalize to the β-actin protein levels.

Furthermore, it is known that the downregulation of stem genes concomitant with differentiation is mediated by the exchange of histones variants in the chromatin. An example is the replacement of histone H2A by the macroH2A histones that have a larger C-terminal region (Buschbeck and Di Croce, 2010; Buschbeck et al., 2009). MacroH2A are histone variants that are associated with gene transcription inhibition and differentiation (Creppe et al., 2012b; Creppe et al., 2012c), as we showed for macroH2A2 (Figure 59C). Besides, macroH2A1.2 histone is known to inhibit the activity of VRK1 by their direct physical interaction (Kim et al., 2012b). Therefore, we tested the potential role of macroH2A histone variants in the regulation of *VRK1* and *CCND1* gene promoters. First, HEK293T cells were transfected with macroH2A variants, together with the long proximal *VRK1* promoter (-1028 to + 52) region expressing plasmid, cloned in pGL2-b-luciferase vector. Renilla-luciferase was used as internal control. We observed that macroH2A1.2 and macroH2A2, but not macroH2A1.1 inhibited the promoter of *VRK1* (Figure 64A). Similar results was obtained using increased doses of macroH2A histone isoforms instead of a single concentration (Figure 64B). Additionally, we determined if macroH2A histone variants were also capable to inhibit the effect of Sox2 on the *VRK1* gene promoter. Therefore, HEK293T cells were transfected with a plasmid expressing the long proximal *VRK1* promoter (-1028 to + 52) region, alongside with myc-FLAG-Sox2 and increased

concentrations of the macroH2A histone variants. It was observed that macroH2A1.2 and macroH2A2 proteins, but not macroH2A1.1 histone, were able to block the activating effect of Sox2 on the *VRK1* proximal promoter (Figure 64C).

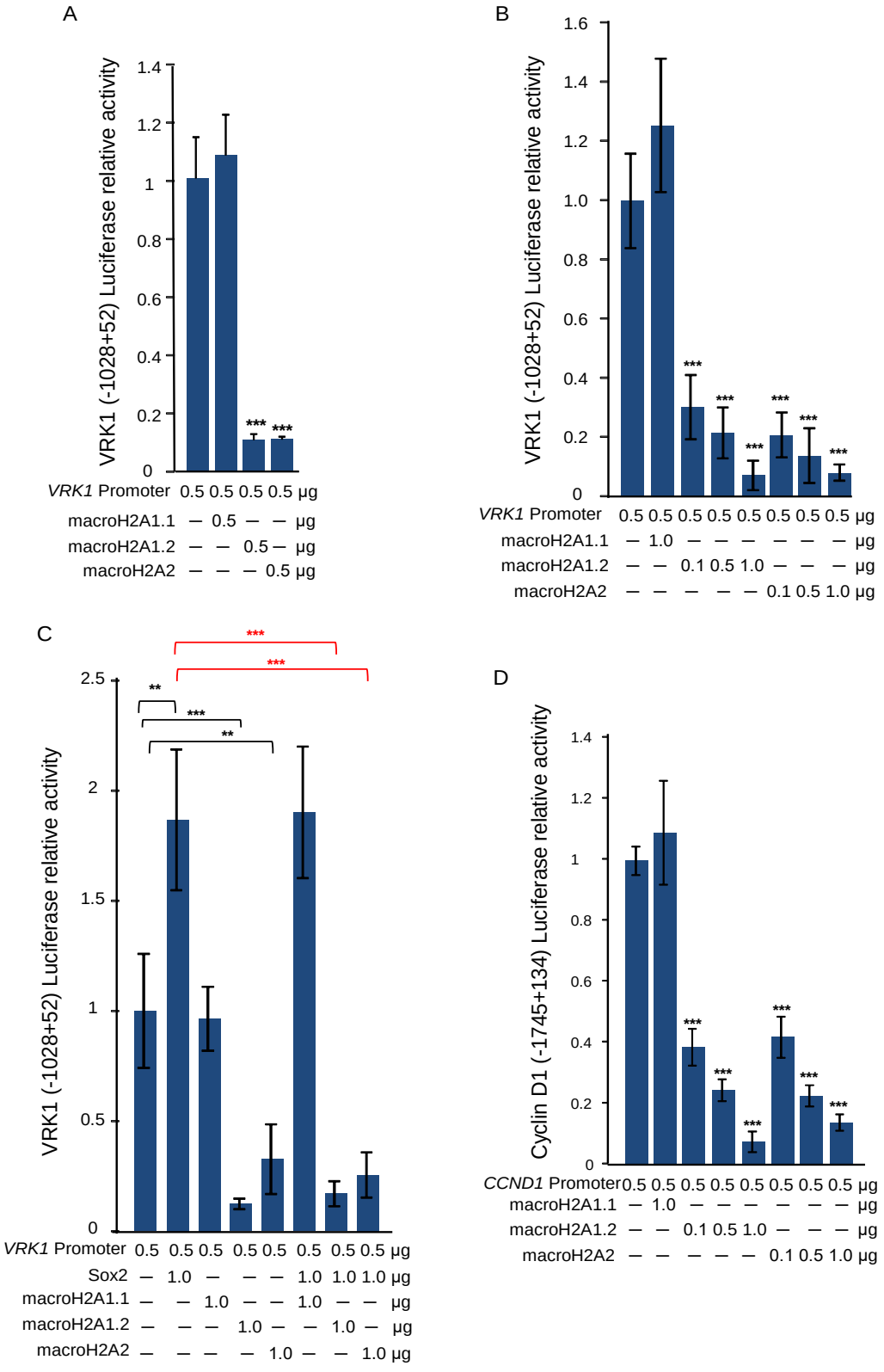

Figure 64. Inhibition of *VRK1* and *CCND1* expression by macroH2A histones. A) The cells were transfected with macroH2A histone variants (pCMV-Tag2A-FLAG-mH2A1.1; pCMV-Tag2A-FLAG-mH2A1.2; pCMV-Tag2A-FLAG-mH2A2) and with pGL2-b-luciferase-VRK1 (-1028+52) vector. B) Cells were transfected with increased concentrations (0.1, 0.5 and 1.0µg) of macroH2A histone variants (pCMV-Tag2A-FLAG-mH2A1.1; pCMV-Tag2A-FLAG-mH2A1.2; pCMV-Tag2A-FLAG-mH2A2) and with pGL2-b-luciferase-VRK1 (-1028+52) vector. C) The cells were transfected with increased concentrations (0.1, 0.5 and 1.0µg) of macroH2A histone variants (pCMV-Tag2A-FLAG-mH2A1.1; pCMV-Tag2A-FLAG-mH2A1.2; pCMV-Tag2A-FLAG-mH2A2), together with myc-FLAG-Sox2 (pCMV6-myc-FLAG-SOX2) and with pGL2-b-luciferase-VRK1 (-1028+52) vector. D) The cells were transfected with increased concentrations (0.1, 0.5 and 1.0µg) of macroH2A histone variants (pCMV-Tag2A-FLAG-mH2A1.1; pCMV-Tag2A-FLAG-mH2A1.2; pCMV-Tag2A-FLAG-mH2A2) and with pA3-CycD1-Prom-Luc (-1745+134). All the experiments were performed in HEK293T and used Renilla-luciferase as internal control. Besides, pGL2-Control plasmid expressing luciferase under the SV40 promoter was used as positive control and pGL2-basic, a promoter-less plasmid, was used as negative and background control. The experiment was performed in triplicate, three times (Student's Test: *<0.05; **<0.005; ***<0.0005).

Finally, the potential regulatory effect of macroH2A histone variants on *CCND1* gene promoter was also studied. Thus, HEK293T cells were transfected with increased concentrations of macroH2A proteins and with the long proximal *CCND1* gene promotor (-1745 to +134), which was cloned in a pGL2-b-luciferase vector. Renilla-luciferase was used as internal control. Once again, we observed that both macroH2A1.2 and macroH2A2 were able to inhibit *CCND1* gene promoter, while macroH2A1.1 had no effect (Figure 64D).

1.9 VRK1 effect on Sox2 protein stability

Lately, we decided to study whether VRK1 had an effect on Sox2 stability. Therefore, NT2 cells were transfected with a siRNA targeting VRK1 (siVRK1-02) and a non-targeting siRNA (siControl) during 72 hours. Then, the cells were treated with CHX and harvest at distinct time periods. We observed that VRK1 depletion did not affected the stability of endogenous Sox2 in NT2 (Figure 65A). Moreover, we tested if Sox2 overexpression affected VRK1 stability in HEK293T cells. So, myc-FLAG-Sox2 was transfected and 48 hours later the cells were

treated with CHX during 24 hours. We did not observe any effect of Sox2 on VRK1 stability (Figure 65B).

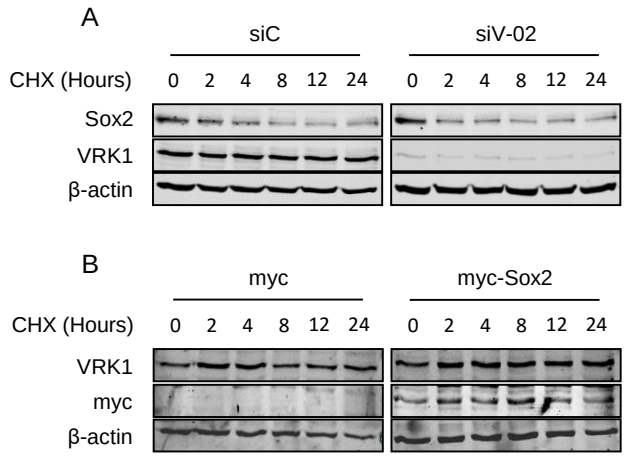

Figure 65. Sox2 stability is unaffected by VRK1, while VRK1 stability is not affected by Sox2. A) NT2 cells were transfected with a specific siRNA targeting VRK1 (siVRK1-02 = siV-02) and with a non-targeting siRNA (siControl = siC). 72 hours later cells were treated with cycloheximide (CHX) and the experimental points harvest at distinct times. Sox2 was detected with a rabbit monoclonal anti-Sox2 antibody. B) HEK293T cells were transfected with myc-FLAG-Sox2 (pCMV6-myc-FLAG-Sox2) or with an empty vector (pCMV6-myc-FLAG) and 48 hours later treated with CHX. The experimental points were harvest at different times during 24 hours.

2.1 VRK1 interaction with Oct4, Klf4 and Nanog

Besides Sox2, we decided to test whether VRK1 interacted with other reprogramming factors such as Oct4, Nanog, Klf4 and c-Myc. Concerning Oct4, we studied first the potential interaction between transfected VRK1 and Oct4 in HEK293T cells. Therefore, the cells were transfected with myc-FLAG-Oct4 alone or alongside with HA-VRK1. Then, protein extracts were immunoprecipitated with a rabbit polyclonal anti-FLAG antibody, or with a rabbit polyclonal anti-HA antibody or with a mouse monoclonal anti-VRK1 (1B5) antibody. VRK1 was detected in Oct4 immunoprecipitate with a mouse monoclonal anti-HA antibody or with a mouse monoclonal anti-VRK1 (1B5) antibody. Oct4 was detected in VRK1 immunoprecipitate with a mouse monoclonal anti-FLAG antibody or with a rabbit polyclonal anti-FLAG antibody. In all the experiments we observed that VRK1 interacted with Oct4 (Figure 66A-D).

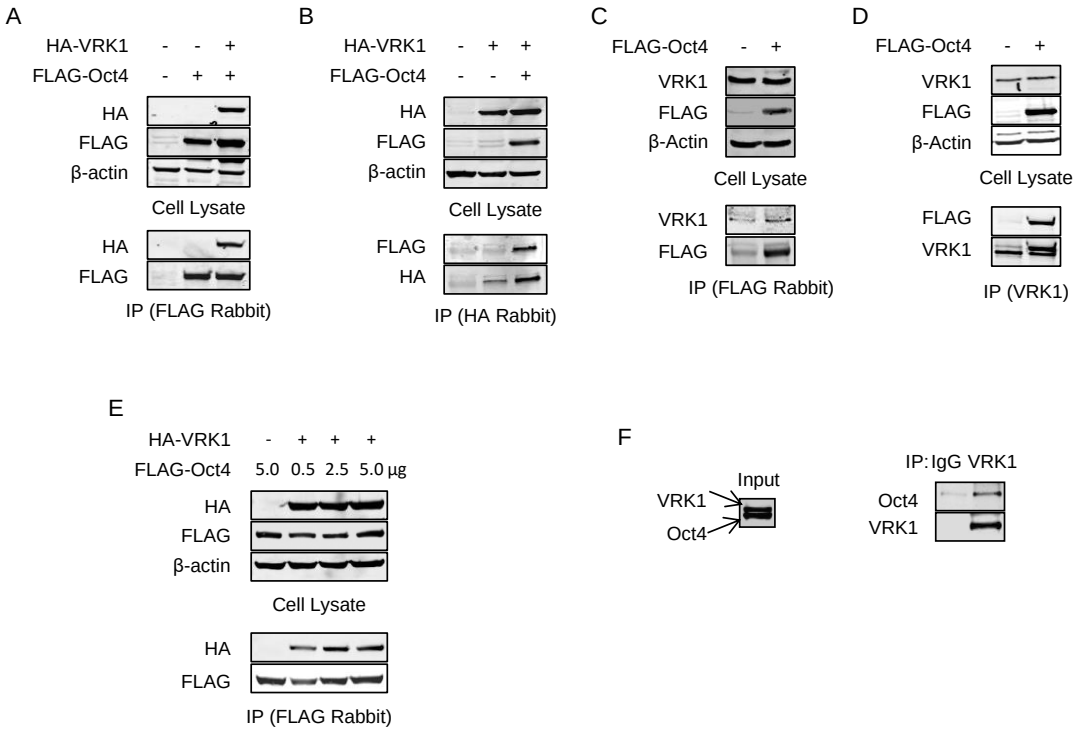

Figure 66. Reprogramming factor Oct4 interacts with VRK1. A) HEK293T cells were transfected with pCMV6-myc-FLAG-Oct4 and pCEFL-HA-VRK1. Oct4 was immunoprecipitated with a rabbit polyclonal anti-FLAG antibody and VRK1 was detected, by immunoblot, with a mouse monoclonal anti-HA antibody. B) HEK293T cells were transfected with pCEFL-HA-VRK1 and pCMV6-myc-FLAG-Oct4. VRK1 was immunoprecipitated with a rabbit polyclonal anti-HA antibody and Oct4 was detected, by immunoblot, with a mouse monoclonal anti-FLAG antibody. C) FLAG-Tagged Oct4 (pCMV6-myc-FLAG-Oct4) was transfected in HEK293T cells and Oct4 was immunoprecipitated with a rabbit polyclonal anti-FLAG antibody. VRK1 was detected with a mouse monoclonal anti-VRK1 (1B5) antibody. D) FLAG-Tagged oct4 (pCMV6-myc-FLAG-Oct4) was transfected in HEK293T cells and VRK1 was immunoprecipitated with a mouse monoclonal anti-VRK1 (1B5) antibody. A mouse monoclonal anti-HA (IgG) antibody was used as control of IP. Oct4 was detected with a rabbit polyclonal anti-FLAG antibody. E) HEK293T cells were transfected with a stable concentration of pCEFL-HA-VRK1 and increased doses of pCMV6-myc-FLAG-Oct4. Oct4 was immunoprecipitated with a rabbit polyclonal anti-FLAG antibody and VRK1 was detected, by immunoblot, with a mouse monoclonal anti-HA antibody. F) VRK1 was immunoprecipitated, from NT2 extracts, with a mouse monoclonal anti-VRK1 (1B5) antibody and Oct4 was detected with a rabbit monoclonal anti-Oct4 antibody. A mouse monoclonal anti-HA (IgG) antibody was used as control of IP.

Also, a stable concentration of HA-VRK1 was transfected with increased doses of myc-FLAG-Oct4. Next, Oct4 was immunoprecipitated with a rabbit polyclonal anti-FLAG antibody and VRK1 was detected with a mouse monoclonal anti-HA antibody. Again, we observed that VRK1 and Oct4 interacted, being the interaction, in this case, dependent on Oct4 concentration (Figure 66E). Finally, we verified the interaction between endogenous VRK1 and Oct4 proteins. NT2 extracts were immunoprecipitated with a mouse monoclonal anti-VRK1 (1B5) antibody and Oct4 was detected using a rabbit monoclonal anti-Oct4 antibody. Again, VRK1 interacted with Oct4 (Figure 66F).

Subsequently, we analyzed the potential interaction between VRK1 and the transcriptional factor Nanog. Thus, NT2 extracts were immunoprecipitated with a mouse monoclonal anti-VRK1 (1B5) antibody and Nanog was detected using a rabbit monoclonal anti-Nanog antibody. We observed that VRK1 interacted with Nanog (Figure 67).

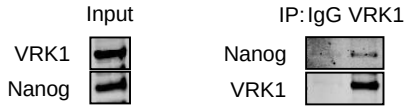

Figure 67. VRK1 interacts with reprogramming factor Nanog. VRK1 was immunoprecipitated, from NT2 extracts, with a mouse monoclonal anti-VRK1 (1B5) antibody and Nanog was detected with a rabbit monoclonal anti-Nanog antibody. A mouse monoclonal anti-HA (IgG) antibody was used as control of IP.

Next, we focused our attention on the potential interaction between VRK1 and Klf4. Therefore, HEk293T cells were transfected with myc-FLAG-Klf4 alone or together with HA-VRK1. Afterward, protein extracts were immunoprecipitated with a rabbit polyclonal anti-FLAG antibody, or with a rabbit polyclonal anti-HA antibody or with a mouse monoclonal anti-VRK1 (1B5) antibody. VRK1 was detected in Klf4 immunoprecipitate with a mouse monoclonal anti-HA antibody or with a mouse monoclonal anti-VRK1 (1B5) antibody. Klf4 was detected in VRK1 immunoprecipitate with a mouse monoclonal anti-FLAG antibody or with a rabbit polyclonal anti-FLAG antibody. We observed that VRK1 interacts with Klf4 (Figure 68).

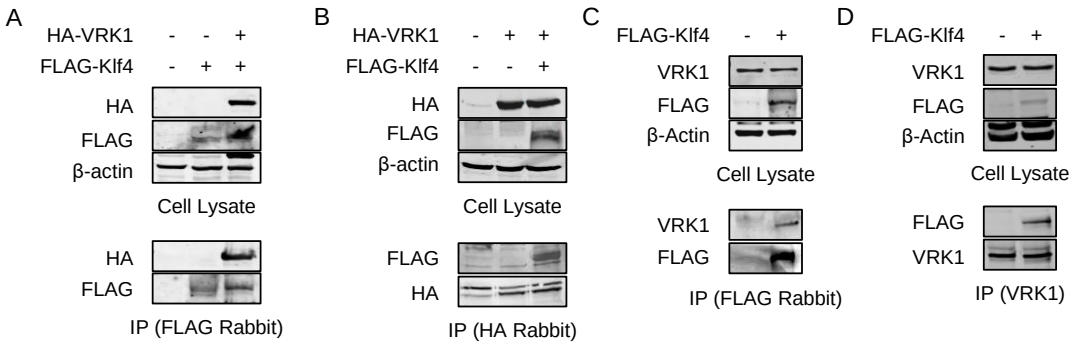

Figure 68. Reprogramming factor Klf4 interacts with VRK1. A) HEK293T cells were transfected with pCMV6-myc-FLAG-Klf4 and pCEFL-HA-VRK1. Klf4 was immunoprecipitated with a rabbit polyclonal anti-FLAG antibody and VRK1 was detected, by immunoblot, with a mouse monoclonal anti-HA antibody. B) HEK293T cells were transfected with pCEFL-HA-VRK1 and pCMV6-myc-FLAG-Klf4. VRK1 was immunoprecipitated with a rabbit polyclonal anti-HA antibody and Klf4 was detected, by immunoblot, with a mouse monoclonal anti-FLAG antibody. C) FLAG-Tagged Klf4 (pCMV6-myc-FLAG-Klf4) was transfected in HEK293T cells and Klf4 was immunoprecipitated with a rabbit polyclonal anti-FLAG antibody. VRK1 was detected with a mouse monoclonal anti-VRK1 (1B5) antibody. D) FLAG-Tagged Klf4 (pCMV6-myc-FLAG-Klf4) was transfected in HEK293T cells and VRK1 was immunoprecipitated with a mouse monoclonal anti-VRK1 (1B5) antibody. A mouse monoclonal anti-HA (IgG) antibody was used as control of IP. Klf4 was detected with a rabbit polyclonal anti-FLAG antibody.

Finally, we verified if VRK1 interacted with the transcriptional factor c-Myc. Therefore, NT2 extracts were immunoprecipitated with a mouse monoclonal anti-VRK1 (1B5) antibody and c-Myc was detected using a rabbit polyclonal anti-c-Myc antibody. We did not observe any interaction between VRK1 and c-Myc (Figure 69).

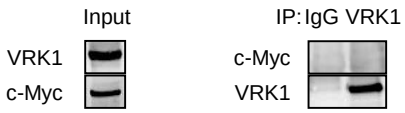

Figure 69. VRK1 and c-Myc do not interact. VRK1 was immunoprecipitated, from NT2 extracts, with a mouse monoclonal anti-VRK1 (1B5) antibody and c-Myc was detected with a rabbit polyclonal anti-c-Myc antibody. A mouse monoclonal anti-HA (IgG) antibody was used as control of IP.

3.1 Effect of Sox2-Oct4 complex on *VRK1* gene promoter

Sox2 was described to be in some cases a weak/ moderate modulator of gene transcription, during embryonic development, pairing with several partner factors to potentiate its transcriptional activity. In fact, the transcriptional factors Sox2 and Oct4 had been reported to form a stable complex that is important in the regulation of *NANOG* gene promoter activity (Kamachi et al., 2000; Rodda et al., 2005). Attending to the fact that *VRK1* gene promoter was average activated by Sox2, we studied the potential co-operation between Sox2 and Oct4 on the activation of this gene promoter. Initially, we decided to verify that in fact Sox2 forms a stable complex with Oct4. Therefore, NT2 cells were immunoprecipitated with a mouse monoclonal anti-Sox2 antibody and Oct4 was detected, by immunoblot, in Sox2 immunoprecipitate with a rabbit monoclonal anti-Oct4 antibody. Indeed, it was observed that Sox2 interacts with Oct4 (Figure 70A). Similar result was obtained between transfected proteins (Figure 70B). Next, we tested if the long proximal *VRK1* gene promoter was modulated by Oct4, by itself. HEK293T cells were transfected with myc-FLAG-Oct4, alongside with the long proximal *VRK1* promoter (-1028 to + 52) region expressing plasmid, cloned in pGL2-b-luciferase vector. Renilla-luciferase was used as internal control. Oct4 did not activated or repressed the *VRK1* gene promoter (Figure 70C). Finally, we analyzed the potential co-operation between both transcriptional factors Sox2 and Oct4 on the activation of *VRK1* gene promoter. Therefore, HEK293T cells were transfected with both myc-FLAG-Sox2 and myc-FLAG-Oct4, together with the long proximal *VRK1* promoter (-1028 to + 52) region expressing plasmid, cloned in pGL2-b-luciferase vector. Once again, Renilla-luciferase was used as internal control. We confirmed that Sox2 activated *VRK1* gene promoter, but Oct4 did not potentiate Sox2 effect (Figure 70D). The analysis of proximal *VRK1* (-1028 to +52) gene promoter sequence confirmed the absence of consensus target sequences for Oct4 (Zhou and Liu, 2008), which could explain the lack of promoter activation by Oct4 (Figure 71).

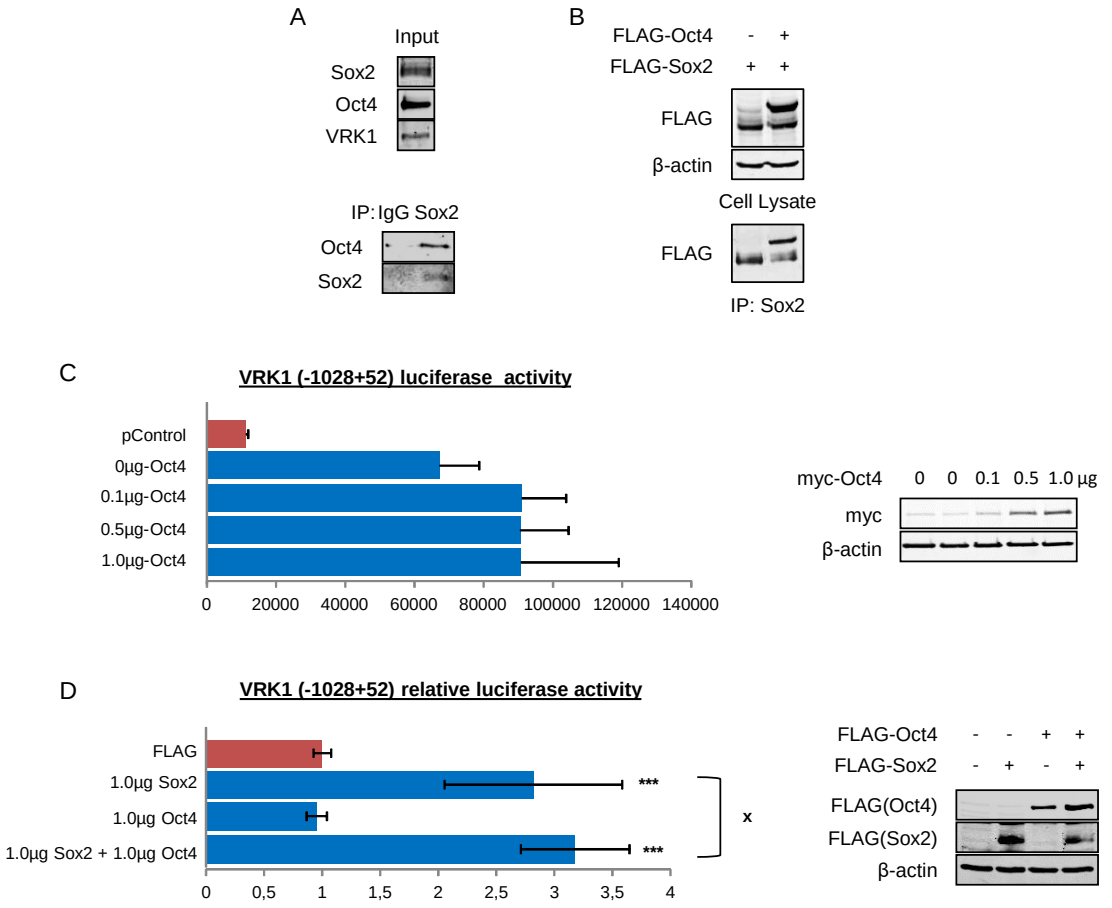

Figure 70. Sox2 and Oct4 did not co-operate on the activation of *VRK1* promoter.

A) NT2 cells were immunoprecipitated with a mouse monoclonal anti-Sox2 antibody and Oct4 was detected, by immunoblot, with a rabbit monoclonal anti-Oct4 antibody. B) HEK293T cells were transfected with pCMV6-myc-FLAG-Sox2 and pCMV6-myc-FLAG-Oct4. Sox2-myc-FLAG tagged protein was immunoprecipitated with a mouse monoclonal anti-Sox2 antibody and Oct4-myc-FLAG tagged protein was detected with a rabbit polyclonal anti-FLAG antibody. C) HEK293T cells were transfected with increased concentrations (0.1, 0.5 and 1.0µg) of Oct4 (pCMV6-myc-FLAG-Oct4) and with pGL2-b-luciferase-VRK1 (-1028+52) vector. D) HEK293T cells were transfected with both transcriptional factors Sox2 (pCMV6-myc-FLAG-Sox2) and Oct4 (pCMV6-myc-FLAG-Oct4), together with pGL2-b-luciferase-VRK1 (-1028+52) vector. All the luciferase assays used Renilla-luciferase as internal control. Besides, pGL2-Control plasmid expressing luciferase under the SV40 promoter was used as positive control and pGL2-basic, a promoter-less plasmid, was used as negative and background control. The experiment was performed in triplicate, three times (Student's Test: *<0.05; **<0.005; ***<0.0005).

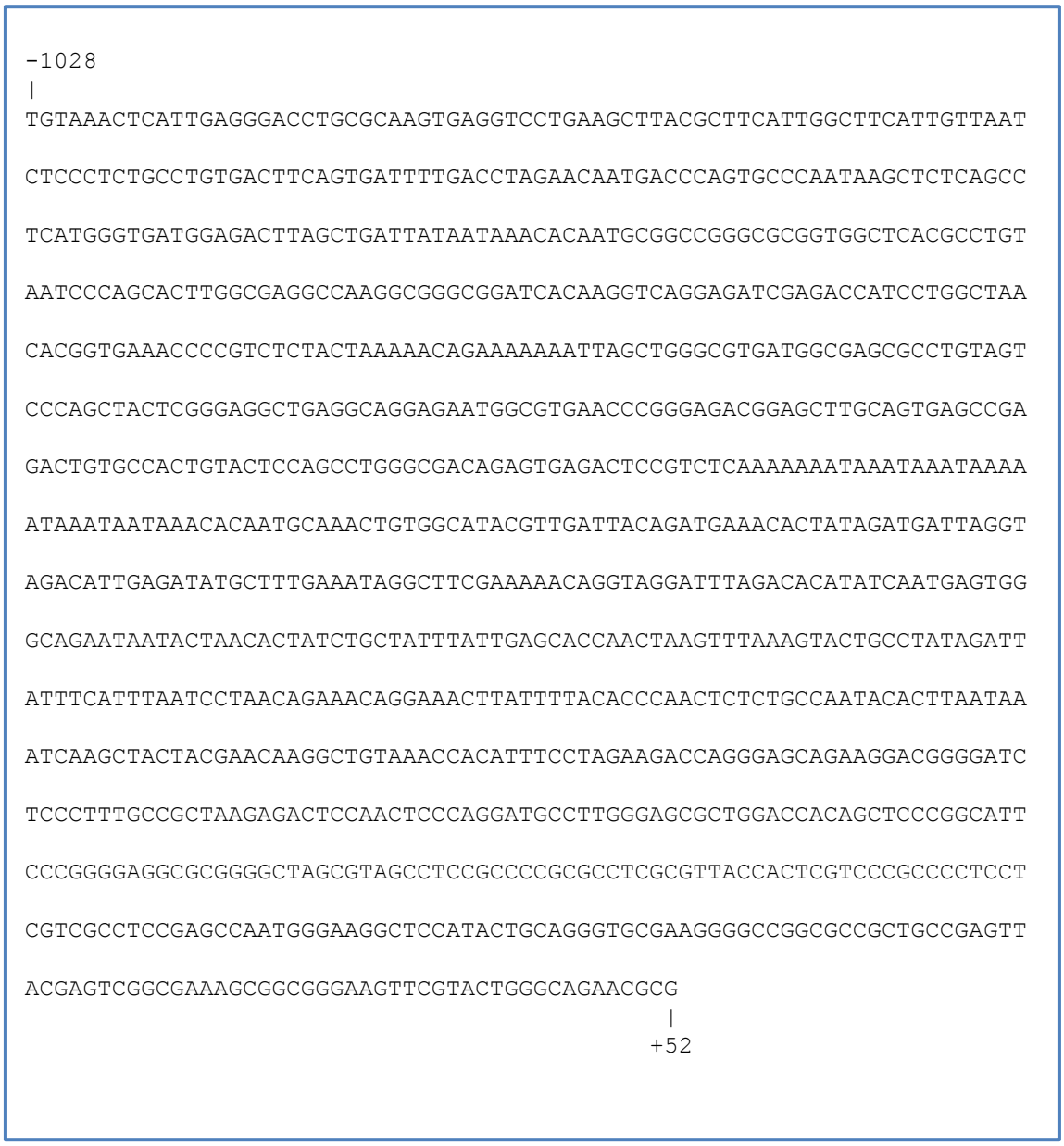

Figure 71. Oct4 consensus target sequences on the proximal promoter (-1028+52) of the human *VRK1* gene. The sequence did not present DNA binding motifs to Oct4 transcription factor.

Discussion

Part 1. Implication of VRK1 in the regulation of AurKB mitotic localization and activity

1.1 Role of VRK1 on the regulation of AurKB activity during mitosis

Human VRK1 is implicated in the correct progression of cell cycle. This observation derives mainly from VRK1 gene expression knockdown assays, where induction of G0/G1 cell cycle arrest is observed, as a result of a reduction on the levels of cyclin A, cyclin D1, PCDNA, among other proliferation markers (Lee et al., 2015; Valbuena et al., 2008b; Valbuena et al., 2011b). Nevertheless, VRK1 regulates also numerous mechanisms during mitosis, more precisely, in the G2/M phase transition, indicating a role not only in interphase but also later, during the mitotic phases. Indeed, VRK1 regulates the nuclear envelope assembly and disassembly, as well as the mitotic Golgi fragmentation and, plays a major role on the chromatin condensation during the G2/M transition, phosphorylating the Thr3 and Ser10 residues on the histone H3, as previously described (Gorjanacz et al., 2008; Lopez-Sanchez et al., 2009; Nichols et al., 2006a). Indeed, our results undeniably show that the depletion of VRK1 causes a decrease in both H3T3ph and H3S10ph, as previously reported (Kang et al., 2007b). Nonetheless, using specific antibodies against histone H3 phosphorylation and through a kinase assay with cold ATP, we show that only the Thr3 residue is a direct phosphorylating target of VRK1, in contrast to previously described results. This difference could be related to distinct experimental conditions, but we mostly emphasize the fact that in some kinase assays, performed by Kang and colleagues, GST protein by itself showed H3S10ph, quite similar to recombinant protein GST-VRK1 (Kang et al., 2007b). The condensation of chromatin begins in prophase and is vital to ensure that the chromosomes are highly compacted in the following phases of the cell cycle. Compacted chromatin facilitates the correct bi-orientation of sister chromatids and the segregation of the chromosomes (Kang et al., 2007b; Salzano et al., 2015; Thadani and Uhlmann, 2015; Wilkins et al., 2014). In turn, human AurKB is a member of the aurora kinase family, together with AurKA and AurKC and is

an important element of CPC, along with Survivin, Borealin and INCENP. AurKB activity is fulfilled during mitosis, and it regulates centromere function, chromatin condensation, spindle assembly, chromosome alignment and segregation and, cytokinesis (Bolanos-Garcia, 2005; Carmena and Earnshaw, 2003). AurKB activity is particularly interesting for our work given that this kinase participates in chromatin condensation, via H3S10 phosphorylation (Crosio et al., 2002). Besides, AurKB seems to regulate H3T3ph, through the direct phosphorylation of Haspin, which turns active and phosphorylates H3T3. This phosphorylation targets CPC/ AurKB to centromeric chromatin were this kinase executes its functions (Wang et al., 2010; Wang et al., 2011). Besides histone H3, also transcriptional factor p53 is a common phosphorylation target of VRK1 and AurKB (Gully et al., 2012; Lopez-Sanchez et al., 2014b; Valbuena et al., 2011a; Vega et al., 2004a). Altogether, it seems likely that both VRK1 and AurKB jointly participate in the regulation of specific mitotic mechanisms.

Initially, we studied the hypothetical co-regulation of a known common substrate, histone H3, by VRK1 and AurKB, through kinase assays with radiolabeled [γ-^{32}P] ATP (Cantarero et al., 2015; Crosio et al., 2002; Kang et al., 2007b; Salzano et al., 2015). Our results showed that the ability of AurKB and VRK1 to phosphorylate histone H3 was inhibited, since recombinant proteins incubated alone with the substrate, showed higher levels of histone H3 phosphorylation in comparison to the phosphorylation levels observed when these recombinant proteins were incubated together. A decrease on the autophosphorylation levels of AurKB and VRK1 was also detected, when kinases were incubated with the respective kinase dead partner, indicating that each WT kinase was unable to self-activate by phosphorylation. Therefore, the lack of catalytic activity of both VRK1 and AurKB towards histone H3, could be due to the inability of these kinases to self-activate. Indeed, autophosphorylation of AurKB was previously reported to be essential for its kinase activity towards histone H3 and Vimentin, during cytokinesis (Yasui et al., 2004). On the other hand, VRK1 was described to have a strong autophosphorylation activity, apparently critical to its kinase activity on the transcriptional factor p53 (Lopez-Borges and Lazo, 2000; Nichols and Traktman, 2004). Similar results were obtained in kinase assays with cold ATP and phospho-specific antibodies against

histone H3 phosphorylations and p53 phosphorylation. AurKB negatively affected the phosphorylation of histone H3 and p53, by VRK1, being this effect independent of AurKB kinase activity and dependent on the kinase levels. In turn, VRK1 negatively affected the phosphorylation of histone H3, by AurKB, independently of it kinase activity and dependent on kinase levels. Accordingly, AurKB and VRK1 seemed to be regulating the kinase activity of one another, independently of their kinase activity and dependently on their levels. This is attributed to an unknown mechanism that probably targets the autophosphorylation activity of each kinase. Moreover, the fact that AurKB regulates VRK1 activity is quite fascinating, since the first kinase seems to be regulating both protein kinases that target H3T3 for phosphorylation. The first, through the phosphorylation of Haspin, which is able to phosphorylate H3T3 when activated by AurKB and the second, through the regulation of VRK1, by an unknown mechanism (Wang et al., 2010; Wang et al., 2011). Moreover, it seemed that this regulatory effect was independent of their kinase activity, since no phosphorylation was observed on VRK1 by AurKB or on AurKB by VRK1. Nevertheless, the fact that histone H3 is present in the mix with the recombinant proteins VRK1 and AurKB, might had induced a miss-observation and further experiments were necessary to test whether at least one of the kinases is a phosphorylation target of the other.

Afterwards, we studied the potential formation of a complex between VRK1 and AurKB that could explain the catalytic inhibitory effect detected when kinases were combined together in kinase assays. Physical interaction between human kinases had been previously reported (i.e. VRK1 and Plk3) and therefore it seemed probable that this could also occur between VRK1 and AurKB (Lopez-Sanchez et al., 2009). Indeed, our results showed a clear interaction between exogenous VRK1 and AurKB. Moreover, this interaction occurred independently of VRK1 activity, since VRK1 dead kinase (K179) also interacted with AurKB. Surprisingly, AurKB formed a stronger complex with inactive VRK1, which is compatible with the fact that inactive VRK1 is unable to complete the potential catalytic cycle. Similar results have also been described concerning VRK1 and p53 stable complex (Lopez-Sanchez et al., 2014b). At this point, it would also be relevant to analyze the interaction between VRK1 and AurKB kinase dead

(K106R), to verify if this interaction is also independent of AurKB activity. Additionally, we observed that VRK1 interacted with AurKB, through both amino and carboxy terminals, perhaps due to the tertiary structure of the protein. Nonetheless, it was expected that VRK1 interacted with AurKB mainly through the carboxy terminal region. Evidence showed that VRK1 interacts with several other proteins through the carboxy terminal region, characterized by its low complexity and high flexibility. Besides, the amino terminal kinase domain don't form stable protein complexes, to allow the rapid release of ADP and phosphorylated target proteins (Kim et al., 2012c; Lopez-Sanchez et al., 2014b; Sanz-Garcia et al., 2012).

The interaction between VRK1 and AurKB exogenous proteins was quite consistent in all the performed experiments. Nevertheless, it was crucial to confirm the formation of a stable complex between endogenous VRK1 and AurKB protein kinases. Our results showed that both endogenous VRK1 and AurKB proteins, interacted and that this interaction occurred in mitosis, when AurKB activity and levels are higher. Unfortunately, it was impossible to ensure the precise mitotic phase in which the stable complex between VRK1 and AurKB was formed. In fact, co-localization was not observed between the two mitotic kinases at any stage of mitosis. In early mitotic stages, nearly all VRK1 is located in the cytoplasm, not associated with chromatin, whereas AurKB was linked to centromeric chromatin or chromosomal arms. These distinct localizations agree with previous reports (Cantarero et al., 2015; Carmena and Earnshaw, 2003; Wang et al., 2010) and could mean that the stable complex only involved a small subpopulation of each mitotic kinase. Actually, it has also been showed that a small dynamic pool of cytoplasmic AurKB, continuously exchanged with the centromeric pool of AurKB, before the onset of anaphase (Murata-Hori and Wang, 2002). These AurKB cytoplasmic location resembles more with the VRK1 observed localization and therefore, it could mean that the stable kinase complex was formed between the two protein cytoplasmic subpopulations. In our work, we observe no differences in the formation of VRK1 and AurKB protein complex, when comparing the chromatin associated fraction with the cytoplasmic fraction, in prometaphase arrested cells. Yet, it could be important to repeat this assay, to be sure that the low VRK1 levels observed in the chromatin, in the cell lysate of nocodazole arrested cells, were not an artefact of insufficient washing, during the

separation of cytoplasmic and chromatin fractions. Even facing the impossibility to define a specific stage or stages of mitosis, in which AurKB interacted with VRK1, we can speculate and abridge these stages. Taking into account the fact that nocodazole arrested cells into prometaphase (Pagan et al., 2015) and that the VRK1-AurKB interaction decreased and disappeared in parallel with the H3T3ph, which is dephosphorylated at the onset of anaphase (Qian et al., 2011), we can assume that the mitotic complex formed between the two kinases is most likely to occur during prometaphase and/or metaphase (Figure 72). However we cannot exclude that at the beginning of chromosome segregation, both kinases are still interacting nor that VRK1 and AurKB interaction is formed before prometaphase, during G2 or at prophase.

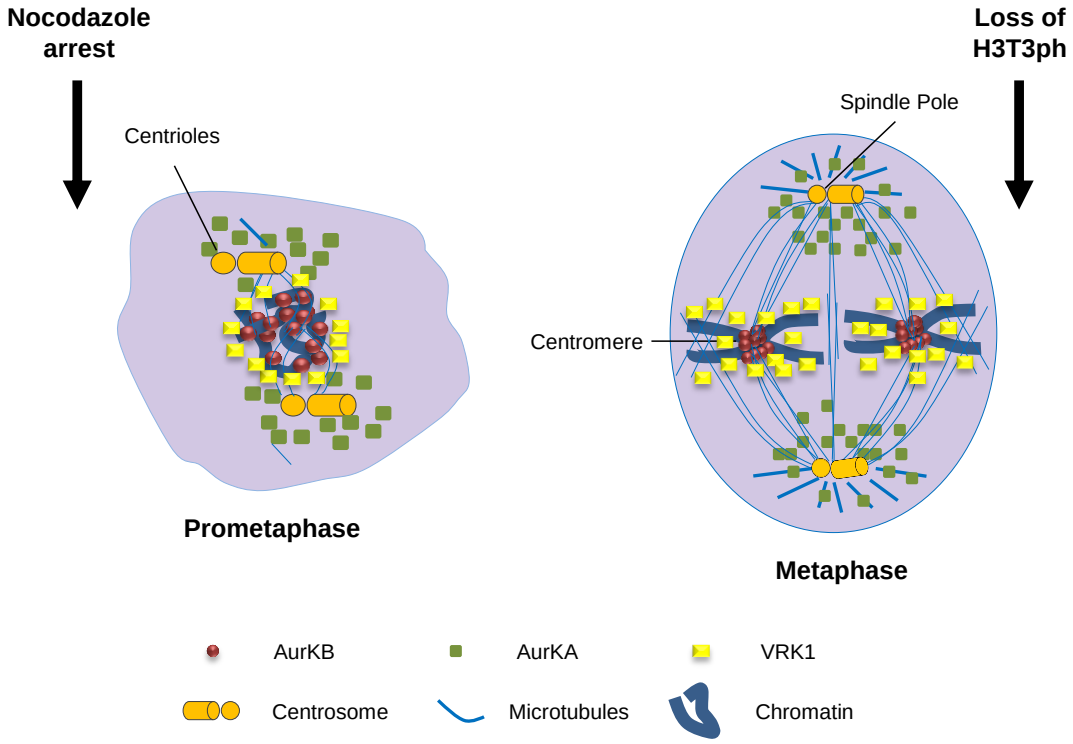

Figure 72. Mitotic stages when AurKB and VRK1 are more likely to interact. The interaction occurs after nocodazole arrest in prometaphase and lasts until the loss of H3T3ph. The dephosphorylation of histone H3 phosphorylation happens in anaphase.

Until the moment, we knew that VRK1 interacted with AurKB, during mitosis and that this interaction interfered with the kinase activity of each member of the complex. Yet, the most expected event would be when a protein kinase interacts with another protein, that the kinase phosphorylates the protein substrate. This occurs to most of the protein kinases in the human kinome,

including VRK1 and AurKB. For example, it was reported that VRK1 phosphorylates p53, histone H3, coilin, histone H2A.X or CREB (Cantarero et al., 2015; Kang et al., 2007b; Salzano et al., 2015; Vega et al., 2004a) and it is phosphorylated by Plk3 (Lopez-Sanchez et al., 2009). In turn, AurKB phosphorylates proteins such as histone H3 and MCAK, and protein kinases like Haspin, and ATM (Hirota et al., 2005; Wang et al., 2011; Yang et al., 2011; Zhang et al., 2007) and it is phosphorylated by Chk1 (Petsalaki et al., 2011). However, in our work, even if our results showed that both kinases interacted, VRK1 was not a phosphorylation target of AurKB and vice versa. Yet, we cannot discard that at least one of the two protein kinases is a substrate for phosphorylation by the other. In fact, using a tool to predict kinase-specific phosphorylation sites, the *GPS* software, VRK1 was determined as a high-score potential substrate for AurKB phosphorylation. At this point, it is curious to observe that VRK1 could be a phosphorylation substrate of AurKB, alike the mitotic protein kinase Haspin (Wang et al., 2011). Both VRK1 and Haspin phosphorylate H3T3 and therefore the existence of a regulatory feedback mechanism is highly probable, in which AurKB regulates the phosphorylation of histone H3, through the phosphorylation of Haspin (Qian et al., 2013; Wang et al., 2010; Wang et al., 2011) and maybe by phosphorylating VRK1. Less likely to occur is the phosphorylation of AurKB by VRK1, since the phosphorylating scores and thresholds, given by the *GPS* analysis, were very low. Accordingly, it could be important to repeat the kinase assay, in order to verify the potential phosphorylation of VRK1 by AurKB, using immunoprecipitated AurKB from nocodazole arrested cells, instead of recombinant GST-AurKB protein. AurKB immunoprecipitated from prometaphase arrested cells, could have a distinct activation status and/ or different tertiary conformation and therefore, it could be able to phosphorylate VRK1. Moreover, it is important to notice that AurKB is the enzymatic core of the CPC, but depends on other members of the complex (notably INCENP) for its localization and activity (Floyd et al., 2013). So, it could be necessary to use the CPC complex, instead of AurKB alone, in order to prove that VRK1 is a phosphorylation target of the CPC enzymatic member, AurKB.

At this point, it seemed that the formation of a stable complex between VRK1 and AurKB, was directly involved in the regulation of their autophosphorylation and consequently in the control of their kinase activity. A

regulation that seems regardless of phosphorylation on one another and that occurs during mitosis (Figure 73).

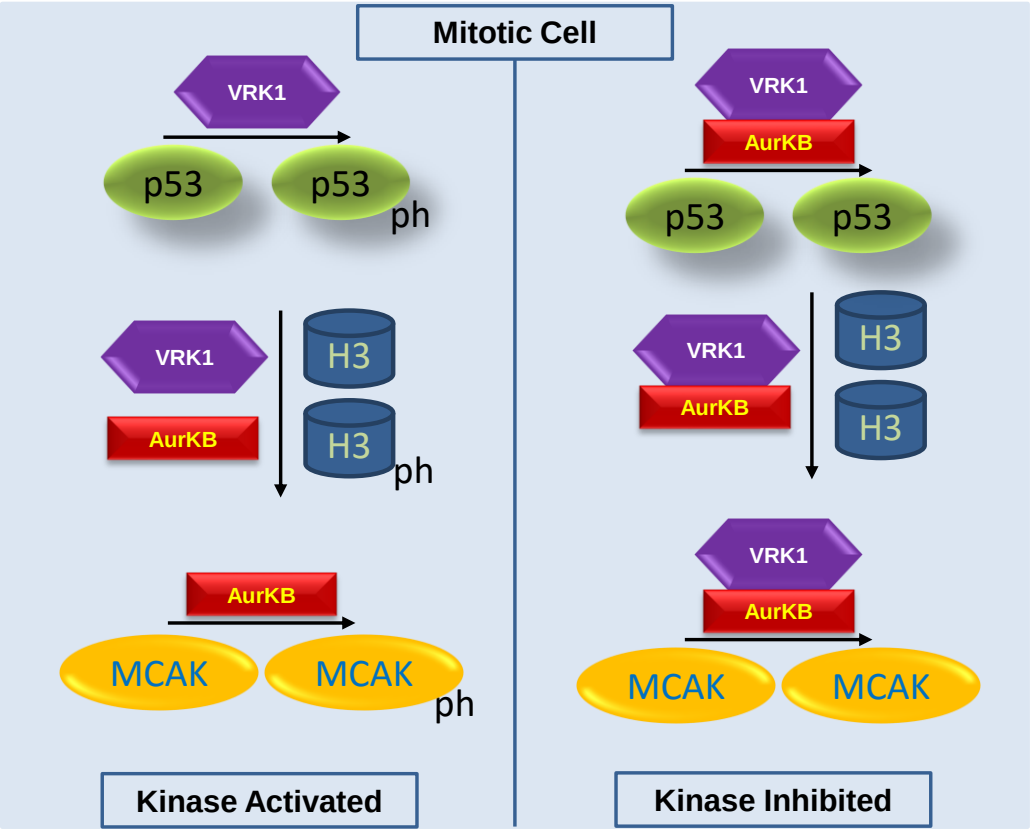

Figure 73. Schematically representation of AurKB and VRK1 inhibitory complex. The formation of a stable complex between VRK1 and AurKB inhibits their kinase activity, probably due to repressed autophosphorylation activity. The examples are potential targets of regulation, when the kinases interact. Non-interacting AurKB is able to phosphorylate MCAK and histone H3, while non-interacting VRK1 is able to phosphorylate p53 and histone H3. The phosphorylation of p53, by VRK1, was not demonstrated to occur during mitosis, but it was used as an example of VRK1 substrate. However, we cannot exclude that VRK1 phosphorylates p53 in response to DNA damage during mitosis.

Nonetheless, it's unclear the phosphorylation targets that may be affected by the AurKB and VRK1 mitotic inhibition, due to their interaction. The phosphorylation of histone H3, is an obvious candidate as the main final target of this regulation, but our results showed that the levels of H3T3ph (VRK1-dependent) and H3S10ph (AurKB-dependent) were on top, during the mitotic stages in which VRK1 interacted with AurKB. Still, we need take into account that

the histone H3 phosphorylation is a dynamic process, involving numerous protein kinases and phosphatases, which are responsible for the modulation of histone H3 phosphorylation, in a given location at a given time. (Baek, 2011; Jeong et al., 2013; Sugiyama et al., 2002). Accordingly, interacting VRK1 and AurKB could be inhibiting the phosphorylation in one precise chromatin location, while non-interacting VRK1 and AurKB are phosphorylating the histone at a different point of the chromatin. Besides, it is important to confirm the exact time or stage within the VRK1 and AurKB complex is formed and whether it occurs before or after histone H3 phosphorylation. Therefore, it could be important to release cells from thymidine arrest and analyze whether this interaction appears before or after mitotic phosphorylation of histone H3.

Furthermore, it could be interesting to test other of the most likely targets to be regulated by this complex, during the early stages of mitosis, the MCAK. This protein form dimers that assemble at the end of microtubules to form an ATP-hydrolyzing complex that processively depolymerizes microtubules. Moreover, MCAK is phosphorylated by AurKB in three different sites (Thr95, Ser110, Ser196), creating a two-site phosphoregulatory mechanisms, which targets kinesin to chromosomal arms or centromeres. The binding of MCAK to chromatin precedes its centromeric localization and creates a dynamic pool of MCAK protein set to load on the centromeres. Thr95ph associates MCAK with the chromosome arms, whereas Ser196ph promotes de disassociation of the chromosome arms. Se196ph also inhibits the microtubule depolymerizing activity of MCAK. In turn, MCAK centromere targeting is accomplished by a balance between Ser110ph and dephosphorylation of Thr95. MCAK located in the centromeres is relevant to correct mal-attachments of kinetochores to microtubules, and so for proper chromosomal alignment and segregation. Centromeric MCAK is hyper-phosphorylated on Ser110 and hypo-phosphorylated on Ser196 at mal-attached kinetochores (Andrews et al., 2004; Zhang et al., 2007). Altogether, it could be relevant to analyze the effect of VRK1 knockdown on the regulation of MCAK activity and localization, by AurKB phosphorylation. For example, uncontrolled phosphorylation of MCAK on T95 could affect its centromeric localization and consequently mal-attachment correction. Moreover, continuous phosphorylation of S196 could inhibit MCAK activity, leading to the formation of mal-attachment. The formation of uncorrected

mal-attachment could lead to improper chromosomal alignment and segregation and culminate in cell cycle arrest. Indeed, unpublished microscopic video data from our lab, revealed that VRK1 knockdown induces incomplete segregation, associated with the formation of chromosomal bridges during segregation. Besides, it could be fascinating to study whether VRK1 could also phosphorylate and regulate MCAK activity and localization or if VRK1 could participate in the mitotic spindle formation, through an independent pathway. In fact, it is known that RCC1 generates a highly local concentration of Ran-GTP around the chromatin which in turn induces the local nucleation of microtubules and mitotic spindle formation. Moreover, inactive RanGDP interacts with VRK1 and inhibits its kinase activity, whereas VRK1 activity is recovered if it is free, or bound to Ran in its active conformation (RanGTP), or to Ran activated by RCC1 (Carazo-Salas et al., 1999; Sanz-Garcia et al., 2008). Accordingly, VRK1 could be regulating the mitotic spindle formation in co-operation with a Ran-dependent pathway and with an AurKB-dependent pathway.

Finally, it could be important to analyze the effect of AurKB and VRK1 double depletion, especially on cell proliferation. Either by using specific siRNAs targeting VRK1 and AurKB, or by using specific kinase inhibitors, even if the actual panorama on VRK1 inhibitors is not encouraging (Kim et al., 2015; Kim et al., 2014; Vazquez-Cedeira et al., 2011). Knowing that both kinase proteins are implicated in cell cycle division and that their kinase activity seems strictly regulated by one another, a double depletion could induce a higher effective cell arrest and lower cell proliferation, with potential promising results for the therapeutics.

1.2 Implication of VRK1 on the control of AurKB localization during mitosis

The centromeric localization and accumulation of CPC, and consequently of AurKB, during the early stages of mitosis, has been reported to depend on the phosphorylation of histone H3 on Thr3 by Haspin, and on the phosphorylation of histone H2A on Thr120 by Bub1. Moreover, it is known that H3T3ph serves as a docking site for Survivin and the H2AT120ph is a binding site for Borealin via Sgo1. Therefore, loss of H3T3ph leads to CPC-AurKB mislocalization at the centromeres and increased AurKB dispersion on the chromatin (Rosasco-Nitcher

et al., 2008; Wang et al., 2010; Wang et al., 2011; Watanabe, 2010). Altogether and since H3T3 is a direct phosphorylation target of VRK1 (Kang et al., 2007b; Salzano et al., 2015), it is likely that AurKB centromeric localization, may depend also on VRK1 kinase activity, as much as it depends on Haspin kinase activity. Indeed, our results show that VRK1 depletion led to a re-location of AurKB from centromeres and chromosomal arms to a more diffuse state on the chromatin, in prometaphase arrested cells. This result is sustained by the decreased number of cells with yellow dots, consequence of diminished ACA and AurKB co-localization, and by the reduced overlapping pixels calculated by Pearson's correlation coefficient. Furthermore, our results showed that VRK1 depletion led to a decrease in the interaction between the mitotic kinase AurKB and histone H3, potentially due to the loss of H3T3ph. Altogether, these results fundamentally demonstrate that VRK1 downregulation induced a loss of H3T3ph, which affected the direct binding of Survivin to the phosphorylated histone. Since AurKB is associated with histone H3 phosphorylated via Survivin, the loss of interaction with the histone protein led to an alteration on its localization, since the kinase is unable to accumulate on the centromeres (Figure 74).

Nevertheless, it is always important to notice that interaction between histone H3 and AurKB, during early stages of mitosis, depends constantly on Survivin, since this protein binds directly to the phosphorylated histone H3 (Wang et al., 2010). Therefore, it could be also important to analyze the interaction of histone H3 and Survivin, when VRK1 is depleted. We should observe an equal decrease on the interaction between histone H3 and Survivin, similarly to what was observed between AurKB and histone H3. Besides, it could be also important to confirm the direct association of Survivin and AurKB with H3T3ph, apart from their association with histone H3 (Figure 73).

Moreover, the centromeric localization of AurKB, depends also on the binding of Borealin via Shugoshin-1 to phosphorylated H2AT120 (Kawashima et al., 2010; Watanabe, 2010). This phosphorylation was associated with Bub1 in humans, but in D*rosophila* the phosphorylation of H2AT119, which corresponds to human H2AT120, was attributed to NHK-1, a *Drosophila* orthologous gene to human VRK1 (Aihara et al., 2004; Brittle et al., 2007). Therefore, it could be important to study whether human VRK1 phosphorylates H2AT120 and if so, whether this phosphorylation is also critical for the centromeric localization of

CPC and consequently of AurKB. Human VRK1 could be regulating AurKB localization and accumulation on centromeric chromatin through both H3T3ph and H2AT120ph. Likewise, it could be stimulating to assess the potential relationship between both the human mitotic Ser/ Thr kinases VRK1 and Haspin. These kinases may act synergistically or synchronously on the regulation of mitotic H3T3ph, and consequently one could be regulating the other or both could be regulated upstream by some unknown mechanism.

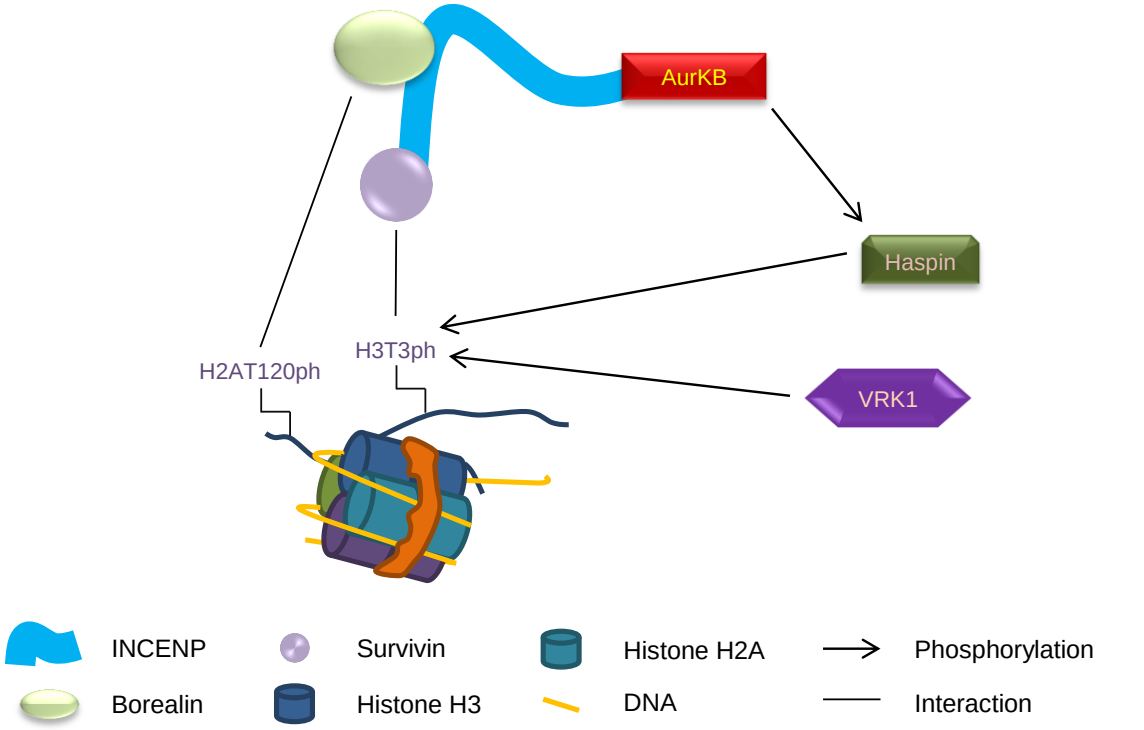

Figure 74. Role of VRK1 on AurKB localization and accumulation on centromeres. VRK1 phosphorylates the histone H3 on the residue Thr3 (H3T3ph), which is critical for the binding to the centromeric chromatin of CPC and therefore of AurKB, via Survivin. The potential implication of VRK1 on the phosphorylation of histone H2A on the Thr120 and on the regulation of AurKB localization and accumulation through this phosphorylation residue remains unexplored. This figure has been updated from Figure 12.

Additionally, the potential regulation of AurKB ubiquitination, by VRK1 was also explored. It is known that VRK1 protects Coilin of ubiquitination and degradation, in the proteasome (Cantarero et al., 2015) and has been reported that AurKB ubiquitination regulates the kinase degradation and the CPC/ AurKB transition from chromosome to the central spindle during anaphase (Chen et al.,

2013; Maerki et al., 2009; Sumara et al., 2007; Teng et al., 2012). So, AurKB ubiquitination, and therefore its degradation or localization, could be regulated in some way by VRK1. Our results showed that ubiquitination of AurKB seemed diminished when VRK1 was depleted, but an overall decrease in the ubiquitination on the cell lysate was also observed. Such remark may indicate that VRK1 plays an important role on global protein ubiquitination instead of a specific and limited part on the ubiquitination of AurKB. Nevertheless, if in fact VRK1 is required for the ubiquitination of AurKB, it could indicate that VRK1 is essential for the degradation of AurKB or that VRK1 is important for the re-location of AurKB. Since our results showed that the overexpression of VRK1 stabilizes overexpressed AurKB, we are more inclined to rule out the potential role of VRK1 on the AurKB degradation, through the UPP. However, it is necessary to confirm the implication of VRK1 on AurKB ubiquitination and re-localization.

Summarizing this section, our work showed a well-organized biological link between both AurKB and VRK1. VRK1 regulates the localization of AurKB on the centromeres, at least by phosphorylating the H3T3, which is a relevant binding site for CPC via Survivin. Then, VRK1 regulates the activity of AurKB through the physical interaction with the kinase, during the early stages of mitosis. The two kinases form a stable complex that inhibits not only the kinase activity of AurKB, but also VRK1. This regulatory mechanism affects the phosphorylation of specific mitotic targets of AurKB and VRK1, as it could be p53 and histone H3.

Part 2. Regulation of VRK1 by Sox2 during cell proliferation and differentiation

2.1 Implication of VRK1 and Sox2 on the regulation of cell proliferation

The reprogramming factor Sox2 regulates the self-renewal of stem cells as well as cellular differentiation, which culminates into a specific tissue after several rounds of cell division. Recently, Sox2 was also associated with cancer development, including in the regulation of cell proliferation, wherein the role of the transcriptional factor is lightly explored (Basu-Roy et al., 2012; Tompkins et al., 2011). On the other hand, the role of VRK1 on cell proliferation is better documented. VRK1 participates in G0 exit and G1 entry, chromatin compaction in G2/M or in the regulation of nuclear envelope assembly and disassembly, in addition to mitotic Golgi complex fragmentation. VRK1 knockdown causes cell cycle arrest and decreased cell proliferation (Kang et al., 2007b; Lopez-Sanchez et al., 2009; Nichols et al., 2006b; Vega et al., 2004a). Thus, all the results pointed for a potential connection between VRK1 and Sox2 on the regulation of cell proliferation. Accordingly, our results showed that VRK1 and Sox2 were expressed in a cellular subpopulation of the highly proliferative epithelial basal layer, in normal tonsil stratified epithelium, while it is lost in cells terminally differentiated. VRK1 pattern conform the previous results obtained from our group, where it was also observed that the kinase co-localize with Ki67 and p63 in dividing cells, but not in differentiated cells. This suggests a role for VRK1 in cell proliferation and in cell differentiation, when the levels of the kinase need to be lower (Valbuena et al., 2008b). In turn, Sox2 was also demonstrated to have a similar expression in the pituitary gland and esophagus epithelium (DeWard et al., 2014; Fauquier et al., 2008), in which Sox2 has a role within the amplification compartment, more precisely on the regulation of self-renewal. Also interesting was the fact that Sox2 was expressed in the lymphoid follicles of tumoral tissue, whereas it was not detected in normal tissue. Therefore, the detection of upregulated levels of Sox2 on a tumor sample could indicate that Sox2 is critical

for cancer development and/ or maintenance. Indeed, self-renewal genes, including Sox2 were reported to be significantly expressed in several tumor samples and in cancer cell lines, showing a significant relationship with tumor grade (Amini et al., 2014). Likewise, Sox2 was also demonstrated to be overexpressed in breast tumor cells, displaying even higher levels in a subpopulation of tamoxifen resistant cells (Piva et al., 2014). This results indicate that Sox2 might be a potential tumor marker in the diagnosis and/or prognosis of cancer.

Moreover, our results showed that VRK1 and Sox2 co-localized and formed a stable complex in the nuclei of various cancer cell lines, such as HEK293T, breast cancer cell lines MCF7 and MDA-MB-231 or NT2. This is consistent with all known interactions of VRK1, as chromatin kinase, with transcription factors such as p53, ATF2, c-Jun or CREB, as well as the p300 acetyltransferase transcriptional coactivator (Guermah et al., 2006; Kang et al., 2008a; Lopez-Sanchez et al., 2014a; Sevilla et al., 2004a; Sevilla et al., 2004b). Also, VRK1 was described as part of Oct4 interactome in addition to the one of Nanog, which could indicate a straight relationship between the kinase with the regulatory network for self-renewal and pluripotency (Ding et al., 2012). In fact, could be interesting to study, during embryonic development, the relationship between VRK1 and self-renewal genes and the implication of this connection in early cell faith decision. Undeniably, VRK1 had been confirmed to be overexpressed at the time of massive cellular expansion during murine hematopoietic embryo development, as well as in murine developing retina, which validates a potential role of importance for the kinase during embryogenesis (Dorrell et al., 2004; Vega et al., 2003). Furthermore, our results showed that VRK1 was also able to phosphorylate the transcriptional factor Sox2 in *in vitro* kinase assays. The interaction with and the phosphorylation of many others transcriptional factors, by VRK1, was previous described (Guermah et al., 2006; Kang et al., 2008a; Lopez-Sanchez et al., 2014a; Sevilla et al., 2004a; Sevilla et al., 2004b). Nevertheless, it is important further studies to dissect which Sox2 residues are phosphorylation targets of VRK1 and to explain the relevance of this phosphorylation(s). The analysis of Sox2 sequence with *GPS* software tool, which predicts kinase-specific phosphorylation sites indicated that VRK1 might phosphorylate, with high probability, the transcriptional factor in several

Seri and Thr residues: Thr85, Thr118, Thr211, Ser212, Thr256, Ser257 and Ser258. Except Thr85, which is located in the HMG domain, all the other residues are part of the transactivation domain, Therefore, it seem probable that Sox2 phosphorylation, by VRK1, is essential for the modulation of the transcriptional factor activity. Actually, Sox2 has been demonstrated to be phosphorylated on the Thr118, by AKT, in ESCs. This phosphorylation stabilizes Sox2, enhancing its transcriptional activity and its cooperation in the reprogramming of mouse embryonic fibroblasts by making the induction of iPSCs more efficient. (Jeong et al., 2010).

The co-localization of VRK1 and Sox2 in the proliferation compartment, as well as their interaction, pointed that both are likely to contribute to the control of cell proliferation. Indeed, our results showed that depletion of either Sox2 or VRK1 caused a similar reduction in the rate of cell duplication, alongside with the loss of phospho-Rb, cyclins D1 and A, PCNA, all associated to active proliferation. Depletion of Sox2 or VRK1 also resulted in accumulation of p27, an inhibitor of cell cycle progression. These results come in line with previous reports in human WS1 fibroblasts, when VRK1 was depleted, and in MCF7, when Sox2 was downregulated (Chen et al., 2008a; Valbuena et al., 2008b).

When cells initiate their first self-renewal asymmetric division it is necessary the cooperation of Sox2 with other proliferation associated proteins, among which VRK1 stands out as a potential candidate. At this point the transcriptional factor Sox2 associates with the chromatin kinase VRK1 that is connected to several aspect of cell proliferation (Valbuena et al., 2011c) as well to chromatin remodeling (Salzano et al., 2015). Our results showed that Sox2 increases *VRK1* gene expression, by targeting Sox2 response elements in *VRK1* proximal promoter that has several Sox2 target sequences approximately one kilobase upstream of the transcription initiation site, a position consistent with that identified in other Sox2 targets (Fang et al., 2011b; Lodato et al., 2013). Thus, the regulation of *VRK1* gene by Sox2 is fully consistent with a role for VRK1 as an initiator of cell proliferation (Valbuena et al., 2008b). Moreover, it is important to notice that the activation of *VRK1* gene promoter, by Sox2, even though relatively low, is enough to increase the levels of one of the most abundant kinases in the nucleus at least twice, as our results showed by WB and IF. Yet,

taking into account that Sox2 could be considered a modest activator of *VRK1* gene transcription, by itself, it could important to further explore potential partners to Sox2 for the co-activation of *VRK1* gene promoter. Our results demonstrated that Oct4, one of the most common Sox2 associated partners, was not able to increase *VRK1* gene promoter, by itself or alongside with Sox2. A results consistent to the fact that *VRK1* proximal promoter lack Oct4 target sequences (Zhou and Liu, 2008). However, another potential candidate to explore could be PAX6, a transcriptional regulator in the early development of the ocular system, central nervous system, and gastrointestinal system (Chien et al., 2009). PAX6 was also described to form with Sox2 a co-DNA-binding partner complex that regulates the initiation of lens development and eye morphogenesis (Kamachi et al., 2001; Kondoh et al., 2004; Smith et al., 2009). On *VRK1* gene promoter, PAX-6 has one response element immediately upstream of one Sox2 target sequence, as analyzed through the *Transfac* database (Figure 75). Yet, the possible association between Sox2 and PAX6 on the regulation of *VRK1* gene promoter, might be better tested during the early stages of embryonic development, where VRK1 plays also a role (Dorrell et al., 2004; Vega et al., 2003).

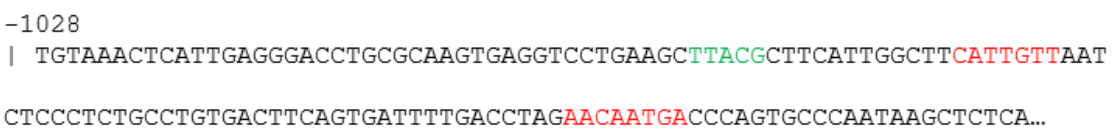

Figure 75. Sox2 and PAX6 target sequences on the proximal promoter (-1028+52) of the human *VRK1* gene. Sox2 and PAX6 response elements are indicated in red and green, respectively.

However, neither Sox2 nor VRK1 are direct regulators of the cell cycle initiation and progression. This indicates that they have to regulate key genes or proteins implicated in cell cycle, among which *CCND1* is a major candidate (Malumbres and Barbacid, 2009). Thus, Sox2 and VRK1 as proliferation regulators, have to co-operate in the control of cell cycle specific genes, as *CCND1*, which is regulated by both Sox2 (Chen et al., 2008a) and VRK1 (Kang et al., 2008b) by themselves. Moreover, Sox2 depending on its levels and therefore on its affinity for its target sequence can also function as an inhibitor of cyclin D1 expression (Hagey and Muhr, 2014). Our results showed that VRK1

and Sox2 individually activated the *CCND1* gene promoter, and that this effect was potentiated when both proteins were combined. Therefore, it is clear that both proteins are necessary to and co-operate on the regulation of cell cycle progression and proliferation, at least through the modulation of *CCND1* gene promoter. Likewise, *CCND1* gene expression is in part controlled by the CREB transcription factor (Kang et al., 2008b). In this context, it is important to notice that *CREB* gene expression is regulated by Sox2 (Iida et al., 2012) and CREB protein is a phosphorylation target of VRK1 (Kang et al., 2008b). Consequently, it is likely that depending on CREBSer133 phosphorylation levels, there are different threshold of responses. In dividing cells low levels of phospho-CREB are required for cell cycle progression and in cells that are differentiated, and in which a different set of genes is required to fulfill their specific function, a higher level of phosphorylation may be necessary. According to our results, it is noteworthy that the highest phosphorylation level of CREB in Ser133 was detected in RA-differentiated NT2 cells, at a time when Sox2 and VRK1 levels had already declined. Accordingly, it is possible that in differentiated cells, CREBSer133 phosphorylation is mediated by different kinases, not VRK1, among which lie the calcium/calmodulin-dependent protein kinase types II and IV (Matthews et al., 1994). This might indicate that CREB phosphorylation might have different roles depending on whether it is participating in cell cycle progression or in cellular differentiation.

Furthermore, the activity of VRK1 is regulated by an auto-regulatory loop with some of its targets, as has been described in the context of p53 (Valbuena et al., 2007b; Valbuena et al., 2006a) and now in the context of Sox2. In fact, our results displayed that the accumulation of VRK1 protein, negatively down-regulated the Sox2 protein and its mRNA levels. A result that is complemented by VRK1 depletion assays, in which Sox2 levels were upregulated. This could indicate that even if cell fate is already determined and ongoing, VRK1 is still necessary to maintain proliferation, whereas Sox2 levels are almost undetectable and probably dispensable to cell proliferation. In line, with the role of VRK1 on the phosphorylation of Sox2, it could be interesting to analyze whether the changes observed on Sox2 levels, when VRK1 varies, are related to its phosphorylation state. Moreover, it could be important to study, the mechanisms

by which VRK1 affects Sox2. VRK1 is not a transcriptional factor and so, it must be an active part of a larger transcriptional complex that regulates Sox2.

The cells already differentiated do not divide and this implies that proliferative proteins must to be downregulated. In fact, our results showed a significant loss on proliferative associated proteins such as the reprogramming factors Sox2, Oct4 and Nanog, both Cyclins B1 and D1 and VRK1, during NT2 cell differentiation with RA (Figure 76). The lower and slower rate of VRK1 downregulation is likely to be a consequence of the high stability of this protein (Valbuena et al., 2008b). As originally stipulated, the RA-differentiation state of the cells was confirmed by the morphological reorganization of α-tubulin and by detecting the corresponding increase in macroH2A2 isoform, N-cadherin, βIII-tubulin, PAX6 and CREB phosphorylated in Ser133, and the decrease in Vimentin (Buschbeck et al., 2009; Creppe et al., 2012a; Fang et al., 2003; Kakhki et al., 2013; Megiorni et al., 2005; Pleasure and Lee, 1993; Pleasure et al., 1992; Podrygajlo et al., 2009; Spinella et al., 1999).

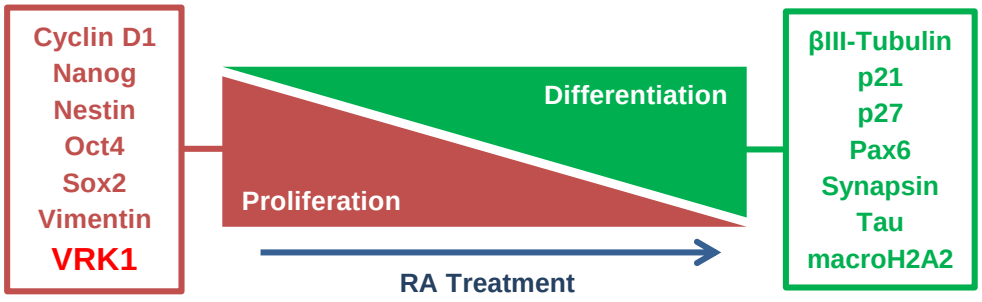

Figure 76 – VRK1 is downregulated during cell differentiation. NT2 cells were differentiated in neurons-like with upon retinoic acid (RA). In turn, macroH2A2 isoform increases during cell differentiation. This figure has been updated from Figure 15.

Contextualizing, it is likely that when VRK1 accumulates, it is able to activate *CCND1* by itself and also downregulate *SOX2* by an unknown mechanism. This latter outcome is consistent with the upregulation of pluripotency transcription factors, Sox2, Oct4 and c-myc, observed upon luteolin treatment, an inhibitor of VRK1 (Kim et al., 2014; Liu et al., 2015). Moreover, high expression of VRK1 can stabilize p53 and consequently contribute to the necessary cell cycle arrest to permit differentiation. Besides, inhibition of proliferation and facilitation of differentiation is mediated by changes in chromatin,

which can be induced by the incorporation of histone variants. In this context the role of macroH2A isoforms is relevant as our results demonstrated. MacroH2A variants 1.2 and 2 can inhibit the VRK1 promoter by themselves, and also prevent the activating effect of Sox2 on the *VRK1* and *CCND1* promoters, which facilitates cell differentiation.

All told, our work has identified a functional biological connection between the reprogramming transcriptional factor Sox2 and the human VRK1 protein kinase. At first Sox2 directly activates *VRK1* gene expression and both proteins cooperate in activation of the *CCND1* expression, which consequently promotes cell proliferation. Moreover, VRK1 contributes, by an unknown mechanism, to the downregulation of *SOX2*, reducing cell proliferation and facilitating cell differentiation. Meanwhile, macroH2A2 variant contributes to cell differentiation by completely shutting down VRK1 in terminally differentiated cells. Therefore, both VRK1 and Sox2 are downregulated in the process of final differentiation. Our data shows a coordinated role for these proteins in the transition from cell division to cell differentiation (Figure 77).

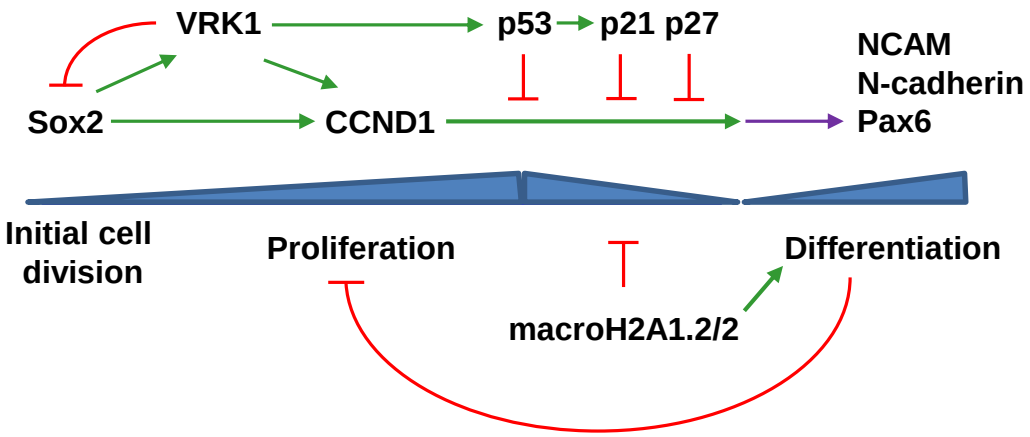

Figure 77 – Diagram of Sox2 and VRK1 roles in the regulation of cell proliferation and differentiation. Red lines indicate inhibition and green lines indicate activation.

The role of human **VRK1** within the tumor phenotype appears to be complex, since it may have roles of both **oncogene** and **tumor suppressor gene**. VRK1 is a strong facilitator of **cell cycle progression** and **proliferation** (Kang et al., 2007a; Molitor and Traktman, 2013; Valbuena et al., 2008b), through various mechanisms, to which we add two new. One by regulating the **localization and activity** of the mitotic **AurKB** and the other through a **regulatory feedback loop** with the reprogramming transcriptional factor **Sox2,** which facilitates also cell **differentiation**. Besides, many tumors feature very high levels of VRK1 protein which is consistent with an oncogenic role of wild-type VRK1. In turn, VRK1 is also a positive regulator of p53, as well as an important player of the genomic stability network, which is important to maintain cell homeostasis. In this context the role of VRK1 is similar to that of other tumor suppressor genes or tumor predisposition genes (Lopez-Borges and Lazo, 2000; Lopez-Sanchez et al., 2014a; Salzano et al., 2015; Salzano et al., 2014; Sanz-Garcia et al., 2012; Valbuena et al., 2011a; Vega et al., 2004b). In any case, VRK1 is not mutated in human cancer, and the very rare mutations described are associated with neurodegenerative diseases (Gonzaga-Jauregui et al., 2013b; Nguyen et al., 2015; Renbaum et al., 2009a; Vinograd-Byk et al., 2015). Thus, the complexity of VRK1 functions might be a reflection of its late appearance in evolution as organisms become more complex, and where VRK1 appears to play a coordinating role of diverse signaling processes and functions in vertebrates.

Conclusions

Conclusions

This work led to the following conclusions:

1a) VRK1 regulates AurKB localization and activity. VRK1 positions AurKB at the centromeres, during mitosis, at least through the phosphorylation of histone H3 on its Thr3 residue. VRK1 depletion causes the displacement of AurKB from the centromeres to a more diffuse state on the chromatin.

1b) VRK1 and AurKB form a stable complex, in early mitosis, which inhibits the catalytic activity of each kinase. This effect seems independent of their kinase activity and seems to aim kinase specific phosphorylation targets such as the histone H3 and the transcriptional factor p53.

2a) VRK1 is regulated by, and cooperates coordinately with the transcriptional factor Sox2 on the regulation of cell cycle progression, activating the *CCND1* gene expression. Depletion of either VRK1 or Sox2, reduces the rate of cell duplication, alongside with decreased levels of proliferation-associated proteins, including cyclin D1.

2b) VRK1 contributes to *SOX2* downregulation, creating a regulatory feedback loop, which promotes cell differentiation over proliferation. As the cells are terminally differentiating, the macroH2A2 variant completely shuts down *VRK1*. Proliferative proteins such as Sox2 and VRK1, as well as cyclin D1, are downregulated in terminally differentiated cells.

Bibliography

Aihara, H., Nakagawa, T., Yasui, K., Ohta, T., Hirose, S., Dhomae, N., Takio, K., Kaneko, M., Takeshima, Y., Muramatsu, M.*, et al.* (2004). Nucleosomal histone kinase-1 phosphorylates H2A Thr 119 during mitosis in the early Drosophila embryo. Genes & development *18*, 877-888.

Amini, S., Fathi, F., Mobalegi, J., Sofimajidpour, H., and Ghadimi, T. (2014). The expressions of stem cell markers: Oct4, Nanog, Sox2, nucleostemin, Bmi, Zfx, Tcl1, Tbx3, Dppa4, and Esrrb in bladder, colon, and prostate cancer, and certain cancer cell lines. Anatomy & cell biology *47*, 1-11.

Andersen, J.S., Lam, Y.W., Leung, A.K., Ong, S.E., Lyon, C.E., Lamond, A.I., and Mann, M. (2005). Nucleolar proteome dynamics. Nature *433*, 77-83.

Andrews, P.D., Ovechkina, Y., Morrice, N., Wagenbach, M., Duncan, K., Wordeman, L., and Swedlow, J.R. (2004). Aurora B regulates MCAK at the mitotic centromere. Dev Cell *6*, 253-268.

Baek, S.H. (2011). When signaling kinases meet histones and histone modifiers in the nucleus. Molecular cell *42*, 274-284.

Baldassarre, G., Boccia, A., Bruni, P., Sandomenico, C., Barone, M.V., Pepe, S., Angrisano, T., Belletti, B., Motti, M.L., Fusco, A.*, et al.* (2000). Retinoic acid induces neuronal differentiation of embryonal carcinoma cells by reducing proteasome-dependent proteolysis of the cyclin-dependent inhibitor p27. Cell growth & differentiation : the molecular biology journal of the American Association for Cancer Research *11*, 517-526.

Bannister, A.J., and Kouzarides, T. (2011). Regulation of chromatin by histone modifications. Cell Res *21*, 381-395.

Barcia-Sanjurjo, I., Vazquez-Cedeira, M., Barcia, R., and Lazo, P.A. (2013). Sensitivity of the kinase activity of human vaccinia-related kinase proteins to toxic metals. Journal of biological inorganic chemistry : JBIC : a publication of the Society of Biological Inorganic Chemistry *18*, 473-482.

Barcia, R., Lopez-Borges, S., Vega, F.M., and Lazo, P.A. (2002). Kinetic properties of p53 phosphorylation by the human vaccinia-related kinase 1. Archives of biochemistry and biophysics *399*, 1-5.

Basu-Roy, U., Bayin, N.S., Rattanakorn, K., Han, E., Placantonakis, D.G., Mansukhani, A., and Basilico, C. (2015). Sox2 antagonizes the Hippo pathway to maintain stemness in cancer cells. Nature communications *6*, 6411.

Basu-Roy, U., Seo, E., Ramanathapuram, L., Rapp, T.B., Perry, J.A., Orkin, S.H., Mansukhani, A., and Basilico, C. (2012). Sox2 maintains self renewal of tumor-initiating cells in osteosarcomas. Oncogene *31*, 2270-2282.

Berger, S.L. (2007). The complex language of chromatin regulation during transcription. Nature *447*, 407-412.

Bhoumik, A., and Ronai, Z. (2008). ATF2: a transcription factor that elicits oncogenic or tumor suppressor activities. Cell cycle (Georgetown, Tex) *7*, 2341-2345.

Bihani, T., and Hinds, P.W. (2011). Mitosis hit with an ATM transaction fee: aurora B-mediated activation of ATM during mitosis. Molecular cell *44*, 513-514.

Birnboim, H.C., and Doly, J. (1979). A rapid alkaline extraction procedure for screening recombinant plasmid DNA. Nucleic acids research *7*, 1513-1523.

Bischoff, J.R., Anderson, L., Zhu, Y., Mossie, K., Ng, L., Souza, B., Schryver, B., Flanagan, P., Clairvoyant, F., Ginther, C.*, et al.* (1998). A homologue of Drosophila aurora kinase is oncogenic and amplified in human colorectal cancers. The EMBO journal *17*, 3052-3065.

Blanco, S., Klimcakova, L., Vega, F.M., and Lazo, P.A. (2006). The subcellular localization of vaccinia-related kinase-2 (VRK2) isoforms determines their different effect on p53 stability in tumour cell lines. The FEBS journal *273*, 2487-2504.

Blanco, S., Santos, C., and Lazo, P.A. (2007). Vaccinia-related kinase 2 modulates the stress response to hypoxia mediated by TAK1. Molecular and cellular biology *27*, 7273-7283.

Blanco, S., Sanz-Garcia, M., Santos, C.R., and Lazo, P.A. (2008). Modulation of interleukin-1 transcriptional response by the interaction between VRK2 and the JIP1 scaffold protein. PloS one *3*, e1660.

Bolanos-Garcia, V.M. (2005). Aurora kinases. Int J Biochem Cell Biol *37*, 1572-1577.

Boumahdi, S., Driessens, G., Lapouge, G., Rorive, S., Nassar, D., Le Mercier, M., Delatte, B., Caauwe, A., Lenglez, S., Nkusi, E.*, et al.* (2014). SOX2 controls tumour initiation and cancer stem-cell functions in squamous-cell carcinoma. Nature *511*, 246-250.

Bowles, J., Schepers, G., and Koopman, P. (2000). Phylogeny of the SOX family of developmental transcription factors based on sequence and structural indicators. Developmental biology *227*, 239-255.

Boyle, K.A., and Traktman, P. (2004). Members of a novel family of mammalian protein kinases complement the DNA-negative phenotype of a vaccinia virus ts mutant defective in the B1 kinase. Journal of virology *78*, 1992-2005.

Brittle, A.L., Nanba, Y., Ito, T., and Ohkura, H. (2007). Concerted action of Aurora B, Polo and NHK-1 kinases in centromere-specific histone 2A phosphorylation. Experimental cell research *313*, 2780-2785.

Brown, J.R., Koretke, K.K., Birkeland, M.L., Sanseau, P., and Patrick, D.R. (2004). Evolutionary relationships of Aurora kinases: implications for model organism studies and the development of anti-cancer drugs. BMC Evol Biol *4*, 39.

Buschbeck, M., and Di Croce, L. (2010). Approaching the molecular and physiological function of macroH2A variants. Epigenetics *5*, 118-123.

Buschbeck, M., Uribesalgo, I., Wibowo, I., Rue, P., Martin, D., Gutierrez, A., Morey, L., Guigo, R., Lopez-Schier, H., and Di Croce, L. (2009). The histone variant macroH2A is an epigenetic regulator of key developmental genes. Nature structural & molecular biology *16*, 1074-1079.

Cantarero, L., Sanz-Garcia, M., Vinograd-Byk, H., Renbaum, P., Levy-Lahad, E., and Lazo, P.A. (2015). VRK1 regulates Cajal body dynamics and protects coilin from proteasomal degradation in cell cycle. Scientific reports *5*, 10543.

Carazo-Salas, R.E., Guarguaglini, G., Gruss, O.J., Segref, A., Karsenti, E., and Mattaj, I.W. (1999). Generation of GTP-bound Ran by RCC1 is required for chromatin-induced mitotic spindle formation. Nature *400*, 178-181.

Carmena, M., and Earnshaw, W.C. (2003). The cellular geography of aurora kinases. Nature reviews Molecular cell biology *4*, 842-854.

Carmena, M., Lombardia, M.O., Ogawa, H., and Earnshaw, W.C. (2014). Polo kinase regulates the localization and activity of the chromosomal passenger complex in meiosis and mitosis in Drosophila melanogaster. Open Biol *4*, 140162.

Carmena, M., Pinson, X., Platani, M., Salloum, Z., Xu, Z., Clark, A., Macisaac, F., Ogawa, H., Eggert, U., Glover, D.M.*, et al.* (2012a). The chromosomal passenger complex activates Polo kinase at centromeres. PLoS Biol *10*, e1001250.

Carmena, M., Wheelock, M., Funabiki, H., and Earnshaw, W.C. (2012b). The chromosomal passenger complex (CPC): from easy rider to the godfather of mitosis. Nature reviews Molecular cell biology *13*, 789-803.

Castro, A., Arlot-Bonnemains, Y., Vigneron, S., Labbe, J.C., Prigent, C., and Lorca, T. (2002). APC/Fizzy-Related targets Aurora-A kinase for proteolysis. EMBO reports *3*, 457-462.

Chakravarthy, S., Gundimella, S.K., Caron, C., Perche, P.Y., Pehrson, J.R., Khochbin, S., and Luger, K. (2005). Structural characterization of the histone variant macroH2A. Molecular and cellular biology *25*, 7616-7624.

Chambers, I., and Tomlinson, S.R. (2009). The transcriptional foundation of pluripotency. Development *136*, 2311-2322.

Chan, K.C., Chan, L.S., Ip, J.C., Lo, C., Yip, T.T., Ngan, R.K., Wong, R.N., Lo, K.W., Ng, W.T., Lee, A.W.*, et al.* (2015). Therapeutic targeting of CBP/beta-catenin signaling reduces cancer

stem-like population and synergistically suppresses growth of EBV-positive nasopharyngeal carcinoma cells with cisplatin. Scientific reports *5*, 9979.

Chang, L., and Karin, M. (2001). Mammalian MAP kinase signalling cascades. Nature *410*, 37-40.

Cheeseman, I.M., Anderson, S., Jwa, M., Green, E.M., Kang, J., Yates, J.R., 3rd, Chan, C.S., Drubin, D.G., and Barnes, G. (2002). Phospho-regulation of kinetochore-microtubule attachments by the Aurora kinase Ipl1p. Cell *111*, 163-172.

Cheetham, G.M., Knegtel, R.M., Coll, J.T., Renwick, S.B., Swenson, L., Weber, P., Lippke, J.A., and Austen, D.A. (2002). Crystal structure of aurora-2, an oncogenic serine/threonine kinase. The Journal of biological chemistry *277*, 42419-42422.

Chen, B.B., Glasser, J.R., Coon, T.A., and Mallampalli, R.K. (2013). Skp-cullin-F box E3 ligase component FBXL2 ubiquitinates Aurora B to inhibit tumorigenesis. Cell death & disease *4*, e759.

Chen, S., Li, X., Lu, D., Xu, Y., Mou, W., Wang, L., Chen, Y., Liu, Y., Li, X., Li, L.Y*., et al.* (2014). SOX2 regulates apoptosis through MAP4K4-survivin signaling pathway in human lung cancer cells. Carcinogenesis *35*, 613-623.

Chen, Y., Shi, L., Zhang, L., Li, R., Liang, J., Yu, W., Sun, L., Yang, X., Wang, Y., Zhang, Y*., et al.* (2008a). The molecular mechanism governing the oncogenic potential of SOX2 in breast cancer. The Journal of biological chemistry *283*, 17969-17978.

Chen, Y., Shi, L., Zhang, L., Li, R., Liang, J., Yu, W., Sun, L., Yang, X., Wang, Y., Zhang, Y*., et al.* (2008b). The molecular mechanism governing the oncogenic potential of SOX2 in breast cancer. J Biol Chem *283*, 17969-17978.

Chien, Y.H., Huang, H.P., Hwu, W.L., Chien, Y.H., Chang, T.C., and Lee, N.C. (2009). Eye anomalies and neurological manifestations in patients with PAX6 mutations. Molecular vision *15*, 2139-2145.

Choi, Y.H., Park, C.H., Kim, W., Ling, H., Kang, A., Chang, M.W., Im, S.K., Jeong, H.W., Kong, Y.Y., and Kim, K.T. (2010). Vaccinia-related kinase 1 is required for the maintenance of undifferentiated spermatogonia in mouse male germ cells. PloS one *5*, e15254.

Chou, Y.T., Lee, C.C., Hsiao, S.H., Lin, S.E., Lin, S.C., Chung, C.H., Chung, C.H., Kao, Y.R., Wang, Y.H., Chen, C.T*., et al.* (2013). The emerging role of SOX2 in cell proliferation and survival and its crosstalk with oncogenic signaling in lung cancer. Stem cells (Dayton, Ohio) *31*, 2607-2619.

Chu, Y., Yao, P.Y., Wang, W., Wang, D., Wang, Z., Zhang, L., Huang, Y., Ke, Y., Ding, X., and Yao, X. (2011). Aurora B kinase activation requires survivin priming phosphorylation by PLK1. J Mol Cell Biol *3*, 260-267.

Collignon, J., Sockanathan, S., Hacker, A., Cohen-Tannoudji, M., Norris, D., Rastan, S., Stevanovic, M., Goodfellow, P.N., and Lovell-Badge, R. (1996). A comparison of the properties of Sox-3 with Sry and two related genes, Sox-1 and Sox-2. Development *122*, 509-520.

Costelloe, T., Fitzgerald, J., Murphy, N.J., Flaus, A., and Lowndes, N.F. (2006). Chromatin modulation and the DNA damage response. Experimental cell research *312*, 2677-2686.

Creppe, C., Janich, P., Cantarino, N., Noguera, M., Valero, V., Musulen, E., Douet, J., Posavec, M., Martin-Caballero, J., Sumoy, L*., et al.* (2012a). MacroH2A1 regulates the balance between self-renewal and differentiation commitment in embryonic and adult stem cells. Molecular and cellular biology *32*, 1442-1452.

Creppe, C., Janich, P., Cantarino, N., Noguera, M., Valero, V., Musulen, E., Douet, J., Posavec, M., Martin-Caballero, J., Sumoy, L*., et al.* (2012b). MacroH2A1 regulates the balance between self-renewal and differentiation commitment in embryonic and adult stem cells. Mol Cell Biol *32*, 1442-1452.

Creppe, C., Posavec, M., Douet, J., and Buschbeck, M. (2012c). MacroH2A in stem cells: a story beyond gene repression. Epigenomics *4*, 221-227.

Crosio, C., Fimia, G.M., Loury, R., Kimura, M., Okano, Y., Zhou, H., Sen, S., Allis, C.D., and Sassone-Corsi, P. (2002). Mitotic phosphorylation of histone H3: spatio-temporal regulation by mammalian Aurora kinases. Molecular and cellular biology *22*, 874-885.

Curtin, J.C., Dragnev, K.H., Sekula, D., Christie, A.J., Dmitrovsky, E., and Spinella, M.J. (2001). Retinoic acid activates p53 in human embryonal carcinoma through retinoid receptor-dependent stimulation of p53 transactivation function. Oncogene *20*, 2559-2569.

Dai, J., Sullivan, B.A., and Higgins, J.M. (2006). Regulation of mitotic chromosome cohesion by Haspin and Aurora B. Dev Cell *11*, 741-750.

DeLuca, K.F., Lens, S.M., and DeLuca, J.G. (2011). Temporal changes in Hec1 phosphorylation control kinetochore-microtubule attachment stability during mitosis. Journal of cell science *124*, 622-634.

DeWard, A.D., Cramer, J., and Lagasse, E. (2014). Cellular heterogeneity in the mouse esophagus implicates the presence of a nonquiescent epithelial stem cell population. Cell Rep *9*, 701-711.

Dhillon, N., and Hoekstra, M.F. (1994). Characterization of two protein kinases from Schizosaccharomyces pombe involved in the regulation of DNA repair. The EMBO journal *13*, 2777-2788.

Ding, J., Xu, H., Faiola, F., Ma'ayan, A., and Wang, J. (2012). Oct4 links multiple epigenetic pathways to the pluripotency network. Cell Res *22*, 155-167.

Dorrell, M.I., Aguilar, E., Weber, C., and Friedlander, M. (2004). Global gene expression analysis of the developing postnatal mouse retina. Investigative ophthalmology & visual science *45*, 1009-1019.

Dumaz, N., and Meek, D.W. (1999). Serine15 phosphorylation stimulates p53 transactivation but does not directly influence interaction with HDM2. The EMBO journal *18*, 7002-7010.

Eastman, A. (2004). Cell cycle checkpoints and their impact on anticancer therapeutic strategies. Journal of cellular biochemistry *91*, 223-231.

Eini, R., Stoop, H., Gillis, A.J., Biermann, K., Dorssers, L.C., and Looijenga, L.H. (2014). Role of SOX2 in the etiology of embryonal carcinoma, based on analysis of the NCCIT and NT2 cell lines. PloS one *9*, e83585.

Eyers, P.A., Churchill, M.E., and Maller, J.L. (2005). The Aurora A and Aurora B protein kinases: a single amino acid difference controls intrinsic activity and activation by TPX2. Cell cycle (Georgetown, Tex) *4*, 784-789.

Fang, H., Chartier, J., Sodja, C., Desbois, A., Ribecco-Lutkiewicz, M., Walker, P.R., and Sikorska, M. (2003). Transcriptional activation of the human brain-derived neurotrophic factor gene promoter III by dopamine signaling in NT2/N neurons. The Journal of biological chemistry *278*, 26401-26409.

Fang, W.T., Fan, C.C., Li, S.M., Jang, T.H., Lin, H.P., Shih, N.Y., Chen, C.H., Wang, T.Y., Huang, S.F., Lee, A.Y.*, et al.* (2014). Downregulation of a putative tumor suppressor BMP4 by SOX2 promotes growth of lung squamous cell carcinoma. International journal of cancer Journal international du cancer *135*, 809-819.

Fang, X., Yoon, J.G., Li, L., Tsai, Y.S., Zheng, S., Hood, L., Goodlett, D.R., Foltz, G., and Lin, B. (2011a). Landscape of the SOX2 protein-protein interactome. Proteomics *11*, 921-934.

Fang, X., Yoon, J.G., Li, L., Yu, W., Shao, J., Hua, D., Zheng, S., Hood, L., Goodlett, D.R., Foltz, G.*, et al.* (2011b). The SOX2 response program in glioblastoma multiforme: an integrated ChIP-seq, expression microarray, and microRNA analysis. BMC genomics *12*, 11.

Fang, X., Yu, W., Li, L., Shao, J., Zhao, N., Chen, Q., Ye, Z., Lin, S.C., Zheng, S., and Lin, B. (2010). ChIP-seq and functional analysis of the SOX2 gene in colorectal cancers. Omics : a journal of integrative biology *14*, 369-384.

Fauquier, T., Rizzoti, K., Dattani, M., Lovell-Badge, R., and Robinson, I.C. (2008). SOX2-expressing progenitor cells generate all of the major cell types in the adult mouse pituitary gland. Proceedings of the National Academy of Sciences of the United States of America *105*, 2907-2912.

Feng, R., Zhou, S., Liu, Y., Song, D., Luan, Z., Dai, X., Li, Y., Tang, N., Wen, J., and Li, L. (2013). Sox2 protects neural stem cells from apoptosis via up-regulating survivin expression. The Biochemical journal *450*, 459-468.

Fernandez, I.F., Blanco, S., Lozano, J., and Lazo, P.A. (2010). VRK2 inhibits mitogen-activated protein kinase signaling and inversely correlates with ErbB2 in human breast cancer. Molecular and cellular biology *30*, 4687-4697.

Fernandez, I.F., Perez-Rivas, L.G., Blanco, S., Castillo-Dominguez, A.A., Lozano, J., and Lazo, P.A. (2012). VRK2 anchors KSR1-MEK1 to endoplasmic reticulum forming a macromolecular complex that compartmentalizes MAPK signaling. Cellular and molecular life sciences : CMLS *69*, 3881-3893.

Finetti, P., Cervera, N., Charafe-Jauffret, E., Chabannon, C., Charpin, C., Chaffanet, M., Jacquemier, J., Viens, P., Birnbaum, D., and Bertucci, F. (2008). Sixteen-kinase gene expression identifies luminal breast cancers with poor prognosis. Cancer research *68*, 767-776.

Fischle, W., Tseng, B.S., Dormann, H.L., Ueberheide, B.M., Garcia, B.A., Shabanowitz, J., Hunt, D.F., Funabiki, H., and Allis, C.D. (2005). Regulation of HP1-chromatin binding by histone H3 methylation and phosphorylation. Nature *438*, 1116-1122.

Fleck, O., and Nielsen, O. (2004). DNA repair. Journal of cell science *117*, 515-517.

Floyd, S., Whiffin, N., Gavilan, M.P., Kutscheidt, S., De Luca, M., Marcozzi, C., Min, M., Watkins, J., Chung, K., Fackler, O.T.*, et al.* (2013). Spatiotemporal organization of Aurora-B by APC/CCdh1 after mitosis coordinates cell spreading through FHOD1. Journal of cell science *126*, 2845-2856.

Fournier, M.V., Martin, K.J., Kenny, P.A., Xhaja, K., Bosch, I., Yaswen, P., and Bissell, M.J. (2006). Gene expression signature in organized and growth-arrested mammary acini predicts good outcome in breast cancer. Cancer research *66*, 7095-7102.

Fu, J., Bian, M., Jiang, Q., and Zhang, C. (2007). Roles of Aurora kinases in mitosis and tumorigenesis. Molecular cancer research : MCR *5*, 1-10.

Gao, F., Wei, Z., An, W., Wang, K., and Lu, W. (2013). The interactomes of POU5F1 and SOX2 enhancers in human embryonic stem cells. Scientific reports *3*, 1588.

Gaspar-Maia, A., Qadeer, Z.A., Hasson, D., Ratnakumar, K., Leu, N.A., Leroy, G., Liu, S., Costanzi, C., Valle-Garcia, D., Schaniel, C.*, et al.* (2013). MacroH2A histone variants act as a barrier upon reprogramming towards pluripotency. Nature communications *4*, 1565.

Gimenez-Abian, J.F., Sumara, I., Hirota, T., Hauf, S., Gerlich, D., de la Torre, C., Ellenberg, J., and Peters, J.M. (2004). Regulation of sister chromatid cohesion between chromosome arms. Curr Biol *14*, 1187-1193.

Girouard, S.D., Laga, A.C., Mihm, M.C., Scolyer, R.A., Thompson, J.F., Zhan, Q., Widlund, H.R., Lee, C.W., and Murphy, G.F. (2012). SOX2 contributes to melanoma cell invasion. Laboratory investigation; a journal of technical methods and pathology *92*, 362-370.

Glover, D.M., Leibowitz, M.H., McLean, D.A., and Parry, H. (1995). Mutations in aurora prevent centrosome separation leading to the formation of monopolar spindles. Cell *81*, 95-105.

Gohard, F.H., St-Cyr, D.J., Tyers, M., and Earnshaw, W.C. (2014). Targeting the INCENP IN-box-Aurora B interaction to inhibit CPC activity in vivo. Open Biol *4*, 140163.

Goldberg, J.M., Manning, G., Liu, A., Fey, P., Pilcher, K.E., Xu, Y., and Smith, J.L. (2006). The dictyostelium kinome--analysis of the protein kinases from a simple model organism. PLoS genetics *2*, e38.

Gonzaga-Jauregui, C., Lotze, T., Jamal, L., Penney, S., Campbell, I.M., Pehlivan, D., Hunter, J.V., Woodbury, S.L., Raymond, G., Adesina, A.M.*, et al.* (2013a). Mutations in VRK1 associated with complex motor and sensory axonal neuropathy plus microcephaly. JAMA neurology *70*, 1491-1498.

Gonzaga-Jauregui, C., Lotze, T., Jamal, L., Penney, S., Campbell, I.M., Pehlivan, D., Hunter, J.V., Woodbury, S.L., Raymond, G., Adesina, A.M.*, et al.* (2013b). Mutations in VRK1 associated with complex motor and sensory axonal neuropathy plus microcephaly. JAMA Neurol *70*, 1491-1498.

Gorjanacz, M., Klerkx, E.P., Galy, V., Santarella, R., Lopez-Iglesias, C., Askjaer, P., and Mattaj, I.W. (2007). Caenorhabditis elegans BAF-1 and its kinase VRK-1 participate directly in post-mitotic nuclear envelope assembly. The EMBO journal *26*, 132-143.

Gorjanacz, M., Klerkx, E.P., Galy, V., Santarella, R., Lopez-Iglesias, C., Askjaer, P., and Mattaj, I.W. (2008). Caenorhabditis elegans BAF-1 and its kinase VRK-1 participate directly in post-mitotic nuclear envelope assembly. Embo J *26*, 132-143.

Goto, H., Yasui, Y., Kawajiri, A., Nigg, E.A., Terada, Y., Tatsuka, M., Nagata, K., and Inagaki, M. (2003). Aurora-B regulates the cleavage furrow-specific vimentin phosphorylation in the cytokinetic process. The Journal of biological chemistry *278*, 8526-8530.

Gubbay, J., Collignon, J., Koopman, P., Capel, B., Economou, A., Munsterberg, A., Vivian, N., Goodfellow, P., and Lovell-Badge, R. (1990). A gene mapping to the sex-determining region of the mouse Y chromosome is a member of a novel family of embryonically expressed genes. Nature *346*, 245-250.

Guermah, M., Palhan, V.B., Tackett, A.J., Chait, B.T., and Roeder, R.G. (2006). Synergistic functions of SII and p300 in productive activator-dependent transcription of chromatin templates. Cell *125*, 275-286.

Gully, C.P., Velazquez-Torres, G., Shin, J.H., Fuentes-Mattei, E., Wang, E., Carlock, C., Chen, J., Rothenberg, D., Adams, H.P., Choi, H.H*., et al.* (2012). Aurora B kinase phosphorylates and instigates degradation of p53. Proceedings of the National Academy of Sciences of the United States of America *109*, E1513-1522.

Guse, A., Mishima, M., and Glotzer, M. (2005). Phosphorylation of ZEN-4/MKLP1 by aurora B regulates completion of cytokinesis. Curr Biol *15*, 778-786.

Hagey, D.W., and Muhr, J. (2014). Sox2 acts in a dose-dependent fashion to regulate proliferation of cortical progenitors. Cell Rep *9*, 1908-1920.

Han, X., Fang, X., Lou, X., Hua, D., Ding, W., Foltz, G., Hood, L., Yuan, Y., and Lin, B. (2012). Silencing SOX2 induced mesenchymal-epithelial transition and its expression predicts liver and lymph node metastasis of CRC patients. PloS one *7*, e41335.

Hanks, S.K., and Hunter, T. (1995). Protein kinases 6. The eukaryotic protein kinase superfamily: kinase (catalytic) domain structure and classification. FASEB journal : official publication of the Federation of American Societies for Experimental Biology *9*, 576-596.

Hans, F., and Dimitrov, S. (2001). Histone H3 phosphorylation and cell division. Oncogene *20*, 3021-3027.

Haraguchi, T., Koujin, T., Segura-Totten, M., Lee, K.K., Matsuoka, Y., Yoneda, Y., Wilson, K.L., and Hiraoka, Y. (2001). BAF is required for emerin assembly into the reforming nuclear envelope. Journal of cell science *114*, 4575-4585.

Harashima, H., Dissmeyer, N., and Schnittger, A. (2013). Cell cycle control across the eukaryotic kingdom. Trends in cell biology *23*, 345-356.

Harper, J.V. (2005). Synchronization of cell populations in G1/S and G2/M phases of the cell cycle. Methods in molecular biology (Clifton, NJ) *296*, 157-166.

Hayashi-Takanaka, Y., Yamagata, K., Nozaki, N., and Kimura, H. (2009). Visualizing histone modifications in living cells: spatiotemporal dynamics of H3 phosphorylation during interphase. The Journal of cell biology *187*, 781-790.

Herreros-Villanueva, M., Zhang, J.S., Koenig, A., Abel, E.V., Smyrk, T.C., Bamlet, W.R., de Narvajas, A.A., Gomez, T.S., Simeone, D.M., Bujanda, L*., et al.* (2013). SOX2 promotes dedifferentiation and imparts stem cell-like features to pancreatic cancer cells. Oncogenesis *2*, e61.

Higgins, J.M. (2001). Haspin-like proteins: a new family of evolutionarily conserved putative eukaryotic protein kinases. Protein science : a publication of the Protein Society *10*, 1677-1684.

Hirota, T., Lipp, J.J., Toh, B.H., and Peters, J.M. (2005). Histone H3 serine 10 phosphorylation by Aurora B causes HP1 dissociation from heterochromatin. Nature *438*, 1176-1180.

Hsu, J.Y., Sun, Z.W., Li, X., Reuben, M., Tatchell, K., Bishop, D.K., Grushcow, J.M., Brame, C.J., Caldwell, J.A., Hunt, D.F*., et al.* (2000). Mitotic phosphorylation of histone H3 is governed by Ipl1/aurora kinase and Glc7/PP1 phosphatase in budding yeast and nematodes. Cell *102*, 279-291.

Huang, H., Weng, H., Zhou, H., and Qu, L. (2014). Attacking c-Myc: targeted and combined therapies for cancer. Current pharmaceutical design *20*, 6543-6554.

Hunter, T. (1995). Protein kinases and phosphatases: the yin and yang of protein phosphorylation and signaling. Cell *80*, 225-236.

Hurd, P.J., Bannister, A.J., Halls, K., Dawson, M.A., Vermeulen, M., Olsen, J.V., Ismail, H., Somers, J., Mann, M., Owen-Hughes, T.*, et al.* (2009). Phosphorylation of histone H3 Thr-45 is linked to apoptosis. The Journal of biological chemistry *284*, 16575-16583.

Hussenet, T., Dali, S., Exinger, J., Monga, B., Jost, B., Dembele, D., Martinet, N., Thibault, C., Huelsken, J., Brambilla, E.*, et al.* (2010). SOX2 is an oncogene activated by recurrent 3q26.3 amplifications in human lung squamous cell carcinomas. PloS one *5*, e8960.

Hutz, K., Mejias-Luque, R., Farsakova, K., Ogris, M., Krebs, S., Anton, M., Vieth, M., Schuller, U., Schneider, M.R., Blum, H.*, et al.* (2014). The stem cell factor SOX2 regulates the tumorigenic potential in human gastric cancer cells. Carcinogenesis *35*, 942-950.

Iida, H., Suzuki, M., Goitsuka, R., and Ueno, H. (2012). Hypoxia induces CD133 expression in human lung cancer cells by up-regulation of OCT3/4 and SOX2. International journal of oncology *40*, 71-79.

Isobe, K., Cheng, Z., Nishio, N., Suganya, T., Tanaka, Y., and Ito, S. (2015). Reprint of "iPSCs, aging and age-related diseases". N Biotechnol *32*, 169-179.

Iv Santaliz-Ruiz, L.E., Xie, X., Old, M., Teknos, T.N., and Pan, Q. (2014). Emerging role of nanog in tumorigenesis and cancer stem cells. International journal of cancer Journal international du cancer *135*, 2741-2748.

Jackson, S.P., and Bartek, J. (2009). The DNA-damage response in human biology and disease. Nature *461*, 1071-1078.

Jeong, C.H., Cho, Y.Y., Kim, M.O., Kim, S.H., Cho, E.J., Lee, S.Y., Jeon, Y.J., Lee, K.Y., Yao, K., Keum, Y.S.*, et al.* (2010). Phosphorylation of Sox2 cooperates in reprogramming to pluripotent stem cells. Stem cells (Dayton, Ohio) *28*, 2141-2150.

Jeong, M.W., Kang, T.H., Kim, W., Choi, Y.H., and Kim, K.T. (2013). Mitogen-activated protein kinase phosphatase 2 regulates histone H3 phosphorylation via interaction with vaccinia-related kinase 1. Molecular biology of the cell *24*, 373-384.

Jia, X., Li, X., Xu, Y., Zhang, S., Mou, W., Liu, Y., Liu, Y., Lv, D., Liu, C.H., Tan, X.*, et al.* (2011). SOX2 promotes tumorigenesis and increases the anti-apoptotic property of human prostate cancer cell. J Mol Cell Biol *3*, 230-238.

Justilien, V., Walsh, M.P., Ali, S.A., Thompson, E.A., Murray, N.R., and Fields, A.P. (2014). The PRKCI and SOX2 oncogenes are coamplified and cooperate to activate Hedgehog signaling in lung squamous cell carcinoma. Cancer cell *25*, 139-151.

Kakhki, S.A., Shahhoseini, M., and Salekdeh, G.H. (2013). Comparative SRY incorporation on the regulatory regions of pluripotency/differentiation genes in human embryonic carcinoma cells after retinoic acid induction. Molecular and cellular biochemistry *376*, 145-150.

Kalantzaki, M., Kitamura, E., Zhang, T., Mino, A., Novak, B., and Tanaka, T.U. (2015). Kinetochore-microtubule error correction is driven by differentially regulated interaction modes. Nature cell biology *17*, 421-433.

Kallio, M.J., McCleland, M.L., Stukenberg, P.T., and Gorbsky, G.J. (2002). Inhibition of aurora B kinase blocks chromosome segregation, overrides the spindle checkpoint, and perturbs microtubule dynamics in mitosis. Curr Biol *12*, 900-905.

Kamachi, Y., Uchikawa, M., and Kondoh, H. (2000). Pairing SOX off: with partners in the regulation of embryonic development. Trends in genetics : TIG *16*, 182-187.

Kamachi, Y., Uchikawa, M., Tanouchi, A., Sekido, R., and Kondoh, H. (2001). Pax6 and SOX2 form a co-DNA-binding partner complex that regulates initiation of lens development. Genes & development *15*, 1272-1286.

Kamaraj, B., Kumar, A., and Purohit, R. (2013). Evolutionary reconstruction and population genetics analysis of aurora kinases. PloS one *8*, e75763.

Kamath, R.S., Fraser, A.G., Dong, Y., Poulin, G., Durbin, R., Gotta, M., Kanapin, A., Le Bot, N., Moreno, S., Sohrmann, M.*, et al.* (2003). Systematic functional analysis of the Caenorhabditis elegans genome using RNAi. Nature *421*, 231-237.

Kang, T.H., and Kim, K.T. (2006). Negative regulation of ERK activity by VRK3-mediated activation of VHR phosphatase. Nature cell biology *8*, 863-869.

Kang, T.H., and Kim, K.T. (2008). VRK3-mediated inactivation of ERK signaling in adult and embryonic rodent tissues. Biochimica et biophysica acta *1783*, 49-58.

Kang, T.H., Park, D.Y., Choi, Y.H., Kim, K.J., Yoon, H.S., and Kim, K.T. (2007a). Mitotic histone H3 phosphorylation by vaccinia-related kinase 1 in mammalian cells. Mol Cell Biol *27*, 8533-8546.

Kang, T.H., Park, D.Y., Choi, Y.H., Kim, K.J., Yoon, H.S., and Kim, K.T. (2007b). Mitotic histone H3 phosphorylation by vaccinia-related kinase 1 in mammalian cells. Molecular and cellular biology *27*, 8533-8546.

Kang, T.H., Park, D.Y., Kim, W., and Kim, K.T. (2008a). VRK1 phosphorylates CREB and mediates CCND1 expression. Journal of cell science *121*, 3035-3041.

Kang, T.H., Park, D.Y., Kim, W., and Kim, K.T. (2008b). VRK1 phosphorylates CREB and mediates CCND1 expression. J Cell Sci *121*, 3035-3041.

Kawajiri, A., Yasui, Y., Goto, H., Tatsuka, M., Takahashi, M., Nagata, K., and Inagaki, M. (2003). Functional significance of the specific sites phosphorylated in desmin at cleavage furrow: Aurora-B may phosphorylate and regulate type III intermediate filaments during cytokinesis coordinatedly with Rho-kinase. Molecular biology of the cell *14*, 1489-1500.

Kawashima, S.A., Yamagishi, Y., Honda, T., Ishiguro, K., and Watanabe, Y. (2010). Phosphorylation of H2A by Bub1 prevents chromosomal instability through localizing shugoshin. Science (New York, NY) *327*, 172-177.

Kelly, A.E., Sampath, S.C., Maniar, T.A., Woo, E.M., Chait, B.T., and Funabiki, H. (2007). Chromosomal enrichment and activation of the aurora B pathway are coupled to spatially regulate spindle assembly. Dev Cell *12*, 31-43.

Kim, D., Kim, C.H., Moon, J.I., Chung, Y.G., Chang, M.Y., Han, B.S., Ko, S., Yang, E., Cha, K.Y., Lanza, R.*, et al.* (2009). Generation of human induced pluripotent stem cells by direct delivery of reprogramming proteins. Cell Stem Cell *4*, 472-476.

Kim, J., Choi, Y.H., Chang, S., Kim, K.T., and Je, J.H. (2012a). Defective folliculogenesis in female mice lacking Vaccinia-related kinase 1. Scientific reports *2*, 468.

Kim, S.H., Ryu, H.G., Lee, J., Shin, J., Harikishore, A., Jung, H.Y., Kim, Y.S., Lyu, H.N., Oh, E., Baek, N.I.*, et al.* (2015). Ursolic acid exerts anti-cancer activity by suppressing vaccinia-related kinase 1-mediated damage repair in lung cancer cells. Scientific reports *5*, 14570.

Kim, W., Chakraborty, G., Kim, S., Shin, J., Park, C.H., Jeong, M.W., Bharatham, N., Yoon, H.S., and Kim, K.T. (2012b). Macro Histone H2A1.2 (MacroH2A1) Protein Suppresses Mitotic Kinase VRK1 during Interphase. J Biol Chem *287*, 5278-5289.

Kim, W., Chakraborty, G., Kim, S., Shin, J., Park, C.H., Jeong, M.W., Bharatham, N., Yoon, H.S., and Kim, K.T. (2012c). Macro histone H2A1.2 (macroH2A1) protein suppresses mitotic kinase VRK1 during interphase. The Journal of biological chemistry *287*, 5278-5289.

Kim, Y.S., Kim, S.H., Shin, J., Harikishore, A., Lim, J.K., Jung, Y., Lyu, H.N., Baek, N.I., Choi, K.Y., Yoon, H.S.*, et al.* (2014). Luteolin suppresses cancer cell proliferation by targeting vaccinia-related kinase 1. PloS one *9*, e109655.

Klein, U.R., Nigg, E.A., and Gruneberg, U. (2006). Centromere targeting of the chromosomal passenger complex requires a ternary subcomplex of Borealin, Survivin, and the N-terminal domain of INCENP. Molecular biology of the cell *17*, 2547-2558.

Klerkx, E.P., Lazo, P.A., and Askjaer, P. (2009). Emerging biological functions of the vaccinia-related kinase (VRK) family. Histology and histopathology *24*, 749-759.

Kollareddy, M., Dzubak, P., Zheleva, D., and Hajduch, M. (2008). Aurora kinases: structure, functions and their association with cancer. Biomed Pap Med Fac Univ Palacky Olomouc Czech Repub *152*, 27-33.

Kondo, T., Isoda, R., Ookusa, T., Kamijo, K., Hamao, K., and Hosoya, H. (2013). Aurora B but not rho/MLCK signaling is required for localization of diphosphorylated myosin II regulatory light chain to the midzone in cytokinesis. PloS one *8*, e70965.

Kondoh, H., Uchikawa, M., and Kamachi, Y. (2004). Interplay of Pax6 and SOX2 in lens development as a paradigm of genetic switch mechanisms for cell differentiation. The International journal of developmental biology *48*, 819-827.

Kouzarides, T. (2007). Chromatin modifications and their function. Cell *128*, 693-705.

Kuroda, T., Tada, M., Kubota, H., Kimura, H., Hatano, S.Y., Suemori, H., Nakatsuji, N., and Tada, T. (2005). Octamer and Sox elements are required for transcriptional cis regulation of Nanog gene expression. Molecular and cellular biology *25*, 2475-2485.

Lancaster, O.M., Cullen, C.F., and Ohkura, H. (2007). NHK-1 phosphorylates BAF to allow karyosome formation in the Drosophila oocyte nucleus. The Journal of cell biology *179*, 817-824.

Lazo, P.A., and Santos, C.R. (2011). Interference with p53 functions in human viral infections, a target for novel antiviral strategies? Reviews in medical virology *21*, 285-300.

Lee, N., Kwon, J.H., Kim, Y.B., Kim, S.H., Park, S.J., Xu, W., Jung, H.Y., Kim, K.T., Wang, H.J., and Choi, K.Y. (2015). Vaccinia-related kinase 1 promotes hepatocellular carcinoma by controlling the levels of cell cycle regulators associated with G1/S transition. Oncotarget *6*, 30130-30148.

Leis, O., Eguiara, A., Lopez-Arribillaga, E., Alberdi, M.J., Hernandez-Garcia, S., Elorriaga, K., Pandiella, A., Rezola, R., and Martin, A.G. (2012). Sox2 expression in breast tumours and activation in breast cancer stem cells. Oncogene *31*, 1354-1365.

Lengerke, C., Fehm, T., Kurth, R., Neubauer, H., Scheble, V., Muller, F., Schneider, F., Petersen, K., Wallwiener, D., Kanz, L.*, et al.* (2011). Expression of the embryonic stem cell marker SOX2 in early-stage breast carcinoma. BMC cancer *11*, 42.

Lens, S.M., and Medema, R.H. (2003). The survivin/Aurora B complex: its role in coordinating tension and attachment. Cell cycle (Georgetown, Tex) *2*, 507-510.

Li, C., Yan, Y., Ji, W., Bao, L., Qian, H., Chen, L., Wu, M., Chen, H., Li, Z., and Su, C. (2012a). OCT4 positively regulates Survivin expression to promote cancer cell proliferation and leads to poor prognosis in esophageal squamous cell carcinoma. PloS one *7*, e49693.

Li, H., Collado, M., Villasante, A., Matheu, A., Lynch, C.J., Canamero, M., Rizzoti, K., Carneiro, C., Martinez, G., Vidal, A.*, et al.* (2012b). p27(Kip1) directly represses Sox2 during embryonic stem cell differentiation. Cell Stem Cell *11*, 845-852.

Li, X., Xu, Y., Chen, Y., Chen, S., Jia, X., Sun, T., Liu, Y., Li, X., Xiang, R., and Li, N. (2013). SOX2 promotes tumor metastasis by stimulating epithelial-to-mesenchymal transition via regulation of WNT/beta-catenin signal network. Cancer letters *336*, 379-389.

Lin, F., Lin, P., Zhao, D., Chen, Y., Xiao, L., Qin, W., Li, D., Chen, H., Zhao, B., Zou, H.*, et al.* (2012). Sox2 targets cyclinE, p27 and survivin to regulate androgen-independent human prostate cancer cell proliferation and apoptosis. Cell proliferation *45*, 207-216.

Lipp, J.J., Hirota, T., Poser, I., and Peters, J.M. (2007). Aurora B controls the association of condensin I but not condensin II with mitotic chromosomes. Journal of cell science *120*, 1245-1255.

Liu, A., Yu, X., and Liu, S. (2013a). Pluripotency transcription factors and cancer stem cells: small genes make a big difference. Chinese journal of cancer *32*, 483-487.

Liu, H., Du, L., Wen, Z., Yang, Y., Li, J., Dong, Z., Zheng, G., Wang, L., Zhang, X., and Wang, C. (2013b). Sex determining region Y-box 2 inhibits the proliferation of colorectal adenocarcinoma cells through the mTOR signaling pathway. International journal of molecular medicine *32*, 59-66.

Liu, K., Lin, B., Zhao, M., Yang, X., Chen, M., Gao, A., Liu, F., Que, J., and Lan, X. (2013c). The multiple roles for Sox2 in stem cell maintenance and tumorigenesis. Cellular signalling *25*, 1264-1271.

Liu, L., Peng, Z., Xu, Z., and Wei, X. (2015). Effect of luteolin and apigenin on the expression of Oct-4, Sox2, and c-Myc in dental pulp cells with in vitro culture. Biomed Res Int *2015*, 534952.

Lodato, M.A., Ng, C.W., Wamstad, J.A., Cheng, A.W., Thai, K.K., Fraenkel, E., Jaenisch, R., and Boyer, L.A. (2013). SOX2 co-occupies distal enhancer elements with distinct POU factors in ESCs and NPCs to specify cell state. PLoS Genet *9*, e1003288.

Lopez-Borges, S., and Lazo, P.A. (2000). The human vaccinia-related kinase 1 (VRK1) phosphorylates threonine-18 within the mdm-2 binding site of the p53 tumour suppressor protein. Oncogene *19*, 3656-3664.

Lopez-Sanchez, I., Sanz-Garcia, M., and Lazo, P.A. (2009). Plk3 interacts with and specifically phosphorylates VRK1 in Ser342, a downstream target in a pathway that induces Golgi fragmentation. Molecular and cellular biology *29*, 1189-1201.

Lopez-Sanchez, I., Valbuena, A., Vazquez-Cedeira, M., Khadake, J., Sanz-Garcia, M., Carrillo-Jimenez, A., and Lazo, P.A. (2014a). VRK1 interacts with p53 forming a basal complex that is activated by UV-induced DNA damage. FEBS Lett *588*, 692-700.

Lopez-Sanchez, I., Valbuena, A., Vazquez-Cedeira, M., Khadake, J., Sanz-Garcia, M., Carrillo-Jimenez, A., and Lazo, P.A. (2014b). VRK1 interacts with p53 forming a basal complex that is activated by UV-induced DNA damage. FEBS letters *588*, 692-700.

Lu, D., Hsiao, J.Y., Davey, N.E., Van Voorhis, V.A., Foster, S.A., Tang, C., and Morgan, D.O. (2014). Multiple mechanisms determine the order of APC/C substrate degradation in mitosis. The Journal of cell biology *207*, 23-39.

Luijsterburg, M.S., and van Attikum, H. (2011). Chromatin and the DNA damage response: the cancer connection. Molecular oncology *5*, 349-367.

Lundberg, I.V., Lofgren Burstrom, A., Edin, S., Eklof, V., Oberg, A., Stenling, R., Palmqvist, R., and Wikberg, M.L. (2014). SOX2 expression is regulated by BRAF and contributes to poor patient prognosis in colorectal cancer. PloS one *9*, e101957.

Maerki, S., Olma, M.H., Staubli, T., Steigemann, P., Gerlich, D.W., Quadroni, M., Sumara, I., and Peter, M. (2009). The Cul3-KLHL21 E3 ubiquitin ligase targets aurora B to midzone microtubules in anaphase and is required for cytokinesis. The Journal of cell biology *187*, 791-800.

Maiato, H., DeLuca, J., Salmon, E.D., and Earnshaw, W.C. (2004). The dynamic kinetochore-microtubule interface. Journal of cell science *117*, 5461-5477.

Malumbres, M., and Barbacid, M. (2007). Cell cycle kinases in cancer. Curr Opin Genet Dev *17*, 60-65.

Malumbres, M., and Barbacid, M. (2009). Cell cycle, CDKs and cancer: a changing paradigm. Nat Rev Cancer *9*, 153-166.

Manning, G., Plowman, G.D., Hunter, T., and Sudarsanam, S. (2002a). Evolution of protein kinase signaling from yeast to man. Trends in biochemical sciences *27*, 514-520.

Manning, G., Whyte, D.B., Martinez, R., Hunter, T., and Sudarsanam, S. (2002b). The protein kinase complement of the human genome. Science (New York, NY) *298*, 1912-1934.

Mansukhani, A., Ambrosetti, D., Holmes, G., Cornivelli, L., and Basilico, C. (2005). Sox2 induction by FGF and FGFR2 activating mutations inhibits Wnt signaling and osteoblast differentiation. The Journal of cell biology *168*, 1065-1076.

Mao, D.D., Gujar, A.D., Mahlokozera, T., Chen, I., Pan, Y., Luo, J., Brost, T., Thompson, E.A., Turski, A., Leuthardt, E.C*., et al.* (2015). A CDC20-APC/SOX2 Signaling Axis Regulates Human Glioblastoma Stem-like Cells. Cell Rep *11*, 1809-1821.

Maresca, T.J., and Salmon, E.D. (2010). Welcome to a new kind of tension: translating kinetochore mechanics into a wait-anaphase signal. Journal of cell science *123*, 825-835.

Marill, J., Idres, N., Capron, C.C., Nguyen, E., and Chabot, G.G. (2003). Retinoic acid metabolism and mechanism of action: a review. Current drug metabolism *4*, 1-10.

Martin, G.R. (1981). Isolation of a pluripotent cell line from early mouse embryos cultured in medium conditioned by teratocarcinoma stem cells. Proceedings of the National Academy of Sciences of the United States of America *78*, 7634-7638.

Matthews, R.P., Guthrie, C.R., Wailes, L.M., Zhao, X., Means, A.R., and McKnight, G.S. (1994). Calcium/calmodulin-dependent protein kinase types II and IV differentially regulate CREB-dependent gene expression. Mol Cell Biol *14*, 6107-6116.

Meadows, J.C., and Millar, J.B. (2015). Sharpening the anaphase switch. Biochemical Society transactions *43*, 19-22.

Megiorni, F., Mora, B., Indovina, P., and Mazzilli, M.C. (2005). Expression of neuronal markers during NTera2/cloneD1 differentiation by cell aggregation method. Neuroscience letters *373*, 105-109.

Meppelink, A., Kabeche, L., Vromans, M.J., Compton, D.A., and Lens, S.M. (2015). Shugoshin-1 Balances Aurora B Kinase Activity via PP2A to Promote Chromosome Bi-orientation. Cell Rep *11*, 508-515.

Mitchison, T.J., and Salmon, E.D. (2001). Mitosis: a history of division. Nature cell biology *3*, E17-21.

Molitor, T.P., and Traktman, P. (2013). Molecular genetic analysis of VRK1 in mammary epithelial cells: depletion slows proliferation in vitro and tumor growth and metastasis in vivo. Oncogenesis *2*, e48.

Molitor, T.P., and Traktman, P. (2014). Depletion of the protein kinase VRK1 disrupts nuclear envelope morphology and leads to BAF retention on mitotic chromosomes. Molecular biology of the cell *25*, 891-903.

Monsalve, D.M., Merced, T., Fernandez, I.F., Blanco, S., Vazquez-Cedeira, M., and Lazo, P.A. (2013). Human VRK2 modulates apoptosis by interaction with Bcl-xL and regulation of BAX gene expression. Cell death & disease *4*, e513.

Murata-Hori, M., and Wang, Y.L. (2002). Both midzone and astral microtubules are involved in the delivery of cytokinesis signals: insights from the mobility of aurora B. The Journal of cell biology *159*, 45-53.

Musacchio, A. (2011). Spindle assembly checkpoint: the third decade. Philos Trans R Soc Lond B Biol Sci *366*, 3595-3604.

Najmabadi, H., Hu, H., Garshasbi, M., Zemojtel, T., Abedini, S.S., Chen, W., Hosseini, M., Behjati, F., Haas, S., Jamali, P.*, et al.* (2011). Deep sequencing reveals 50 novel genes for recessive cognitive disorders. Nature *478*, 57-63.

Nezu, J., Oku, A., Jones, M.H., and Shimane, M. (1997). Identification of two novel human putative serine/threonine kinases, VRK1 and VRK2, with structural similarity to vaccinia virus B1R kinase. Genomics *45*, 327-331.

Nguyen, T.P., Biliciler, S., Wiszniewski, W., and Sheikh, K. (2015). Expanding Phenotype of VRK1 Mutations in Motor Neuron Disease. Journal of clinical neuromuscular disease *17*, 69-71.

Nichols, R.J., and Traktman, P. (2004). Characterization of three paralogous members of the Mammalian vaccinia related kinase family. The Journal of biological chemistry *279*, 7934-7946.

Nichols, R.J., Wiebe, M.S., and Traktman, P. (2006a). The vaccinia-related kinases phosphorylate the N' terminus of BAF, regulating its interaction with DNA and its retention in the nucleus. Mol Biol Cell *17*, 2451-2464.

Nichols, R.J., Wiebe, M.S., and Traktman, P. (2006b). The vaccinia-related kinases phosphorylate the N' terminus of BAF, regulating its interaction with DNA and its retention in the nucleus. Molecular biology of the cell *17*, 2451-2464.

Nishiyama, T., Sykora, M.M., Huis in 't Veld, P.J., Mechtler, K., and Peters, J.M. (2013). Aurora B and Cdk1 mediate Wapl activation and release of acetylated cohesin from chromosomes by phosphorylating Sororin. Proceedings of the National Academy of Sciences of the United States of America *110*, 13404-13409.

Nolen, B., Taylor, S., and Ghosh, G. (2004). Regulation of protein kinases; controlling activity through activation segment conformation. Molecular cell *15*, 661-675.

Ohi, R., Coughlin, M.L., Lane, W.S., and Mitchison, T.J. (2003). An inner centromere protein that stimulates the microtubule depolymerizing activity of a KinI kinesin. Dev Cell *5*, 309-321.

Ouyang, J., Yu, W., Liu, J., Zhang, N., Florens, L., Chen, J., Liu, H., Washburn, M., Pei, D., and Xie, T. (2015). Cyclin-Dependent Kinase-Mediated Sox2 Phosphorylation Enhances the Ability of Sox2 to Establish the Pluripotent State. The Journal of biological chemistry.

Pagan, J.K., Marzio, A., Jones, M.J., Saraf, A., Jallepalli, P.V., Florens, L., Washburn, M.P., and Pagano, M. (2015). Degradation of Cep68 and PCNT cleavage mediate Cep215 removal from the PCM to allow centriole separation, disengagement and licensing. Nature cell biology *17*, 31-43.

Park, C.H., Choi, B.H., Jeong, M.W., Kim, S., Kim, W., Song, Y.S., and Kim, K.T. (2011). Protein kinase Cdelta regulates vaccinia-related kinase 1 in DNA damage-induced apoptosis. Molecular biology of the cell *22*, 1398-1408.

Pasque, V., Radzisheuskaya, A., Gillich, A., Halley-Stott, R.P., Panamarova, M., Zernicka-Goetz, M., Surani, M.A., and Silva, J.C. (2012). Histone variant macroH2A marks embryonic differentiation in vivo and acts as an epigenetic barrier to induced pluripotency. Journal of cell science *125*, 6094-6104.

Paweletz, N. (2001). Walther Flemming: pioneer of mitosis research. Nature reviews Molecular cell biology *2*, 72-75.

Pawson, T., and Scott, J.D. (2005). Protein phosphorylation in signaling--50 years and counting. Trends in biochemical sciences *30*, 286-290.

Petersen, J., and Hagan, I.M. (2003). S. pombe aurora kinase/survivin is required for chromosome condensation and the spindle checkpoint attachment response. Curr Biol *13*, 590-597.

Petsalaki, E., Akoumianaki, T., Black, E.J., Gillespie, D.A., and Zachos, G. (2011). Phosphorylation at serine 331 is required for Aurora B activation. The Journal of cell biology *195*, 449-466.

Pinsky, B.A., and Biggins, S. (2005). The spindle checkpoint: tension versus attachment. Trends in cell biology *15*, 486-493.

Piva, M., Domenici, G., Iriondo, O., Rabano, M., Simoes, B.M., Comaills, V., Barredo, I., Lopez-Ruiz, J.A., Zabalza, I., Kypta, R.*, et al.* (2014). Sox2 promotes tamoxifen resistance in breast cancer cells. EMBO molecular medicine *6*, 66-79.

Pleasure, S.J., and Lee, V.M. (1993). NTera 2 cells: a human cell line which displays characteristics expected of a human committed neuronal progenitor cell. J Neurosci Res *35*, 585-602.

Pleasure, S.J., Page, C., and Lee, V.M. (1992). Pure, postmitotic, polarized human neurons derived from NTera 2 cells provide a system for expressing exogenous proteins in terminally differentiated neurons. The Journal of neuroscience : the official journal of the Society for Neuroscience *12*, 1802-1815.

Podrygajlo, G., Tegenge, M.A., Gierse, A., Paquet-Durand, F., Tan, S., Bicker, G., and Stern, M. (2009). Cellular phenotypes of human model neurons (NT2) after differentiation in aggregate culture. Cell and tissue research *336*, 439-452.

Prigent, C., and Dimitrov, S. (2003). Phosphorylation of serine 10 in histone H3, what for? Journal of cell science *116*, 3677-3685.

Qian, J., Beullens, M., Lesage, B., and Bollen, M. (2013). Aurora B defines its own chromosomal targeting by opposing the recruitment of the phosphatase scaffold Repo-Man. Curr Biol *23*, 1136-1143.

Qian, J., Lesage, B., Beullens, M., Van Eynde, A., and Bollen, M. (2011). PP1/Repo-man dephosphorylates mitotic histone H3 at T3 and regulates chromosomal aurora B targeting. Curr Biol *21*, 766-773.

Renbaum, P., Kellerman, E., Jaron, R., Geiger, D., Segel, R., Lee, M., King, M.C., and Levy-Lahad, E. (2009a). Spinal muscular atrophy with pontocerebellar hypoplasia is caused by a mutation in the VRK1 gene. Am J Hum Genet *85*, 281-289.

Renbaum, P., Kellerman, E., Jaron, R., Geiger, D., Segel, R., Lee, M., King, M.C., and Levy-Lahad, E. (2009b). Spinal muscular atrophy with pontocerebellar hypoplasia is caused by a mutation in the VRK1 gene. American journal of human genetics *85*, 281-289.

Riggi, N., Knoechel, B., Gillespie, S.M., Rheinbay, E., Boulay, G., Suva, M.L., Rossetti, N.E., Boonseng, W.E., Oksuz, O., Cook, E.B.*, et al.* (2014). EWS-FLI1 Utilizes Divergent Chromatin Remodeling Mechanisms to Directly Activate or Repress Enhancer Elements in Ewing Sarcoma. Cancer cell *26*, 668-681.

Riggi, N., Suva, M.L., De Vito, C., Provero, P., Stehle, J.C., Baumer, K., Cironi, L., Janiszewska, M., Petricevic, T., Suva, D.*, et al.* (2010). EWS-FLI-1 modulates miRNA145 and SOX2 expression to initiate mesenchymal stem cell reprogramming toward Ewing sarcoma cancer stem cells. Genes & development *24*, 916-932.

Rodda, D.J., Chew, J.L., Lim, L.H., Loh, Y.H., Wang, B., Ng, H.H., and Robson, P. (2005). Transcriptional regulation of nanog by OCT4 and SOX2. The Journal of biological chemistry *280*, 24731-24737.

Rosasco-Nitcher, S.E., Lan, W., Khorasanizadeh, S., and Stukenberg, P.T. (2008). Centromeric Aurora-B activation requires TD-60, microtubules, and substrate priming phosphorylation. Science (New York, NY) *319*, 469-472.

Rothenberg, S.M., Concannon, K., Cullen, S., Boulay, G., Turke, A.B., Faber, A.C., Lockerman, E.L., Rivera, M.N., Engelman, J.A., Maheswaran, S.*, et al.* (2015). Inhibition of mutant EGFR in lung cancer cells triggers SOX2-FOXO6-dependent survival pathways. eLife *4*.

Ruan, Q., Wang, Q., Xie, S., Fang, Y., Darzynkiewicz, Z., Guan, K., Jhanwar-Uniyal, M., and Dai, W. (2004). Polo-like kinase 3 is Golgi localized and involved in regulating Golgi fragmentation during the cell cycle. Experimental cell research *294*, 51-59.

Ruchaud, S., Carmena, M., and Earnshaw, W.C. (2007). Chromosomal passengers: conducting cell division. Nature reviews Molecular cell biology *8*, 798-812.

Salzano, M., Sanz-Garcia, M., Monsalve, D.M., Moura, D.S., and Lazo, P.A. (2015). VRK1 chromatin kinase phosphorylates H2AX and is required for foci formation induced by DNA damage. Epigenetics *10*, 373-383.

Salzano, M., Vazquez-Cedeira, M., Sanz-Garcia, M., Valbuena, A., Blanco, S., Fernandez, I.F., and Lazo, P.A. (2014). Vaccinia-related kinase 1 (VRK1) confers resistance to DNA-damaging agents in human breast cancer by affecting DNA damage response. Oncotarget *5*, 1770-1778.

Santos, C.R., Rodriguez-Pinilla, M., Vega, F.M., Rodriguez-Peralto, J.L., Blanco, S., Sevilla, A., Valbuena, A., Hernandez, T., van Wijnen, A.J., Li, F.*, et al.* (2006). VRK1 signaling pathway in the context of the proliferation phenotype in head and neck squamous cell carcinoma. Molecular cancer research : MCR *4*, 177-185.

Sanz-Garcia, M., Lopez-Sanchez, I., and Lazo, P.A. (2008). Proteomics identification of nuclear Ran GTPase as an inhibitor of human VRK1 and VRK2 (vaccinia-related kinase) activities. Molecular & cellular proteomics : MCP *7*, 2199-2214.

Sanz-Garcia, M., Monsalve, D.M., Sevilla, A., and Lazo, P.A. (2012). Vaccinia-related kinase 1 (VRK1) is an upstream nucleosomal kinase required for the assembly of 53BP1 foci in response to ionizing radiation-induced DNA damage. The Journal of biological chemistry *287*, 23757-23768.

Sanz-Garcia, M., Vazquez-Cedeira, M., Kellerman, E., Renbaum, P., Levy-Lahad, E., and Lazo, P.A. (2011). Substrate profiling of human vaccinia-related kinases identifies coilin, a Cajal body nuclear protein, as a phosphorylation target with neurological implications. Journal of proteomics *75*, 548-560.

Sarkar, A., and Hochedlinger, K. (2013). The sox family of transcription factors: versatile regulators of stem and progenitor cell fate. Cell Stem Cell *12*, 15-30.

Scheeff, E.D., Eswaran, J., Bunkoczi, G., Knapp, S., and Manning, G. (2009). Structure of the pseudokinase VRK3 reveals a degraded catalytic site, a highly conserved kinase fold, and a putative regulatory binding site. Structure (London, England : 1993) *17*, 128-138.

Schnoder, T.M., Arreba-Tutusaus, P., Griehl, I., Bullinger, L., Buschbeck, M., Lane, S.W., Dohner, K., Plass, C., Lipka, D.B., Heidel, F.H.*, et al.* (2015). Epo-induced erythroid maturation is dependent on Plcgamma1 signaling. Cell death and differentiation *22*, 974-985.

Schober, C.S., Aydiner, F., Booth, C.J., Seli, E., and Reinke, V. (2011). The kinase VRK1 is required for normal meiotic progression in mammalian oogenesis. Mechanisms of development *128*, 178-190.

Sessa, F., Mapelli, M., Ciferri, C., Tarricone, C., Areces, L.B., Schneider, T.R., Stukenberg, P.T., and Musacchio, A. (2005). Mechanism of Aurora B activation by INCENP and inhibition by hesperadin. Molecular cell *18*, 379-391.

Sevilla, A., Santos, C.R., Barcia, R., Vega, F.M., and Lazo, P.A. (2004a). c-Jun phosphorylation by the human vaccinia-related kinase 1 (VRK1) and its cooperation with the N-terminal kinase of c-Jun (JNK). Oncogene *23*, 8950-8958.

Sevilla, A., Santos, C.R., Vega, F.M., and Lazo, P.A. (2004b). Human vaccinia-related kinase 1 (VRK1) activates the ATF2 transcriptional activity by novel phosphorylation on Thr-73 and Ser-62 and cooperates with JNK. The Journal of biological chemistry *279*, 27458-27465.

Shannon, K.B., Canman, J.C., and Salmon, E.D. (2002). Mad2 and BubR1 function in a single checkpoint pathway that responds to a loss of tension. Molecular biology of the cell *13*, 3706-3719.

Shchemelinin, I., Sefc, L., and Necas, E. (2006). Protein kinases, their function and implication in cancer and other diseases. Folia biologica *52*, 81-100.

Shechter, D., Dormann, H.L., Allis, C.D., and Hake, S.B. (2007). Extraction, purification and analysis of histones. Nature protocols *2*, 1445-1457.

Sinclair, A.H., Berta, P., Palmer, M.S., Hawkins, J.R., Griffiths, B.L., Smith, M.J., Foster, J.W., Frischauf, A.M., Lovell-Badge, R., and Goodfellow, P.N. (1990). A gene from the human sex-determining region encodes a protein with homology to a conserved DNA-binding motif. Nature *346*, 240-244.

Singh, S., Trevino, J., Bora-Singhal, N., Coppola, D., Haura, E., Altiok, S., and Chellappan, S.P. (2012). EGFR/Src/Akt signaling modulates Sox2 expression and self-renewal of stem-like side-population cells in non-small cell lung cancer. Molecular cancer *11*, 73.

Smith, A.N., Miller, L.A., Radice, G., Ashery-Padan, R., and Lang, R.A. (2009). Stage-dependent modes of Pax6-Sox2 epistasis regulate lens development and eye morphogenesis. Development *136*, 2977-2985.

Smith, E., and Shilatifard, A. (2010). The chromatin signaling pathway: diverse mechanisms of recruitment of histone-modifying enzymes and varied biological outcomes. Molecular cell *40*, 689-701.

Smith, S.L., Bowers, N.L., Betticher, D.C., Gautschi, O., Ratschiller, D., Hoban, P.R., Booton, R., Santibanez-Koref, M.F., and Heighway, J. (2005). Overexpression of aurora B kinase (AURKB) in primary non-small cell lung carcinoma is frequent, generally driven from one allele, and correlates with the level of genetic instability. Br J Cancer *93*, 719-729.

Soufi, A. (2014). Mechanisms for enhancing cellular reprogramming. Curr Opin Genet Dev *25*, 101-109.

Spinella, M.J., Freemantle, S.J., Sekula, D., Chang, J.H., Christie, A.J., and Dmitrovsky, E. (1999). Retinoic acid promotes ubiquitination and proteolysis of cyclin D1 during induced tumor cell differentiation. The Journal of biological chemistry *274*, 22013-22018.

Stewart, S., and Fang, G. (2005). Destruction box-dependent degradation of aurora B is mediated by the anaphase-promoting complex/cyclosome and Cdh1. Cancer research *65*, 8730-8735.

Stokes, M.P., Rush, J., Macneill, J., Ren, J.M., Sprott, K., Nardone, J., Yang, V., Beausoleil, S.A., Gygi, S.P., Livingstone, M.*, et al.* (2007). Profiling of UV-induced ATM/ATR signaling pathways. Proceedings of the National Academy of Sciences of the United States of America *104*, 19855-19860.

Stolzenburg, S., Rots, M.G., Beltran, A.S., Rivenbark, A.G., Yuan, X., Qian, H., Strahl, B.D., and Blancafort, P. (2012). Targeted silencing of the oncogenic transcription factor SOX2 in breast cancer. Nucleic acids research *40*, 6725-6740.

Sudakin, V., Chan, G.K., and Yen, T.J. (2001). Checkpoint inhibition of the APC/C in HeLa cells is mediated by a complex of BUBR1, BUB3, CDC20, and MAD2. The Journal of cell biology *154*, 925-936.

Sudakin, V., Ganoth, D., Dahan, A., Heller, H., Hershko, J., Luca, F.C., Ruderman, J.V., and Hershko, A. (1995). The cyclosome, a large complex containing cyclin-selective ubiquitin ligase activity, targets cyclins for destruction at the end of mitosis. Molecular biology of the cell *6*, 185-197.

Sugiyama, K., Sugiura, K., Hara, T., Sugimoto, K., Shima, H., Honda, K., Furukawa, K., Yamashita, S., and Urano, T. (2002). Aurora-B associated protein phosphatases as negative regulators of kinase activation. Oncogene *21*, 3103-3111.

Sumara, I., Quadroni, M., Frei, C., Olma, M.H., Sumara, G., Ricci, R., and Peter, M. (2007). A Cul3-based E3 ligase removes Aurora B from mitotic chromosomes, regulating mitotic progression and completion of cytokinesis in human cells. Dev Cell *12*, 887-900.

Takahashi, K., and Yamanaka, S. (2006). Induction of pluripotent stem cells from mouse embryonic and adult fibroblast cultures by defined factors. Cell *126*, 663-676.

Takeshita, M., Koga, T., Takayama, K., Ijichi, K., Yano, T., Maehara, Y., Nakanishi, Y., and Sueishi, K. (2013). Aurora-B overexpression is correlated with aneuploidy and poor prognosis in non-small cell lung cancer. Lung cancer (Amsterdam, Netherlands) *80*, 85-90.

Tan, B.T., Park, C.Y., Ailles, L.E., and Weissman, I.L. (2006). The cancer stem cell hypothesis: a work in progress. Laboratory investigation; a journal of technical methods and pathology *86*, 1203-1207.

Tanno, Y., Kitajima, T.S., Honda, T., Ando, Y., Ishiguro, K., and Watanabe, Y. (2010). Phosphorylation of mammalian Sgo2 by Aurora B recruits PP2A and MCAK to centromeres. Genes & development *24*, 2169-2179.

Taylor, S.S., and Kornev, A.P. (2011). Protein kinases: evolution of dynamic regulatory proteins. Trends in biochemical sciences *36*, 65-77.

Teng, C.L., Hsieh, Y.C., Phan, L., Shin, J., Gully, C., Velazquez-Torres, G., Skerl, S., Yeung, S.C., Hsu, S.L., and Lee, M.H. (2012). FBXW7 is involved in Aurora B degradation. Cell cycle (Georgetown, Tex) *11*, 4059-4068.

Terada, Y. (2001). Role of chromosomal passenger complex in chromosome segregation and cytokinesis. Cell structure and function *26*, 653-657.

Thadani, R., and Uhlmann, F. (2015). Chromosome condensation: weaving an untangled web. Curr Biol *25*, R663-666.

Tompkins, D.H., Besnard, V., Lange, A.W., Keiser, A.R., Wert, S.E., Bruno, M.D., and Whitsett, J.A. (2011). Sox2 activates cell proliferation and differentiation in the respiratory epithelium. American journal of respiratory cell and molecular biology *45*, 101-110.

Towbin, H., Staehelin, T., and Gordon, J. (1979). Electrophoretic transfer of proteins from polyacrylamide gels to nitrocellulose sheets: procedure and some applications. Proceedings of the National Academy of Sciences of the United States of America *76*, 4350-4354.

Ubersax, J.A., and Ferrell, J.E., Jr. (2007). Mechanisms of specificity in protein phosphorylation. Nature reviews Molecular cell biology *8*, 530-541.

Vader, G., Cruijsen, C.W., van Harn, T., Vromans, M.J., Medema, R.H., and Lens, S.M. (2007). The chromosomal passenger complex controls spindle checkpoint function independent from its role in correcting microtubule kinetochore interactions. Molecular biology of the cell *18*, 4553-4564.

Vader, G., and Lens, S.M. (2008). The Aurora kinase family in cell division and cancer. Biochimica et biophysica acta *1786*, 60-72.

Vagnarelli, P. (2012). Mitotic chromosome condensation in vertebrates. Experimental cell research *318*, 1435-1441.

Valbuena, A., Blanco, S., Vega, F.M., and Lazo, P.A. (2008a). The C/H3 domain of p300 is required to protect VRK1 and VRK2 from their downregulation induced by p53. PloS one *3*, e2649.

Valbuena, A., Castro-Obregon, S., and Lazo, P.A. (2011a). Downregulation of VRK1 by p53 in response to DNA damage is mediated by the autophagic pathway. PloS one *6*, e17320.

Valbuena, A., Lopez-Sanchez, I., and Lazo, P.A. (2008b). Human VRK1 is an early response gene and its loss causes a block in cell cycle progression. PloS one *3*, e1642.

Valbuena, A., Lopez-Sanchez, I., Vega, F.M., Sevilla, A., Sanz-Garcia, M., Blanco, S., and Lazo, P.A. (2007a). Identification of a dominant epitope in human vaccinia-related kinase 1 (VRK1) and detection of different intracellular subpopulations. Archives of biochemistry and biophysics *465*, 219-226.

Valbuena, A., Sanz-Garcia, M., Lopez-Sanchez, I., Vega, F.M., and Lazo, P.A. (2011b). Roles of VRK1 as a new player in the control of biological processes required for cell division. Cellular signalling *23*, 1267-1272.

Valbuena, A., Sanz-Garcia, M., Lopez-Sanchez, I., Vega, F.M., and Lazo, P.A. (2011c). Roles of VRK1 as a new player in the control of biological processes required for cell division. Cell Signal *23*, 1267-1272.

Valbuena, A., Suarez-Gauthier, A., Lopez-Rios, F., Lopez-Encuentra, A., Blanco, S., Fernandez, P.L., Sanchez-Cespedes, M., and Lazo, P.A. (2007b). Alteration of the VRK1-p53 autoregulatory loop in human lung carcinomas. Lung cancer (Amsterdam, Netherlands) *58*, 303-309.

Valbuena, A., Vega, F.M., Blanco, S., and Lazo, P.A. (2006a). p53 downregulates its activating vaccinia-related kinase 1, forming a new autoregulatory loop. Mol Cell Biol *26*, 4782-4793.

Valbuena, A., Vega, F.M., Blanco, S., and Lazo, P.A. (2006b). p53 downregulates its activating vaccinia-related kinase 1, forming a new autoregulatory loop. Molecular and cellular biology *26*, 4782-4793.

van Dam, H., and Castellazzi, M. (2001). Distinct roles of Jun : Fos and Jun : ATF dimers in oncogenesis. Oncogene *20*, 2453-2464.

van den Berg, D.L., Snoek, T., Mullin, N.P., Yates, A., Bezstarosti, K., Demmers, J., Chambers, I., and Poot, R.A. (2010). An Oct4-centered protein interaction network in embryonic stem cells. Cell Stem Cell *6*, 369-381.

van der Horst, A., and Lens, S.M. (2014). Cell division: control of the chromosomal passenger complex in time and space. Chromosoma *123*, 25-42.

van der Waal, M.S., Saurin, A.T., Vromans, M.J., Vleugel, M., Wurzenberger, C., Gerlich, D.W., Medema, R.H., Kops, G.J., and Lens, S.M. (2012). Mps1 promotes rapid centromere accumulation of Aurora B. EMBO reports *13*, 847-854.

Vazquez-Cedeira, M., Barcia-Sanjurjo, I., Sanz-Garcia, M., Barcia, R., and Lazo, P.A. (2011). Differential inhibitor sensitivity between human kinases VRK1 and VRK2. PloS one *6*, e23235.

Vazquez-Cedeira, M., and Lazo, P.A. (2012). Human VRK2 (vaccinia-related kinase 2) modulates tumor cell invasion by hyperactivation of NFAT1 and expression of cyclooxygenase-2. The Journal of biological chemistry *287*, 42739-42750.

Vega, F.M., Gonzalo, P., Gaspar, M.L., and Lazo, P.A. (2003). Expression of the VRK (vaccinia-related kinase) gene family of p53 regulators in murine hematopoietic development. FEBS letters *544*, 176-180.

Vega, F.M., Sevilla, A., and Lazo, P.A. (2004a). p53 Stabilization and accumulation induced by human vaccinia-related kinase 1. Molecular and cellular biology *24*, 10366-10380.

Vega, F.M., Sevilla, A., and Lazo, P.A. (2004b). p53 Stabilization and accumulation induced by human vaccinia-related kinase 1. Mol Cell Biol *24*, 10366-10380.

Vermeulen, K., Van Bockstaele, D.R., and Berneman, Z.N. (2003). The cell cycle: a review of regulation, deregulation and therapeutic targets in cancer. Cell proliferation *36*, 131-149.

Vinograd-Byk, H., Sapir, T., Cantarero, L., Lazo, P.A., Zeligson, S., Lev, D., Lerman-Sagie, T., Renbaum, P., Reiner, O., and Levy-Lahad, E. (2015). The Spinal Muscular Atrophy with Pontocerebellar Hypoplasia Gene VRK1 Regulates Neuronal Migration through an Amyloid-beta Precursor Protein-Dependent Mechanism. J Neurosci *35*, 936-942.

Wang, D., Lu, P., Zhang, H., Luo, M., Zhang, X., Wei, X., Gao, J., Zhao, Z., and Liu, C. (2014a). Oct-4 and Nanog promote the epithelial-mesenchymal transition of breast cancer stem cells and are associated with poor prognosis in breast cancer patients. Oncotarget *5*, 10803-10815.

Wang, F., Dai, J., Daum, J.R., Niedzialkowska, E., Banerjee, B., Stukenberg, P.T., Gorbsky, G.J., and Higgins, J.M. (2010). Histone H3 Thr-3 phosphorylation by Haspin positions Aurora B at centromeres in mitosis. Science (New York, NY) *330*, 231-235.

Wang, F., Ulyanova, N.P., van der Waal, M.S., Patnaik, D., Lens, S.M., and Higgins, J.M. (2011). A positive feedback loop involving Haspin and Aurora B promotes CPC accumulation at centromeres in mitosis. Curr Biol *21*, 1061-1069.

Wang, X., Ji, X., Chen, J., Yan, D., Zhang, Z., Wang, Q., Xi, X., and Feng, Y. (2014b). SOX2 enhances the migration and invasion of ovarian cancer cells via Src kinase. PloS one *9*, e99594.

Watanabe, Y. (2010). Temporal and spatial regulation of targeting aurora B to the inner centromere. Cold Spring Harb Symp Quant Biol *75*, 419-423.

Waters, K., Yang, A.Z., and Reinke, V. (2010). Genome-wide analysis of germ cell proliferation in C.elegans identifies VRK-1 as a key regulator of CEP-1/p53. Developmental biology *344*, 1011-1025.

Wee, C.D., Kong, L., and Sumner, C.J. (2010). The genetics of spinal muscular atrophies. Current opinion in neurology *23*, 450-458.

Wei, Y., Mizzen, C.A., Cook, R.G., Gorovsky, M.A., and Allis, C.D. (1998). Phosphorylation of histone H3 at serine 10 is correlated with chromosome condensation during mitosis and meiosis in Tetrahymena. Proceedings of the National Academy of Sciences of the United States of America *95*, 7480-7484.

Weina, K., and Utikal, J. (2014). SOX2 and cancer: current research and its implications in the clinic. Clinical and translational medicine *3*, 19.

Werner, M., and Glotzer, M. (2008). Control of cortical contractility during cytokinesis. Biochemical Society transactions *36*, 371-377.

Wiebe, M.S., Nichols, R.J., Molitor, T.P., Lindgren, J.K., and Traktman, P. (2010). Mice deficient in the serine/threonine protein kinase VRK1 are infertile due to a progressive loss of spermatogonia. Biology of reproduction *82*, 182-193.

Wilkins, B.J., Rall, N.A., Ostwal, Y., Kruitwagen, T., Hiragami-Hamada, K., Winkler, M., Barral, Y., Fischle, W., and Neumann, H. (2014). A cascade of histone modifications induces chromatin condensation in mitosis. Science (New York, NY) *343*, 77-80.

Williamson, K.A., Hever, A.M., Rainger, J., Rogers, R.C., Magee, A., Fiedler, Z., Keng, W.T., Sharkey, F.H., McGill, N., Hill, C.J.*, et al.* (2006). Mutations in SOX2 cause anophthalmia-esophageal-genital (AEG) syndrome. Human molecular genetics *15*, 1413-1422.

Wu, F., Zhang, J., Wang, P., Ye, X., Jung, K., Bone, K.M., Pearson, J.D., Ingham, R.J., McMullen, T.P., Ma, Y.*, et al.* (2012). Identification of two novel phenotypically distinct breast cancer cell subsets based on Sox2 transcription activity. Cellular signalling *24*, 1989-1998.

Wysocka, J., Reilly, P.T., and Herr, W. (2001). Loss of HCF-1-chromatin association precedes temperature-induced growth arrest of tsBN67 cells. Molecular and cellular biology *21*, 3820-3829.

Xiang, R., Liao, D., Cheng, T., Zhou, H., Shi, Q., Chuang, T.S., Markowitz, D., Reisfeld, R.A., and Luo, Y. (2011). Downregulation of transcription factor SOX2 in cancer stem cells suppresses growth and metastasis of lung cancer. Br J Cancer *104*, 1410-1417.

Xie, S., Wang, Q., Ruan, Q., Liu, T., Jhanwar-Uniyal, M., Guan, K., and Dai, W. (2004). MEK1-induced Golgi dynamics during cell cycle progression is partly mediated by Polo-like kinase-3. Oncogene *23*, 3822-3829.

Xu, N., Papagiannakopoulos, T., Pan, G., Thomson, J.A., and Kosik, K.S. (2009). MicroRNA-145 regulates OCT4, SOX2, and KLF4 and represses pluripotency in human embryonic stem cells. Cell *137*, 647-658.

Yamagishi, Y., Honda, T., Tanno, Y., and Watanabe, Y. (2010). Two histone marks establish the inner centromere and chromosome bi-orientation. Science (New York, NY) *330*, 239-243.

Yang, C., Tang, X., Guo, X., Niikura, Y., Kitagawa, K., Cui, K., Wong, S.T., Fu, L., and Xu, B. (2011). Aurora-B mediated ATM serine 1403 phosphorylation is required for mitotic ATM activation and the spindle checkpoint. Molecular cell *44*, 597-608.

Yang, N., Hui, L., Wang, Y., Yang, H., and Jiang, X. (2014). SOX2 promotes the migration and invasion of laryngeal cancer cells by induction of MMP-2 via the PI3K/Akt/mTOR pathway. Oncology reports *31*, 2651-2659.

Yasui, Y., Urano, T., Kawajiri, A., Nagata, K., Tatsuka, M., Saya, H., Furukawa, K., Takahashi, T., Izawa, I., and Inagaki, M. (2004). Autophosphorylation of a newly identified site of Aurora-B is indispensable for cytokinesis. The Journal of biological chemistry *279*, 12997-13003.

Yu, J., Vodyanik, M.A., Smuga-Otto, K., Antosiewicz-Bourget, J., Frane, J.L., Tian, S., Nie, J., Jonsdottir, G.A., Ruotti, V., Stewart, R.*, et al.* (2007). Induced pluripotent stem cell lines derived from human somatic cells. Science (New York, NY) *318*, 1917-1920.

Yu, T., Chen, X., Zhang, W., Liu, J., Avdiushko, R., Napier, D.L., Liu, A.X., Neltner, J.M., Wang, C., Cohen, D.*, et al.* (2015). KLF4 regulates adult lung tumor-initiating cells and represses K-Ras-mediated lung cancer. Cell death and differentiation.

Zaret, K.S., and Carroll, J.S. (2011). Pioneer transcription factors: establishing competence for gene expression. Genes & development *25*, 2227-2241.

Zelko, I., Kobayashi, R., Honkakoski, P., and Negishi, M. (1998). Molecular cloning and characterization of a novel nuclear protein kinase in mice. Archives of biochemistry and biophysics *352*, 31-36.

Zhang, X., Lan, W., Ems-McClung, S.C., Stukenberg, P.T., and Walczak, C.E. (2007). Aurora B phosphorylates multiple sites on mitotic centromere-associated kinesin to spatially and temporally regulate its function. Molecular biology of the cell *18*, 3264-3276.

Zhang, Y., Jiang, C., Li, H., Lv, F., Li, X., Qian, X., Fu, L., Xu, B., and Guo, X. (2015). Elevated Aurora B expression contributes to chemoresistance and poor prognosis in breast cancer. Int J Clin Exp Pathol *8*, 751-757.

Zhao, C., Li, Y., Zhang, M., Yang, Y., and Chang, L. (2015). miR-126 inhibits cell proliferation and induces cell apoptosis of hepatocellular carcinoma cells partially by targeting Sox2. Human cell *28*, 91-99.

Zhou, Q., and Liu, J.S. (2008). Extracting sequence features to predict protein-DNA interactions: a comparative study. Nucleic acids research *36*, 4137-4148.

Zhuang, X., Semenova, E., Maric, D., and Craigie, R. (2014). Dephosphorylation of barrier-to-autointegration factor by protein phosphatase 4 and its role in cell mitosis. The Journal of biological chemistry *289*, 1119-1127.

Acknowledgments

Aqui, perdido numa biblioteca entre dezenas de pessoas de ‘’careta’’ pesada e tentando encontrar inspiração para criar uma boa ‘’portada’’ para este trabalho, lembrou-me que ainda me falta escrever umas quantas linhas a agradecer a todas as pessoas de que alguma forma estão envolvidas nesta fase da minha carreira. Poderia dizer nesta fase linda, nesta fase estupenda, nesta fase feliz, o que não seria mentira, mas parecer-me-ia um cliché e prefiro o fazer após o dia do juízo final ou como alguns o apelidam: ‘’el día de lectura de la tesis’’. No entanto, ‘’umas quantas linhas’’ não são fáceis e não serão suficientes para escrever tudo aquilo que poderia ser realmente dito e todas as emoções que neste momento aparecem dentro de mim. De qualquer forma, e tentando não me esquecer de ninguém aqui vai.

En primero lugar quiero agradecer a mi supervisor y mentor de este trabajo, Pedro A. Lazo-Zbikowski por la enorme oportunidad que me ha dado para hacer el doctorado, aceptando en su grupo y por todos los enseñamientos y motivación, durante estos cuatro años, mismo cuando el mundo de la ciencia nos ata en el tiempo. ¡Un enorme placer conocerlo y trabajar con usted!

Gracias a todos mi compañeros de laboratorio y del CIC. Espero no me olvidar de nadie. Agradezco a Carlos e Sonia, a María y Ángel. A María, Sara y Vanesa del laboratorio 5, mis compañeras de cuarto de cultivos y conversación. A Mariana, por me facilitar la llegada a Salamanca y por su amistad que viene de Coimbra. Agradezco a Jose, uno verdadero y grande amigo, lo cual voy a echar de menos por todas las longas conversaciones. Agradezco a Martiña por me ayudar y mucho en mi formación y por ser el primero vinculo en la incorporación en el laboratorio. Ah…y las tartas y bizcochos, los cuales no me puedo olvidar. A Marcella por todos los momentos italiano-españoles-portugueses y todas las expresiones que me van atormentar toda mi vida. A Isa por su inteligencia y enseñamientos, sin olvidar el lado humano y los momentos divertidos fuera del laboratorio. A Gema, Nacho e Elena, los últimos y más recientes miembros del laboratorio 4. Mismo que nuestros momentos fuera de laboratorio han sido pocos y curtos me he encantado conocerlos. Espero que tenga todo el suceso no solo en laboratorio, pero igualmente fuera del. Y tu Elena, espero que encuentres un compañero de pasillo, tan espectacular como yo. A Virginia, la mejor persona que conocí en Salamanca durante todos estos cuatro años y que me ayudó y

mucho en todos los momentos. Una mujer genuinamente amable y que nunca olvidaré. Muchas gracias! Durante estos años muchos salieran y muchos otros entrarán, todavía nadie tenderá mi afecto como vosotras: Lara y Diana! Dra. Lara Cantarero, fuiste la primera amiga que tuve en Salamanca (creo que la única con más de 45 años) y así seguirás siendo. Gracias por todo, principalmente por momentos en que poco más quedaba que nosotros. Nunca me olvidaré de los cuatro años en que los pasaste corrigiendo el portuñol. Eu ‘’posso’’ salir de Salamanca, pero ‘’nenguno’’ me retirará esto. Y gracias Diana. Vivir en tu mundo fui de las mejores experiencias que tuve. Es una persona 10 (en 5) estrellas. Nada me encantaba más que escuchar reír, dentro o fuera del laboratorio. Tu alegría y bondad infectaba a todos y así me recordaré de ti para la eternidad. Espero que las placas tectónicas empecen a trabajar más activamente y al revés para que te veamos más cerca de nosotros. La distancia es inmensa y espero que volvas a Europa rápidamente.

Obrigado a todos os meus amigos. A todos aqueles me conhecem faz 31 anos ou aqueles que apareceram nos últimos tempos. Em especial quero agradecer a todos os membros do tão famoso e apelidado grupo: o ‘’Boda’’. Fábio, Fernando, Filipa, Luísa, Pedro, Pedro, Quitéria, Silvino, Steve, Susana, Tiago e Vasco. Todos vocês, em maior ou menor grau fazem parte desta história e assim espero que sigam sendo. Onde quer que eu esteja ou vocês estejam, conhecemo-nos bem para saber que mesmo passados todos estes anos, e cada um num lugar distinto e com uma vida preenchida, ainda estamos todos sentados no académico a partilhar uma cerveja e a ver um jogo qualquer de uma liga que pouco interessa. Obrigado Sofia, André, Sr. Fernando e D. Teresa. Faz pouco tempo que entraram na minha vida, mas fico feliz por dizer que somos toda uma grande e feliz família. Obrigado por tudo, pela preocupação, pelos conselhos, pelas conversas e pela alegria em cada visita.

Obrigado a toda a minha família. Obrigado ao meu Pai, a minha Mãe e ao meu irmão. Adoro-vos faz 31 anos e para os próximos 90 anos assim será. Depois logo poderemos fazer um apanhado das coisas e decidir qual a próxima meta. Obrigado pelo vosso sacrifício e por todo o carinho e paciência que me deram e continuam a dar para que eu tenha tudo o necessário para triunfar. Espero que sintam honra no que alcancei. Faço-o em parte por vocês. Pai, tudo o que me

ensinaste e mesmo que não pareça, uso-o para ser melhor pessoa e melhor profissional. Espero que um dia o meu filho me olhe e sinta o mesmo orgulho, por me ter como pai, como eu sinto em relação a ti. Por tudo que passaste para que os teus filhos fossem felizes e alcançassem uma vida melhor do que a tiveste. Obrigado! Mãe, obrigado por todo o carinho, por rires de todas as minhas coisas, por nunca me ter faltado nada, mesmo quando significava um sacrifício enorme para ti. Tuas palavras seguem-me fazendo feliz e sempre que estou em casa sinto-me como uma criança amada. Toda a minha vida estiveste ao meu lado, ouvindo meus problemas e alegrias e aconselhando-me o melhor que podias e sabias. Nunca esquecei teus sacrifícios e teu amor. Obrigado! Mica, faz 29 anos que tenho que aturar-te. És o melhor irmão que algum dia poderia ter tido. Somos como água e vinho, mas nas horas da verdade estás presente e se necessário sacrificando-te por mim e pelos demais. Nunca percas tua capacidade de dar vida até aos mortos. Luta sempre pelos teus objetivos, porque foi esse teu espírito lutador que me contagiou e fez de mim melhor. Que o diga o meu ombro, que ainda sente dor de tanta pancada que ali levava. Bons velhos tempos, em que andar a ‘’porrada’’ era um modo de demonstrar afeto e de aprendizagem entre irmão. Obrigado também a minha avó. Gostaria que pudesses assistir a tudo o que alcance. Ficarias orgulhosa de mim, depois de tudo que me ensinaste e sacrificaste. Onde quer que estejas avô, amo-te e obrigado!

E apenas falta-me agradecer a duas pessoas mais. E que pessoas. As duas que dão mais cor e muita alegria há minha vida. Obrigado Ana e Vasco! Amo-vos! Ana, no dia que te conheci, senti que irias revolucionar o meu pequeno mundo, de uma forma ou da outra. E não é que acertei. Nunca vivi momentos de alegria, de afeto e emotivos como os que vivi contigo ao meu lado. Tu dás-me tranquilidade, concentração, amor, inteligência, bondade, vida, entre muitas outras coisas e por isso nunca te poderei pagar devidamente. Obrigado por me aturares, o que não é fácil para o deixar claro, por seres a minha melhor amiga, por me ajudares em todos os meus projetos, por dares tudo de ti por aqueles que tu amas e por todos os teus pormenores do dia-a-dia, que de alguma forma dão sempre ritmo há minha vida. E que ritmo…diga-se de passagem. Espero que saibas que sem ti, pouco mais restaria que uma vida sem rumo. És a minha

bussola. E quanto a ti Vasquito, obrigado por estes 19 meses alucinantes e a alta velocidade. Espero que um dia estejas tu a escrever os agradecimentos na tua tese de doutoramento e que tudo o que eu te possa ensinar esteja na tua mente. Mas por favor, escreve qualquer coisa melhor do que isto que para aqui escrevi. Além disso, quando uma dia leres esta tese, já que será leitura obrigatória para ti durante a primária, espero que sintas orgulho no teu pai. Tudo isto é para ti!

Obrigado